The chemical manipulation of meta-stable brine super-saturated with gypsum: forcing precipitation by overriding the inhibitory effect of antiscalants on crystal formation

by

Daniël Hendrik Gerber

Thesis submitted in partial fulfillment

of the requirements for the Degree

of

MASTER OF SCIENCE IN ENGINEERING

(CHEMICAL ENGINEERING)

in the Faculty of Engineering

at Stellenbosch University

Supervised by

Prof. A.J. Burger

December 2011

Declaration

By submitting this thesis electronically, I declare that the entirety of the work contained therein is my own, original work, that I am the sole author thereof (save to the extent explicitly otherwise stated), that reproduction and publication thereof by Stellenbosch University will not infringe any third party rights and that I have not previously in its entirety or in part submitted it for obtaining any qualification.

Signature Date

Abstract

Desalination, by means of reverse osmosis (RO), in combination with other processes, can produce potable water at high recoveries. Antiscalants are generally used to reduce scaling on equipment surfaces and to improve water recovery during RO by slowing down the precipitation kinetics of sparingly soluble salts in the RO feed, thereby allowing concentration levels in the RO brine at several times the solubility limit of these salts. In addition, a fraction of the concentrate may be recycled back to the feed of the RO-membrane to improve the overall recovery, but only after the super saturated salts in the concentrate have been precipitated. The inhibitory character of the antiscalants (which are rejected into the concentrate stream) complicates the removal of salt from the concentrate and therefore prohibits such recycling.

The focus of this study is aimed at properly understanding some of the parameters that influence the functionality or effectiveness of antiscalants used in high sulphate waters, with the purpose to override the effect of the antiscalant in the concentrate stream and force precipitation of the super saturated salts in solution.

A batch crystallization technique, which considers the precipitation of calcium sulphate dehydrate (gypsum) from a solution of changing super saturation, was used to perform precipitation tests 1) on synthetically prepared solutions, super saturated with gypsum and 2) industrial concentrate, rich in sulphate (produced by concentrating acid mine drainage (AMD) by means of a lab scale RO unit). During batch crystallization, the precipitation process was observed by means of monitoring the depletion of calcium, using a calcium selective electrode (ISE). Deductions concerning the kinetics of precipitation were made from observing two kinetic variables (response variables) *e.g.* the induction time and the growth rate (t_{C80} – inferential variable).

Two antiscalants have been evaluated in this study: a phosphonate based antiscalant (HYDREX) and a polyacrylate antiscalant (BULAB), at concentrations of 4 mg/l and 12 mg/l. The objective was to chemically and physically manipulate the antiscalant effectiveness, override its effect and force precipitation of gypsum by means of changing parameters in the system, such as the temperature (15°C- 25°C), pH (4-10), ferric chloride concentration (2-10 mg/l) or seeding the solution with gypsum seed at a concentration of 0-2000 mg/l. In addition, lime and a combination of gypsum and lime were also used for seeding at concentrations of 2000 mg/l.

The induction time, prior to precipitation, was found to be most strongly affected by the change in seed concentration and pH at a given antiscalant concentration. Seed at a concentration of 2000 mg/l was sufficient in most cases to immediately override the effect of HYDREX and BULAB (at 4-12 mg/l) and produce ~ 0 minutes induction time. A pH of 10 increased the adsorption capacity of HYDREX and BULAB, leading to longer induction times (exceeding 24 hours in some cases). At a pH of 4 the adsorption capacity was very low for both HYDREX and BULAB (lower) leading to shorter induction times (zero to 100 minutes). It was especially in the 'no-seed' cases that the effect of pH on the induction time was prominent.

The rate of precipitation (crystal growth rate) was increased at a temperature of 25°C, compared to 15°C (the rate increased two fold for an increase in 10°C). The addition of lime-seed, instead of gypsum, (at 2000 mg/l) produced growth rates, two times higher compared to when gypsum was used at the same conditions. In Addition, seeding with lime produced induction times (150 minutes for HYDREX and 50 minutes for BULAB) prior to precipitation, compared to zero induction time when gypsum was used at the same conditions. It was proven that an induction time could be eliminated by adding a combination of gypsum and lime both at a concentration of 2000 mg/l. with the added benefit of the higher growth rate.

An increase in the calcium concentration increased the crystal growth rate in the presence of HYDREX. The presence of a high pH, however caused the effect of calcium on the growth (in the presence of BULAB) to be overshadowed. At a higher pH the growth rate of gypsum slowed down as a result of the increase in adsorption capacity of the polymer onto the crystal surface.

The interaction of the antiscalant with $FeCl_3$ seemed to be important with regard to crystal growth. Higher ferric concentrations (10 mg/l) were sufficient to limit the inhibitory effect of 12 mg/l antiscalant (HYDREX and BULAB) on the crystal growth rate. Conversely, low ferric concentration resulted in slower growth rates in the presence of an antiscalant.

The best conditions (within the scope of the current study), sufficient 1) to override the inhibitory effect of antiscalants (HYDREX and BULAB) and 2) to produce rapid precipitation of gypsum, lie in the use of seeding with gypsum and lime (2000 mg/l), adding ferric chloride (10 mg/l), lowering the pH to 4 or lower (which can only be obtained when lime is not added) and setting the solution temperature to a moderate value of 25°C or higher.

These 'best' conditions were subsequently applied to a concentrate, produced from concentrating AMD in a RO unit, and proved to be even more successful in overriding the effect of HYDREX and BULAB than in synthetic aqueous solutions. The induction times of precipitation of AMD in all cases

were ~ 0 minutes, whereas the growth rate increased threefold compared to the synthetic tests. The presence of additional foreign precipitates of aluminum, calcium and magnesium as well as an increased $[SO_4^{2-}]$ x $[Ca^{2+}]$ product of 3.73 (AMD concentrate) vs. 3.46 (synthetic solutions) is thought to be responsible for the increase in precipitation kinetics when only gypsum seed was used.

The addition of lime caused an increase in the precipitation potential of the brine by increasing the calcium concentration. Although the addition of lime caused an increase in the pH to 12.3 (at which point the antiscalant was most effective), the increase in pH is likely to cause an increase in the natural carbonate in the water, which would stimulate $CaCO_3$ precipitation. The $CaCO_3$ precipitate would be responsible for the adsorption of antiscalants, reducing their efficiency.

Opsomming

Ontsouting by wyse van tru-osmose (TO), in samewerking met ander prosesse, kan help om drink-water te lewer teen verhoogte herwinning. Tipies word antiskaalmiddels gebruik om bevuiling op die oppervlak van toerusting te verminder en terselfdetyd herwinning te verhoog deurdat dit die presipitasiekinetika van superversadigde soute in die TO voerwater vertraag. Dit lei daartoe dat water (superversadig met soute) deur die membraansisteem kan beweeg, sonder om bevuiling te veroorsaak. 'n Breukdeel van die konsentraat kan herwin word na die TO voer om sodoende die algehele waterherwinning te verhoog. Dit kan egter eers gebeur nadat die soute in die konsentraat neergeslaan en verwyder is. Die inhirente 'vertragingskarakter' van antiskaalmiddels (wat ook in die konsentraat stroom beland) kompliseer die verwydering van sout vanuit die konsentraat en verhoed so herwinning.

Die fokus van hierdie studie is daarop gemik om die parameters wat die funksionaliteit of effektiwiteit van antiskaalmiddels (wat in sulfaatryke waters gebruik word), beter te verstaan. Die doel is daarop gemik om die betrokke antiskaalmiddel se effek te kanselleer asook presipitasie van die superversadigde soute in oplossing aan te help.

'n Lot ('batch') kristallisasietegniek wat die presipitasie van kalsiumsulfaatdehidraat (gips) beskou vanuit 'n oplossing waar die konsentrasie verander soos presipitasie plaasvind, is gebruik om presipitasietoetse uit te voer 1) op oplossings wat sinteties versadig is met gips en 2) op sulfaatryke AMD (gekonsentreer met behulp van 'n laboratoriumskaal TO eenheid). Die presipitasie proses is in elke geval waargeneem, deur die vermindering van die kalsium konsentrasie in die oplossing dop te hou, met die gebruik van 'n kalsiumselektiewe elektrode. Afleidings rakende die kinetika van presipitasie is gemaak deur twee responsveranderlikes dop te hou: die induksietyd en die kristal groeitempo (t_{C80}).

Twee antiskaalmiddels by 'n konsentrasies van 4 dpm (deetjies per miljoen) en 12 dpm is evalueer: 'n fosfonaat (HYDREX) and poliakrilaat (BULAB). Die doel was om die antiskaalmiddel se werking chemies en fisies te manipuleer, hul werking teen te werk en presipitasie van gips te forseer. Die manipulasie het geskied deur die volgende parameters te verander: temperatuur (15°C-25°C), pH (4-10), $FeCl_3$ (2-10 mg/l) of saad byvoeging (gips: 2000 mg/l). Kalsiumhidroksied (gebuste kalk) en 'n kombinasie van gips en gebluste kalk is ook gebruik by konsentrasies van 2000 mg/l.

Die induksietyd (by ‘n spesifieke antiskaalmiddel konsentrasie) is die sterkste beïnvloed deur ‘n verandering in saad konsentrasie en pH verandering. In die meeste gevalle was ‘n saad konsentrasie van 2000 mg/l voldoende om die induksie effek van beide HYDREX en BULAB te vernietig en nul-minute induksietyd is verkry. ‘n pH van 10 het gelei tot die verhoging van die adsorpsiekapasiteit van HYDREX en BULAB wat gelei het tot langer induksietye (in sommige gevalle het dit 24 uur oorskry). By ‘n pH van 4 was die adsorpsie kapasiteit van beide antiskaalmiddels baie laag (laer vir BULAB) en induksie-tye is beperk tot 100 minute. Dit is veral wanneer geen saad toegevoeg is nie wat die effek van pH prominent was.

Die tempo van presipitasie was verhoog by ‘n temperatuur van 25°C (2 keer hoër as by 15°C). Die byvoeging van gebluste kalk teen 2000 mg/l het ‘n kristal groeitempo, 2 keer hoër as in die teenwoordigheid van gips gelewer. Gebluste kalk saad byvoeging het egter gelei tot ‘n indukisetyd (150 minute vir HYDREX en 50 minute vir BULAB). Hierdie probleem is oorkom deur ‘n kombinasie van gips en gebluste kalk te gebuik teen ‘n konsentrasie van 2000 mg/l. Geen induksie tyd is waargeneem met die voordeel van ‘n hoër presipitasietempo (kristal groei).

‘n Verhoging van kalsium konsentrasie verhoog die kristal groei tempo in die teenwoordigheid van HYDREX. Nietemin, die invloed van pH oorskadu die invloed van kalsium op die groei tempo (in die teenwoordigheid van BULAB). By ‘n hoë pH word die kristal groei tempo vertraag as gevolg van die verhoging van die adsorpsiekapasiteit van die antiskaalmiddel. Die interaksie van $FeCl_3$ met die antiskaalmiddel blyk van belang te wees. By hoë $FeCl_3$ konsentrasies (10 dpm), is die werking van beide HYDREX en BULAB (12 dpm) beperk.

Die ‘beste’ kondisies (verkry binne die konteks van hierdie studie), 1) om die vertragingseffek van HYDREX en BULAB teen te werk en 2) spoedige presipitasie van gips te bewerk, lê in die gebruik van saad (gips en gebluste kalk teen 2000 mg/l), die byvoeging van $FeCl_3$ (10 mg/l), ‘n lae pH (4 of laer, wat natuurlik net tersprake is wanneer slegs gips as saad gebruik word aangesien geluste kalk die pH sal lig) asook ‘n relatiewe hoë temperatuur (25°C).

Hierdie ‘beste’ kondisies is toegepas in AMD konsentraat om die effek van HYDREX en BULAB te vernietg en gips te presipiteer en die gevolg was dat dit selfs meer suksesvol was as in sintetiese oplossings. In elke geval is die induksietyd na nul minute toe verminder, terwyl die kristal groei tempo 3 maal verhoog het in vergelyking met die sintetiese toetse. Die teenwoordigheid van onsuiwerhede insluitende aluminium, kalsium, magnesium sowel as ‘n verhoging in die $[SO_4^{2-}]x[Ca^{2+}]$ produk (3.73 teenoor 3.46 vir sintetiese toetse), blyk verantwoordelik te wees vir die versnelling van die kinetika.

Met die byvoeging van gebluste kalk is dit waarskynlik dat die verhoging van die pH (12.3) lei tot die verhoging van natuurlike karbonate in die water wat weer $CaCO_3$ stimlueer. Die teenwoordigheid van $CaCO_3$ kan verantwoordelik gehou word vir bykomende nukleasie en groei, sowel as die deaktivering van antiskaal effektiwiteit.

Acknowledgements

- All the glory to JESUS who stuck it out with me – for wisdom, guidance, peace and companionship.
- Veolia, thank you for the opportunity.
- Prof. Burger for wisdom, hard words and patience.
- My parents, two wonderful sisters and friends for support and always believing in me.
- Calisto Kazembe – late night discussions and wisdom of life.
- Oom Anton, Oom Jannie, Oom Vincent, Alvin, Elton and Lucas for assistance in the lab.
- Hanlie Botha for always being willing to help.
- Tannie Juliana for compassion and always helping even in the dire straits.
- Stefan Bekker for a great friend – thanks for running the race with me.
- DB and Jeanne for I&W.
- Frans van Schalkwyk and Dirk Bosman – companions for life.
- Colleagues of A-601.
- Family at SHOFAR for prayer and support.
- Helderberg zone legends (Chris, Andre and the boys), Oom Derk-Jan and tannie Rene.
- Nini van der Merwe – blessing of year one.
- Aerolene for friendship.
- Mohau Phiri – a great friend.
- Amelia, Anri en Steve – dankie vir die retreat.
- The HILLSONG team.
- Ingrid Wolfaardt.

Table of contents

Abbreviations and symbols

Symbol/Abbreviation	Description
AA	Atomic Absorption spectrophotometry
A_{DH}	Constant (temperature dependent)
a_{DH}	Ionic size parameter
α_i	Activity of a species
Al_2O_3	Aluminium oxide (alumina)
AMD	Acid Mine Drainage
AS	Antiscalant
Ω	Saturation ratio
B_{DH}	Constant (temperature dependent)
Ca^{2+}	Calcium ion
$[Ca^{2+}]$	Calcium ion concentration (M)
$CaCO_3$	Calcium carbonate (calcite)
$CaSO_4.2H_2O$	Calcium sulphate dehydrate (gypsum)
$CaSO_4.½H_2O$	Calcium sulphate hemihydrate
$CaSO_4$	Calcium sulphate anhydrite
CF	Concentration factor
CMC	Carboxymethyl cellulose
c_i	Concentration of molecular species (mol/kg)
CO_2	Carbon dioxide
C_{80}	Calcium concentration at t_{C80}
C*	Calcium concentration at equilibrium
DOE	Design of Experiments
E	Observed potential (V)

E_a	Reference potential (V)
EDTA	Ethylene diaminetetraacetic acid
ENTMP	N,N,N',N'-ethylenediaminetetra (methylenephosphonic acid)
ϵ	Dielectric constant for water
F	Faraday's constant ($9.648x10^4$ C/equivalent)
$FeCl_3$	Ferric chloride (used in text as FERRIC)
Fe^{3+}	Ferric ion
Fe^{2+}	Ferrous ion
$Fe(OH)_3(s)$	Ferric hydroxide solids
FeS_2	Pyrite
$f(\Phi)$	Correction factor (classical nucleation theory)
ΔG_{crit}	Critical Gibbs energy
γ_i	Activity coefficient of a given species
HEDP	1-hydroxyethylidine-1,1-diphosphonic acid
HESG	Heterogeneous seeded growth
HOSG	Homogeneous seeded growth
HYDREX	Phosphonate based antiscalant
IP	Ionic product
ISA	Ionic strength adjuster for calcium
ISE	Ion Selective Electrode
J	Salt rejection
k'	Crystal growth rate constant ($M^{-1}.min^{-1}$)
$KFe_3(SO_4)_2(OH)_6$	Kaolin (mineral)
K_{sp}	Solubility product
M	Concentration of ionic species (mol/l)

m	Concentration of ionic species (mol/l)
m_{eq}	Concentration of ionic species at equilibrium (mol/l)
$Mg(OH)_2$	Magnesium hydroxide
MgO	Magnesium oxide
mM	mMol/liter
MSF	Multi stage flash distillation
$MgSO_4.7H_2O$	Magnesium sulphate
MW	Molecular weight
N_A	Avogadro's number
NaCl	Sodium chloride
Na_2CO_3	Sodium carbonate
NaOH	Sodium hydroxide (caustic soda)
NROC	Natural RO concentrates
NTMP	Nitrilotri(methylene phosphonic acid)
PAA	Polyacrylic acid
PACl	Polyaluminium chloride
PGA	Polyglutamic acid
PMA	Polymaleic acid
PolyDADMAC	Polydiallyldimethylammonium chloride
Q_f	Retentate flow rate (or volume)
Q_p	Permeate flow rate (or volume)
R	Universal gas constant
R	Water recovery
r_{crit}^2	Critical nuclei radius
RO	Reverse Osmosis
SDS	Sodium dodecyl sulphate
SEM	Scanning Electron Microscopy

SHMP	Sodium Hexametaphosphate
SI	Saturation index
SiO_2	Silicon oxide (Silica)
S_n	Constant -function of the number of growth sites available in solution
SO_4^{2-}	Sulphate ion
$[SO_4^{2-}]$	Sulphate ion concentration (mol/l)
SPARRO	Slurry Precipitation and Recycle Reverse Osmosis
SPP	Sodium pyrophosphate
STPP	Sodium tripolyphosphate
σ	Interfacial tension (J/m^2)
TENTMP	N,N,N',N'-triethylenediaminetetra (methylenephosphonic acid)
t_{C80}	Inferential growth rate. Point in time at which 80 % of the precipitation process is complete.
t_g	Time required for the nucleus to grow to a visible size
t_i	Time required for the critical nucleus to form
t_{ind}	Induction time
V_m	Molar volume for gypsum [74.69 ($cm^3.mol^{-1}$)]
x_i	Concentration of molecular species (mol/l)
z_i	Charge of molecular species

List of figures

List of tables

Chapter 1 - Introduction

1.1 Problem statement and focus of the study

Not only do antiscalants prevent scale formation of sparingly soluble salts in processes such as multi-stage flash distillation (MSF) and reverse osmosis (RO), it also helps to increase water recovery during RO by inhibiting nucleation kinetics of the sparingly soluble salts as they become super saturated in the RO process. The inhibitory effect of these same antiscalants inhibits further separation of water and salt in the concentrate stream. The focus of this study is aimed at the proper understanding of the factors that influence the functionality of antiscalants in high sulfate water with the purpose to override the effect of the antiscalants and force precipitation of the salts (gypsum in this case) in the concentrate.

1.2 The water situation in South Africa

Twelve years ago, Scholes *et al.* (1999) already stated*: "South Africa's available freshwater resources are already almost fully utilized and under stress. At the projected population growth and economic development rates, it is unlikely that the projected demand on water resources in South Africa will be sustainable. Water will increasingly become the limiting resource in South Africa, and supply will become a major restriction to the future socio-economic development of the country in terms of quantity and quality."*

South Africa is a semi-arid, water-stressed country with an average annual rainfall of approximately 450 mm per year, well below the world average rainfall of 860 mm per year.

In addition, research by van den Berg (2009) states that the main contributors to the degradation of water quality in South Africa are the discharge of urban and industrial effluents into rivers, high salinity irrigation return flows, wash-off and leachate from mining operations as well as wash-off from areas with insufficient sanitation.

In the mining industry, which makes out 8 % of the total water usage (Basson *et al.*, 1997), great potential exists for recycle and re-use of water. However, methods currently employed for the desalination of such waste water, including ion exchange and membrane treatment, produce saline effluents that require additional management (Nathoo *et al.*, 2009).

1.3 Brine treatment background

During desalination processes, such as reverse osmosis or flash distillation, water is typically recovered to the point at which precipitation of super saturated, sparingly soluble salts occur in the concentrate. This point is determined by the scaling potential of the feed water, which is related to the water chemistry, temperature and pre-treatment employed. Pre-treatment is applied to prevent sparingly soluble salts (*e.g.* gypsum, calcium carbonate, barite, etc.) from precipitating on process equipment, pipes and membranes and can consist of either one, or a combination, of processes such as softening by precipitation, pH adjustment and the addition of antiscalants. In addition, pre-dosing of antiscalants have shown to help increase water recovery from 50 % up to 90 % by slowing down the precipitation kinetics of super saturated sparingly soluble salts in solution (Bonne *et al.*, 2000).

To further improve water recovery during a process such as reverse osmosis (RO), a fraction of the RO concentrate (brine) can be recycled back to the feed, after precipitating the super saturated salt in solution. However, antiscalants present in the brine leads to the stabilization of the super saturated solution (Yang *et al.*, 2007) and appropriate pre-treatment of the brine should therefore be employed prior to recycle.

Softening by precipitation is a common method used to remove excess salt from stable super saturated brine. Softening is dependent on the addition of alkaline compounds such as hydrated lime-$Ca(OH)_2$, caustic soda (NaOH) and/or soda-ash (Na_2CO_3) to produce highly super saturated conditions, which can both stimulate and sustain precipitation of calcium salts such as $CaCO_3$ and $CaSO_4.2H_2O$ (Rahardianto *et al.*, 2010).

Seeded precipitation is another form of brine crystallization, and makes use of the benefit that RO concentrates are already super saturated with respect to the scalant under scrutiny. Seeded precipitation has the advantage of reduced chemical consumption, as seed can be re-used and recycled (Tait *et al.*, 2009).

Other brine treatment methods, some of which are more directly focused on destroying or degrading antiscalants include:

- addition of coagulants such as ferric chloride (Kim *et al.*, 2009), PACl (Aluminium) or SDS (Yang *et al.*, 2007) to the brine, which cause antiscalants to preferentially complex with the coagulant molecules rather than with the crystal surface, resulting in reduced efficiency of their inhibitory power,

- the addition of inorganic particles (Yang *et al.*, 2008a), which serves the same purpose as seed material, creating additional nucleation sites for crystal growth and,
- chemical or electrochemical oxidation, which causes antiscalants to be chemically degraded.

The literature study (Chapter 2) presents different brine treatment strategies in more detail.

1.4 Motivation and objective of research

Total water recovery can be improved during a compounded process that includes multiple desalination and precipitation stages. After desalination by means of RO (or other related methods), super saturated salts in the concentrate stream (brine) can be removed and the water recycled back to the RO feed. During pre-treatment (prior to RO), antiscalants are added to prevent scaling on the membrane surface and improve water recovery by slowing down precipitation kinetics of sparingly soluble salts in solution. Antiscalants do not build up in the system and are rejected together with the brine. Effective brine concentration specifically considers the deactivation or destruction of the antiscalant molecules.

This work, specifically focuses on the treatment of brines as could typically be produced by desalination of high sulphate AMD. These brines are characterized by high levels of sulphate and moderate levels of calcium and are prone to calcium sulphate dehydrate (gypsum) scaling.

The aim of the study was to determine to which extent precipitation kinetics (in the presence of antiscalants) could be accelerated by means of chemical manipulation of the RO concentrate.

The bulk of the work was performed on synthetically prepared aqueous solutions, super saturated with gypsum. Subsequent verification of findings was performed by selected tests on RO-concentrated AMD.

Chapter 2 - Literature review

2.1 Flow diagram

The following diagram depicts the logic in the inclusion of each part of the literature review.

	OUTLINE OF LITERATURE	REMARK
2.2	Sulfidic mine water	**[Origin of problem water]**
2.2.1	Reverse Osmosis (RO)	**[Treatment of problem water]**
2.3	The calcium sulphate -water equilibrium	**[Characteristic of problem water]**
2.4	Precipitation	
2.5	Thermodynamics of calcium sulphate dehydrate	
2.6	Kinetics of calcium sulphate dehydrate	**[Mechanism of precipitation of gypsum]**
2.6.1	Nucleation	
2.6.2	Growth	
2.7	Factors influencing gypsum precipitation kinetics	
2.7.1	Temperature	
2.7.2	Super saturation/ super saturation ratio	**[Factors influencing the mechanism of precipitation]**
2.7.3	Seeding	
2.7.4	Admixtures	
2.7.5	Anionic admixture	
2.8	Antiscalants suitable for gypsum inhibition	**[Refers to 2.7.4] - specific admixture used to pre-treat RO feed water**
2.8.1	Overview	**[Considers important literature about antiscalants]**
2.8.2	Adsorption Mechanism	
2.9	Factors that influence behaviour of antiscalants	
2.9.1	The interaction between antiscalant, temperature and super saturation	**[Factors that influence mechanism of antiscalant]**
2.9.2	pH	
2.9.3	Cationic impurities	
2.10	RO-concentrate treatment	
2.10.1	CESP process	
2.10.2	Coagulant and surfactant addition – de-super saturation	**[Novel techniques used to treat meta-stable brines]**
2.10.3	Addition of inorganic particles	
2.10.4	Air-blow and organic inducers	
2.10.5	More seeded precipitation processes	

2.2 Sulfidic mine water

Metallic ore deposits (Cu, Pb, Zn, Au, Ni, U, and Fe), phosphate ores, coal seams, oil shales and some mineral sands contain rich amounts of sulphides. Mining activities are mainly responsible for the exposure of these sulphide-rich resources to natural weathering (oxidation), which over time have resulted in one of the largest environmental problems aside from global warming today – acid mine drainage (AMD) (Lottermoser, 2007).

Of all the sulphide-containing minerals, pyrite (FeS_2) is the most abundant and is generally associated with coal and metal ores (Lottermoser, 2007). Under oxidative conditions (refer to reactions A-D), pyrite is oxidized to Fe^{2+} (ferrous iron). When ferrous iron comes in contact with oxygen-rich surface waters, further oxidation to Fe^{3+} (ferric iron) takes place. The stability of ferric iron has a strong pH dependency. At a pH below 3.5, Fe^{3+} will further act as a catalyst to oxidise pyrite according to reaction C. At a pH above 3.5, Fe^{3+} will precipitate as $Fe(OH)_3(s)$. The formation of this precipitate generates H^+ ions and buffers the pH at around 2.5-3.5, giving rise to the characteristic acidity of sulfidic mine waters (Brown *et al.*, 2002).

$$FeS_{2(s)} + \frac{7}{2}O_2 + H_2O \rightarrow 2SO_4^{2-} + Fe^{2+} + 2H^+ \quad \text{(A)}$$

$$Fe^{2+} + \frac{1}{4}O_2 + H^+ \rightarrow Fe^{3+} + \frac{1}{2}H_2O \quad \text{(B)}$$

$$FeS_2(s) + 14Fe^{+3} + 8H_2O \rightarrow 2SO_4^{2-} + 15Fe^{2+} + 16H^+ \quad \text{(C)}$$

$$Fe^{3+} + 3H_2O \rightarrow Fe(OH)_3(s) + 3H^+ \quad \text{(D)}$$

AMD run-off, seepage, ponds, streams etc. contain precipitates such as gypsum ($CaSO_4.2H_2O$), epsomite ($MgSO_4.7H_2O$) and jarosite $KFe_3(SO_4)_2(OH)_6$ of which gypsum is the most abundant. The Ca^{2+} (constituent of gypsum) are produced either by 1) the weathering of carbonate and silicate minerals such as dolomite, calcite and plagioclase or 2) as a result of the neutralization of AMD waters (Lottermoser, 2007).

Neutralization (or softening), is used to remove certain dissolved minerals from the water which causes scaling on process equipment, pipes etc. Materials such as soda ash, caustic soda, sodium carbonate, lime, limestone, dolomite and calcite are among the most common materials used for this application. The increase in the pH during neutralization, results in the precipitation of hydroxides of iron, magnesium, calcium etc., after which precipitates of these metals are removed proficiently (Brown *et al.*, 2002).

Neutralisation reactions between AMD waters and calcite result in gypsum precipitation (Lottermoser, 2007):

$$CaCO_{3(s)} + H_2SO_{4(aq)} + 2H_2O_{(l)} \rightarrow CaSO_4 \cdot 2H_2O_{2(s)} + H_2CO_{3(aq)} \quad \text{(E)}$$

The same observation is made when lime is used to neutralise AMD water:

$$Ca(OH)_2(s) + H_2SO_4 \rightarrow CaSO_4.2H_2O\ (s) \quad \text{(F)}$$

Neutralization can also help to partially remove sulphate from scaling waters as observed in reaction F (Geldenhuys *et al.*, 2001). Additional sulphate removal takes place either with the use of ion exchange, electro-dialysis, adsorption or reverse osmosis (Droste, 1997).

When the ionic concentration of Ca^{2+} and SO_4^{2-} increase beyond the solubility limit of gypsum, severe scaling takes place (gypsum precipitation is not influenced by pH and is dependent on the detailed chemical analysis of the water). The solubility limit of sparingly soluble salts puts a limiting factor on the recovery of water during desalination processes such as reverse osmosis (RO), and multi-stage flash distillation etc. For illustration purposes, only RO will be discussed henceforth.

2.2.1 Reverse Osmosis (RO)

Conceptually, RO is a pressure driven filtration process based on the concept of a semi-permeable membrane, which allows selective separation of water and dissolved matter. Pressure (substantially greater than the osmotic pressure) is applied to the solute side of the membrane (containing most dissolved components), and forces the water through the membrane to produce an almost pure solvent (Sourinajan, 1970).

Water recovery (R) during RO is defined as the fraction feed water recovered as product (permeate):

$$R = \frac{Q_P}{Q_F} \tag{2.1}$$

The concentration of salts in the brine is related to the water recovery by the following expression where CF is referred to as the concentration factor and J the salt rejection:

$$CF = \frac{1 + R \cdot J - R}{1 - R} \tag{2.2}$$

Because salt rejection of most membranes is close to unity (95-98 %), the expression in equation 2.2 could be simplified as:

$$CF \approx \frac{1}{1 - R} \tag{2.3}$$

Feed water chemistry can limit water recovery during RO to as low as 50 % (Wilf and Ricklis, 1983). Effective pre-treatment of RO feed water, by means of antiscalant addition have however shown to improve recovery up to 90 % (Bonne *et al.*, 2000). Additionally, water recovery can be increased by further concentrating the RO concentrate and recycling the cleaner water back as feed to the RO module. Antiscalants that end up in the RO concentrate stream however cause the salt in the brine stream to exhibit meta-stable behaviour, preventing precipitation and subsequent concentration of brine. To effectively treat such brine, it is necessary to have knowledge of:

1) The precipitation kinetics and thermodynamics of the precipitating system
2) The mechanism and behaviour of antiscalants.

Section 2.10 considers some of the more novel technologies which can be applied for RO concentrate treatment.

2.3 The calcium sulphate -water equilibrium

In a system containing only calcium, sulphate and pure water, three primary hydration states or molecular forms can exist (Ben Ahmed *et al.*, 2008): $CaSO_4.2H_2O$ (gypsum), $CaSO_4.½H_2O$ (hemihydrate) and $CaSO_4$ (anhydrite). There is also a fourth hydration state, called the 'soluble' anhydrite (Posnjak, 1938). Gypsum and the insoluble anhydrite form are the only ones recognised as being stable (Power *et al.*, 1964). The different molecular forms are interchangeable and depend strongly on the temperature.

To illustrate the transition between the different molecular forms in pure water at atmospheric pressure, consider the solubility-temperature relationship in **Figure 1**. The majority of researchers (Partridge & White, 1929; Posnjak, 1938; Power *et al.*,1964) have come to the conclusion that the transition temperature between gypsum and the insoluble anhydrite is approximately 40°C. These researchers all considered the 'solubility method'. A limitation of this method is that none of the transitional reactions between different hydration states could be adequately reversed as a result of slow kinetics (Blount and Dickson, 1973).

Hardie (1967) challenged the status quo and calculated the transition temperature to be approximately 63.5°C, which is far removed from the data obtained from mainstream research. In addition, he successfully reversed the reaction from anhydrite to gypsum. Moreover, Blount & Dickson (1973) calculated the transition temperature to be 56°C, using a method different to that of Hardie (1967). Nonetheless, the work of Blount & Dickson (1973) agrees best with that of Hardie (1967).

Why there is a discrepancy between the measured transition temperatures in different studies is not clear. Nonetheless, there is consensus that below 40°C gypsum is the only stable phase.

In addition, the solubility of each of the molecular forms and consequently the transition temperature is also affected by the presence of additional dissolved salts.

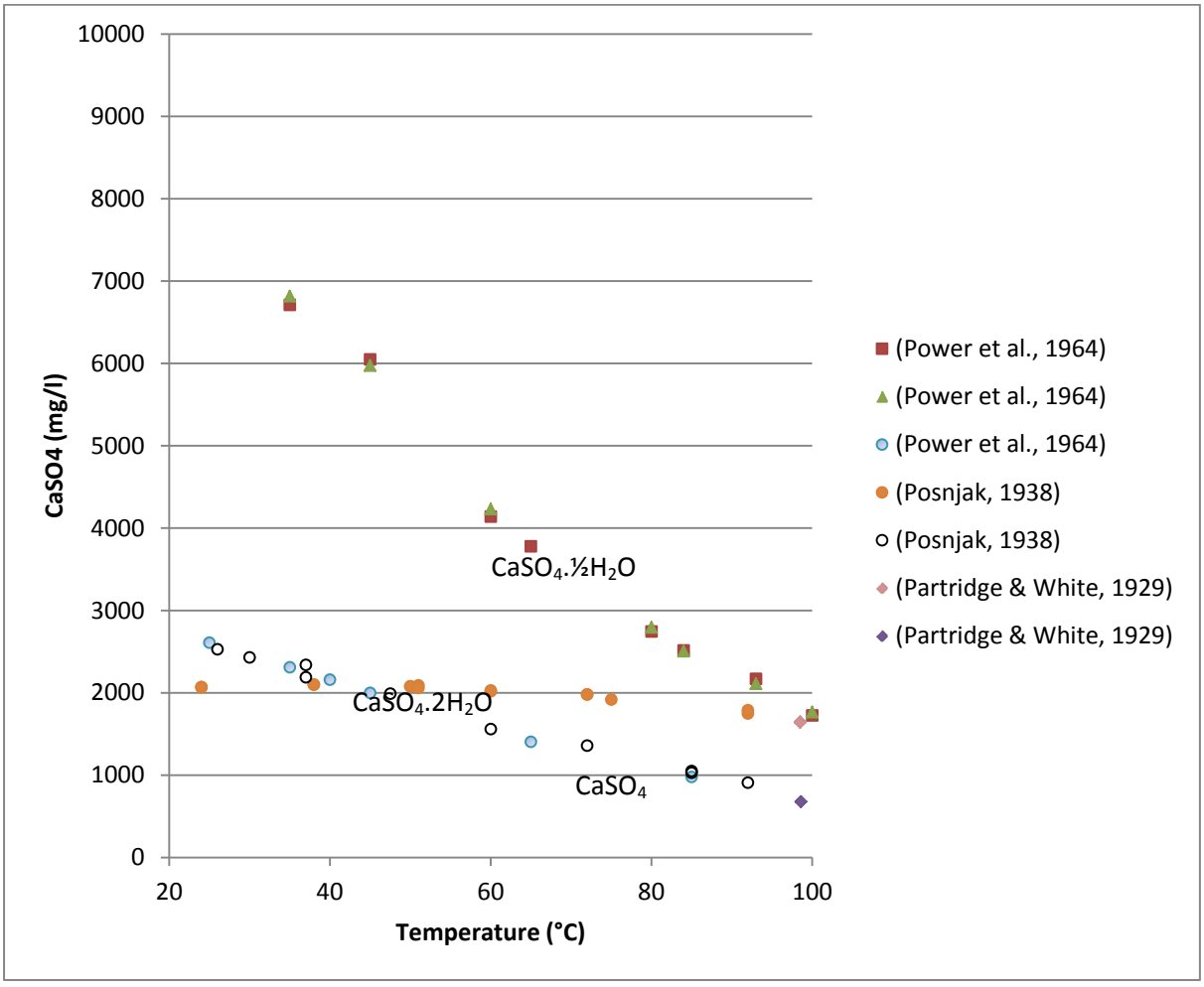

Figure 1: *Solubility of calcium sulphate hydrates in water at different temperatures*

Blount & Dickson (1973) studied the gypsum-anhydrite system in equilibrium with NaCl and showed that increasing amounts of NaCl reduced the transition temperature between gypsum and the anhydrite phases: 0 M NaCl = 56°C, 2 M NaCl = 48°±4°C, 4 M NaCl = 36°±4°C and 6 M NaCl = 20°±4°C. This work correlated well with published data by Hardie (1967).

Block & Waters (1968) considered the $CaSO_4$-Na_2SO_4-NaCl-water system at temperatures 25°C to 100°C. They found that at 25°C-70°C and 0-4 M NaCl the only calcium sulphate hydrate form was gypsum. Only at 85°C the gypsum changed to the anhydrite from.

In conclusion, temperature as well as the ionic strength, has a strong influence on the transition between different hydration states. At low temperatures and low ionic strengths gypsum is expected to be the prevailing molecular state.

2.4 **Precipitation**

In general there is some dispute about the definitions of crystallization and precipitation. However, in actual fact there is little that divides these phenomena. It is maybe best to think of precipitation as representing fast crystallization. The tempo at which precipitation takes place is said to be as a result of the level of super saturation governing the process. Generally materials that are rather insoluble lead to precipitated products, as the low solubility causes the super saturation to be increased. The high super saturation levels ensure that the primary nucleation rates are high (nucleation rate plays an important role in precipitation). Normally when the super saturation is high, a large number of minute crystals are produced (10^{11} and 10^{16} per cm^{-3}). Super saturation, necessary for precipitation, can in some cases be produced by a chemical reaction. In this case precipitation is referred to as reactive crystallization. Moreover precipitation is generally carried out at a constant temperature and does not rely on cooling to produce super saturation (Söhnel and Garside, 1992).

Precipitation consists of a number of individual steps as well as kinetic processes (refer to **Figure 2**).

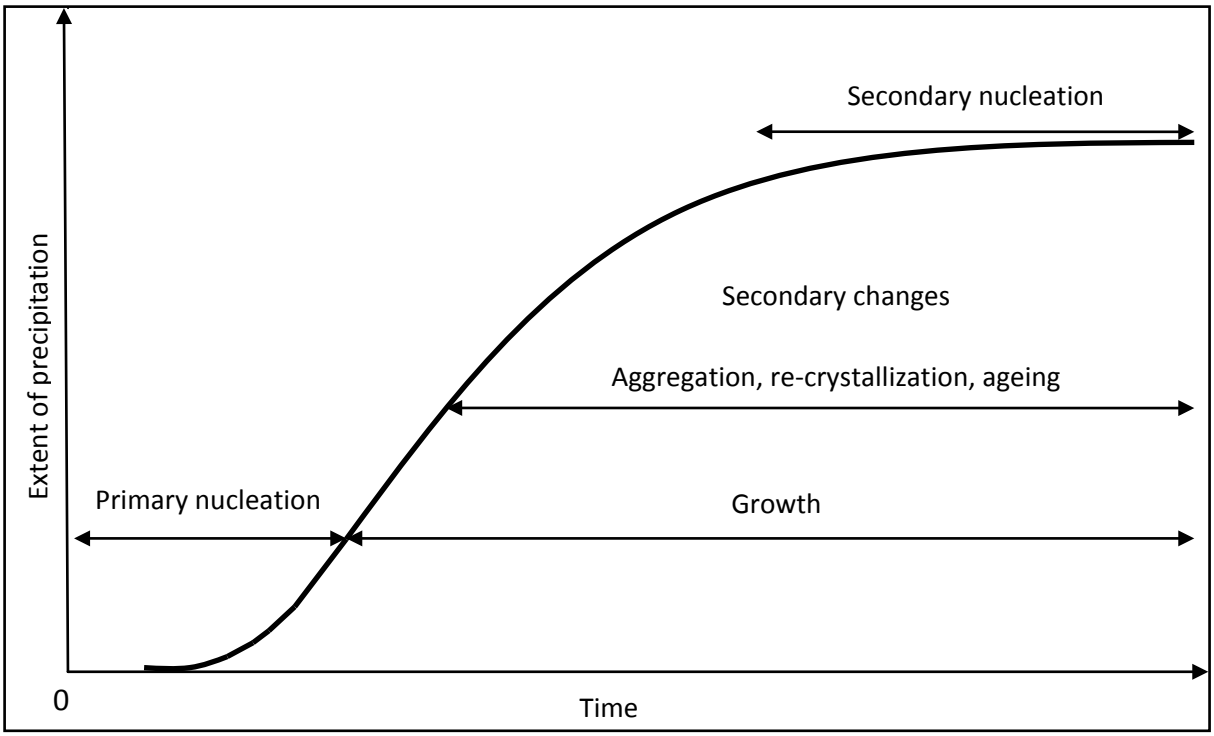

Figure 2: *Kinetic processes of precipitation (Re-drawn from Söhnel and Garside,1992)*

Central to understanding the kinetics of precipitation is the nucleation and growth processes. The current research is concerned with gypsum crystallization and therefore kinetic concepts will be

considered in the light of the calcium sulphate-water system. The thermodynamics of crystallization will be considered henceforth.

2.5 Thermodynamics of calcium sulphate dehydrate

The characteristic reaction which describes the formation of gypsum from calcium and sulphate in an aqueous solution is given as,

$$Ca^{2+} + SO_4^{2-} \leftrightarrow CaSO_4.2H_2O \qquad (G)$$

The thermodynamic driving force for gypsum crystallization in this reaction is the change in Gibbs free energy between a super saturated state and a state of equilibrium (Nielsen, 1984) and is given as,

$$\Delta G = -\frac{RT}{2}\ln\Omega \qquad (2.4)$$

Where R is the universal gas constant (8.314 J/mol.K), T is the absolute temperature of the solution expressed in degrees Kelvin and Ω is the super saturation ratio with respect to gypsum. The super saturation ratio indicates to what extent a solution is super saturated with respect to equilibrium at a given temperature, and is calculated according to:

$$\Omega = \frac{(\alpha_{Ca^{2+}})(\alpha_{SO_4^{2-}})}{K_{sp}} \qquad (2.5)$$

α represents the ionic activity or 'effective concentration' of a given species in a complex solution. K_{sp} represents the solubility product of gypsum and is unique for a given temperature. K_{sp} defines how much of a given salt will be soluble at a prescribed temperature and is expressed as:

$$K_{sp} = \gamma_{Ca^{2+}}.[Ca^{2+}]_{eq} \cdot \gamma_{SO_4^{2-}}.[SO_4^{2-}]_{eq} \qquad (2.6)$$

2.5.1 The activity

In an ideal solution where there is no interaction between the different components in the solution, the activity of each species (α_i) is equal to its concentration. In a real solution, interaction between components becomes important and the activity coefficient (γ_i) is used to describe the deviation from ideality (Söhnel and Garside, 1992).

The activity, α is written as:

$$\alpha_i = \gamma_i x_i \tag{2.7}$$

Where, γ_i is the activity coefficient and x_i is the concentration of a given species. The activity coefficient is a function of the ionic strength, which is calculated as follows:

$$I = \frac{1}{2}\sum_I (C_I Z_I^2) \tag{2.8}$$

Where, C_I is the concentration of a given species in moles/kg and Z_I is the charge of the species *i*. For dilute solutions (ionic strength <1x10^{-4} M), ions are assumed to exert ideal behaviour and the activity coefficient of each species simplifies to 1 (Koretsky, 2004). At higher ionic strengths, the activity coefficient for a species decreases. This behaviour is more pronounced for species with a higher valence. For an accurate calculation of the activity coefficient for solutions with an ionic strength less than 0.1 M, the Debye-Huckel equation can be used (Pytcowicz, 1979; Snoeyink & Jenkins, 1980)

$$\log(\gamma_i) = -A_{DH} Z_i^2 \left(\frac{I^{1/2}}{1 + a_{DH} B_{DH} I^{1/2}} \right) \tag{2.9}$$

$$A_{DH} = 1.82x10^6 (\epsilon T)^{-3/2} \tag{2.10}$$

$$B_{DH} = 50.3(\epsilon T)^{-1/2} \tag{2.11}$$

A_{DH} and B_{DH} are both temperature dependent constants; ϵ is the dielectric constant of water and $a_{DH}$is the ionic size parameter.

For ionic strengths up to 0.5 M the Davies equation is sufficient:

$$\log(\gamma_i) = -A_{DH} Z_i^2 \left(\frac{I^{1/2}}{1 + I^{1/2}} - 0.2I \right) \tag{2.12}$$

At ionic strengths higher than 0.5 M (up to 6 molal), the Pitzer equation (Pitzer, 1991) can be applied.

The mean activity coefficient of a solute, MX, in a mixed electrolyte according to the Pitzer equation is given by equation 2.13, where m_i is the molality of either the cations or anions in solution. v_M and v_X are the number of ions M and X per molecule, with electric charges z_M and z_X. A_Φ is the Debye-Huckel coefficient for the osmotic coefficient (0.3915 mol.kg^{-1}, at 25°C in water), b and a are two adjustable parameters with values of 1.2 and 2 respectively. Parameters $\beta^{(1)}$ and $\beta^{(0)}$ define the second virial coefficient (temperature-dependent correction factor, used to explain the deviation from ideal gas behaviour, caused by inter-particle interactions), representing specific interaction parameters for pure electrolytes. Values for the second virial coefficients have been extensively tabulated in the DIPPR (Design Institute of Physical Properties Data) database. C_{MX} describes the third virial coefficient. This term is usually quite small and sometimes negligible. Predictions of the third virial coefficient have been made by De Santis and Grande, 1979.

$$\begin{aligned}\mathrm{Ln}\,\gamma_{MX} = {} & |z_M z_X| F \frac{v_M}{v}\sum_a m_a\left[2B_{Ma} + ZC_{Ma} + 2\left(\frac{v_X}{v_M}\right)\Phi_{\mathrm{Xa}}\right] \\ & + \frac{v_X}{v}\sum_c m_c\left[2B_{cX} + ZC_{cX} + 2\left(\frac{v_M}{v_X}\right)\Phi_{\mathrm{Mc}}\right] \\ & + \sum_c\sum_a m_c m_a \frac{1}{v}[2v_M z_M C_{ca} + v_M\psi_{Mca} + v_X\psi_{caX}] + \\ & + \sum_{c<}\sum_{c'} m_c m_{c'}\frac{v_X}{v}\psi_{cc'X} \\ & + \sum_{a<}\sum_{a'} m_a m_{a'}\frac{v_M}{v}\psi_{Maa'} + 2\sum_n m_n(v_M\lambda_{nM} + v_X\lambda_{nX})/v\end{aligned} \tag{2.13}$$

The indices c and c’ apply to all cations, whereas the indices **a** and **a’** apply to all anions.

$$\mathrm{Z} = \sum_{\mathrm{c}} \mathrm{m_c z_c} = \sum_{\mathrm{c}} \mathrm{m_a |z_c|} \tag{2.14}$$

$$\mathrm{F} = f^{\gamma} + \sum_{\mathrm{c}}\sum_{\mathrm{a}} m_c m_a B'_{ca} + \sum_{\mathrm{c}<}\sum_{\mathrm{c}'} m_c m_{c'}\Phi'_{cc'} + \sum_{\mathrm{a}<}\sum_{\mathrm{a}'} m_a m_{a'}\Phi'_{aa'} + \tag{2.15}$$

$$\mathrm{B_{MX}} = \beta^{(0)}_{\mathrm{MX}} + \beta^{(1)}_{\mathrm{MX}}\frac{1}{2I}\left[1 - \left(1 + 2\sqrt{I}\right)\exp\left(-2\sqrt{I}\right)\right] \tag{2.16}$$

$$B'_{MX} = \frac{\beta^{(1)}_{MX}}{2I^2}\left[-1 + \left(1 + 2\sqrt{I} + 2I\right)\exp\left(-2\sqrt{I}\right)\right] \quad (2.17)$$

$$C_{MX} = \frac{C^{\Phi}_{MX}}{2|z_M z_X|^{1/2}} \quad (2.18)$$

$$f^{\gamma} = -A_{\Phi}\left[\frac{I^2}{\left(1 + bI^{1/2}\right)} + \frac{2}{b}ln\left(1 + bI^{1/2}\right)\right] \quad (2.19)$$

$$v = v_M + v_X \quad (2.20)$$

The parameters Φ, Φ' and ψ arise from additional combinations of the individual second and third virial coefficients. The parameters, containing an apostrophe correspond to the derivative of the parameter with respect to the ionic strength. The parameters $\lambda_{n\ldots}$ are related to the interactions between a molecule, n, and an ion.

To analyse complex systems, calculation of an activity coefficient by hand can become a really tedious operation. Software such as OLI, Visual MINTEQ and Phreeq have been developed to simplify this process and predict speciation of an aqueous solution using advanced thermodynamic models.

2.6 Kinetics of calcium sulphate dehydrate

To quantify the kinetic behaviour of a system subject to crystallization, the nucleation and growth characteristics of system should be fully understood. This is especially important for process engineers who design and build and specify (size) process equipment according to time constraints such as the retention time of an operation.

2.6.1 Nucleation

When water is heated at atmospheric pressure, it is accepted that phase transition (boiling) will take place at 100°C. However it has been shown that pure water (essentially free from any form of solid particles), which does not make contact with any solid surface can only start to boil at a temperature as high as 279.5°C (Apfel, 1972). This is as a result of the phenomenon of nucleation.

The transition from one phase X to another Y, will only take place once some of the Y-nucleus has formed in phase X. It is only at this stage that Y can increase until the transition has reached

completion. Because the formation of nuclei can be very slow, the transition from one phase to another does not take place once thermodynamically favourable conditions have been met. In practice (crystallization) the question is always, "how fast will the nuclei of a new phase come into existence at a given super saturation" (Söhnel and Garside, 1992).

The definition of nucleation depends strongly on the mechanism which is responsible for nucleus formation. The different mechanisms of nucleation can be represented as follows (Söhnel and Garside, 1992):

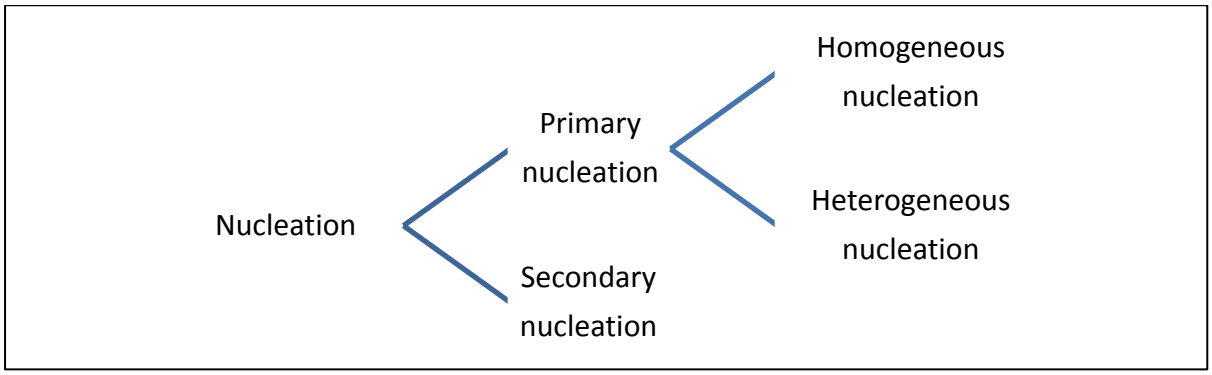

During primary nucleation, the "formation of the new solid phase is not influenced by presence of the solid phase being formed" (Söhnel and Garside, 1992). A distinction could be made between two types of primary nucleation: homogeneous nucleation and heterogeneous nucleation. During homogeneous nucleation, the formation of a new solid phase is not influenced by the presence of any solid phase. Essentially, pure homogenous precipitation is very difficult to achieve as there are always solid particles present even in pure water. During heterogeneous nucleation, the creation of a new solid phase is initiated by the presence of an alien phase. On the other hand, during secondary nucleation, the formation of a solid phase is promoted by the presence of the solid phase of the material being crystallized (Söhnel and Garside, 1992).

In practical terms the nucleation period (refer to **Figure 3**) is expressed as the induction period of crystallization, which is quantified, as the time elapsed between the formation of a super saturated state and the first physical changes observed in the precipitating system. These changes can be an increase in the turbidity (Kim *et al.*, 2009; Sarig *et al.*, 1975; Shih *et al.*, 2004; Shih *et al.*, 2006), a decrease in the measured solution concentration (Le Gouellec & Elimelech, 2002; Rahardianto *et al.*, 2010; Shih *et al.*, 2004) or conductivity (McCartney & Alexander, 1958; Weijnen *et al.*, 1983; Weijnen & van Rosmalen, 1985).

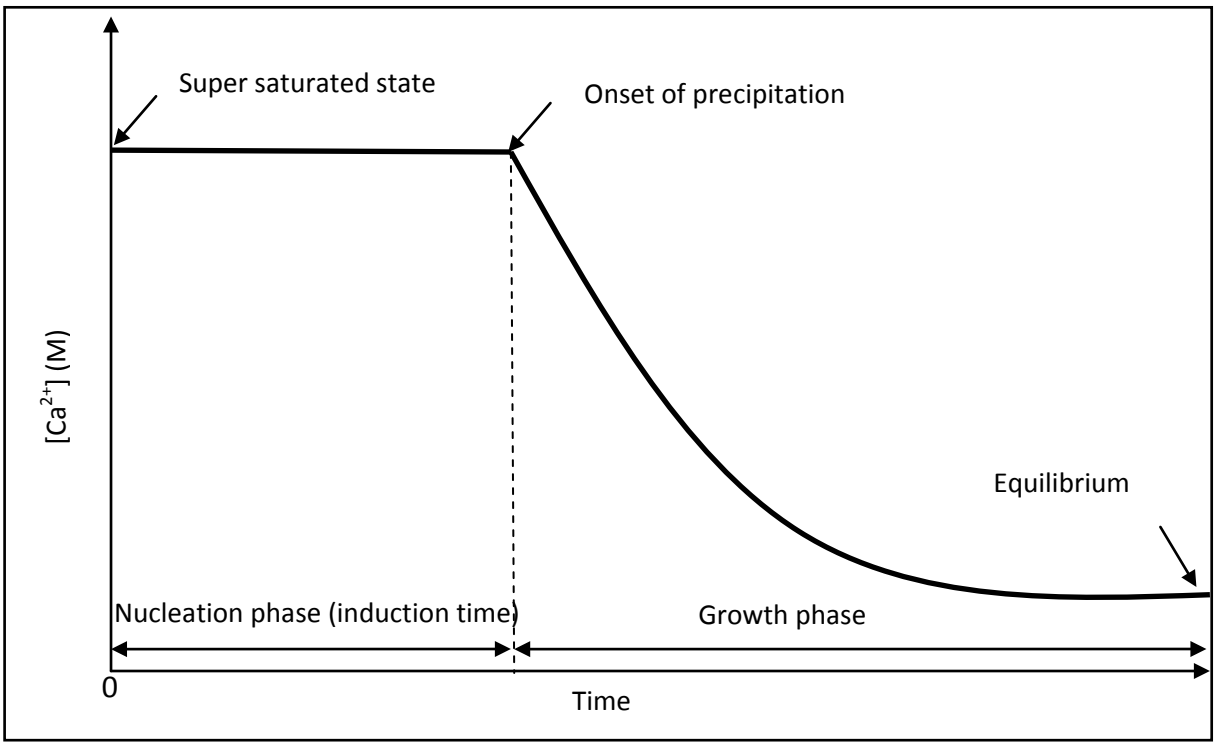

Figure 3: *Conceptual kinetic growth curve of gypsum precipitation*

When determined by an optically driven process (visual or turbidity change), the induction period (t_{ind}) is the sum of the time required for the critical nucleus to form (t_i) and the time that is necessary for the nucleus to grow to a visible size (t_g) (Söhnel and Mullin, 1988):

$$t_{ind} = t_i + t_g \tag{2.21}$$

The instance where the induction time is determined by a decrease in the concentration, t_g, represents the time taken for an ample amount of solute to deposit onto the nuclei, such that a change in the concentration is observed.

For both homogeneous and heterogeneous nucleation, the induction time with relation to changes in temperature, super saturation, inorganics and organics can be explained by the following equation, which has been derived from classical nucleation theory (Söhnel and Mullin, 1988):

$$\log(t_{ind}) = B + \frac{C}{T^3(\log\Omega)^2} \tag{2.22}$$

The relationship between temperature or super saturation and the induction period can easily be derived from equation 2.22. However the influence of factors such as inorganics and organics on the nucleation kinetics can be quantified by observing a change in σ, the interfacial tension, which is

related to the slope, *C*, of equation 2.22, by the following expression (Ben Ahmed, Tlili and Ben Amor, 2008):

$$C = \frac{\alpha N_A \sigma^3 V_m^2 f(\theta)}{(2.3RT)^3} \quad (2.23)$$

α is the geometric (shape) factor of a spherical nucleus and is equal to 16 π/3. *f*(Φ) is a correction factor; during pure homogeneous nucleation *f*(Φ) is equal to 1; when heterogeneous nucleation takes place *f*(Φ) is equal to 0.01. V_m is the molar volume for gypsum and equals 74.69 ($cm^3.mol^{-1}$); R is a gas constant (J/mol.K), N_A is Avogadro's number (mol^{-1}) and σ is the interfacial tension (J/m^2) (Ben Ahmed, Tlili and Ben Amor, 2008).

The nucleation rate, *J* (number of nuclei per unit time), is related to the temperature, level of super saturation and interfacial tension according to the following equation,

$$J = F \cdot \exp\left(\frac{-\alpha\sigma^3 V_m^2 N_A f(\theta)}{(2.3RT\log\Omega)^3}\right) \quad (2.24)$$

F (in equation 2.24) is called the frequency constant or the pre-exponential factor. For the critical nucleus to be formed, the free energy needed can be calculated as follows,

$$J = F \cdot \exp\left(\frac{-\Delta G_{crit}}{RT}\right) \quad (2.25)$$

The size of the critical nucleus can then be calculated from the following equation:

$$\Delta G_{crit} = \frac{4}{3}\pi r_{crit}^2 \sigma \quad (2.26)$$

2.6.2 Growth

The growth phase is defined as the period between the onset of precipitation (the induction time) and equilibrium (refer to **Figure 3**). The rate of crystal growth can be defined as the perpendicular displacement rate of any given crystal face (Söhnel and Garside, 1992).

It is generally accepted that gypsum precipitation can be expressed by a second order equation with respect to the calcium concentration (Liu and Nancollas, 1970) and has found application in numerous studies (Amjad, 1985; Amjad & Hooley, 1986; Amjad, 1988; Gill & Nancollas, 1979; Hoang *et al.*, 2007; Liu & Nancollas, 1970; Liu & Nancollas, 1973; Liu & Nancollas, 1975). Mathematically the expression is given as:

$$-\frac{\mathrm{dm}}{\mathrm{dt}} = \mathrm{k'S_n(m - m_{eq})^2} \tag{2.27}$$

See also section 11.8 for the use of equation 2.27.

m= $[Ca^{2+}]$ (Where $[Ca^{2+}] = [SO_4^{2-}]$) represents the concentration of free ions in solutions at a given moment in time and has units of [mol/l], m_{eq} is concentration of the ion at equilibrium at a particular ionic strength and temperature, S_n is a function of the number of growth sites available in solution (generally added as seed crystals) and k' is the growth rate constant, expressed in units: $M^{-1}.min^{-1}$. The effect of different process conditions on the growth kinetics is expressed in the growth rate constant.

2.7 Factors influencing gypsum precipitation kinetics

Each system subject to precipitation is unique and is affected by a number of variables such as process conditions, impurities (admixtures) in the system etc. According to literature, the following factors have shown to be among those, which have an important influence on the nucleation and growth kinetics of gypsum:

- Temperature
- Super saturation/ super saturation ratio
- Seeding
- Admixtures (foreign components which are ionic in nature)

The following section helps to quantify and simplify the relationship between gypsum kinetics and the factors listed above.

2.7.1 Temperature

2.7.1.1 Temperature-induction time relationship

"Homogeneous nucleation is essentially only influenced by the temperature and the presence of admixtures of an ionic nature" (Söhnel and Garside, 1992).

A temperature increase shortens the induction period of precipitation (Amjad, 1988; Amjad & Hooley, 1986; Liu & Nancollas, 1975). This temperature-induction time relationship takes on logarithmic form and is accurately explained by classical nucleation theory (equation 2.22). It has been shown that a 10°C change in temperature causes the induction period under a fixed set of conditions to be reduced by a factor of 2 approximately, independent of the system (refer to **Table 1**).

Pure system (no impurities or antiscalants) induction times for a range of operating conditions are shown in **Figure 4**.

Table 1: *Effect of temperature on the precipitation kinetics of gypsum (In the presence of some antiscalants)*

Antiscalant type	Temp (°C)	Seed (mg/l)	Antiscalant concentration	Induction period (minutes)	Growth rate ($M^{-1}.min^{-1}$)
TENTMP[a]	25	1930	1.89 x10^{-6} M	440	2.58
[Ca^{2+}] = 0.04M	35			210	5.90
	45			87	10.04
	55			45	19.8
P-AA[b]	25	2000	0.25 mg/l	240	
(MW: 6000)	35			86	
[Ca^{2+}] = 0.035 M	50			33	
pH=7					
PAA[c]	25	2000	0.2 mg/l	265	0.298
(MW:5100)	35			130	0.61
[Ca^{2+}]=0.0363M	45			12	1.06

[a](Liu and Nancollas, 1975)

[b](Amjad, 1988)

[c](Amjad and Hooley, 1986)

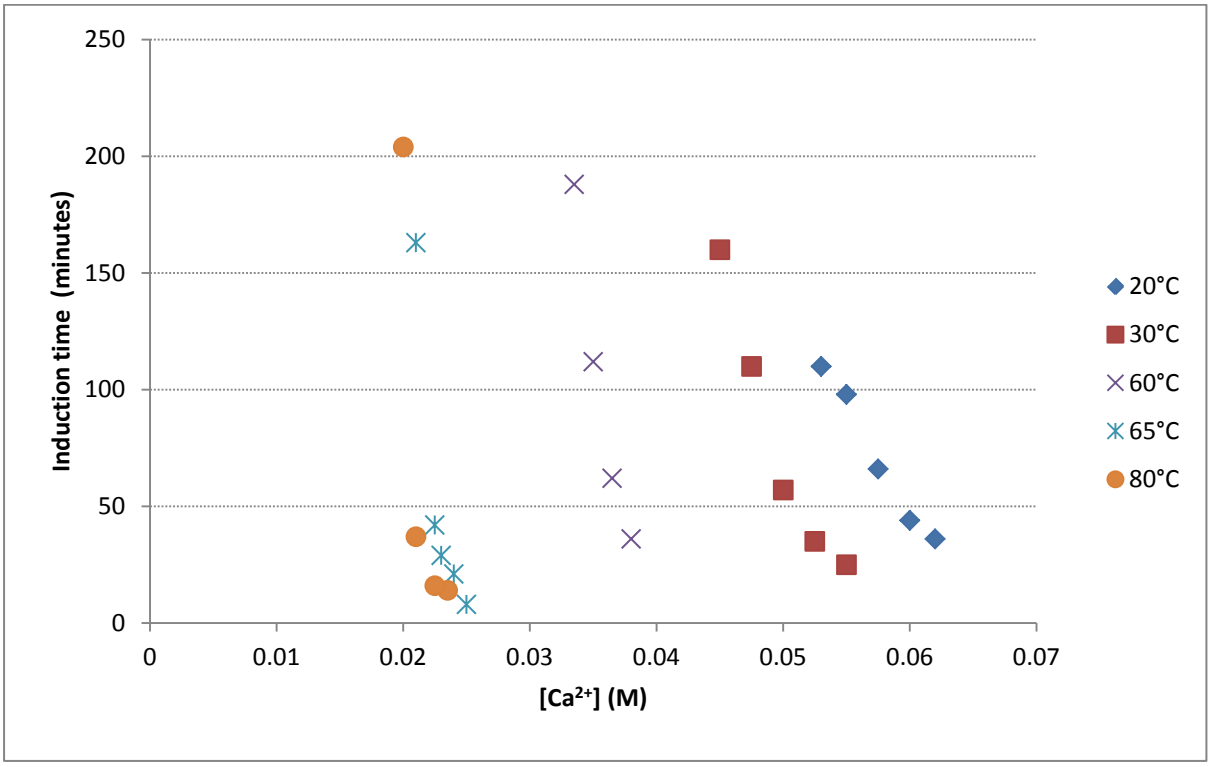

Figure 4: *Induction time-[Ca^{2+}] relationship at various temperatures.* (Klepetsanis and Koutsoukos, 1991) *and* (Klepetsanis *et al.*, 1999).

2.7.1.2 Temperature-growth rate relationship

The relationship between the kinetic growth rate constant (k') and the temperature can be explained by an Arrhenius type relationship, where the growth rate increases exponentially with temperature (Hoang *et al.*, 2007; Liu & Nancollas, 1973). Extensive research on account of precipitation of gypsum in the temperature range 15-50°C have found values for the growth rate constant (k') to be within the range 0-8 $M^{-1}.min^{-1}$ (Liu & Nancollas, 1970; Amjad & Hooley, 1986; Amjad, 1988). The Arrhenius representation of these values is illustrated in **Figure 5**. The discrepancy in the magnitude of the growth rate between various studies can be attributed to differences in solution chemistry, differences in seed morphology and concentration, etc.

Ben Ahmed *et al.* (2008) suggested that the nucleation kinetics is favored at temperatures below 50°C, and that temperature only holds important implications for the growth rate constant at temperatures above 50°C.

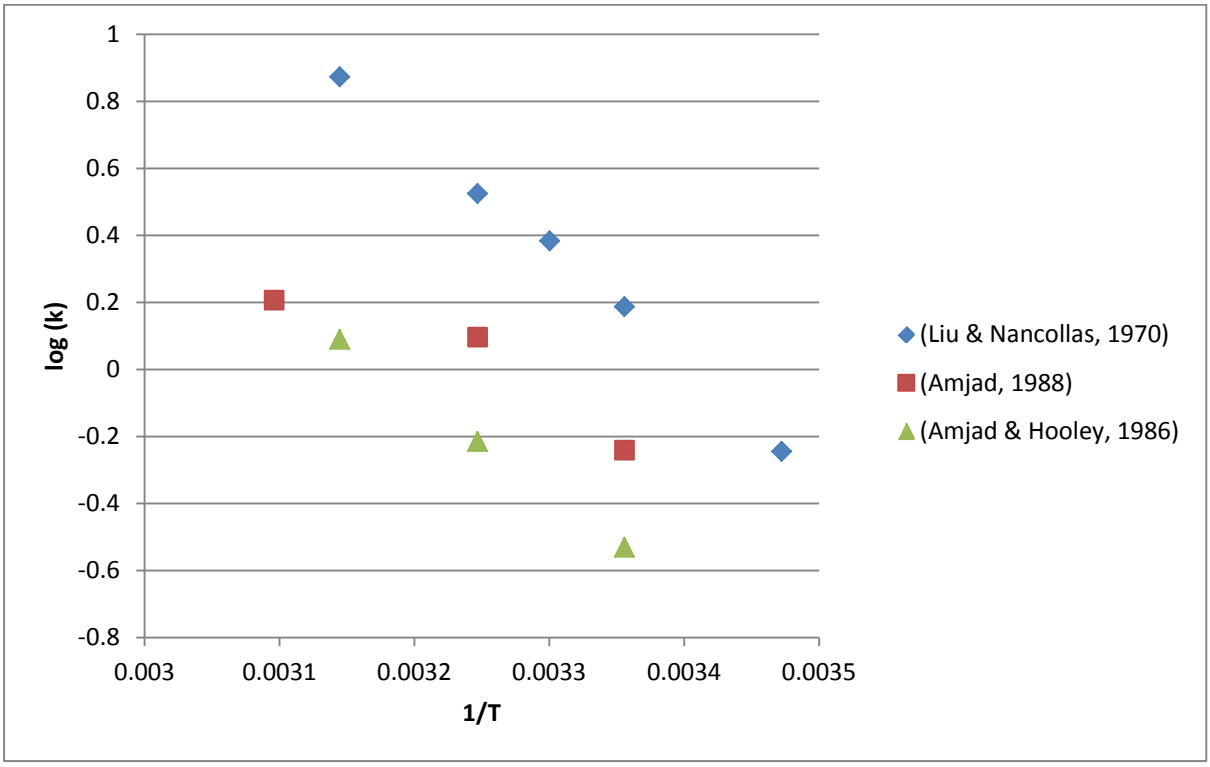

Figure 5: *Arrhenius plot of [log(k) versus 1/T] at different solution concentrations (temperature in units of Kelvin)*

2.7.2 Super saturation/ super saturation ratio

Super saturation is a key variable in any precipitation process and is indeed central to the definition of precipitation (Söhnel and Garside, 1992). This term is described as the degree at which a given system subject to precipitation is super saturated (or oversaturated) relative to the equilibrium concentration at a given temperature. Mathematically this term is expressed as:

$$\Omega = \frac{(\alpha_{Ca^{2+}})(\alpha_{SO_4^{2-}})}{K_{sp}} \tag{2.5}$$

The degree of super saturation affects growth and nucleation kinetics by determining the amount of precipitating molecules that arrive at the nuclei surface at any given time. Because Ω is directly proportional to α_{Ca}^{2+} and α_{Ca}^{2+} is directly proportional to $[Ca^{2+}]$, it is safe to say that Ω is directly proportional $[Ca^{2+}]$ and therefore also to $[Ca^{2+}][SO_4^{2-}]$, when $[SO_4^{2-}]$ is constant .

2.7.2.1 Super saturation-induction time relationship

According to classical nucleation theory (equation 2.22), the log of the induction time is inversely proportional to square of the log of the saturation level (Ben Ahmed *et al.*, 2008; Klepetsanis *et al.*, 1999). **Figure 6** clearly shows this relationship between the induction period and

the concentration of calcium at a fixed temperature of 25°C. At higher temperatures (**Figure 4**), this effect is magnified and lower induction times can be expected (Hamdona, Nessim and Hamza, 1993).

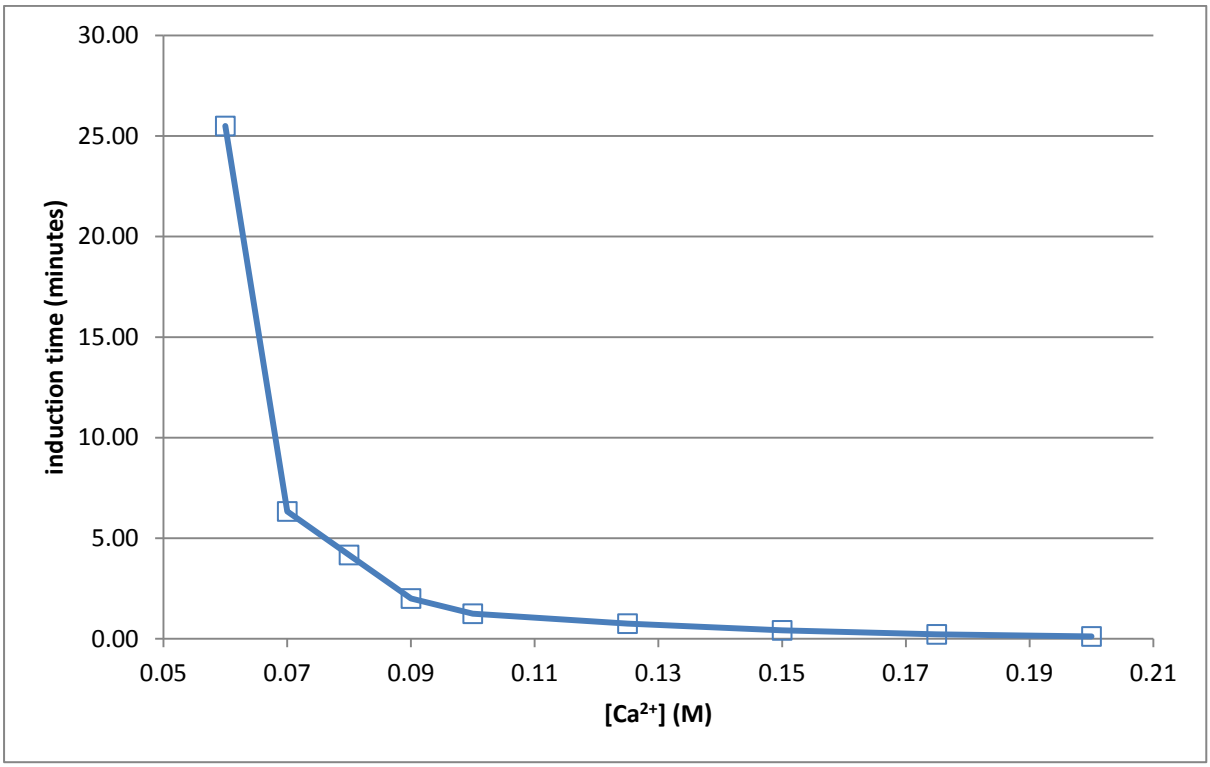

Figure 6: *Plot of induction time against total calcium concentration, T= 25°C. 0.5 M sodium chloride medium,* redrawn from Liu and Nancollas (1973).

2.7.2.2 Super saturation-growth rate relationship

The precipitation reaction of gypsum in water follows variable order kinetic rate expressions with respect to the saturation level.

Klepetsanis *et al.* (1999) proposed that a linear relationship exists between the growth rate and the relative super saturation ($[Ca^{2+}]$: 0.02-0.045 M; temperature: 25-80°C) which suggests a spiral growth mechanism. Scanning force microscopy, however failed to recognize the occurrence of spirals in the calcium sulphate dehydrate crystals. In addition, a linear model provided a poor fit to the data.

Hamdona *et al.* (1993) expressed this same relationship ($[Ca^{2+}]$: 0.04-0.056 M, temperature: 25°C) using the following mathematical expression:

$$R = {}^{dm}/_{dt} = k\sigma^{n} \qquad (2.28)$$

A plot of the log(R) vs. log(σ) yielded a linear relationship with n, the order of the reaction, being equal to 3.6. This suggests a poly-nuclear process. Using the same semi-empirical growth model, Klepetsanis & Koutsoukos (1991) found an apparent rate order where n=5. The same author however states that this equation should not be used too rigorously to draw any conclusions concerning the mechanism of crystal growth.

Liu & Nancollas (1973) studied the effect of super saturation on the linear growth rate of gypsum. It was proposed that a second order relationship could satisfactorily explain the relationship between the saturation level and the crystal growth rate at lower saturation levels ([Ca^{2+}]: 0.028-0.0424 M, temperature: 25°C). The deviation from this second order relationship is explained in terms of two-dimensional surface nucleation.

To conclude: from literature it is hard to elucidate the exact mathematical relationship between the saturation level and the growth rate. The discrepancies between data from different authors could possibly be explained by the difference in experimental procedures, reagents etc.

2.7.3 Seeding

The rate of precipitation at low super saturation levels is generally low and can be induced by seeding the solution (Lewis & Nathoo, 2006). The effect of seed on precipitation kinetics is largely dependent on the type, morphology and concentration of the seed. The effect of seed on the kinetics is also affected by the chemistry of the precipitating system.

2.7.3.1 Seed type

A distinction is made between two modes of seeded growth:

1. Heterogeneous seeded growth(HESG)
2. Homogeneous seeded growth (HOSG)

HESG takes place when the seed has a different chemical structure than the nucleating phase. When there is a close resemblance between the chemical structure of the seed and the nucleating phase it is referred to as, epitaxial growth (Gill and Nancollas, 1979).

On the other hand, HOSG takes place when the seed and the nucleating phase have similar chemical structures.

Upon the addition of seed to an oversaturated solution during HESG, the stimulation of crystal growth is subject to additional heterogeneous nucleation in the solution (Söhnel and Garside, 1992)

and on the crystal surface (Liu and Nancollas, 1970), the extent of which depends on the seed concentration.

Gill & Nancollas (1979) showed that barite and calcite seed crystals can de-super saturate a solution where gypsum is the precipitation phase (also refer to **Table 2**). In the case of both barite and calcite, an induction time prior to the growth phase was observed. Interestingly enough the growth rate following the induction period was higher in the presence of both barite and calcite compared to gypsum. It is suggested, that an increase in the growth rate is related to the addition of growth sites formed during the nucleation phase. This surface nucleation was also observed from scanning electron micrographs.

In addition, Yang *et al.* (2008a) and Yang *et al.* (2008b) studied the use of a range of different inorganic, seed crystals including gypsum, kaolin ($Al_2O_3.2SiO_2.2H_2O$), Al_2O_3, dolomite, MgO and diatomite (80 % SiO_2, 15 % Al_2O_3) and calcite to test their effectiveness as precipitation-stimulating media in a system super saturated with gypsum. In all cases, gypsum caused immediate precipitation of the meta-stable super saturated solution, whereas the effect of other inorganic particles was subject to the specifics of the system and the specific inorganic particle. In most cases, precipitation took place almost immediately as result of the large quantity of added seed (10-20 g/l). There seems however to be a short nucleation phase prior to precipitation. The rate of precipitation was also found to be lower in the presence of foreign particles compared to when gypsum was used. This observation seems to be contradictory to the observation made by Gill & Nancollas (1979), however when compared, the seed concentration in studies conducted by Yang *et al.* (2008a) and Yang *et al.* (2008b) were high enough to partially overcome the nucleation phase and almost immediately stimulate growth. An abundance of growth sites, which causes an increase in the growth rate, are not formed as the induction periods are relatively short in the presence of growth on foreign particles.

HESG is attractive because it causes the rate of precipitation to increase relative to HOSG; however large induction times can lead to long unwanted retention times during large scale applications.

Table 2: *Effect of seed type on nucleation and growth kinetics of calcium sulphate dehydrate* (Gill and Nancollas, 1979)

Seed type	Seed (mg/l)	Induction time (minutes)	k' ($M^{-1}.min^{-1}$)
gypsum	400	0	0.2612
calcite	400	90	0.9288
barite	400	75	1.2044
barite	107	55	1.866
barite	200	75	0.5524
barite	850	50	1.94

2.7.3.2 Seed quantity

The induction period preceding the precipitation process as well as the crystal growth rate is dependent on the amount of available 'identifiable' growth sites in solution relative to the level of saturation. By the term 'identifiable' it means that the growth sites are of the same type as the precipitating phase.

When the number of growth sites, relative to the saturation level during HOSG is insufficient (too little seed or a very large saturation level), or when growth sites are obstructed by adsorbed impurities, an induction period will be observed. Amjad (1985) showed that when the seed concentration for a fixed solution concentration ($[Ca^{2+}]$=0.0479 M) was reduced from 1990 to 790 mg/l, the induction period increased from 0 to 80 minutes as there was not enough growth sites available to effect precipitation. Interestingly enough, the growth rate increased from 0.866 $M^{-1}.min^{-1}$ to 1.51 $M^{-1}.min^{-1}$, which points to an increase in the number of growth sites during the nucleation period. Similar observations were made by Amjad & Hooley (1986) and Liu & Nancollas (1970), (refer to **Table 3**).

Concerning the seed-growth rate relationship (Amjad, 1985; Amjad & Hooley, 1986; Liu & Nancollas, 1970) found that the growth rate is proportional to the quantity of seed added initially. The growth rate increases as the seed quantity increases; refer to **Table 3** for data. The effect of the seed on the kinetics concentration is dependent on the system in its complexity and no simple, mathematical formula can accurately explain its effect.

Table 3: *Kinetic data: the relationship between seed (gypsum) quantity and gypsum kinetics at different conditions*

Seed (mg/l)	$[Ca^{2+}]$ (M)	Temp (°C)	Induction time (minutes)	k' ($M^{-1}.min^{-1}$)	Source
247	0.0363	35	50	0.55	(Amjad and Hooley, 1986)
1213			0	0.58	
1327			0	0.61	
2487			0	1.2	
440	0.035	25	67	2.57	(Amjad, 1988)
880			0	1.37	
1890	0.0464	25	0	2.97	(Liu and Nancollas, 1970)
1333	0.0442	25	0	0.565	(Liu and Nancollas, 1970)
2133			0	0.955	

2.7.3.3 Seed morphology

Finally the morphology of gypsum crystals plays an important role in how seed addition affects precipitation kinetics. Consider HOSG:

Generally, two types of morphologically distinct gypsum crystals exist: plates and needles (Seewoo *et al.*, 2004). Different morphological forms are distinguished from one another by their size, shape, and surface area. Needle-shaped crystals are thin and elongated with lengths in the range 80-120 µm (Liu and Nancollas, 1970) and are generally synthesized from solutions with a lower level of super saturation (<0.3 M). Plate-like crystals are shorter, thicker, more robust crystals with a greater specific surface area than needle-shaped crystals and are synthesized from highly concentrated solutions (>0.75 M) in the range of 25-50 µm (Liu & Nancollas, 1970; Seewoo *et al.*, 2004).

Liu & Nancollas (1970), Liu& Nancollas (1973) and Lewis & Nathoo (2006) found that the addition of plate-like crystals to a super saturated solution causes higher growth rates than when needle-like crystals were added (Refer to **Table 4**). This was also observed by Seewoo *et al.* (2004) who showed that plate-like crystals resulted in more rapid de-super saturation of a given solution than needle-like crystals. They also proposed that the increased growth kinetics is as a result of an increase in specific surface area, which is higher in the case of plate-like crystals. The effect of a difference in morphology seemed to be significant up to 4 % seed by volume, above which the effect of morphology became insignificant (Seewoo *et al.*, 2004).

Table 4: *Effect of gypsum seed morphology on gypsum growth kinetics*

Morphology	Seed (mg/l)	$[Ca^{2+}]$ (M)	k' ($M^{-1}.min^{-1}$)	Source
Plates	310	0.0273	0.58	(Liu and Nancollas, 1970)
Plates	390	0.0310	0.58	(Liu and Nancollas, 1970)
Plates	880	0.0458	1.37	(Liu and Nancollas, 1973)
Plates	880	0.0464	1.37	(Liu and Nancollas, 1970)
Plates	980	0.0468	1.52	(Liu and Nancollas, 1970)
Plates	1890	0.0442	2.97	(Liu and Nancollas, 1973)
Plates	1890	0.0442	2.97	(Liu and Nancollas, 1970)
Needles	2520	0.0390	1.43	(Liu and Nancollas, 1970)
Needles	2780	0.0438	1.55	(Liu and Nancollas, 1970)
Needles	2780	0.0438	1.66	(Liu and Nancollas, 1970)
Needles	3030	0.0460	1.80	(Liu and Nancollas, 1973)
Needles	2870	0.0330	1.97	(Liu and Nancollas, 1970)

2.7.4 Admixtures

Dissolved admixtures influence heterogeneous nucleation, where they are adsorbed on the surface of the precipitating solid phase, or on the hetero-nuclei already present in the solution. In addition these admixtures influence nucleation where they form complexes with the nucleating matter (Söhnel and Garside, 1992).

In general, the extent to which an admixture will influence nucleation is determined by the concentration of the admixture, and increases with increasing concentration. Both the admixture and the nucleating substance compete to adsorb onto the surface of the nucleus. When the amount of nucleating molecules that arrive at the crystal surface is high, the admixtures are prevented from adsorbing at the active sites on the crystal surface. Conversely, when the amount of admixture arriving at the crystal surface is rather high, the super saturation should be increased to increase the number of solute molecules arriving at the crystal surface (Söhnel and Garside, 1992).

2.7.4.1 Cationic admixtures

Hamdona *et al.* (1993) and Hamdona & Al Hadad (2007) showed that small concentrations of cations in solution can reduce the crystallization rate of gypsum up to 70% and that the effect increases upon increase of the cation concentration (refer to Table 5). Conversely, Rashad *et al.*, (2004) showed that aluminium (Al^{3+}) at a concentration of 0-2 % could result in an increase in gypsum precipitation kinetics. Hamdona *et al.* (1993) and Hamdona & Al Hadad (2007) proposed that the inhibiting effect of cations on the precipitation rate of gypsum is as a result of cations that adsorb onto crystal surface, which causes a restriction of crystal growth. Adsorption effects were described

by means of a Langmuir adsorption isotherm. Moreover, it was shown that the inhibiting effect of cations is considerably weaker at higher levels of super saturation.

Table 5: *Effect of cations on nucleation and growth kinetics of gypsum*

Additive	Concentration	Effect on kinetics		Source
		Growth Rate	Nucleation	
Mg^{2+} (MgO)[a]	0-3 %	(-)	(-)	(Rashad *et al.*, 2004)
Mg^{2+}[d]	1-12x10^{-6} (M)	(-) 8-38 % inhibition	N/A	(Hamdona and Al Hadad, 2007)
Mg^{2+}[b]	5-50 x10^{-5} (M)	(-) 17-65 % inhibition	N/A	(Hamdona *et al.*, 1993)
Mg^{2+}[c]	5-50 x10^{-5} (M)	(-) 20-71 % inhibition	N/A	(Hamdona *et al.*, 1993)
Al^{3+} (Al_2O_3)[a]	0-2 % 3 %	**(+)** (-)	**(+)** (-)	(Rashad *et al.*, 2004)
Cr^{3+}[d]	1-12x10^{-6} (M)	(-) 16-51 % inhibition	N/A	(Hamdona and Al Hadad, 2007)
Fe^{3+}[d]	1-12 x10^{-6} (M)	(-) 27-64 % inhibition	N/A	(Hamdona and Al Hadad, 2007)
Fe^{3+}[b]	20-50 x10^{-5} (M)	(-) 8-18 % inhibition	N/A	(Hamdona *et al.*, 1993)
Fe^{3+}[c]	20-50 x10^{-5} (M)	(-) 10-25 % inhibition	N/A	(Hamdona *et al.*, 1993)
Cu^{2+}[d]	1-12 x10^{-6} (M)	(-) 34-70 % inhibition	N/A	(Hamdona and Al Hadad, 2007)
Cd^{2+}[d]	1-12 x10^{-6} (M)	(-) 34-70 % inhibition	N/A	(Hamdona and Al Hadad, 2007)
Cd^{2+}[b]	5-50 x10^{-5} (M)	(-) 12-55 % inhibition	N/A	(Hamdona *et al.*, 1993)
Cd^{2+}[c]	5-50 x10^{-5} (M)	(-) 14-61 % inhibition	N/A	(Hamdona *et al.*, 1993)

Table 5 *Continues*

$Pb^{2+[b]}$	5-50 $x10^{-5}$ (M)	(-) 7-31 % inhibition	N/A	(Hamdona *et al.*, 1993)
$Pb^{2+[c]}$	5-50 $x10^{-5}$ (M)	(-) 10-37 % inhibition	N/A	(Hamdona, Nessim and Hamza, 1993)

[a]Conditions simulate phosphonic acid production (Temperature = 80°C), SR (Calcium) =1.088

[b] σ=4.1

[c] σ=3.7 ($\sigma=(IP)^{½}-K_{Sp}^{½}$)

[d]σ=1.32

2.7.5 Anionic admixture

In this instance, the only anionic admixtures that will be considered are antiscalants; c.f. section 2.8 for a detailed discussion.

2.8 Antiscalants suitable for gypsum inhibition

2.8.1 Overview

Numerous studies have been conducted since the late 1950's on the evaluation of different compounds, as suitable candidates for gypsum growth inhibition. Studies have pointed out that some proteinaceous material, organic acids, polyelectrolytes and phosphonates are amongst the most suitable molecules used for inhibition of gypsum precipitation**.** This section provides an overview of some of the most significant work that has been done in this regard and aims to dissect the different components that make a molecule suitable as an antiscalant.

2.8.1.1 Proteinaceous material

McCartney & Alexander (1958) showed that additives most likely to exhibit a retarding effect on gypsum precipitation are those containing polar groups on their chain structure such as proteinaceous and polycarboxylic material. They found that keratin and gelatine can cause significant reduction of gypsum growth. Similarly, observations with respect to gelatine were made by Liu & Nancollas (1973) and Liu & Nancollas (1975), who showed that gelatine caused growth rate reduction at concentrations 0-120 mg/l. Even at low concentrations (13 mg/l) it caused a significant growth rate reduction (2.5 to 0.75 $M^{-1}.min^{-1}$). Yet at high concentrations (100 mg/l), gelatine never caused a complete interruption of growth. It is suggested that gelatine adsorption takes place at specific growth sites and that adsorption at the crystal surface is not strong. Liu & Nancollas (1973) showed the interaction between gelatine and gypsum by means of a Langmuir adsorption isotherm.

2.8.1.2 Organic acids

McCartney & Alexander (1958) reported that organic acids such as aconitic, maleic, citric, fumaric, glycolic, and succinic acid could enhance the apparent solubility of gypsum. In addition, McCartney & Alexander (1958) made similar conclusions regarding malonic, succinic and citric acid. Sarig *et al.* (1975) showed that polyglutamic acid (PGA) is a suitable growth inhibitor for gypsum. Its suitability as a growth inhibitor is correlated to its molecular structure, in which case there is a close resemblance between the inhibitor (PGA) and the crystal (gypsum) lattice - 8 Angstrom and 8.1 Angstrom respectively. The addition of alanine to the PGA structure to form a copolymer of PGA, resulted in weaker retardation of gypsum precipitation compared to when pure PGA was used.

2.8.1.3 Polyelectrolytes

McCartney & Alexander (1958) showed that carboxymethyl cellulose (CMC) and polyacrylic acid (PAA) at considerably low concentrations (0.13-1.3 mg/l) caused complete inhibition of gypsum growth for an undefined period of time. Since, numerous studies (Amjad,1985; Amjad, 1988; Oner *et al.*, 1998; Weijnen & van Rosmalen, 1985) have confirmed PAA and its copolymers as suitable candidates for gypsum growth inhibition. However, its considerable capacity to inhibit growth (high induction times) at very low concentrations, have limited the evaluation of PAA in kinetic studies to very low concentrations (≈2 mg/l). In all cases, it was found that PAA causes a complete inhibition of growth for a defined period of time (several minutes-24 hours) after which growth takes place at a rate comparable to that of a pure solution.

The effectiveness of a PAA is not only limited by the concentration, (increasing with increasing concentration) but has been found to be strongly affected by the molecular weight and its molecular structure, which can vary according to substituent ions.

McCartney & Alexander (1958) discovered that the retarding power of polyelectrolytes increased with increasing molecular weight. A similar observation was made by Oner *et al.* (1998) for high molecular weight block copolymers of PAA at MW: 2000-18000. Contrary to these findings, Amjad (1985) showed that PAA is more effective at low molecular weights and that its efficiency increased with decreasing molecular weight in the range 3500-50000. This observation was confirmed by a number of additional studies: Amjad & Hooley (1986) considered molecular weights: MW 2100-50000; Amjad (1988) considered MW: 900-250000; and Amjad (1988), MW: 2600-50000. Amjad (1988) found that inhibition reached an optimum at a MW of 2100, below which the inhibition decreased. It is suggested that at MW lower than 2000, weaker inhibition is caused as a result of a decrease in bonding possibilities. Furthermore, Oner *et al.* (1998) studied polyacrylic acids, MW: 1200-240 000 as well polymethacrylic acids (PMA), MW: 8000-34000 and found that at lower molecular weights, the inhibitory efficiency was the highest- no optimum was observed. Polymethacrylic acids were also found to be less efficient that polyacrylic acids.

The molecular structure of the antiscalant is very important regarding its inhibitory capacity. Oner *et al.* (1998) showed that the addition of a methyl group to PAA, resulting in a methacrylic acid (PMAA) caused a reduction the inhibitory capacity of the molecule. Similar observations have been made by McCartney & Alexander (1958) and Weijnen & van Rosmalen (1985). It has been suggested, that the lower inhibition of PMAA is caused by an increase in hydrophobicity as well as a decrease in anionic charge density caused by the addition of the methyl group.

Weijnen & van Rosmalen (1985) studied the effect of different substituent ions on the efficiency of polymaleic acid (PMA) and polyacrylic acid (PAA)-based molecules and compared it to pure PMA and PAA. Partial substitution of carboxylic acid groups by sulphonic or phenyl sulphonic groups caused a reduction in efficiency of PAA. Moreover, the phenyl group was least effective as a result of its hydrophobic character and resulted in a decrease in the anionic charge density of the molecule. When substituted with a methyl group, the efficiency of the inhibitor reduced compared to the pure PAA. This is attributed to the increased hydrophobicity and lower anionic charge density of the molecule. The addition of an amide group showed to increase the effectiveness of PAA; even though the carboxylic acid groups are reduced, the amide group actively bonds with the crystal surface to compensate for this disadvantage. It is suggested that the amino part of the amide is active in hydrogen bridge formation between the water molecules and the crystal anions. PAA was found to be more effective than PMA at lower retention times. This was also confirmed by Amjad & Hooley (1986). However, at increased crystal growth PMA efficiency surpassed that of PAA. The effectiveness of PMA compounds could be related to their hydrophylicity. The one with fewer hydrophobic groups was found to be more effective.

Oner *et al.* (1998) showed that the inhibitory capacity of structured molecules is more effective than randomly structured molecules by comparing the efficiency of random and block copolymers of buthylmethacrylate-methacrylic acid. Block copolymers were considerably more effective than random copolymers. Moreover it was established that the acid content of polymers is an important factor and an increase in the acid content causes the inhibitory capacity to increase.

Other factors that influence polyelectrolytes are related to changes in process conditions and are discussed in section 2.9.

2.8.1.4 Phosphonates

Phosphates and phosphonate based molecules have also shown to exhibit variable behaviour with regard to their ability to inhibit gypsum precipitation.

Liu & Nancollas (1973) showed that TENTMP and ENTMP cause total inhibition of gypsum growth for a period of 8 hours (maximum time of experimental run) at concentrations as low as $1x10^{-6}$ M. At lower concentrations, a clear induction time was observed, which increased upon increase in antiscalant concentration. A similar observation was made by Liu & Nancollas (1975), who studied TENTMP and ENTMP at concentrations of 0.63-$2.52x10^{-6}$ M and 0.63-$1.89x10^{-6}$ M respectively. For TENTMP, it was shown that complete inhibition of growth takes place for a defined period after which growth commences at a rate comparable to the pure solution. For ENTMP, the growth rate

following the induction period was considerably lower than for a pure solution. ENTMP was also found to be a stronger antiscalant than TENTMP at the same concentration. The mechanism that governs inhibition by phosphates and phosphonates is discussed in section 2.8.2.

Liu & Nancollas (1973) showed that HEDP, an organophosphate, at a concentration of $10x10^{-6}$ M had no effect on inhibiting gypsum growth. Amjad (1985), Amjad (1988) and Amjad & Hooley (1986) showed that HEDP had a negligible effect on the induction period and growth rate. In addition Weijnen *et al.* (1983) showed that HEDP could not inhibit gypsum precipitation at concentrations below 10^{-7} M, but that complete inhibition was accomplished at concentrations above $2x10^{-5}$ M. This confirms that the power of inhibitors is extremely dependent on their concentration.

In addition, Liu & Nancollas (1973) showed that NTMP resulted in a marked inhibition of gypsum at very low concentrations ($1x10^{-4}$-$1x10^{-5}$ M). Strangely, the growth rate increased upon increase in antiscalant concentration; still being lower than the growth rate from a pure solution. It was suggested that the adsorption of impurities on the crystal surface caused the formation of active growth centres, which stimulated further growth.

Moreover, Amjad (1985), Amjad (1988), Amjad & Hooley (1986) and Logan and Kimura (1985) showed that sodium hexametaphosphate (SHMP) caused temporary inhibition of gypsum crystal growth after which growth recommenced at a measurable rate. Amjad (1985) pointed out that an increase in the concentration of SHMP (0.25-0.5 mg/l) only results in an increase in the induction period and that under these conditions the rate of crystal growth was almost independent of the concentration of SHMP.

It was also shown by Amjad (1988), that SHMP was more effective than SPP. Amjad (1985) further pointed out that SPP and STPP had a negligible effect on crystal growth rate, which was confirmed by Amjad & Hooley (1986).

To summarise, molecules that are effective in inhibiting the nucleation and growth of gypsum are those that cause retardation or complete inhibition of nucleation and growth kinetics of the precipitating phase at low inhibitor concentrations (0 – 10 mg/l). These include polyelectrolytes and phosphonate molecules. The molecular structure of the inhibitor molecule is important: those with polar groups, with lattice structures matching that of the precipitating ion and with the low number of hydrophobic side chains or other constituent ions is most effective. Molecules with well defined molecular structures are also more effective growth inhibitors than randomly structured molecules. Increasing the concentration of the inhibitor molecule increases its inhibitory capacity. In addition, the molecular weight plays a significant role with regard to the efficiency of polyelectrolyte inhibitor

molecules. At lower molecular weights (approximately 2000 g/mol) polyelectrolytes are more effective than at higher molecular weights.

2.8.2 Adsorption Mechanism

The inhibitory action of effective antiscalants could be explained by an adsorption mechanism, where inhibitor molecules would adsorb onto the crystal surface or nuclei, and restrict crystal growth. Amjad (1985) proposed that only the most active sites (kinks and terraces) on the crystal surface are poisoned by these growth inhibitors through preferential adsorption. Meanwhile sites of lower energy *e.g.* steps, continue to slowly grow, forming bunched-up macro steps (Weijnen and van Rosmalen, 1985) until adsorbed molecules are completely enveloped and incorporated into the crystal lattice, at which point growth would commence at a rate comparable to that of a crystal grown from a pure solution.

This section aims explain the interaction between growth inhibitors and crystal surfaces, and explains their preferential adsorption. The aim is to provide credibility to the adsorption theory by investigating the influence of antiscalants on:

- gypsum precipitation kinetics and,
- crystal habit (morphology)

Since phosphonates and polyelectrolytes are among the most effective antiscalants used for gypsum inhibition (which is the main precipitant in the current study), the discussion in the following sections is confined to these two antiscalant types.

2.8.2.1 The influence of antiscalants on gypsum precipitation kinetics

This section explains how the adsorption mechanism could be related to the way in which antiscalants affect the nucleation and growth kinetics.

2.8.2.1.1 Nucleation kinetics

2.8.2.1.1.1 Induction time

A common misconception is that chelation or complexation is the mechanism responsible for the retarding action of growth inhibitors.

The difference between the chelating agent EDTA and threshold inhibitors was explicitly shown by Liu & Nancollas (1973) by referring to their influence on gypsum nucleation kinetics. The chelating agents had zero influence on crystal nucleation kinetics, whereas the threshold inhibitors (with the

addition of only a small quantity of growth inhibitor: 1-10 mg/l) caused a significant increase in the induction period of a super saturated solution.

McCartney & Alexander (1958) showed that EDTA do not affect the crystal habit of calcium sulphate (which is known to happen when adsorption takes place) and only caused the growth rate to reduce to the extent that it removed a stoichiometric proportion of the calcium.

Moreover, Hamdona & Al Hadad (2008) showed that complex formation is not responsible for growth retardation of calcium sulphate dehydrate in the presence of amino acids (suitable antiscalants), as complex formation should account for less that 1 % of the initial calcium at the highest concentrations of acid investigated.

We can further relate the effect of threshold inhibitors by observing the change in the interfacial tension (c.f. section 2.6). He *et al.* (1994) found that the presence of phosphonates and polycarboxylates lead to an increase in the interfacial tension. Similarly, Ben Ahmed *et al.* (2008) found that the surface tension increases in the presence of RPI (polyacrylic acid) compared to a solution without any growth inhibitor. In addition, the surface tension increased with increasing concentration of RPI.

2.8.2.1.1.2 Nucleation temperature

Nucleation temperature simply refers to the temperature at which rapid nucleation from a super saturated solution is induced (Guo and Severtson, 2004).

Guo & Severtson (2004) related the effect of threshold growth inhibitors polyacrylic acid (PAA) and polymaleic acid (PMA) to the nucleation kinetics of a precipitant by measuring the nucleation temperature of the precipitant at different antiscalant concentrations. The extent to which very small amounts of antiscalants were able to increase the nucleation temperature, indicated that these molecules are able to inhibit growth in excess of what would be expected from solution phase binding of calcium as a result of mere complexation with ions in the crystal surface. This was confirmed by comparing the nucleation temperatures of EDTA with PAA and PMA. It was proposed by Guo & Severtson (2004) that direct interactions between the inhibitor species and the developing nuclei causd this extensive increase in nucleation temperature.

Moreover, measurement of nucleation temperatures over a wide range of concentrations, for a given inhibitor, show that a maximum inhibitor concentration exist at a given level of super saturation above which either a slight or no increase in inhibitor function is seen.

2.8.2.1.2 Growth kinetics

In the majority of kinetic studies on gypsum precipitation, it has been established that antiscalants do not cause a change in the growth rate following the induction period. (Amjad,1985; Amjad, 1988; Oner *et al.*, 1998; Weijnen & van Rosmalen, 1985)

Amjad (1985) explains the independence of the crystal growth rate from the type and concentration of antiscalant by means of an adsorption mechanism, where the inhibitor molecules adsorb onto the faces of the crystals and are subsequently incorporated into the crystal structure of the forming crystals. This concept will be explained in more detail in section 2.8.2.2.4

2.8.2.2 The influence of antiscalants on crystal habit (morphology)

Before explaining the habit (morphology), or 'crystal structure'-altering nature of antiscalants, some concepts regarding the interaction of antiscalants with the crystal surface are explained.

2.8.2.2.1 Inhibitor/crystal interaction

Weijnen & van Rosmalen (1985) proposed that the interaction between the inhibitor and the crystal surface relies on both electrostatic interaction and chemical bonding between the molecule and the crystal surface. In addition Liu& Nancollas (1973) suggested that both complexing and adsorptive actions are operative during inhibitor/crystal interaction.

Electrostatic interaction between the crystal and inhibitor is said to be mainly responsible for the rate at which bonding at the crystal surface takes place, whereas the type and therefore the strength of the chemical bonds formed with the surface will determine the final attachment of the inhibitor ions at the surface.

Regarding the chemical bonding between an inhibitor and the crystal surface, the anionic functional groups of the inhibitors are said to be primarily responsible for the predominant interaction with the crystal surface by coordination of the crystal cations in the surface.

In the next section phosphonates and polyelectrolytes are explained separately:

2.8.2.2.1.1 Phosphonates

The effectiveness of a given inhibitor concentration drastically increases with raising the pH (Weijnen *et al.*, 1983). It is assumed that the effectiveness of phosphonate molecules, as growth inhibitors, are related to the fully dissociated phosphonic groups (c.f. section 2.9.2) (Weijnen and van Rosmalen, 1985).

On the other hand, Weijnen & van Rosmalen (1985) pointed out that an effective inhibitor needs to contain at least one acid group with an un-dissociated hydroxyl group per inhibitor ion. This apparent contradiction could be explained as follows: fully dissociated groups are responsible for ensuring strong electrostatic interaction with the crystal surface, whereas singly protonated groups are probably responsible for the actual binding with the crystal surface.

Where additional functional groups (groups that are unable to coordinate with the surface cations) are connected to the inhibitor molecule, they form hydrogen bridges with surface anions and in some cases with the crystal water molecules. This has proven to enhance phosphonate effectiveness at pH values ≤5 (Weijnen and van Rosmalen, 1985).

2.8.2.2.1.2 Polyelectrolytes

The molecular weight of these molecules is higher than most commercial phosphonate inhibitors Weijnen and van Rosmalen, 1985). It therefore seems that a higher concentration of carboxylic acid groups in the polyelectrolyte molecule is required for effective growth retardation.

For polyelectrolytes, de-protonation is necessary for the inhibitor to be effective, because the primary interaction between the inhibitor and the surface is as a result of electrostatic interaction (Weijnen and van Rosmalen, 1985).

Similar to phosphonate inhibitors, raising the pH increases the affinity between the crystal surface and the inhibitor, which could be attributed to an increase in anionic charge density. In this case, the adsorption capacity is limited by the build-up of charge near the surface due to the fact that not all carboxylic acid groups belonging to the adsorbed segment are involved in complex formation with the crystal surface (Oner *et al.*, 1998).

A clear analogy could therefore be drawn between the mechanism of phosphonates and polyelectrolytes. Ionized carboxylic acid groups, (similar to fully dissociated phosphonic acid groups in phosphonates) are responsible for electrostatic interactions of polyelectrolytes with the crystal surface. In a similar fashion, singly protonated groups in both cases establish the actual bond with cations in the surface (Weijnen and van Rosmalen, 1985).

2.8.2.2.2 Adsorption location

In the spiral growth and in the poly-nuclear growth mechanism prevailing at respectively lower and higher super saturation levels, three possible adsorption sites can be recognised (Nielsen, 1984; Weijnen and van Rosmalen, 1985; Weijnen *et al.,* 1986):

1) terraces on the crystal surfaces between the steps,
2) along the steps and,
3) at the kink sites in the steps.

Note: Crystal growth propagates step wise. During crystal growth, thermal roughening causes steps to have irregularities, producing kinks in the surface which is a crook or bend or similar deformity. Terraces are found between steps (Weijnen *et al.,* 1986).

Depending on the mechanism of the growth inhibitor, one or more of these sites will offer a preferential site for adsorption.

2.8.2.2.2.1 Phosphonates

These molecules are small and produce effective growth retardation at very low concentrations. Weijnen *et al.* (1983) showed that crystal surface coverage of as little as 5 % is needed for complete growth inhibition. Adsorption on the flat parts of the surface (steps) is rather unlikely since in that case, large surface coverage would be needed for growth inhibition. It can be assumed that phosphonate molecules would preferentially adsorb at only the most active sites *e.g.* kinks and terraces (Weijnen and van Rosmalen, 1985).

2.8.2.2.2.2 Polyelectrolytes

Whether preferential adsorption takes place is debatable. Because these molecules can become quite large, entropy loss could become substantial when inhibitor ions are stretched along the steps. We can rather expect adsorption upon the terraces (Ohara and Reid, 1973). It is proposed that a larger surface coverage is needed. If adsorption can take place in a flat configuration upon the surface with few loops and tails, an effective step propagation barrier could be accomplished with less inhibitor molecule.

2.8.2.2.3 The effect of growth inhibitors on the crystal habit or morphology

When additives are present during crystal growth, they are assumed to be adsorbed in different concentrations onto the various types of crystal faces. Given that each type of face has a different surface lattice structure, a different distribution of adsorption sites is found at each face. It is possible that this would result in a different degree of growth retardation for each type of crystal

face which would ultimately lead to distortion of certain crystal faces and changes in the overall crystal morphology (Liu and Nancollas, 1973).

Gypsum crystals grown from pure solutions are smooth and needle shaped. It is estimated that they have a length to width ratio of 10 to 1, and width to thickness ratio of 3 to 1. These crystals are bound by (000), (120), (011) and (111) faces when grown in a pure solution. It has been observed that the (011) faces, gradually disappear in a super saturated solution in which case a more plate like character is adopted (Weijnen and van Rosmalen, 1985).

In the presence of different polyelectrolytes and/or phosphonates, crystal morphology and crystal habit have found to be strongly influenced.

Weijnen & van Rosmalen (1985) studied the effect of polymaleic acid and polyacrylic acid and their structural analogues on gypsum crystal habit. They found that crystals, which were grown in the presence of these inhibitors, result in shorter and thicker crystals than those grown from pure solutions. In the early outgrowth stages, the surface developed a rough character. After 10 to 30 % outgrowth, macro steps develop. Upon further outgrowth the crystal surface becomes smooth. However the grown crystals are severely distorted. It was concluded that (011) and (111) faces, (the least stable of the faces which provide the best bonding possibilities for adsorbing molecules) are most effectively blocked. After sufficient outgrowth, these faces are hardly recognizable as a result of surface roughening. In addition, McCartney & Alexander (1958) indicated that crystal habit modification, were most pronounced on the (111) faces.

He *et al.* (1994) observed that gypsum and barite crystals change from small, thin, sharp and elongated crystals to thick, rounded, less needle-like crystals in the presence of phosphonates and polycarboxylates.

Moreover, McCartney & Alexander (1958) found that gypsum, grown in the presence of keratin and gelatine, produced short, stumpy crystals. It was interesting to note that the habit modification disappeared altogether when the pH was reduced to 3 (c.f. section 2.9.2).

Lee *et al.* (2009) showed that needle-like crystals were exchanged for plate-like crystals in the presence of humic acid. To verify the morphological change, a shape factor was calculated both in the presence of humic acid and in its absence. A distinctive increase in the shape factor from an average of 0.68 in the absence of humic acid to 0.8 in the presence of humic acid (10 mg/l) supports the effect of growth inhibitors on the alteration of crystal habit.

Furthermore, Ben Ahmed *et al.* (2008) studied the effect of RPI (polyacrylate) on precipitated gypsum crystals. SEM images pointed out that short, stubby crystals and large worm-shaped agglomerates are formed in the presence of RPI, which increase with increasing concentration of RPI. XRD tests showed increased peak intensities in the presence of RPI, which confirms that crystals become highly textured. This could be aptly explained by the adsorption of RPI onto the crystal surface.

The agglomerative effect of growth inhibitors on gypsum was also observed by Oner *et al.* (1998). In the presence of block copolymers of n-buthylmethacrylate-b-methacrylic acid, clumps of needle-like crystal aggregates were formed. Crystals were found to be shorter than those grown from pure salt solutions with some star-like agglomerates. In the presence of random copolymers of n-buthylmethacrylate-co-methacrylic acid, larger plate-like crystals were formed. In the presence of PAA not only the needle character of the crystals disappear, they became deformed and covered in a sponge-like mass of very fine crystals. An extensive degree of agglomeration (by visual comparison of SEM photographs) was also witnessed in the presence of PAA.

2.8.2.2.4 Absorption of antiscalants into the crystal structure

As was explained in section 2.8.2.2.1, it is observed that antiscalants preferentially adsorb onto and block the most active growth sites on the crystal surface (kinks and terraces). Antiscalants also preferentially distort certain of the characteristic faces of a crystal (c.f. section 2.8.2.2.3). Moreover it is hypothesized (Weijnen and van Rosmalen, 1985) that sites of lower energy (steps) will continue to grow, while sites of higher energy are blocked. This leads to step bunching, and inevitably to the development of high macro steps which are capable of overgrowing the adsorbed inhibitor molecule. At this point inhibitors are assumed to be completely incorporated into the crystal lattice. This not only leads to a residual decrease in the inhibitor concentration (Amjad and Hooley, 1986) but at this point growth recommences at a rate comparable to that of the pure solution. Note however that most of the test conditions under which these assumptions were made, only considered very low antiscalant concentrations (< 10 mg/l).

Hernandez *et al.* (2006) conducted kinetic tests on gypsum growth under extremely high super saturation and inhibitor concentrations and concluded that a critical inhibitor concentration exists, below which spontaneous precipitation will occur for a specific super saturation. Experiments carried out for different inhibitor concentrations at a fixed solution concentration pointed out that inhibitor concentration decreases over time until a critical value is reached at which point gypsum starts to precipitate. It is hypothesised that during this process the growth inhibitor is constantly

adsorbed onto the crystal surface and then incorporated into the crystal lattice, resulting in a decrease of inhibitor concentration. This continues until the inhibitor is unable to further inhibit the growth and spontaneous precipitation commences.

To conclude this section, the adsorption mechanism of antiscalants such as phosphonates and polyelectrolytes is justified by showing that antiscalants,

1. cause inhibition of precipitation kinetics, beyond what could be expected from complexation or chelation,
2. alter/distort the crystal habit/morphology through adsorbing at specific sites on the crystal surface,
3. are not only adsorbed onto but also incorporated into the crystal structure.

2.9 Factors that influence efficiency of antiscalants

The capacity of an antiscalant to inhibit nucleation and growth of a system under crystallization is dependent on the type of antiscalant, the governing process conditions and the chemistry of the system. This section briefly explains the effect of the following parameters on the efficiency of commercial antiscalants:

1. The concentration of antiscalant
2. Temperature
3. Super saturation
4. pH,
5. Cationic impurities

The effects of the antiscalant concentration, temperature and super saturation are considered together while the effects of pH and cationic impurities are considered separately.

2.9.1 The interaction between antiscalant, temperature and super saturation

Antiscalants cause nucleation kinetics of precipitants in solution to slow down. This is seen by the effect that the addition of small quantities of antiscalant exerts on the induction period.

The extent to which a unit-change in concentration of antiscalant will prolong the induction period (or rather the antiscalant-induction time relationship) of a given system depends firstly on the type of antiscalant (c.f. section 2.8.1 and **Table 6** and **Table 7**). Section 2.8.1 shows that, for the inhibition of gypsum precipitation polyelectrolytes and phosphonates are some of the most efficient antiscalants.

In a system subject to crystallization, (in the absence of impurities in solution) an increase in the concentration of an effective antiscalant subsequently causes the induction period to increase (Refer to **Table 8**). This tendency has been proven for PAA (Amjad, 1985; Amjad & Hooley, 1986; Ben Ahmed *et al.*, 2008; Liu & Nancollas, 1970; Oner *et al.*, 1998; Shih *et al.*, 2004) and phosphonate based antiscalants (Amjad, 1985; Shih *et al.*, 2004; Weijnen *et al.*, 1983). Some researchers hypothesized, that antiscalants slow down kinetics by increasing the interfacial tension between the crystal surface and the solution (Ben Ahmed *et al.*, 2008). As mentioned previously, antiscalants slow down nucleation by blocking the most active growth sites on the crystal surface. An increase in the concentration of antiscalants therefore increases the extent of blockage, resulting in an increase in the induction time.

However, continual increase of the antiscalant concentration does not necessarily add to its efficiency. For a range of different phosphate based antiscalants, Guo & Severtson (2004) showed that the inhibition capacity of each inhibitor reached a maximum at concentration of about 10 mg/l. Similarly Wang *et al.* (2009), who studied the effect of phosphonic copolymer on the inhibition of calcite, observed that the inhibition capacity of this polymer reached a maximum at a concentration of around 10-12 mg/l. It could be assumed that for every system and antiscalant there is an optimum antiscalant concentration above which the inhibition capacity does not change significantly.

Conversely, Hernandez *et al.* (2006) explained that there exists a critical antiscalant concentration below which no inhibition takes place. This concept was demonstrated by showing that, for a system with a fixed chemical makeup, a critical concentration of a given antiscalant exists at which spontaneous precipitation in the absence of an induction period will take place.

The antiscalant-induction time relationship is strongly dependent on the chemistry and temperature of the system. Nucleation and growth kinetics increase with an increase in temperature and super saturation according to classical nucleation theory (c.f. section 2.6). Consequently, a given concentration of antiscalant is less effective when operating conditions are kinetically favourable. (Amjad, 1988; Liu & Nancollas, 1975; Amjad & Hooley, 1986) among others (refer to **Table 9**) have shown that an increase in temperature of 10°C caused a given concentration of antiscalant to reduce in efficiency by a factor of two.

In addition, El Dahan & Hegazy (2000) showed that, to achieve a certain degree of inhibition (*e.g.* 90 %) using a phosphate ester, the concentration of antiscalant had to be increased considerably with an increase in temperature.

Table 6: *Comparison of the effectiveness of different antiscalants (Amjad, 1985), [Ca^{2+}] = 0.0497 M, 0.4 M NaCl (Temperature: 25°C, seed concentration: 2000 mg/l, antiscalant concentration: 0.5 mg/l)*

Antiscalant type	Induction period (minutes)	Growth rate ($M^{-1}.min^{-1}$)
PAA (MW: 3500)	382	0.915
PAA (MW: 10000)	80	0.866
PAA (MW:50000)	0	0.873
SPP	7	0.816
STPP	5	0.783
SHMP	280	0.748
HEDP	2	0.728

Table 7: *Comparison of the effectiveness of different antiscalants* (Amjad and Hooley, 1986)*, [Ca^{2+}] = 0.0363 M (Temperature: 35*°C, seed concentration: 2000 mg/l, antiscalant concentration: 0.2 mg/l)

Antiscalant type	Induction period (minutes)	Growth rate ($M^{-1}.min^{-1}$)
PAA (MW: 2100)	195	0.55
PAA (MW: 5100)	130	0.61
PAA (MW: 6000)	95	0.58
PAA (MW: 10000)	30	0.56
PAA (MW: 50000)	0	0.55
SPP	0	0.56
STPP	0	0.55
SHMP	85	0.61
HEDP	5	0.52

Table 8: *Concentration effect of antiscalants on the induction period during gypsum precipitation*

Antiscalant type	Temp (°C)	Seed (mg/l)	Antiscalant concentration	Induction period (minutes)	Source
PAA (MW: 5100)	35	2000	0.1 mg/l	15	(Amjad and Hooley, 1986)
			0.2 mg/l	130	
			0.3 mg/l	275	
			0.6 mg/l	1225	
			2 mg/l	>1800	
AF-400 (PAA) **[Ca^{2+}] = 0.0497 M**	25	2000	0.25 mg/l	160	(Amjad, 1985)
			0.35 mg/l	290	
			0.5 mg/l	550	
			2 mg/l	>1200	
PAA(MW: 500) **[Ca^{2+}] = 0.0497 M**	25	2000	0.25 mg/l	114	(Amjad, 1985)
			0.5 mg/l	382	
			0.7 mg/l	540	

Table 9: *Effect of temperature on antiscalants efficiency during gypsum precipitation*

Antiscalant type	Temp (°C)	Seed (mg/l)	Antiscalant concentration	Induction period (minutes)	Source
TENTMP **[Ca^{2+}] = 0.04 M**	25	1930	1.89 x10^{-6} M	440	(Liu and Nancollas, 1975)
	35			210	
	45			87	
				45	
PAA **(MW: 6000)** **[Ca^{2+}] = 0.035 M** **pH=7**	25	2000	0.25 mg/l	240	(Amjad, 1988)
	35			86	
	50			33	
PAA **(MW: 5100)**	25	2000	0.2 mg/l	265	(Amjad and Hooley, 1986)
	35			130	
[Ca^{2+}] = 0.0363 M	45			12	

2.9.2 pH

In section 2.8.2 it was explained that the degree to which a polymer would be attracted to a crystal surface depends on both the electrostatics and the chemical bonding between the antiscalant and the crystal surface.

The pH of the solution (subject to crystallization) determines the degree of dissociation of acidic molecules such as phosphonic acids and polyacrylic acids. The degree of dissociation determines the anionic charge density, which again determines the electrostatic interaction with the crystal surface. At low pH values, acidic molecules in their un-dissociated state are assumed to exhibit a low degree of electrostatic interaction. Furthermore, Weijnen & van Rosmalen (1985) explains that polyelectrolytes behave like non-ionic polymers at low pH values and adopt a loopy configuration upon the crystal surface, which is an indication of very weak bonding. As the pH increases, inhibitor molecules begin to dissociate, increasing the anionic charge density on the surface and causes the inhibitor affinity to increase towards the crystal surface.

McCartney & Alexander (1958) showed that at a low pH of 2.5, the degree of dissociation of polyacrylic acid is very low and that the inhibitor has no influence on calcium sulphate crystallization. Upon further increasing the pH to 6, a maximum is reached in terms of inhibitory efficiency. At this stage PAA is estimated to be more than 60 % dissociated. Upon further increase in pH, in which case PAA becomes fully dissociated, no further increase in effectiveness is observed. In addition (Amjad, 1988; Oner *et al.*, 1998; Weijnen & van Rosmalen, 1985) found that at low pH values (2.5-3) the retarding power of polyacrylic acid is insignificant and that its effectiveness is independent of the polymer concentration. They also confirmed the observation made by McCartney & Alexander (1958) that the efficiency of this inhibitor increases with increasing the pH up to a pH of 5.5-6, above which no real increase in performance is witnessed.

pH-efficiency behaviour similar to that of PAA exists for polymaleic acid. Weijnen & van Rosmalen (1985) demonstrated that, at a low pH of 3, polymaleic acid was very ineffective. Upon increasing the pH from 3 to 5 and from 5 to 7, a great increase in inhibitor effectiveness was seen. The increasing affinity of polymers toward the crystal surface can again be explained by an increase in the anionic charge density.

In contrast, He *et al.* (1994) showed that for carboxylic acids, (of which PAA forms part) maximum inhibitory capacity is observed at a pH of 3-4.

For phosphonates, the inhibition capacity is also related to a pH change. Weijnen *et al.* (1983) indicated that, at pH of 3.5, no inhibition of gypsum was observed, while at pH values greater than 7 the growth process was very slow. It was demonstrated that an increase in growth inhibition was observed with an increase in the pH. It is argued that the attraction between the inhibitor and the crystal surface can be attributed to the fully dissociated phosphonate groups. Similarly, He *et al.* (1994) found that the maximum inhibitory capacity of phosphonates occurred at a pH of roughly 7.

2.9.3 Cationic impurities

Cationic impurities in solution have a detrimental effect on antiscalant performance (Gabelich *et al.*, 2002). Some cations form complexes with the inhibitor molecules, and in such a way prevents the inhibitory action of the polymer. In other cases a cation will form hydrates or hydroxylates in solution, which act as large, nucleating sites for crystals and circumvents the inhibitory action of threshold inhibitors by promoting nucleation (Dalvi *et al.*, 2000). Ferric and aluminium ions (well known for their use as coagulants during pre-treatment of RO feed water) have especially drawn attention in this regard.

2.9.3.1 Iron species

When Fe^{3+} is added to an aqueous system, numerous hydrated and hydroxylated species can coexist, depending on the pH according to the following equilibrium (Stumm, 1992):

$$Fe^{3+}(H_2O)_6 \leftrightarrow Fe(OH)^{2+} \leftrightarrow Fe(OH)_2{}^{+} \leftrightarrow Fe(OH)_3 \qquad \text{(H)}$$

When ferric chloride is added to water containing natural alkalinity, the following reaction takes place (Gabelich *et al.*, 2002):

$$2FeCl_3 + 3Ca(HCO_3^-)_2 \rightarrow 2Fe(OH)_3 \downarrow + 3CaCl_2 + 6(CO_2) \qquad \text{(I)}$$

During acidic conditions, hydrated species dominate, while in alkaline solutions hydroxylated species dominate.

Dalvi *et al.* (2000) studied the effect of different iron species (Fe^{3+}, Fe^{2+}, Fe_2O_3, $Fe(OH)_2$, $Fe(OH)_3$ and rust) on the performance of two antiscalants: polymaleic acid and polyphosphonate based antisclant. Both antiscalants were evaluated at a concentration of 2 mg/l and at a temperature of 95°C. It was observed that the presence of iron species Fe^{3+} and $Fe(OH)_3$, at a concentration of 2 mg/l (referring to iron species) caused a considerable reduction in efficiency of the antiscalant. For

polymaleic acid, a reduction in efficiency of 37 % and 32.3 % was observed when Fe^{3+} and $Fe(OH)_3$ was added respectively at concentrations of 2 mg/l. For polyphosphonate, effeciencies of 46.4 % and 40.5 % were reported at the same conditions. Fe_2O_3, $Fe(OH)_2$ and rust affected the performance of both antiscalants to a lesser degree. When the concentration of ferric (Fe^{3+}) was increased from 0.3 to 5 mg/l, the efficiency of both antiscalants decreased considerably. However a further increase in the ferric concentration above 5 mg/l caused no further change in the inhibitor efficiency. Similar observations were made by Rashad *et al.* (2004). It is explained that iron species reduce the antiscalant efficiency by offering nucleation sites in the case of $Fe(OH)_3$ and hydrolyzed chains in the case of ferric iron which would cause either preferential adsorption of the antiscalant molecules onto the iron molecules or the precipitating phase to nucleate on to the iron species. In another study, discussed in section 2.10.2, Kim *et al.* (2009) found that Ferric chloride (Fe^{3+}) at concentrations of up to 2 mg/l, had a severely negative impact on the scale inhibition properties of a polycarboxylic acid scale inhibitor.

Leseur *et al.* (2005) found that at high pH values, iron formed strong complexes with phosphonates in solution. This was not observed at lower pH values. According to Dalvi *et al.* (2000), the complexes can be as a result of 1) the formation of Fe^{2+} ions which will complex with the negatively charged phosphonates ions, or 2) as a result of strong adsorption onto $Fe(OH)_3$ macromolecules in solution.

2.9.3.2 Aluminium species

Aluminium (generally added as Alum, i.e. aluminium sulphate) ions also greatly affect the inhibitory power of threshold growth inhibitors. When alum is added to water containing natural alkalinity, the following general reaction takes place (Gabelich *et al.*, 2002):

$$Al_2(SO_4)_3 \cdot 14H_2O + 3Ca(HCO_3)_2 \rightarrow 2Al(OH)_3 \downarrow + 3CaSO_4 + 6(CO_2) + 14H_2O \qquad (J)$$

Depending on the pH, various ionic forms of aluminium can include: $AlOH^{2+}$, $Al(OH)_2^{+}$, $Al_3(OH)_4^{5+}$ and $Al_{13}O_4(OH)_{24}^{7+}$.

When trace amounts of aluminium are present in the water in the presence of phosphorous-based antiscalants, fouling on reverse osmosis membrane surfaces is a serious problem. It is suggested that phosphorous chelates with the excess aluminium in the water (Gabelich *et al.*, 2002). This same tendency has been found by Gabelich *et al.* (2006).

Shih *et al.* (2006) studied the effect of residual aluminium on the effectiveness of a range of different growth inhibitors. The inhibitors evaluated include polyacrylic acid, phosphino carboxylic acid and other polycarboxylic acids, each at a concentration of 3 mg/l. At concentrations as low as 100 µg/l,

aluminium was able to reduce the efficiency of antiscalants up to 20 or 30 fold compared to the no-alumunium scenario. In some cases, complete inhibition of the antiscalant efficiency was observed. It is proposed that the Aluminium ions in solution compete with the calcium ions to preferentially complex with the anionic polymers, subsequently preventing adsorption of antiscalant molecules onto the crystal surface. An exponential decay of the induction period was seen as the aluminium concentration was increased at a constant antiscalant concentration of 3 mg/l. When the antiscalant dosage was doubled to 6 mg/l, the same destructive effect of the aluminium on the antiscalant effectiveness was not witnessed.

In addition, Akay *et al.* (1998) studied the effect of pH on the capacity of red mud (containing both aluminium and iron) to remove phosphonate from a solution. At a pH of 5.2, 100 % removal efficiency was observed, at pH of 9.2 15 % removal was seen and at a pH of 7.4, 77 % removal and at pH of 3.9, 47 % removal efficiency was observed. It is interesting to note that when phosphate rejection was found to be at a maximum the pH ranged from 5.2 to 7.4 and both iron and aluminium phosphate species were found to be at a minimum.

2.10 **RO-concentrate treatment**

As previously mentioned, water recovery during the use of RO is limited by the feed water chemistry and the type of pre-treatment. In combination with other processes, desalination by means of RO can deliver higher recoveries. Sufficient brine treatment can be an effective way to improve water recovery. In the following section, some brine treatment strategies are discussed.

2.10.1 CESP process

The CESP process (Rahardianto *et al.*, 2010), short for 'chemically enhanced seeded precipitation' is a two-step chemically enhanced seeded precipitation process (CESP). This process is aimed at improving the super saturation of antiscalant, polyacrylic acid (PAA), containing RO brine solutions that are super saturated with respect to gypsum (SI=2.53) and calcium carbonate (SI=20.3). The first step of the process consists of chemical precipitation, where lime is used to 'scavenge' or destroy antiscalant behaviour. This is followed by a seeded precipitation step where gypsum seed is used to precipitate the remaining gypsum in solution. Lime dosage (1.35-3.37 mM) is controlled to prevent raising the pH above the saturation point of $Mg(OH)_{2,}$ which is pH=9.56, in order to prevent it from precipitating. The philosophy behind the prevention of $Mg(OH)_2$ precipitation is to enhance the settling characteristics of the slurry since $Mg(OH)_2$ has poor settling characteristics. During the seeded precipitation step, gypsum seed is added at a concentration between 2.5 or 4 g/l.

The results indicated that, at the lower end of the lime dosage concentration (1.35 mM), insufficient antiscalant scavenging (PAA concentration 3 mg/l - 12 mg/l) takes place; however a lime concentration above 2.7 mM was sufficient to achieve effective antiscalant scavenging, indicating scaling characteristics similar to the baseline (no antiscalant) conditions. Moreover the time allocated for lime treatment had a significant effect on antiscalant removal and the efficiency of sulphate treatment in which case 10-25 minutes proved to be sufficient. With the addition of gypsum seed, equilibrium was reached within 2 hours.

The initial antiscalant concentration had a significant effect on the 'scavenging' process. Although the applied lime dosage of 3.37 mM was sufficient to scavenge the antiscalant at 3 mg/l, it proved to be insufficient at an initial antiscalant concentration of 12 mg/l. In the case where antiscalant scavenging by means of lime treatment alone was insufficient, subsequent seeded precipitation with gypsum caused additional antiscalant scavenging.

The efficiency of recycled crystals (gypsum and calcium carbonate) on gypsum precipitation in the second stage was studied for four consecutive runs. Recycled seed showed a significant loss of active

surface area in the second run (86 % gypsum removal vs. 92 %). In the following runs (3 and 4), the extent of removal stayed almost constant at 84 %.

An advantage of the CESP process is low chemical usage compared to conventional chemical precipitation using only lime, caustic or soda ash, where concentrations of 5.7 mM, 11.4 mM and 6.7xCESP lime dosage, respectively, would be required for the same result using only CESP.

2.10.2 Coagulant and surfactant addition – de-super saturation

Yang *et al.* (2007), studied the de-super saturation of RO brine (oversaturated with gypsum) in the presence of polyaspartic acid (MW: 2000-3000), polyamino polyether methylenephosphonate (MW: 600), an anionic 4.5 generation polyamidoamine and sodium hexametaphosphate (SHMP) each within the concentration range (10-34 mg/l).

Kinetics data indicated that the addition of polyaluminum chloride - PACl (60-240 mg/l), a commercial coagulant could effectively override the effect of all the different antiscalants and cause the super saturated solution to reach equilibrium within 45 minutes. At lower concentrations, PACl was most effective; at the maximum investigated concentration (240 mg/l), PACl caused re-stabilization of initially destabilized particles which reduced its efficiency. In addition, sodium dodecyl sulphate (SDS), a surfactant, (38-300 mg/l) was only effective in disrupting the effect of the polyamino polyether methylenephosphonate antiscalant.

When the coagulant and/ or surfactant were effective in disrupting the inhibitory effect of the antiscalant, a decrease in the antiscalant concentration was observed. It is suggested that the reduction in antiscalant is possibly caused by adsorption of antiscalant onto the precipitating crystals. It was also observed that the addition of gypsum seed at 20 g/l caused immediate precipitation of the meta-stable solution and caused equilibrium to be reached within 10 minutes.

In another study, Kim *et al.* (2009) demonstrated the effect of interaction between ferric chloride and polyDADMAC on the effectiveness of 2 mg/l of a polycarboxylic antiscalant during gypsum (gypsum SI=3.3) precipitation. The addition of 1-2 mg/l ferric chloride reduced the induction time from 270 minutes to approximately 20 minutes, which is longer than the control run which took 10-15 minutes to start precipitating. When the ratio ferric: PolyDADMAC was 10, the relative nucleation rate was slower (approximately 50 minutes induction period) compared to only ferric (35 minutes), in which case the precipitation rate was lower compared to the control); however when the ratio ferric: PolyDADMAC is essentially one, the induction time decreased to approximately 25 minutes,

resulting from an increase in nucleation kinetics. The higher nucleation rate is considered to be as a result of the higher degree of flocculation in the presence of PolyDADMAC. Moreover, it was observed that the addition of ferric (2 mg/l) and PolyDADMAC (10 mg/l) respectively caused an increase in the induction period in the absence of an antiscalant. In both cases a maximum in the induction period (25 minutes for ferric chloride and 23 minutes for polyDADMAC) was displayed which decreased to approximately 15 minutes (baseline or minimum induction time), upon further addition of ferric or PolyDADMAC.

2.10.3 Addition of inorganic particles

Yang *et al.* (2008a) showed that the addition of inorganic particles can induce crystallization of gypsum in RO concentrate in the presence of antiscalant. They studied the effect of six different inorganic particles: gypsum, kaoline ($Al_2O_3.2SiO_2.2H_2O$), Al_2O_3, dolomite, MgO and diatomite (80 % SiO_2, 15 %Al_2O_3) at concentrations of 10-20 g/l on the precipitation kinetics of solutions super saturated with gypsum and containing different organic antiscalants. The antiscalants included: A) polyamino polyether methylenephosphonate, MW: 600 (20 mg/l), B) polyaspartic acid, MW: 2000-3000 (11 mg/l) and C) an anionic 4.5-generation polyamidoamine starburst dendrimerpolymer (30 mg/l). For each run the duration was one hour.

All inorganic particles, except for diatomite were effective in causing precipitation in the presence of the polyaspartic (11 mg/l) acid within 40 minutes. The efficiency of the inorganic particles was as follows: gypsum>kaoline>Al_2O_3>dolomite>MgO>>diatomite. The precipitation rate was much larger in the presence of gypsum and no induction time was observed prior to precipitation.

In the case of the polyamidoamine polymer, all particles were effective in causing precipitation as well as reaching equilibrium within one hour. An induction time of 10 minutes was observed for MgO as well for diatomite. In the presence of gypsum, complete precipitation (< 5 minutes) was very fast compared to the use of other particles (30 minutes to one hour).

In the presence of polyamino polyether methylenephosphonate, all inorganic particles caused precipitation; however precipitation in all cases was slow and equilibrium was slowly reached for each case. Only gypsum resulted in immediate precipitation.

It is suggested that when foreign particles are used as seed material, heterogeneous nucleation must be accomplished before crystal growth can commence.

In addition, Yang *et al.* (2008a) studied the effectiveness of seeding in the presence of SHMP at different concentrations and pH values. At a SHMP concentration of 7 mg/l, gypsum seed was

effective to immediately induce precipitation of solution super saturated with gypsum. At higher concentrations of SHMP the interaction between pH and the antiscalant concentration became more significant. At a SHMP concentration of 34 mg/l at a pH of 7) gypsum seed was ineffective in relieving the state of super saturation within one hour. When the pH was increased to 10 (resulting in the hydrolysis of SHMP), gypsum addition resulted in precipitation of the solution. At a pH of 7, SHMP is very effective and adsorbs strongly to the crystal surface. When the pH is increased to 10, SHMP is hydrolysed to the orthophosphate form, which bonds weakly, resulting in the increased effectiveness of gypsum seed to effect precipitation.

2.10.4 Air-blow and organic inducers

Yang *et al.* (2008b) considered three methods to induce crystallization of gypsum from super saturated solutions containing antiscalants: 1) air-blow method, 2) the addition of an inorganic inducer 3) and a method where method one and two are combined. Two different scaling solutions were used. Antiscalants included: A) polyamino polyether methylenephosphonate, MW: 600 (10 mg/l), B) polyaspartic acid, MW: 2000-3000 (16 mg/l) and C) an anionic 4.5-generation polyamidoamine starburst dendrimer polymer (22 mg/l).

In the case of the air-blow experiment, only 30 % (in the case of polyaspartic acid) and 40 % (in the case of the polyamidoamine polymer) of the calcium could be removed within two hours by precipitating. Calcium was removed by $CaCO_3$ precipitation, through CO_2 removal. In both cases, a pH increase to 8.2 was observed, which confirms the removal of CO_2.

$CaCO_3$ was added as inorganic precipitation inducer at 20 g/l of $CaCO_3$. Calcium removal of 25-40 % was achieved within 2 hours. A pH decrease was noted during the course of the precipitation reaction as a result of the generation of CO_2. When air-blow was combined with calcite induction, calcium removal increased considerably for all antiscalants (up to 50-60 % calcium removal). This is as a result of CO_2 removal, driving the calcite precipitation process according to the Le Chattelier principle.

In addition, it was shown that other inorganic inducers: diatomite, dolomite, kaoline, alumina and MgO could also be used to remove calcium in the presence of antiscalants. All other inducers were found to be slightly less effective than calcite. In combination with air-blow, MgO was the most effective inducer, resulting in 70 % and 80 % calcium removal for solutions 1 and 2. It is argued that the hydration of MgO causes the formation of hydroxyl ions, which accelerates the removal of calcium.

2.10.5 More seeded precipitation processes

2.10.5.1 Seeded slurry and tubular RO (SPARRO)

The Slurry Precipitation and Recycle Reverse Osmosis (SPARRO) process was developed to treat brines containing high amounts of sulphate and calcium. This process makes use of tubular RO membranes and seeded slurry which is recycled and maintained within the membrane system. Seed crystals provide preferential sites for homogeneous nucleation and precipitation, not only to reduce the risk of scaling in the membranes but also to de-super saturate the brine. The process has however found to cause problems with regards to membrane fouling, corrosion, hydrolysis and premature membrane failure (Lewis & Nathoo, 2006).

2.10.5.2 Pure and recycled seeding for high strength wastewater

In a lab-bench-crystallization study, seeded crystallization was used to reduce sulphate levels of high strength wastewater. The addition of gypsum seed crystals (4000 mg/l) to a complex waste-water (2900 mg/l Calcium and 1100 mg/l sulphate,) caused rapid crystallization of gypsum in solution; equilibrium was reached within 2-5 hours. In the event where no seed was added to the waste-water, the rate of crystallization was insignificant. It is suggested, that the large amount of impurities in the waste-water causes the precipitating phase(s) to exhibit meta-stable behaviour, such that seed addition is needed to cause super saturated solutions to precipitate (Tait *et al.*, 2009).

Moreover, some experiments were conducted using recycled seed and it was found that crystallization rates in the presence of the recycled seed were in good agreement with the rates obtained using pure synthetic crystals (Tait *et al.*, 2009).

2.10.5.3 Fixed-bed seeding- de-super saturation

Barium sulphate precipitation was studied on laboratory scale using both super saturated synthetic (without presence of organic matter) and natural RO concentrates (NROC). Bremere *et al.* (1998) and Bremere *et al.* (1999) made use of a fixed bed, de-super saturation unit to reduce the saturation level of RO concentrate, by forced precipitation onto seed crystals. In the case of the synthetic concentrates without the addition of an antiscalant (type unknown), barium removal efficiency was unchanged within 100 hours of operation. However, the addition of an antiscalant to the feed water caused barium removal to decrease. It was concluded that the antiscalant adsorbs to the crystals and poisons growth sites, thereby restricting further growth and barium removal. The same effect was observed for natural NF (nano-filtration) concentrate containing organic material. To destroy the effect of the antiscalant in the NROC, ozone was used to treat water prior to the de-

super saturation phase. However, ozone-treated water caused poisoning of seed crystals. It is suspected that oxidation products from the ozonation reaction - carboxylic acids adsorb on to crystal surfaces and result in poisoning of the seed.

2.11 **Literature summary**

The presence of antiscalant molecules in the concentrate of desalination processes (such as reverse osmosis) creates problems with regard to further optimization of water recovery by preventing the effective separation of salt from the concentrate.

Different methods can be applied to override the effect of the antiscalant in a meta-stable, super saturated solution in order to force precipitation. These include: 1) chemical or seeded precipitation of which the latter can be induced by means of pure gypsum or other inorganic particles, 2) the addition of coagulants, or 3) by means of oxidation.

A study of the calcium sulphate-water equilibrium showed that, at moderate temperatures (below 40°C), which are the conditions that can be encountered in most water treatment plants (excluding thermal operations), $CaSO_4.2H_2O$ (gypsum), is the preferred hydration state or molecular form.

Concerning the precipitating system, the literature indicates the following:

- For every 10°C increase in temperature, the induction time decreases by a factor of two, whereas the growth rate increases exponentially with temperature. Typical induction periods can range from zero minutes to several hours.
- An increase in the level of super saturation (concentration of the precipitating ions) causes the induction period to decrease according to a logarithmic relationship. The relationship between the growth rate and the level of super saturation is unclear and has been shown to exhibit variable order (1-5).
- The addition of seed improves the nucleation kinetics and can diminish the induction period prior to precipitation. The effect of seed depends on the type, concentration and morphology of the seed. Seed, with a molecular structure different to gypsum, can lead to increased growth kinetics; nonetheless it will always be preceded by an induction period. A high concentration of gypsum seed (above 2000 mg/l) with a plate-like structure is best suited to de-super saturates a meta-stable solution.
- Cationic impurities such as Mg^{2+}, Cr^{3+}, Fe^{3+}, Cu^{2+}, $Cd^{2+}$and Pb^{2+} at concentrations below 10^{-4}M have shown to reduce the growth rate of gypsum up to 70 %, whereas small amounts of Al^{3+} can improve the growth of gypsum.
- Moreover, the presence of antiscalants (anionic in nature) at very low concentrations (below 10 mg/l), slows down the nucleation kinetics of gypsum precipitation, causing long induction times (several minutes up to more than 24 hours).

Antiscalants operate by means of adsorption and cause inhibition of precipitation by blocking active growth sites on the crystal nuclei. This is the generally accepted theoretical explanation, which has found only to be justified by 1) the way in which antiscalants affect the kinetics of precipitation and 2) the distortion that antiscalants cause to the crystal morphology. Concerning antiscalants, the literature points out the following:

- The efficiency of a given concentration of antiscalant decreases with increasing precipitation kinetics *e.g.* at higher temperatures (reduces by a factor of 2 for an increase in 10°C) and higher super saturation.
- The adsorption of antiscalants onto the crystal surface is strongly affected by pH, which determines their dissociation and anionic charge density, which again determines their electrostatic interaction with the crystal surface.
    - At low pH values (below 3) the efficiency of both phosphonate based antiscalants and polyacrylate antiscalants are very poor. Efficiency increases with an increase in pH. According to the available literature for phosphonate based antiscalants, maximum efficiency is reached around a pH of 7 and for polyacrylate antiscalants maximum efficiency is reached at around a pH of 6.
- The efficiency of antiscalants is influenced by the presence of cationic impurities such as ferric and aluminium which, at very low concentrations (below 10 mg/l), can cause their complete deactivation, depending on the concentration of antiscalant in solution.

Considering the insight gained from the literature – as summarised above – the experimental work in this study aims to determine, under batch crystallization conditions, how the factors influencing both the kinetics of the precipitating system, as well as the antiscalant mechanism, can be used to 1) override the inhibitory effect of two commercial antiscalant and 2) improve precipitation kinetics.

Chapter 3 - Research objectives and hypotheses

The hypotheses and objectives provided in this chapter are based on an extensive literature study as reported in Chapter 2.

3.1 Hypotheses

Considering a meta-stable solution, super saturated with gypsum in the presence of antiscalants, the induction time for gypsum precipitation can be reduced by the addition of $FeCl_3$, decreasing the pH, addition of gypsum seed and an increase in temperature. These effects are interrelated and can be utilized to enhance precipitation of gypsum from RO concentrate, generated from AMD.

3.2 Research objectives

The aim of the study is to determine to what extent the onset of precipitation and precipitation kinetics (in the presence of antiscalants) can be accelerated by means of chemically manipulating the RO concentrate. A system in which calcium sulphate dehydrate (gypsum) is the precipitating compound is evaluated.

This study consists of two stages. The first is a test phase where crystallization from a synthetic aqueous solution, super saturated with gypsum, is evaluated. During the second phase crystallization tests are performed, using the RO concentrate produced during desalination of AMD (rich in sulphate) with antiscalant. Tests with AMD are only performed to verify the results generated from numerous tests in artificially prepared aqueous solution. Similar trends are observed in real AMD compared to water with no chemical interferences.

3.2.1 Phase 1: batch crystallization of synthetic aqueous solution

The effect of changing process parameters [temperature: 15-25°C and calcium concentration 0.045 M (1804 mg/l) to 0.055 M (2205 mg/l)] on the kinetics of gypsum under conditions of spontaneous precipitation is studied. Aqueous solutions (super saturated with gypsum) are synthetically prepared from AR grade chemicals: calcium chloride and sodium sulphate and distilled water, where calcium concentrations simulate that of typical RO brine from gold and coal mines (refer to **Table 14** for typical AMD feed water). In synthetic aqueous solutions, background ions include NaCl. To prevent complex precipitates and co-precipitation, other cations and anions are excluded.

A phosphonate-based antiscalant (commercial brand name HYDREX) and a polyacrylate antiscalant (commercial brand name BULAB) are studied at concentrations between 4 and 12 mg/l.

Chemical manipulation of the RO concentrate includes changing of the pH (4-10), adding ferric chloride (as $FeCl_3$) (2-10 mg/l) and seeding the solution with lime, gypsum or a combination of lime and gypsum (2000 mg/l).

3.2.2 Phase 2: batch crystallization on AMD water

AMD from a coal mine in Witbank (South-Africa) is concentrated by a factor of 3 (recovery = 67 %) which brings the scaling tendency of gypsum in solution (3.73), c.f. section 11.10, to approximately the same level as during the synthetic tests (3.46). A pilot scale, 2½" spiral wound membrane, is used to concentrate the water. The RO feed is dosed with antiscalant at 4 mg/l, which results in a concentration of ≈12 mg/l in the concentrate stream at the same recovery. The concentrate is then used, instead of synthetically prepared aqueous solution, for batch crystallization tests.

By applying the conditions found to be optimum for overriding the antiscalants (at 12 mg/l) in a synthetic aqueous solution, it is determined whether these same conditions are suitable to override the effect of the antiscalants and force precipitation in more complex AMD.

3.3 Limitations

Because of the vastness of the current field of study, only a narrow range of operating conditions and factors are considered. The following limitations should be taken note of:

- The current study considers the precipitation of gypsum from synthetically prepared aqueous solutions at equimolar concentrations of $[Ca^{2+}]$ and $[SO_4^{2-}]$. In case of the AMD these concentrations are not equimolar.
- One commercial phosphonate based antiscalant (HYDREX) and one commercial polyacrylate antiscalant (BULAB) are evaluated.
- The only coagulant that is evaluated is ferric chloride
- Only 2 types of seed is evaluated: gypsum and lime

All factors studied, including temperature [15-25°C], calcium concentration [0.045 M (1804 mg/l) to 0.055 M (2204 mg/l)], pH [4-10], ferric concentration (as $FeCl_3$) [2-10 mg/l], seed concentration [2000 mg/l] and antiscalant concentration [4-12 mg/l] are considered within a narrow range of values, simulating the conditions found in typical AMD RO brines.

Chapter 4 - Materials and methods

4.1 Introduction

To achieve the research objectives, it is first necessary to develop a means to define the relationship between the kinetics of a system subject to precipitation and the factors that have an influence on the kinetics. This study considers the calcium sulphate- water system (NaCl as background ions), and how antiscalants affect the precipitation kinetics of this system, but more importantly how the process parameters (temperature, pH, and solution concentration) and impurities (ferric concentration and seed concentration) can be used as a tool to override the effect of the antiscalant and force precipitation of gypsum from a meta-stable super saturated solution.

In this chapter 1) an experimental approach (methods, response variables, available experimental and diagnostic tools) and 2) methodology (equipment, software, mathematics, and statistics etc.) are considered.

4.2 Experimental approach

4.2.1 Batch crystallization

A batch crystallization technique is employed which considers precipitation (of calcium sulphate dehydrate in this case) under conditions of changing super saturation: a solution (concentration A) will precipitate, while the level of saturation is decreasing until equilibrium (concentration B) is reached. This method, under conditions of seeded precipitation, has proven to provide reliable and reproducible results (Amjad, 1985; Amjad & Hooley, 1986; Liu & Nancollas, 1970) while under conditions of spontaneous precipitation (in the absence of seed), reproducibility is rather poor (Liu and Nancollas, 1973).

4.2.2 Process monitoring tools

4.2.2.1 Methods used for monitoring of precipitation

Popular methods used for monitoring of gypsum precipitation include: 1) conductivity monitoring (McCartney & Alexander, 1958; Weijnen *et al.*, 1983; Weijnen & van Rosmalen, 1985), 2), turbidity monitoring, (Kim *et al.*, 2009; Sarig *et al.*, 1975; Shih *et al.*, 2004; Shih *et al.*, 2006) or 3) titration methods using EDTA (Amjad, 1985; Amjad & Hooley, 1986; Gill & Nancollas, 1979; Liu & Nancollas, 1973; Liu & Nancollas, 1975) and 4) monitoring of calcium by means of an ion selective electrode, ISE (Le Gouellec & Elimelech, 2002; Rahardianto *et al.*, 2010; Shih *et al.*, 2004).

Conductivity monitoring enables real-time accurate online determination of the precipitation process, especially the induction time. Kinetic data can be inferred from conductivity measurement by relating the conductivity to a concentration value. However, exact concentrations will be hard to infer. Turbidity monitoring is an accurate method to determine the induction time, but cannot provide kinetic precipitation data. Titration methods are accurate but time consuming.

4.2.2.2 Ion selective electrode (ISE)

Calcium measurement by means of an ion selective electrode (ISE) was selected for the current research. This method is fast, simple, relatively accurate and reproducible (Rahardianto *et al.*, 2010; Shih *et al.*, 2004). Measurements are strongly influenced by sample chemistry (ionic interference) and calibration and therefore great care should be taken during sample preparation. The chemicals used for sample preparation, calibration and conditioning are moderately expensive. Nonetheless, this method is economical compared to other techniques. This method is not suitable for continuous, online measurement of a solution of changing composition and samples should therefore be periodically withdrawn from the precipitating solution for preparation and subsequent measurement

4.2.2.3 Atomic absorption (AA)

To ensure reliability of results obtained from ISE measurements, samples were sporadically analysed using AA. The accuracy of this method relies strongly on sample preparation and calibration since measurements are influenced by ionic interference. This method was employed by Hamdona & Al Hadad (2007) for measuring free calcium in solution during calcium sulphate dehydrate precipitation.

4.2.3 Response variables

During each precipitation test, the calcium concentration was monitored at selected time intervals using an ISE electrode. From a kinetic plot of calcium concentration versus time, two responses for each data set were obtained: 1) the induction time (t_{ind}), which was taken as the moment in time at which a sudden decrease in calcium concentration is observed and 2) t_{C80}, an inferential variable used to explain the growth rate. The variable t_{C80} represents a point in the growth curve, at which 80 % of the precipitation process (where the start of the precipitation process is the induction time – t_{ind}) is complete. First C_{80} is calculated (refer to equation 4.1 and **Figure 7**) and then the time t_{C80} is determined from linear interpolation of experimental data. Note that use of an inference variable, t_{C80}, is not a method known to be used in literature and was developed by the author of this study for the purpose of comparing kinetic data. The growth rate constant (k'), which is considered in literature to be the general unit of measure to describe or compare crystal growth under different conditions, was not used for comparative analytical purposes within the scope of this study because of large variability in its calculation. However to compare the current work with that which is found in literature, k'-values provide an invaluable source of information (For calculations c.f. section 11.8).

$$C_{80} = (1 - 0.8) \times (C_0 - C^*) + C^* \quad (4.1)$$

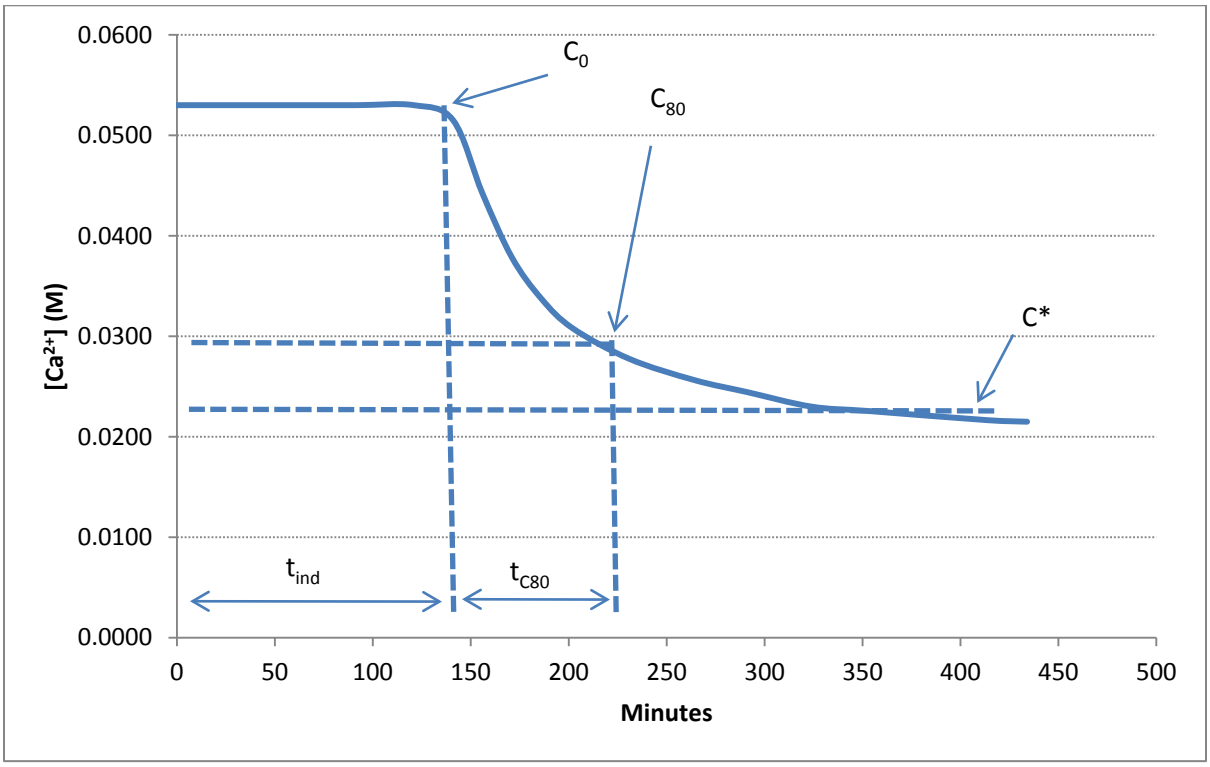

Figure 7: *Graphical interpretation of* t_{C80}

4.2.4 Software tools

4.2.4.1 STATISTICA

The design of experiments (DOE) tool pack was used to generate a factorial design on which the eventual, experimental design would be based.

4.2.4.2 Microsoft Excel 2007

For data analysis, MS Excel 2007 was used. Kinetic plots and other comparative plots were drawn in Excel. The solver function was used to fit a second order rate model to kinetic data, to produce growth rate constants (k') for each kinetic test. In addition, the data analysis tool pack was used to perform additional statistical analysis on the experimental design data set.

4.2.4.3 OLI analyser version 3

In this study, OLI® software is used for thermodynamic calculations and for determining the speciation of aqueous solutions. The activity coefficient models which are embedded in the OLI® system is the Mixed Solvent Electrolyte (MSE) activity coefficient model and the revised Helgeson-Kirkham-Flowers (HKF) model and the aqueous (H+ ions) model. These models constitute the traditional framework, applicable to most multi-component mixtures of chemicals in water, and are able to predict activity coefficients at a wide range of temperatures, pressures and concentrations.

4.3 Methodology – Batch crystallization

In this section, the different experimental designs (methods) introduced earlier are described in terms of design, functionality and reliability (where applicable). The materials and chemicals used, as well as their functionality, are considered and a statistical design approach and experimental preparation and procedure are also provided.

4.3.1 Batch crystallization equipment

Consider the batch crystallization setup (**Figure 8**) used in the current study.

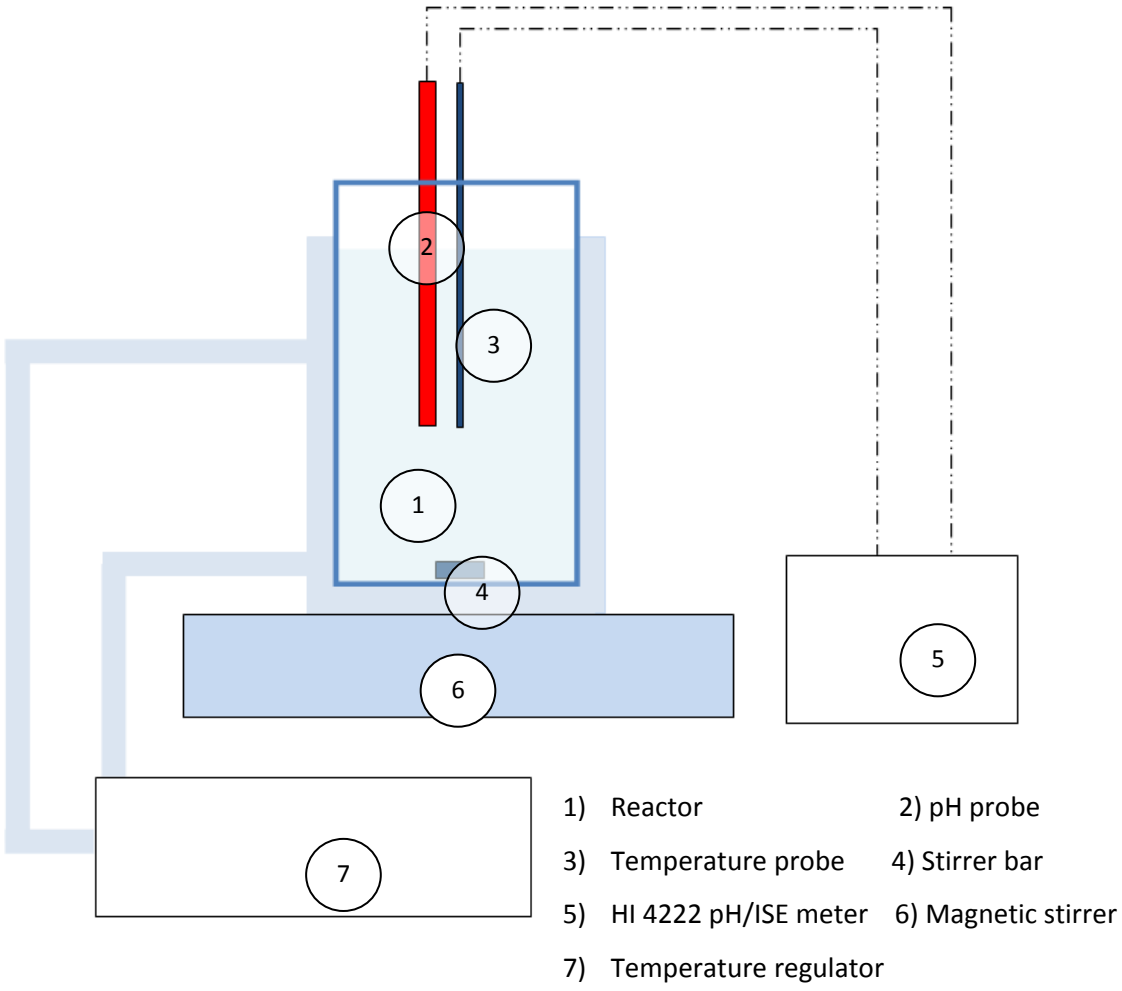

Figure 8: *Simplified schematic of batch crystallization setup*

4.3.1.1 Reactor

The reactor consists of a 600 ml vertical, jacketed, glass vessel of which the working volume is 400 ml. A Teflon cover on top of the reactor provides a snug fit to hold both temperature and pH probes.

4.3.1.2 Stirring equipment

Magnetic stirring is employed using a (30x8 mm) Teflon coated stirrer bar. The rate of stirring is accurately controlled by means of a digitally operated magnetic stirrer (*RET control/t safety control IKAMAG Magnetic stirrer*). Stirring is performed at 400 rpm.

4.3.1.3 Temperature regulatory equipment

A water jacket around the reactor provides a medium for temperature control inside the reactor. A reservoir, in which both heating (by means of a heating element) or cooling (by means of a chiller) takes place, supplies the water to be circulated.

A simple semi-automatic temperature control method is employed: a probe from the ISE/pH meter continually measures the temperature inside the reactor while the temperature is set by manually adjusting the knob on the heater-cooler.

This system provides temperature control within 0.5°C. Keeping in mind that the temperature levels considered are 15°C and 25°C (10°C difference), the error in control is 5 % maximum.

4.3.1.4 pH electrode

The pH of the working solution is monitored by means of a glass pH probe (HI 1006-2005, Hanna Instruments) which is inserted through a Teflon cover on the top of the reactor. The probe is coupled to a pH/ISE meter (HI 4222-01, Hanna Instruments).

To ensure accuracy of measurements, certified standard buffers from Hanna Instruments are used for calibration and calibration is performed at a temperature, close to the operating temperature of the reactor. Moreover, calibration is performed prior to each experimental run. After calibration, the pH/ISE meter displays the status of the probe (0-100 %), which gives a good indication of the accuracy of the probe.

4.3.2 Process monitoring tools

4.3.2.1 Calcium electrode (process monitoring)

A calcium selective electrode (HI 4104 calcium combination electrode, Hanna Instruments) is used to measure calcium concentration of diluted aqueous samples. The electrode utilizes a sensing module comprising a PVC membrane with an organic ion exchanger polymer, which is sensitive to calcium ions. For data display, the probe is connected to a pH/ISE meter (HI4222 -01, Hanna Instruments). For specifications of the probe, c.f. section 11.12.

4.3.2.1.1 Theory of operation (Hanna Instruments, n.d.):

The HI-4104 is a potentiometric device and is used for the rapid determination of free calcium ions in an aqueous solution. The electrode functions as a sensor or an ionic conductor. The HI4104 consists of a combination electrode with an Ag/AgCl reference electrode and gel stabilized Cl^- electrolyte in its inner chamber. The electrolyte in the external chamber is refillable. The PVC membrane on the sensor tip is impregnated with an organic ion-exchanger, which is considered an ionophore, meaning that it is capable of both shielding and carrying the calcium ion in its polar cage through the a-polar regions of the membrane. A charge imbalance develops between the test solution and the internal cell of the sensor. This change in voltage is in response to a change in the ionic activity. When the ionic strength is set, the voltage change is proportional to change in calcium ions in solution. The sensor follows the Nernst equation:

$$E = E_a + 2.3RT/nF \cdot log\alpha_i \quad (4.2)$$

Where, E is the observed potential, E_a is the reference potential, R is the universal gas constant (8.314 J/mol.K), n is the charge on the measured ion, α_i is the ion activity in the sample, T is the absolute temperature (K) and F is the Faraday constant (9.648×10^4 C/equivalent)

4.3.2.1.2 Reliability

The level of consistency of the data obtained by the ISE sensor is highly dependent on whether calibration and sample preparation is adequately performed (for a discussion on the reliability of the data, c.f. section 5.4). During both sample preparation and calibration, the temperature and ionic strength are important factors. Calibration and sample measurement should be performed at the same temperature and the ionic strength of the sample, and the calibration standards used should be

comparable. For the purpose of adjusting the ionic strength of samples and calibration standards an ionic strength adjuster (ISA) is used.

4.3.2.2 Atomic absorption spectrophotometry (AA)

This is a standard analytical method and will not be discussed in detail here. However some detail will be mentioned which was used to ensure accurate AA readings. For the AA readings, a Varian Spectra AA 250 Plus was used.

Samples and calibration standards were diluted so that the concentration of calcium is below 10 mg/l. Samples with higher concentrations have shown to give very large standard deviations. For dilutions of samples and calibration standards 20 ml of a 5000 mg/l lanthanum chloride solution was added and 0.1 M HCl (not distilled water) was used to make up the volume to 100 ml. For a description of the dilution process, c.f. section 4.3.6.1 (Gordon, 2010).

4.3.3 Experimental design

The current study involves determining the joint effect of a number of factors on the nucleation (response 1) and growth kinetics (response 2) of gypsum precipitation. Firstly, a number of hypotheses were formulated from studying relevant literature. A set of preliminary single-factor tests were performed, to evaluate the validity of literature statements, as well as determine the reliability and reproducibility of the chosen experimental procedure. It was concluded that six factors, including temperature, seed concentration, calcium concentration, pH, antiscalant concentration and ferric chloride concentration, significantly affect precipitation kinetics. The levels of the different factors (in other words the range of the factors) were determined by: 1) literature considerations and 2) knowledge from actual plant operating conditions. The temperature levels (15 and 25°C) are typical values during RO operation (Strohwald, 2010). The pH levels (4 and 10) are the limiting values of the ISE probe (HI 4104 calcium combination electrode, Hanna Instruments). For phosphonate and polyacrylate-based antiscalants, concentrations between 4 and 12 mg/l, are typically used during RO pre-treatment (Strohwald, 2010). The $FeCl_3$ concentrations (2 and 10 mg/l) were taken from literature and the seed concentrations (0 and 2000 mg/l) were found to be within the range of seed concentrations most used in literature.

The function of 'experimental design' is to determine which subset of process variables has the greatest influence on the process performance (Montgomery *et al.*, 1998). In the current research, a factorial

design (more specifically a 2^k design) is considered to evaluate the joint effect of all important, identified factors on a given response. This design is suitable, especially as many factors need to be evaluated (Montgomery *et al.*, 1998). With a 2^k design, each factor is evaluated at two levels (high and low). If all the possible combinations of factors are considered (full design), one would end up with 64 experiments (number of experiments = 2^6).

A full, factorial design considers main factor effects, low order interactions and higher order interactions between factors. If we assume that the higher order interactions are negligible, then a fractional factorial design (which involves fewer than the complete set of 2^k runs) can be used to determine information on the main factors as well as on the low-order interaction (Montgomery *et al.*, 1998).

In the current study a 2^{6-2} (16 experiments) design was used (**Table 10**), which proves to be a very economical design with regard to time available and information needed .The level of each factor is given in **Table 11**.

When making use of a fractional, factorial experimental design, one comes across a concept called 'aliasing', or confounding of factor effects. This takes place when the same combination of factor levels is used to compute different factor and interaction effects (Montgomery *et al.*, 1998). Consider for example the aliasing effects in **Table 12** (the coefficient of 1*6 indeed also expresses the combination 2*5 and 3*4).

Furthermore, some centre runs were added during the HYDREX experimental block to add points which could help in determining experimental variance.

Table 10: *Fold-over experimental design*

Standard Run	Design: 2**(6-3) design (+Foldover) (Spreadsheet1)					
	Temp	pH	AS	Ferric	Ca	Seed
1	-1.00000	-1.00000	-1.00000	1.00000	1.00000	1.00000
2	1.00000	-1.00000	-1.00000	-1.00000	-1.00000	1.00000
3	-1.00000	1.00000	-1.00000	-1.00000	1.00000	-1.00000
4	1.00000	1.00000	-1.00000	1.00000	-1.00000	-1.00000
5	-1.00000	-1.00000	1.00000	1.00000	-1.00000	-1.00000
6	1.00000	-1.00000	1.00000	-1.00000	1.00000	-1.00000
7	-1.00000	1.00000	1.00000	-1.00000	-1.00000	1.00000
8	1.00000	1.00000	1.00000	1.00000	1.00000	1.00000
9	1.00000	1.00000	1.00000	-1.00000	-1.00000	-1.00000
10	-1.00000	1.00000	1.00000	1.00000	1.00000	-1.00000
11	1.00000	-1.00000	1.00000	1.00000	-1.00000	1.00000
12	-1.00000	-1.00000	1.00000	-1.00000	1.00000	1.00000
13	1.00000	1.00000	-1.00000	-1.00000	1.00000	1.00000
14	-1.00000	1.00000	-1.00000	1.00000	-1.00000	1.00000
15	1.00000	-1.00000	-1.00000	1.00000	1.00000	-1.00000
16	-1.00000	-1.00000	-1.00000	-1.00000	-1.00000	-1.00000

Table 11: *Representation of factor levels and actual values*

Level	Temperature (°C)	pH	AS concentration (mg/l)	Ferric concentration (mg/l)	$[Ca^{2+}]$* (M)	Seed concentration (mg/l)
-1	15	4	4	2	0.045	0
1	25	10	12	10	0.055	2000

*$[Ca^{2+}]$: 0.045 M = 1804 mg/l; $[Ca^{2+}]$: 0.055 M = 2204 mg/l

Table 12: *Alias structure of experimental design*

	Alias 1	Alias 2
A		
B		
C		
D		
E		
F		
1*2	5*6	
1*3	4*6	
1*4	3*6	
1*5	2*6	
1*6	2*5	3*4
2*3	4*5	
2*4	3*5	

4.3.4 Materials

This section describes all the chemicals used during a typical experimental procedure and are categorised according to their functionality (Refer to **Table 13**):

- 'EXP' – chemicals used in the working solution
- 'CALIB' – chemicals used for calibration purposes
- 'MEAS' – chemicals used during sampling and sample analyses
- 'COND' – chemicals used to condition probes

Table 13: *Chemicals, their functionality and description*

Function	Chemical	Description	Molecular structure	Supplier
EXP	Ferric chloride HYDREX (3220)	$FeCl_3$ (46 % solution)*	$FeCl_3$	Veolia Water Solutions
EXP	HYDREX (4105) **(34 % solids)****	Phosphonate based antiscalant	N/A (pH=5+-0.5)	Veolia Water Solutions
EXP	BULAB (8813) **(34 % solids)****	Polyacrylate antiscalant	N/A (pH=3.5-4.5)	Buckmann Laboratories
EXP	Calcium Sulphate Dehydrate	Seed (pure salt precipitate)	$CaSO_4.2H_2O$	Kimix
EXP	Sodium Sulphate	AR grade Anhydrous salt	Na_2SO_4	Kimix, Merck
EXP	Calcium Chloride	AR grade Anhydrous salt	$CaCl_2$	Merck
CALIB	(HI-4004-01)	0.1 M Calcium Standard	N/A	Hanna Instruments
CALIB	(HI-7010) (HI-7007) (HI-7004)	pH Buffers	N/A	Hanna Instruments
CALIB and MEAS	(HI-4004-00)	ISA, Calcium - Ionic Strength Adjuster	N/A	Hanna Instruments
MEAS	(HI -7082)	ISE electrolyte	3.5 M KCl	Hanna Instruments
MEAS	(HI-7071)	pH probe electrolyte	3.5 M KCl-$AgCl_3$	Hanna Instruments
COND	(HI-70300)	pH electrode cleaning and storage solution	N/A	Hanna Instruments

Table 13 *Continues*

Function	Chemical	Description	Molecular structure	Supplier
COND	(HI-7074)	pH probe inorganic cleaning solution	N/A	Hanna Instruments
COND	(HI-4004-45)	ISE (calcium) probe conditioning and storage solution	N/A	Hanna Instruments

NOTES:

** The $FeCl_3$ product concentrate (HYDREX 3220) is a 46 % solution of $FeCl_3$; however the concentrations throughout the text are based on 100 % $FeCl_3$.*

***Both antiscalants contain 34 % solids by mass. This probably refers to the active ingredients of the antiscalants. These percentages were determined by drying 1g of each antiscalant until no-more change in the weight of the substance was observed. All antiscalant concentrations reported in this study are based on the dilute antiscalant solution (as delivered).*

4.3.5 Experimental preparation

4.3.5.1 Equipment

The reactor is thoroughly cleaned prior to experimentation, or at the end of each run. The cleaning procedure consists of two steps: first a cleaning solution (0.03 M EDTA) is used to rinse the reactor for 15 minutes in order to dissolve/remove calcium and other cationic debris. This is followed by rinsing the reactor with distilled water for 15 minutes to remove the remaining dissolved debris; the reactor is then left to dry.

The pH probe is cleaned, using a special cleaning solution (refer to **Table 13**), after which it is rinsed with distilled water and placed within a conditioning solution, ready for calibration or measuring.

The calcium electrode is thoroughly cleaned inside and out with distilled water. When the electrode is fully assembled, the electrode body is filled with electrolyte (HI-7082) and then placed in a conditioning and storage solution (HI-4004-45) for 30 minutes to 60 minutes prior to calibration. Care should be taken when assembling the probe to make sure that the electrolyte does not drain out too quickly, however slow drainage (4 cm per 24 hour period) is natural. The probe is to be conditioned prior to calibration and must remain in the conditioning solution between measurements.

Care should be taken to ensure that all glassware (pipettes and glass flasks) are clean and dry.

4.3.5.2 Calibration

The pH probe and calcium electrode are calibrated prior to each experiment.

For pH calibration a standard, three point calibration is performed using the following three buffer solutions: 4.01, 7.01 and 10.01 (Hanna Instruments). Calibration is performed at a temperature close to the operating temperature of the reactor.

After thoroughly conditioning the calcium electrode, a three point calibration is performed using standards, which bridge the measured range of values (measured values are 30-130 mg/l). In this case 10 mg/l, 100 mg/l and 1000 mg/l standards are used.

Calcium standards are made from a stock solution of 0.1 M. For the 1000 mg/l standard, 25 ml of the 0.1 M stock solution is made up to 100 ml and an additional 2 ml of ISA (Ionic strength adjuster) is added. For the 100 mg/l standard, 10 ml of a 1000 mg/l stock solution is made up to a 100 ml and 2 ml of ISA is added. Similarly, a 10 mg/l standard is prepared by taking 10 ml of a 100 mg/l stock solution, making it up to 100 ml and adding 2 ml of ISA.

ISA is added to standardize the ionic strength of the standards and samples to be measured. If the ionic strength of the samples is lower than 0.1 M, ISA can be added to standards and samples as explained previously. If the ionic strength of the samples is higher than 0.1 M, special compensation for the background ions need to be made and special standards prepared (Rahardianto *et al.*, 2010). In this study, samples were diluted below an ionic strength of 0.1 M prior to ISA addition.

4.3.5.3 Preparation of super saturated solutions

Anhydrous salts of calcium chloride and sodium sulphate are dried overnight in a vacuum oven at 60-70°C. After salts are removed from the oven it is placed in a desiccator to cool to room temperature (room temperature, depending on seasonal changes will vary between 12 and 20°C). Cool, dried salts are weighed accurately to 3 decimal places. (Note that calcium chloride is known to have an extremely hygroscopic nature, which makes it suitable as desiccant. It is therefore possible that the calcium salts 'dried' in the desiccator absorbs water, rather than to lose water, resulting in a lower NETT calcium concentration than calculated.) Distilled water and A-grade glassware is used to make up super saturated solutions. Calcium chloride dissolves easily in cold water (reacts exothermically with water); however sodium sulphate, even though it is very soluble in cold water, reacts endothermically with water. Heat addition will assist the process. Solutions are left at least 2 hours before use to allow for the dissolution process to be complete.

4.3.5.4 Start-up

After equipment is cleaned and calibrated, as well as stock solutions and super saturated working solutions are prepared, the start-up procedure is as follows (This procedure is standard for all experimental runs.):

4.3.5.4.1 Procedure (time frame)

1. The calcium chloride solution (solution 1) is placed within the reactor and the sodium sulphate solution (solution 2) is placed within the reservoir of the heater-cooler and 20 minutes is allowed for both solutions to reach the pre-determined experimental temperature.
2. Solution 2 is slowly added to solution 1 (while solution 1 is constantly mixed at 400 rpm) by pouring it against the inside of the reactor wall to avoid spurting or bubbles from forming in the solution. The pH probe is now also placed in the solution.
3. One minute after the addition of solution 2, the antiscalant is added. At this stage we assume that the solution is fully mixed and super saturated.
4. If ferric is added to the solution, it takes place two minutes after the addition of solution 2.
5. The pH is adjusted next, three minutes after the addition of solution 2 and three minutes is allocated for the completion of this process.
6. Seed is added 7 minutes after the addition of solution 2
7. The first sample is taken 8 minutes after the addition of solution 2.

Eight minutes might seem like a long time, however in the light of the magnitude of the induction times determined when NO physical or chemical manipulation of the solution takes place, eight minutes is a very short period.

4.3.6 Sampling

Using a pipette, a (10 ml) liquid aliquot is extracted at predetermined time intervals. Sampling takes place 10-30 minutes apart depending on the kinetics of the run. Once precipitation has commenced (the solution will be cloudy), sampling happens typically at time intervals of 10-15 minutes apart.

Following the extraction of the liquid aliquot, the sample is filtered, using a 0.45 µm cellulose acetate (chemically non- reactive membrane) syringe filter. The filtering process ensures that most or all seed or solid particles, which could further encourage precipitation, are removed. 5 ml of the filtered sample is diluted to 100 ml (making a 20x dilution). The dilution is important to reduce the ionic strength to below 0.1 M. Under these conditions, regular calcium ISE standards are sufficient for calibration and measurements are accurate. 2 ml Ionic strength adjuster (ISA) is added to the 100

ml resulting in a final volume of 102 ml. For measurement purposes, the final sample solution is transferred to a 100 ml beaker which is continually stirred using an additional magnetic stirrer. Both the calcium selective electrode and the temperature probe are inserted into the sample. A period of approximately 5-10 minutes is given for the measurement of the probe to stabilize, after which the value is recorded manually.

4.3.6.1 Sampling for AA analysis

A 10 ml liquid aliquot from the reactor is withdrawn and filtered using a 0.45 µm cellulose acetate syringe filter. 5ml of the filtered sample is made up to 100 ml (making a 20x dilution). Instead of using distilled water for the dilution, 0.1 M HCl is used. A second dilution (20x) is made by taking 5 ml of already dilute sample, adding 20 ml of a 5000 mg/l lanthanum chloride to the solution and making it up to 100 ml with 0.1 M HCl. Similarly, 100 ml standards for the AA are made up by adding 20 ml of 5000 mg/l lanthanum chloride and making the solution up to a total volume of 100 ml.

4.3.7 Data handling

A data set for each run consists of a calcium concentration-time relationship. Two responses are calculated from this data set: the induction time and t_{C80} (an inferential response variable that describes the growth rate). Most of the data handling and statistical analysis is performed in MS Excel 2007.

4.4 Methodology – Concentration of AMD from coal mine

During the first experimental phase (synthetic batch crystallization tests), super saturated solutions of gypsum were prepared by adding predetermined concentrations of salt to demineralised water to simulate RO concentrate super saturated with respect to gypsum. During the second experimental phase, AMD (from the Witbank area in South Africa) was concentrated by means of RO and the concentrate was used for batch crystallization tests similar to phase 1.

4.4.1 Equipment description

A schematic of the lab-scale desalination unit using reverse osmosis that was built and used to concentrate mine water (AMD) is shown in **Figure 9**.

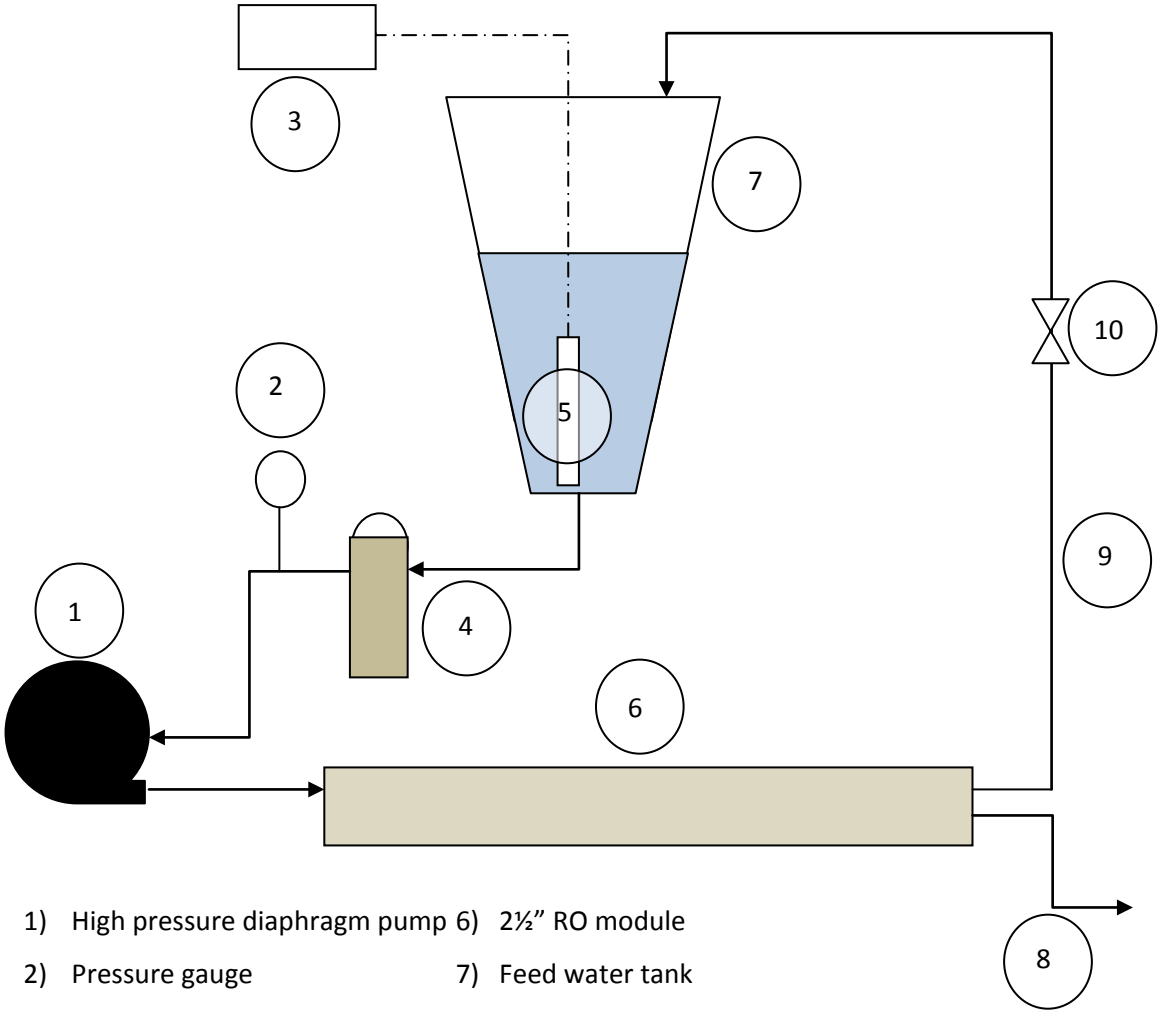

1) High pressure diaphragm pump
2) Pressure gauge
3) pH/conductivity meter
4) Cartridge filter (5µm)
5) Conductivity probe
6) 2½" RO module
7) Feed water tank
8) Permeate
9) RO concentrate
10) Needle valve

Figure 9: *Schematic of lab scale desalination unit*

4.4.1.1 Equipment description

A (Hydra-Cell D -03) diaphragm pump was used to deliver water at a maximum of 11.8 l/min under the governing pressure (20-40 bar). A portable pH/conductivity meter was used to continuously monitor the change in conductivity of the RO concentrate. A 5 micron cartridge filter was used to remove seed crystals and solid debris before recycled brine enters the inlet to the pump. A 2½" spiral wound polyamide RO membrane was used to concentrate AMD.

4.4.2 Method of operation

Water (pre-treated AMD) was loaded into a feed tank – enough to ensure that sufficient head was available to prevent the risk of pump cavitation (In this case more than 2 litres should remain in the feed tank at all times). Once the pump was switched on, pressure began to build-up within the system, pressurising the RO membrane at 20 to 30 bar. The pressure within the module was controlled by a valve on the concentrate line (refer to **Figure 9**). Not only does this valve control the pressure, but also the velocity of the permeate flowing through the membrane. This flux was limited to 20-25 $l/m^2/h$. A lower flux can cause rapid fouling, whereas a larger flux can cause telescoping of the membrane - The membrane is forced like a plug into one end of the membrane housing (Burger, 2010). During operation, permeate (desalinated water) was removed and the concentrate recycled back to the feed tank causing the concentrate to constantly increase in TDS. The conductivity probe which was inserted into the feed tank was used to monitor the conductivity of the water remaining in the system. Once the conductivity of the concentrate reached a predetermined value (the initial value concentrated to a predetermined factor), the pump was switched off, the operation stopped and the concentrate then transferred to the batch crystallization vessel for further treatment.

To ensure that the concentration of the final brine was the same after each "AMD concentration" experiment, the conductivity (measure of the TDS) and the permeate flow rate for each test were recorded and kept constant for each run. With this method, reproducible results were obtained.

4.4.2.1 Flush and prime

Before and after each run, the RO membrane system was flushed twice with 10 litres of demineralised water to ensure that no ions (which could possibly cause scaling or fouling of the membrane and other equipment) were present in the system. After the flush process, the system was drained of excess water. Prior to the actual run, three litres of pre-treated AMD (c.f. section 4.4.2.3) with added antiscalant was used to replace the flush water and again the system was drained of excess fluid.

4.4.2.2 Calibration

The valve position on the RO concentrate discharge was calibrated to ensure that the flux through the membrane, at the operating pressure, fell within an operational margin of 20-25 $l.m^{-2}.h^{-1}$. The RO membrane, with a cross-sectional area of 2.8 m^2, related to an optimum permeate flow rate of 0.8-1 l/min. For calibration purposes a NaCl solution was prepared having the same conductivity as the pre-treated AMD. Several runs were performed using this synthetic aqueous solution to accurately determine the valve position which would allow the correct permeate flow-rate.

4.4.2.3 Pre-treatment

All the AMD (+70 litres) was pre-treated at once to ensure homogeneity of the RO feed water in the subsequent experimental runs. The pre-treatment was done as follows: The pH was adjusted upward using a 1 % (w/w) lime solution. When the pH increases beyond 3, all the Fe^{2+} ions are converted to Fe^{3+} ions. To improve the oxidation process, air was constantly bubbled through the solution while the pH was adjusted. In addition 2 mg/l sodium hypochlorite was added to further assist the oxidation process. During the entire process, the water was continuously stirred. When the pH of the water was stable at a pH of 8, the stirrer was switched off. During this pre-treatment process, not only were all or most of the iron removed, but also most of the aluminium and nickel were also removed as a result of precipitation. The removal of both iron and aluminium from the water is an essential part of the pre-treatment process as these metals tend to cause rapid fouling and degradation of the membrane. The treated water was left to settle overnight and in the morning the clean water was decanted.

Prior to loading the AMD into the feed tank for priming and operation, antiscalant was added to the water at 4 mg/l.

4.4.3 AMD analysis and pre-treatment

Table 14: *Analysis of untreated and pre-treated AMD; original certified data in* **Figure 56** *and* **Figure 57** (c.f. appendix)

	Untreated*	Untreated**	Treated*
Potassium as K (mg/)	14		14
Sodium as Na (mg/)	55	41	60
Calcium as Ca (mg/l)	521	420	614
Magnesium as Mg (mg/l)	235	160	246
Sulphate as SO_4 (mg/l)	2463	3000	2496
Chloride as Cl (mg/l)	15.2	16	21
Alkalinity as $CaCO_3$ (mg/l)	0.0		19
Acidity as $CaCO_3$ (mg/l)	150		0.0
Iron as Fe (mg/l)	31.8		<0.01
Aluminium as Al (mg/l)	124		0.12
Nickel as Ni (mg/l)	28.6		0.07
Manganese as Mn (mg/l)	-	17	4.1
Conductivity (mS/m) @ 25°C	365		365
pH Lab (20°C)	3.2	2.1	7.3

* Acid water from Witbank area (current study) – untreated and treated water

**Acid water from the Navigation coal mine, near Witbank

Chapter 5 - Preliminary results, verification of experimental method and baseline data

5.1 Preliminary Results

After a thorough literature survey was done, some preliminary tests were performed to:

- verify whether the experimental method and analytical methods selected could produce reliable and reproducible results.
- verify whether the factors(which influence gypsum kinetics and antiscalant efficiency) identified by literature are significant namely:
  - Temperature
  - Level of super saturation
  - Ferric chloride concentration
  - Seeding
  - Antiscalant concentration
  - pH
- assess the order of magnitude of the induction times (kinetics),
- provide guidance for the development of a factorial experimental design.

Table 15: *Summary of preliminary results*

Exp	$[Ca^{2+}]$ (M)	Temp (°C)	pH*	Antiscalant concentration	Additive	Induction time (minutes)
P(a)	0.05	15	-	-	-	43
P(b)	0.05	15	-	-	-	42
P(c)	0.05	25	-	-	-	22
P(d)	0.05	25	-	-	-	21
P(e)	0.05	25	-	-	-	19
P(f)	0.05	25	-	-	-	22
P(g)	0.05	25	-	1 mg/l	-	122
P(h)	0.05	25	-	1 mg/l	-	131
P(i)	0.05	25	-	1 mg/l	-	135
P(j)	0.05	25	-	2 mg/l	-	205
P(k)	0.05	25	-	2 mg/l	-	208
P(l)	0.05	25	-	2 mg/l	-	217

Table 15 *Continues*

Exp	$[Ca^{2+}]$ (M)	Temp (°C)	pH	Antiscalant concentration	Additive	Induction time (minutes)
P(m)	0.05	25	-	2 mg/l	$FeCl_3$ (10 mg/l)	20
P(n)	0.05	25	-	2 mg/l	$FeCl_3$ (10 mg/l)	20
P(o)	0.05	25	-	2 mg/l	Alum (10 mg/l)	25
P(p)	0.05	25	-	2 mg/l	Alum (10 mg/l)	20
P(q)	0.05	25	4	2 mg/l	-	106
P(r)	0.05	25	4	2 mg/l	-	103
P(s)	0.05	25	10	2 mg/l	-	215
P(t)	0.05	25	10	2 mg/l	-	205
P(u)	0.05	25	10	2 mg/l	-	150
P(v)	0.05	25	-	2 mg/l	gypsum seed (1000 mg/l)	0
P(w)	0.05	25	-	2 mg/l	gypsum seed (1000 mg/l)	0
P(x)	0.05	25	-	2 mg/l	gypsum seed (500 mg/l)	10

*where no pH values are indicated, these were not measured

5.1.1 Discussion

The preliminary tests have verified that,

- Temperature strongly influences the induction period. At an increase of 10°C, the induction period is reduced by a factor of two. This could be repeated (Exp P (a) to Exp P (f)).
- The addition of a small amount of antiscalant (1-2 mg/l BULAB) caused a significant increase in the induction period (+100 minutes to +200 minutes) compared to when no antiscalant (+20 minutes) was used (Exp P(g)to Exp P(l)).
- The addition of a small amount of ferric chloride (10 mg/l) to a solution containing 2 mg/l antiscalant is sufficient to override the effect of the antiscalant (Exp P (m) and Exp P (n)).
- Alum (10 mg/l) is as efficient as ferric chloride to override the effect of the antiscalant at a concentration of 2 mg/l (Exp P (o) and Exp P (p)).
- The effectiveness of the antiscalant is strongly influenced by pH. The induction time is comparatively lower at low pH-4 than at high pH-10 (compare Exp P(q) and Exp P(r) with Exp P(s) to Exp P(u)).

- The addition of seed to a meta-stable super saturated solution causes a considerable decrease in the induction period. Seed quantity is also important - more seed is equal to shorter induction period.

From the preliminary experimental work, the robustness of the experimental procedure as well as the factors which influence its accuracy was established. It was determined how antiscalants BULAB and HYDREX affect the nucleation kinetics of calcium sulphate dehydrate during precipitation reactions. It was further established what literature has already pointed out namely: that the effect of temperature, level of super saturation, ferric chloride, seeding and antiscalant concentration (individually), all significantly influence the kinetics of calcium sulphate dehydrate precipitation. Moreover all these factors, including a change in pH, influence the effectiveness of antiscalants. It was therefore decided to include these factors in an experimental design in order to determine the interaction of the combination of these factors 1) on the nucleation and growth kinetics of gypsum precipitation and 2) on the efficiency of the antiscalants studied.

5.2 **Baseline data**

Baseline conditions (in the current study) refer to all the possible combinations of temperatures and calcium concentrations used in this study. These conditions have been reported earlier in **Table 11**. The kinetic data at these conditions are presented in **Table 16** and **Figure 10**. At the same baseline conditions, thermodynamic equilibrium concentrations were calculated using OLI Analyser 3.

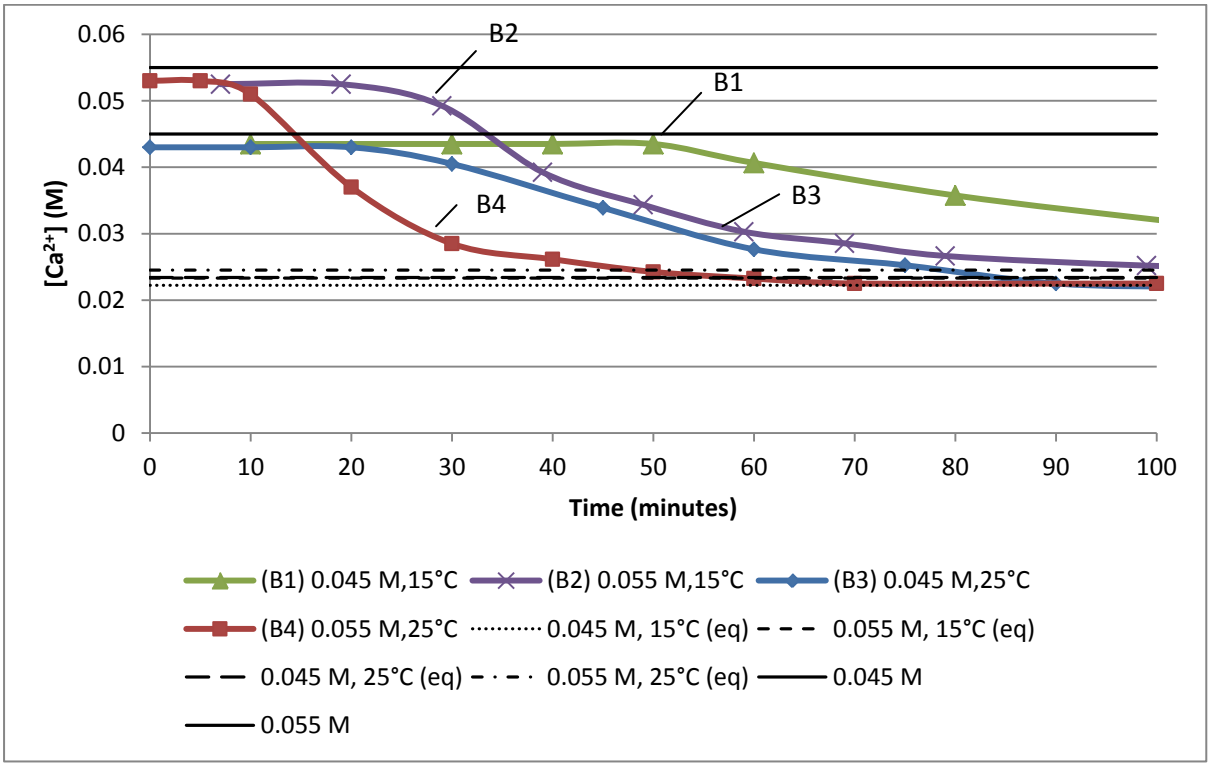

Figure 10: *Kinetic plots for baseline runs (dotted lines signify equilibrium [Ca^{2+}] concentrations)*

Table 16: *Kinetic baseline data*

Exp ID	Temp (°C)	$[Ca^{2+}] = [SO_4^{2-}]$(M)	Induction time (minutes)	t_{c80} (minutes)	k' ($M^{-1}min^{-1}$)
B(1)	15	0.045	50	93	0.83
B(2)	15	0.055	25	37	2.3
B(3)	25	0.045	25	42	2.023
B(4)	25	0.055	10	21	3.32

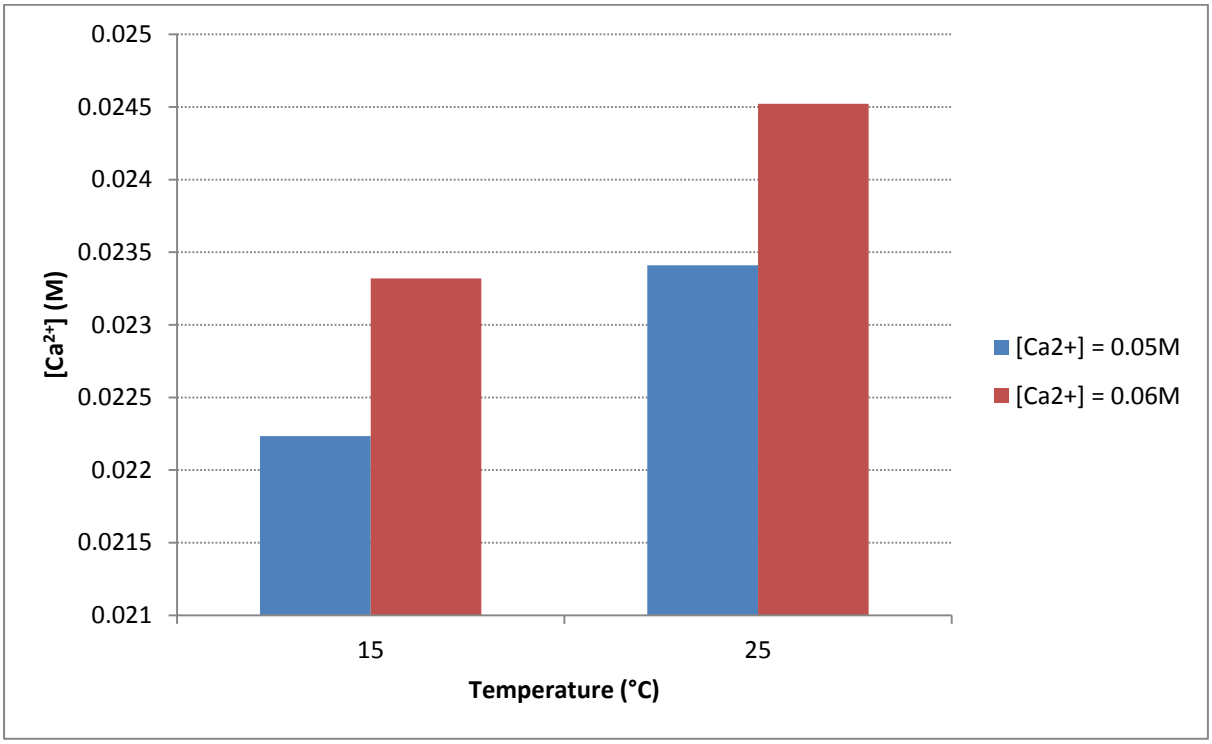

Figure 11: *Thermodynamic equilibrium concentrations according to OLI Analyser 3, based on theoretical calculations.*

5.2.1 Discussion

At a constant solution concentration, an increase in the temperature by 10°C reduces the induction period by a factor of two. This observation was also made during the preliminary testing and confirms the observations made by Liu & Nancollas (1975), Amjad (1988) and Amjad & Hooley (1986). Moreover, the magnitude of the induction times (0 to 50 minutes) at the baseline conditions agrees well with data presented by Klepetsanis & Koutsoukos (1991) and Klepetsanis *et al.* (1999).

The growth rate is a strong function of temperature (compare baseline 1 and 3 as well as 2 and 5). For a temperature increase of 10°C, the growth rate increases by a factor of two. In addition, the growth rate constants (k') within the examined temperature range are in good agreement with that observed by Liu & Nancollas (1970), Amjad (1985), Amjad & Hooley (1986) and Gill & Nancollas (1979).

An increase in calcium concentration at a fixed temperature causes an increase in the nucleation kinetics of gypsum precipitation. For an increase (calcium concentration) from 0.045 M to 0.055 M, the induction time decreased from 25 minutes to 10 minutes at 25°C and from 50 minutes to 25 minutes at 15°C. A similar observation was made by Liu & Nancollas (1973) who showed that the

induction time decreased from 25 minutes to approximately 12 minutes at 25°C for an increase in calcium concentration from 0.045 M to 0.055 M. It further shows that the growth rate increases with calcium concentration. At 25°C the value for t_{C80} changed from 42 to 21 with an increase in 0.01 M of calcium; at 15°C, t_{C80} decreased from 93 minutes to 37 minutes.

5.3 Reproducibility and repeatability of data

From the results obtained during preliminary testing (batch crystallization) it is evident that the obtained induction times are in close agreement for tests performed in replicate. This holds true in the absence of, and in the presence of, antiscalant (refer to Exp P (a) – Exp P (f) as well as Exp P (g) – Exp P (l)). Moreover, excellent reproducibility was obtained when additives such as ferric or alum or seed was introduced. For all replicates and error margin below 5 % was obtained.

Preliminary results include at the most an interaction of 4 factors. During the actual experimental design (where a multitude of factors are interacting-maximum of six factors), **Figure 12** indicates that excellent reproducibility can be obtained with the current equipment and analytical tools. The data displayed in **Figure 12** shows that for five different runs at the same conditions the standard deviation for a given data point at time‘t’ is between 3 and 4 (units deviation from the sample mean or average). For calculations, c.f. section 11.1. Note that these experiments were performed in the presence of seed. When seed was absent from the precipitating solution, the reproducibility of the induction time was poor, as foreseen in literature.

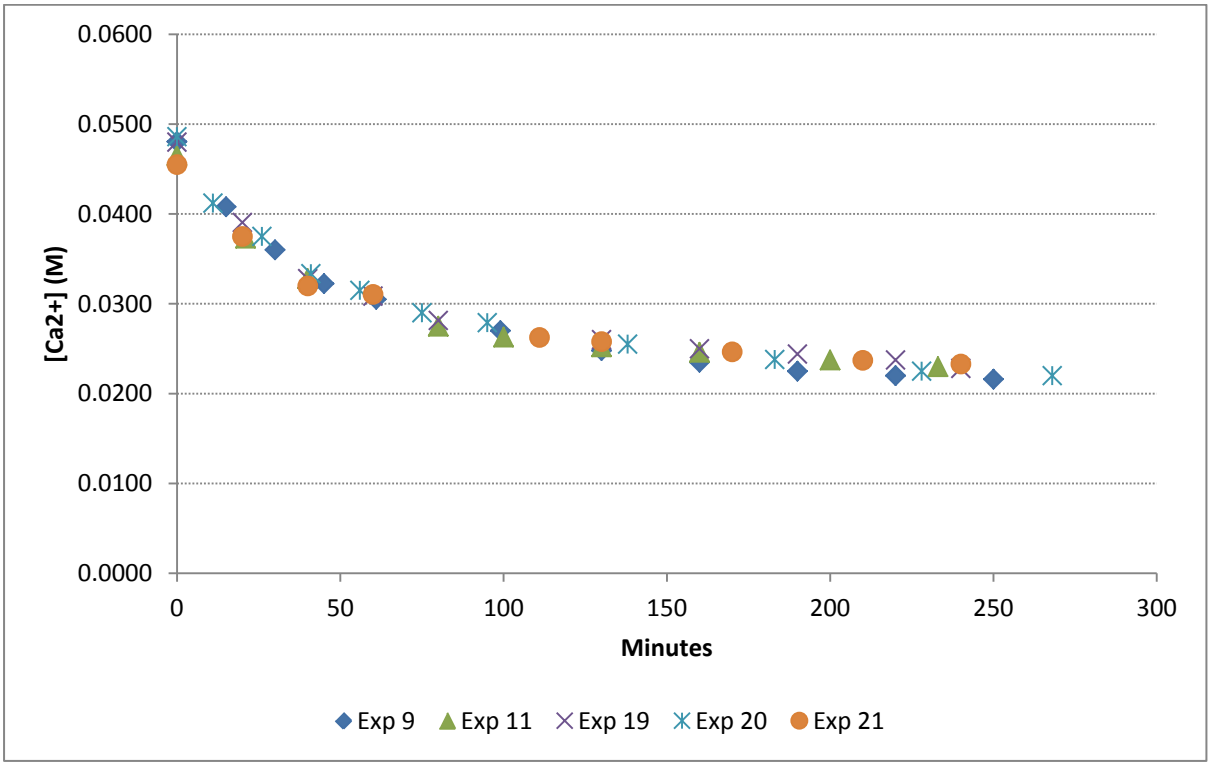

Figure 12: *Kinetic plot to illustrate reproducibility (experiments performed in the presence of HYDREX at the same conditions). For raw data, c.f. section 11.4.*

5.4 Reliability of data

Repeatability of results is one thing but to know if the results that are obtained by the analytical instruments can be trusted is yet another. Great care had been taken to ensure that anhydrous salts, accurate balances and A-grade glassware were used in the preparation of solutions. Because a standard method of preparation was used throughout the testing phase, the same error would be present in all cases.

To verify whether the data obtained by the calcium selective electrode were reliable, spot checks were performed with the use of an atomic absorption spectrophotometry (AA); refer to **Table 42** through to **Table 45** (Appendix). A straight line (y=x) relationship (see **Figure 13**) between the data obtained from the AA and the ISE (two independent analytical methods) shows that the data obtained with the two methods are in close agreement. Therefore it is safe to say that the ISE measurements are reliable.

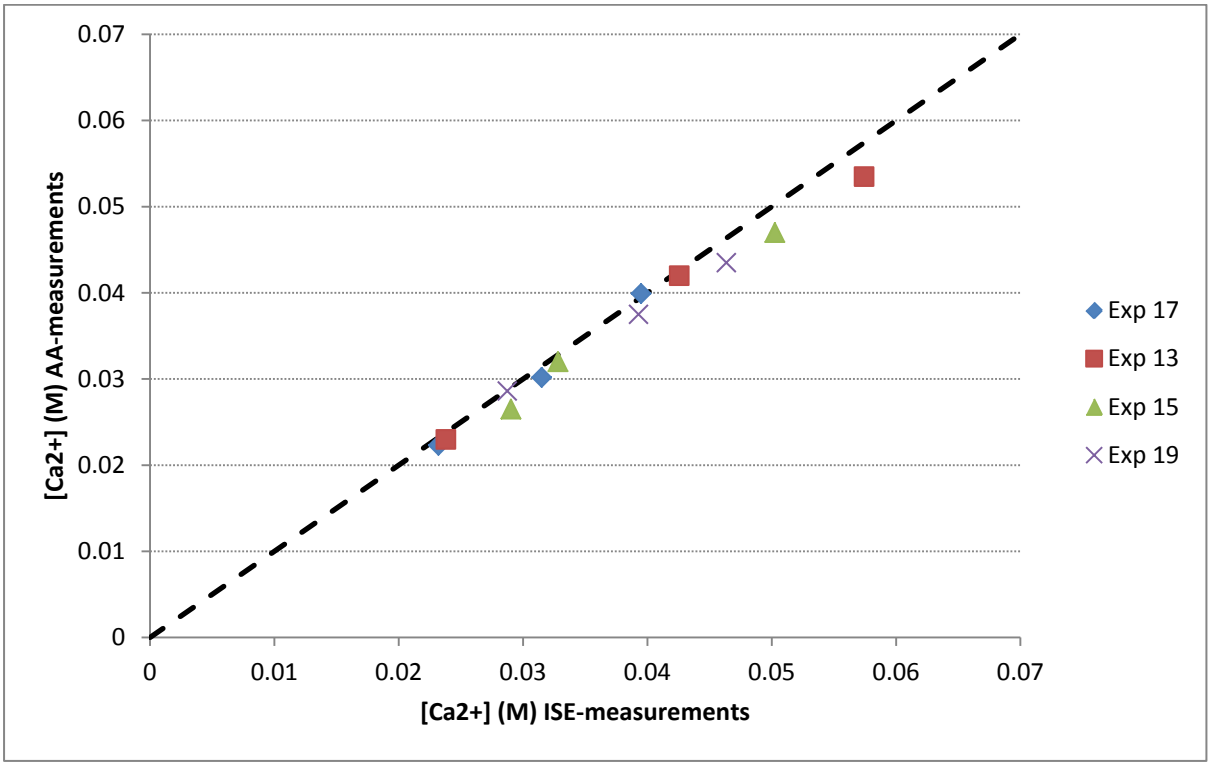

Figure 13: *Agreement between ISE-measurements and AA measurements (HYDREX)*

Chapter 6 - Results and discussion: gypsum batch crystallization from synthetically prepared aqueous solutions

6.1 Introduction

This chapter considers the crystallization of gypsum from synthetically prepared aqueous solutions, either in the presence of a phosphonate based antiscalant (HYDREX) or a polyacrylate antiscalant (BULAB). The influence and interaction between temperature, pH, antiscalant concentration, ferric chloride concentration, calcium concentration and seed concentration on the precipitation kinetics of gypsum is evaluated on the basis of two response variables: the induction time and the growth rate, inferred by 't_{C80}'. In addition to t_{C80}, k'-values are presented as an additional response variable to describe the crystal growth rate.

The current work differs from literature in that it aims to incorporate (into each test) a family of factors, which have all proven to have a distinct influence on either the rate of precipitation, or antiscalant effectiveness, when viewed in isolation in the context of calcium sulphate crystallization. The test is to witness whether these factors in combination could improve the de-activation of the inhibitory power of antiscalants on nucleation kinetics and at the same time improve precipitation of gypsum.

6.2 Antiscalant concentration 4 mg/l

Kinetic plots presented in **Figure 14** through to **Figure 17** illustrate the change in calcium concentration over time at a given set of operating conditions. The only constant in all these experimental cases is the concentration of antiscalant: 4 mg/l (BULAB or HYDREX). Three phases could be distinguished in each kinetic plot. The first is the nucleation phase or induction period (induction time), which is the time before any change in calcium concentration is observed. The second phase is the growth phase which is defined as the period where the concentration of calcium is changing. The third phase is the equilibrium phase which begins at the point in time where no further change in calcium concentration can be observed. In each figure the starting concentration vary between 0.045 M (1804 mg/l) and 0.055 M (2204 mg/l) of calcium. For each of the starting concentrations, a given theoretical equilibrium calcium concentration at a defined temperature could be achieved. The theoretical limits are drawn on each figure as dotted lines.

In **Figure 14** (where BULAB is the antiscalant and the calcium concentration is 0.055 M), experiments 1, 3 and 18 produced zero induction times and growth rates that are similar by visual comparison. Experiment 8 visually produced the fastest growth rate, reaching the equilibrium phase first. Experiment 3 produced an induction time larger than 400 minutes, after which the growth rate commenced at a rate comparable to the cases where no induction time was observed. Note that no seed was added in the case of experiment 3 and that the pH is at a high level of 10.

In **Figure 15** (where HYDREX is the antiscalant and the calcium concentration is 0.055 M) similar observations to **Figure 14** can be made. Again experiments 1, 3 and 18 produce zero induction times. This time (in the presence of HYDREX) experiment 3 produced a shorter induction period (approximately 150 minutes), compared to 400 minutes for BULAB at the same conditions. In addition experiment 1 produced a much slower growth rate compared to the experiment 3 and 18.

Note: **Table 17** and **Table 18** summarise the induction times and inferred growth rates (t_{C80}) calculated from the kinetic plots (in the presence of 4 mg/l antiscalant) displayed in **Figure 14** through to **Figure 17**. In the 'conditions' frame in the figures, 'T ()' refers to temperature in **degrees Celsius**, 'Fe ()' refers to the concentration of ferric chloride as ($FeCl_3$) in **mg/l** and 'S ()' refers to the concentration of seed in **mg/l.**

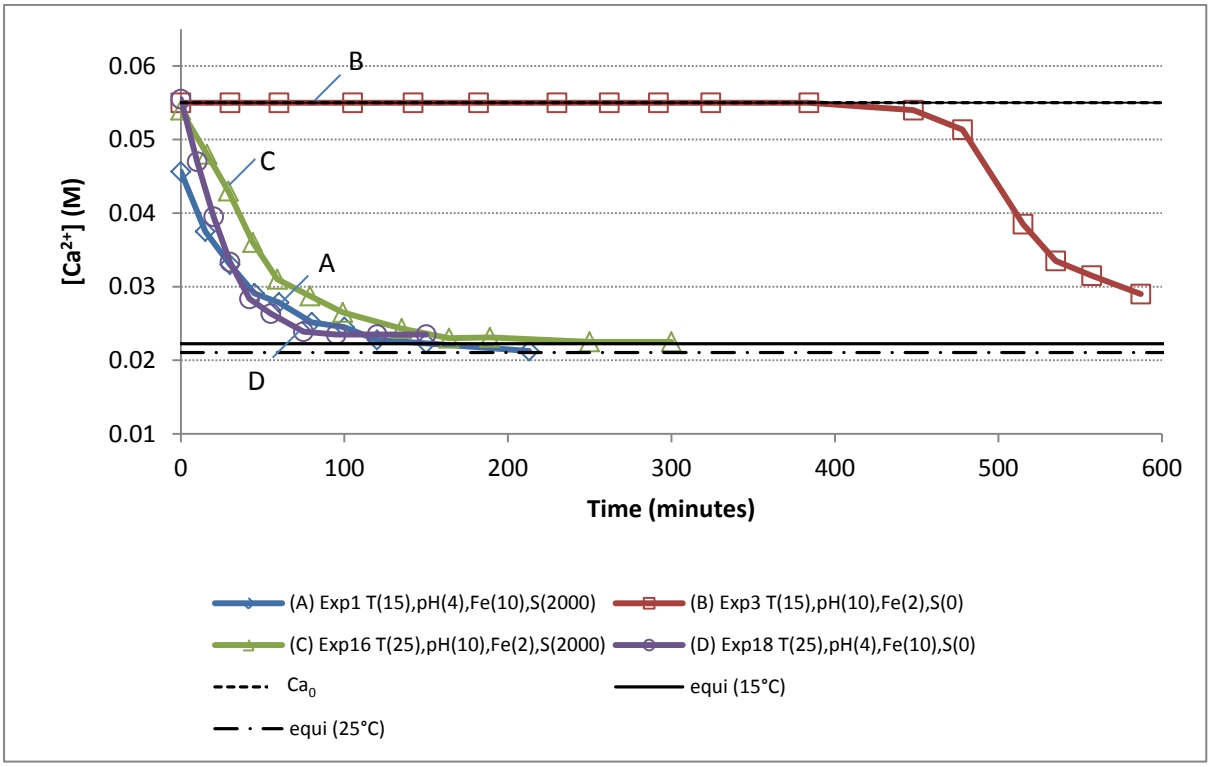

Figure 14: *Kinetic plots of gypsum precipitation, BULAB (4 mg/l), [Ca^{2+}] = 0.055 M (2204 mg/l)*

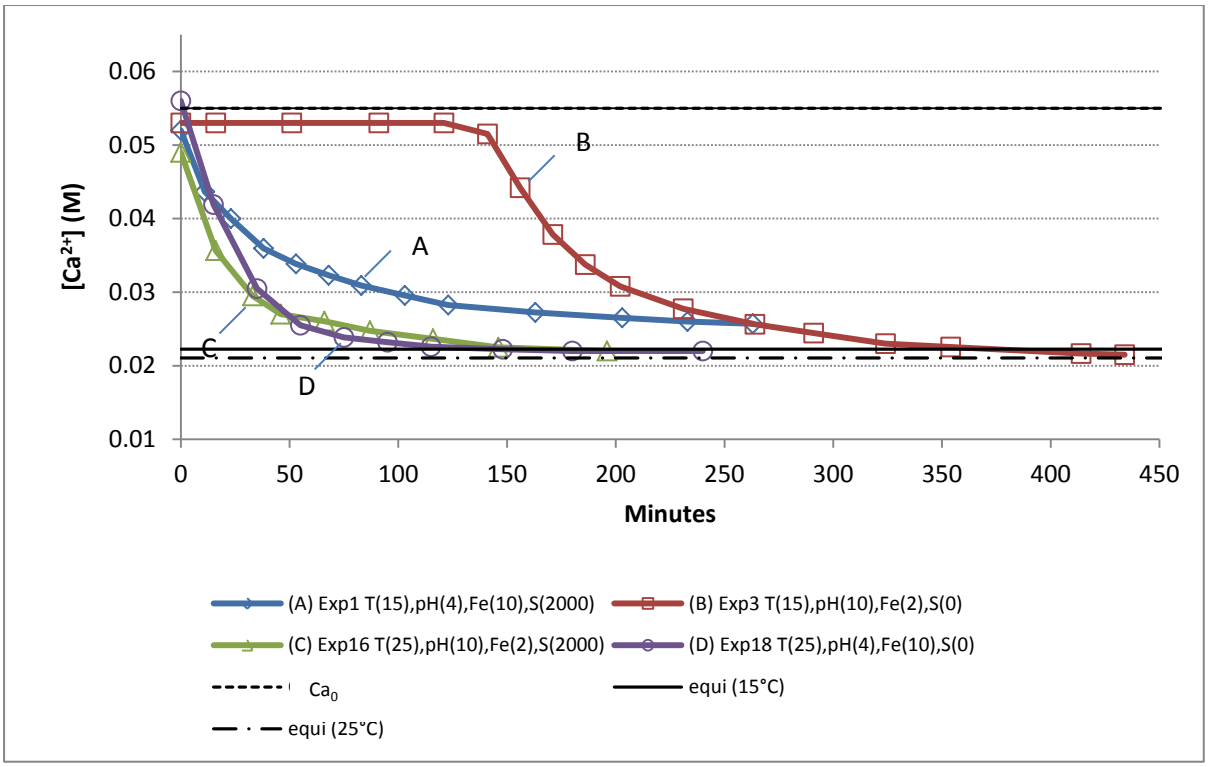

Figure 15: *Kinetic plots of gypsum precipitation, HYDREX (4 mg/l), [Ca^{2+}] = 0.055 M (2204 mg/l)*

From **Figure 16** and **Figure 17**, it is interesting to note that for BULAB and HYDREX, the kinetic plots take on a similar format regarding the magnitude of the induction times, when experiments at the same conditions for different antiscalants are compared, i.e.

t_{ind} (experiment 4) > t_{ind} (experiment 19) > t_{ind} (experiment 17 and 2).

Note that the induction times are observed when no seed is added to solution. In addition, experiment 4 (being at a higher pH than experiment 19), produced the longest induction time. Again BULAB produced longer induction times at the same conditions as HYDREX. Although experiment 17 produced zero induction time, its growth rate is very slow compared to experiment 4. Both these runs reach equilibrium at approximately the same point in time and were carried out at a pH of 10, however, the run at a temperature of 15°C (experiment 17) is far slower compared to the run at 25°C (experiment 4).

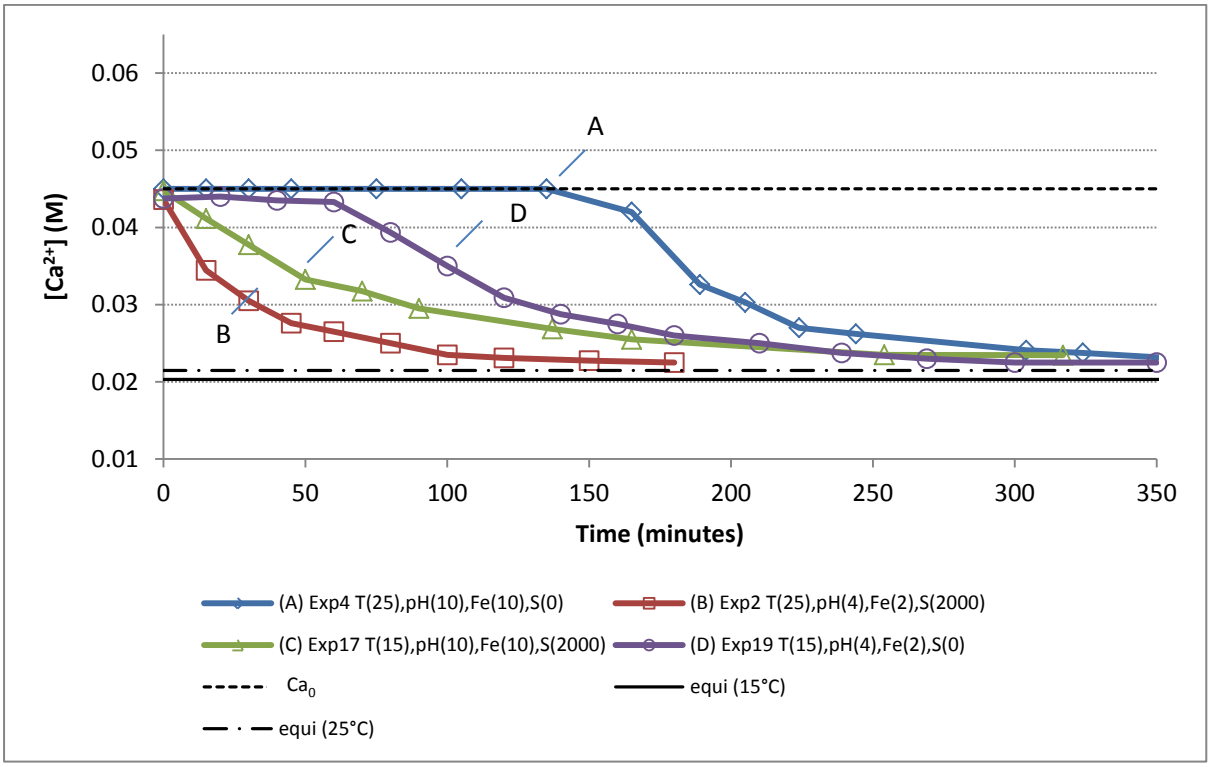

Figure 16: *Kinetic plots of gypsum precipitation, BULAB (4 mg/l), [Ca^{2+}] = 0.045 M (1804 mg/l)*

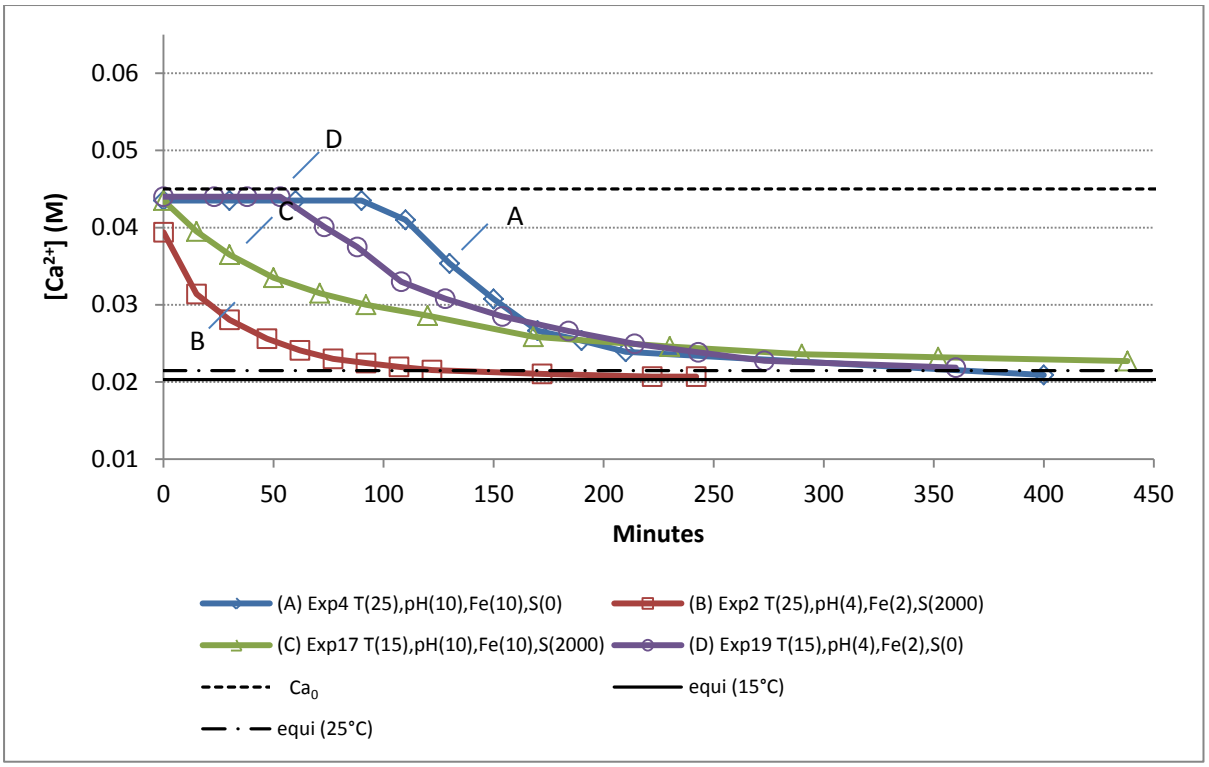

Figure 17: *Kinetic plots of gypsum precipitation, HYDREX (4 mg/l), [Ca^{2+}] = 0.045 M (1804 mg/l)*

Table 17: *Summary of kinetic data: antiscalant concentration (4 mg/l), [Ca^{2+}] = 0.055 M*

Exp ID	Conditions	Induction time (minutes)		t_{C80} (minutes)		k' ($M^{-1}min^{-1}$)	
		HYDREX	BULAB	HYDREX	BULAB	HYDREX	BULAB
1	T(15),pH(4),Fe(10),S(2000)	0	0	82	73	1.07	1.1
3	T(15),pH(10),Fe(2),S(0)	140	450	94	103	0.54	0.61
16	T(25),pH(10),Fe(2),S(2000)	0	0	44	79	1.87	0.47
18	T(25),pH(4),Fe(10),S(0)	0	0	44	38	1.42	0.97

Table 18: *Summary of kinetic data: antiscalant concentration (4 mg/l), [Ca^{2+}] = 0.045 M*

Exp ID	Conditions	Induction time (minutes)		t_{C80} (minutes)		k' ($M^{-1}min^{-1}$)	
		HYDREX	BULAB	HYDREX	BULAB	HYDREX	BULAB
2	T(25),pH(4),Fe(2),S(2000)	0	0	59	57	2.08	1.76
4	T(25),pH(10),Fe(10),S(0)	100	150	86	62	0.92	1.48
17	T(15),pH(10),Fe(10),S(2000)	0	0	156	122	0.56	0.48
19	T(15),pH(4),Fe(2),S(0)	60	70	131	104	0.67	0.72

6.3 Antiscalant concentration 12 mg/l

When comparing the experimental runs of **Figure 18** and **Figure 19** (antiscalant concentration = 12 mg/l; calcium concentration = 0.055 M), kinetic behaviour for BULAB and HYDREX are again in agreement at similar experimental conditions. Induction times for BULAB range between 0-600 minutes and for HYDREX 0- 200 minutes.

In the seeded runs (experiment 8 and 15), zero induction times were observed for both BULAB and HYDREX, with experiment 8 having a larger growth rate than experiment 15, possibly as a result of the higher temperature which would increase the kinetics of precipitation. In the no-seed scenario (experiment 6 and 13) induction times were observed, where the larger pH (both in the case of BULAB and HYDREX) produced the longer induction time. The lengthy induction time for experiment 13 can be related to numerous factors: no seed, low temperature and high pH (c.f. section 6.5.1). The retarding effect on the induction time is more pronounced for BULAB.

Consider experiment 6 for both BULAB and HYDREX: although a longer induction time is observed for experiment 6 (no seed) than for both experiment 8 and 15 (seeded), equilibrium in experiment 6 is reached sooner than for experiment 8 and 15. The faster growth rate for experiment 6 can be related to both the high temperature and low pH (c.f. section 6.5.1 and 6.5.2)

Note: **Table 19** and **Table 20** summarise the induction times and inferred growth rates (t_{C80}) calculated from the kinetic plots (in the presence of 12 mg/l antiscalant) displayed in **Figure 18** through to **Figure 21**.

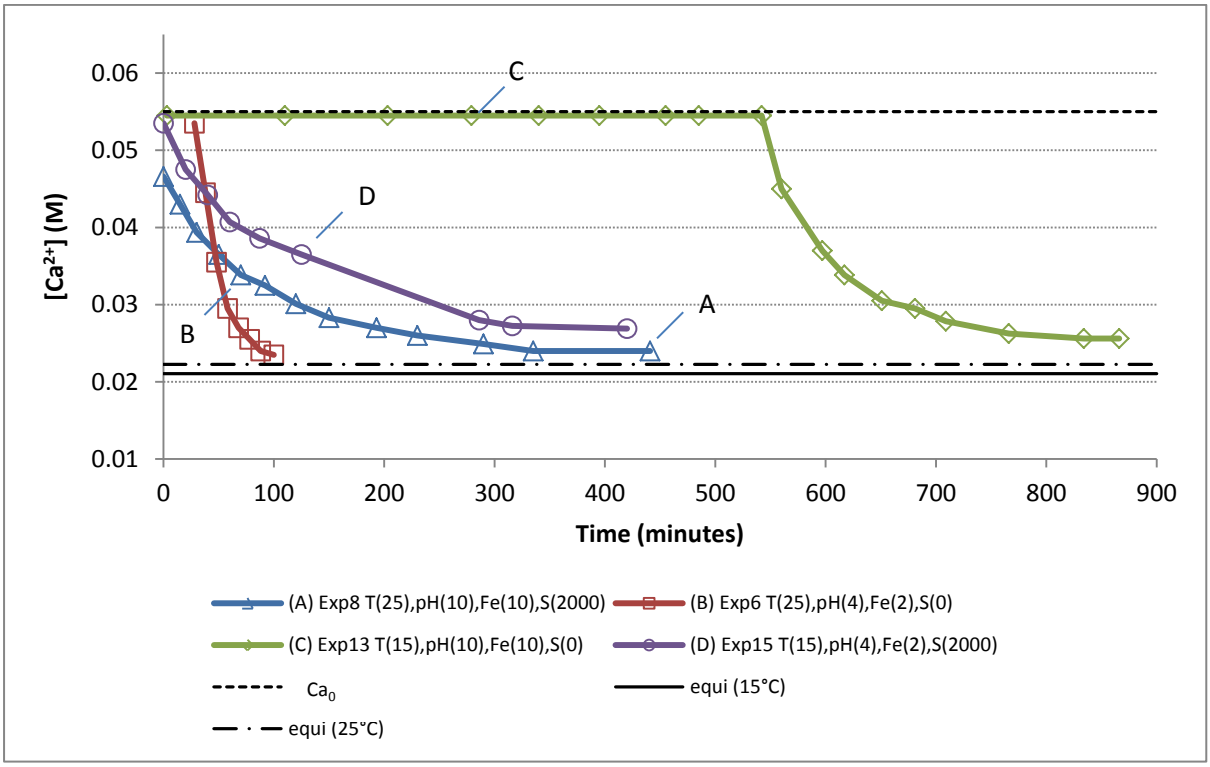

Figure 18: *Kinetic plots of gypsum precipitation, BULAB (12 mg/l), [Ca^{2+}] = 0.055 M (2204 mg/l)*

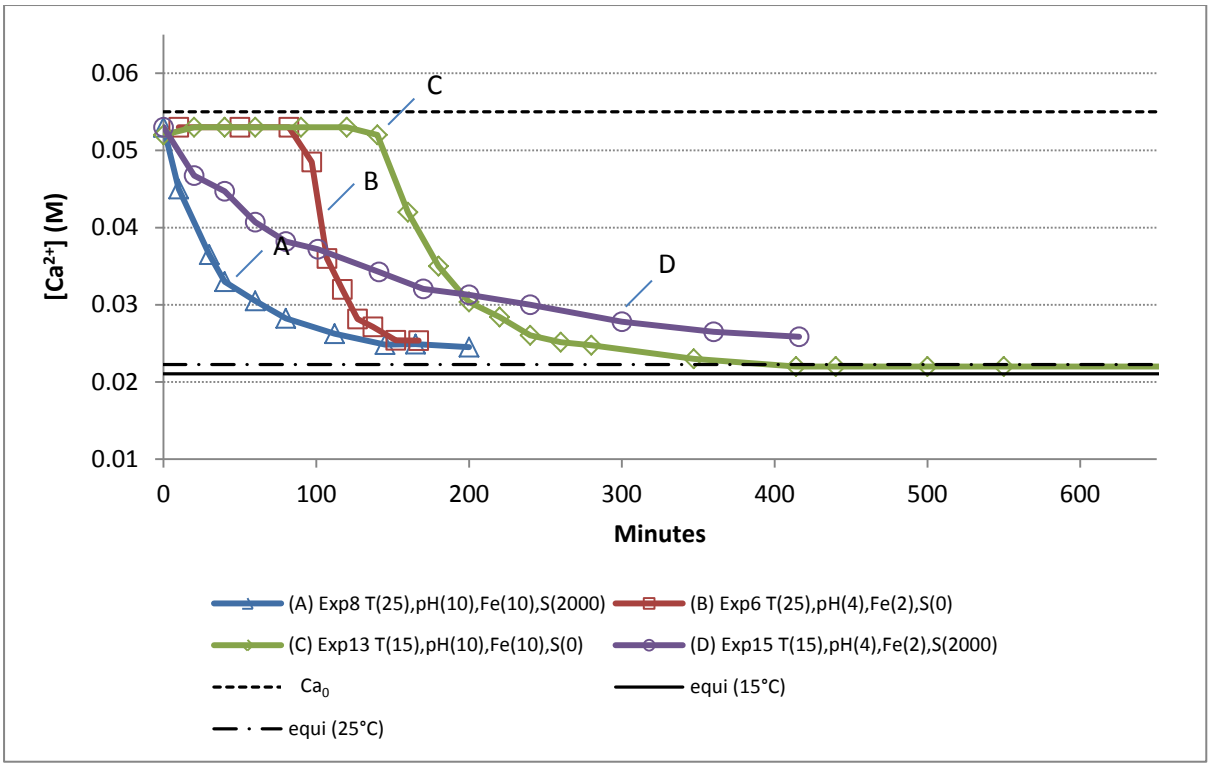

Figure 19: *Kinetic plots of gypsum precipitation, HYDREX (12 mg/l), [Ca^{2+}] = 0.055 M (2204 mg/l)*

At a lower super saturation level (0.045 M calcium), refer to **Figure 20** and **Figure 21** (**Table 19** and **Table 20**), the effect of the high antiscalant concentration on the nucleation kinetics is evident when one observes the slow kinetics of experiment 12 and 7. The induction time of experiment 12 exceeds 24 hours in the case of both BULAB and HYDREX. It is interesting to note that this experiment is carried out without seed, at a high pH and at a low temperature. Experiment 7 is again an exception, producing a lengthy induction time despite the fact that the solution is seeded. Note once more that the pH is at a high level and the temperature low, suppressing the kinetics.

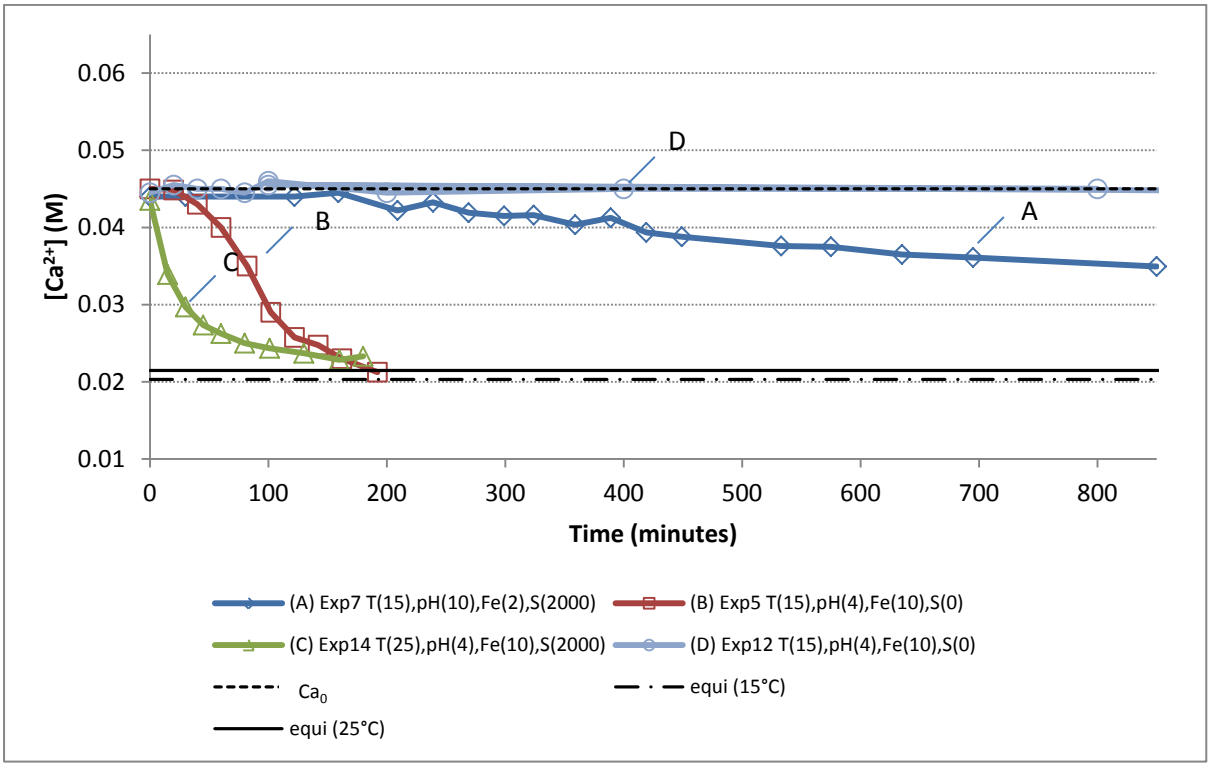

Figure 20: *Kinetic plots of gypsum precipitation, BULAB (12 mg/l), [Ca^{2+}] = 0.045 M (1804 mg/l)*

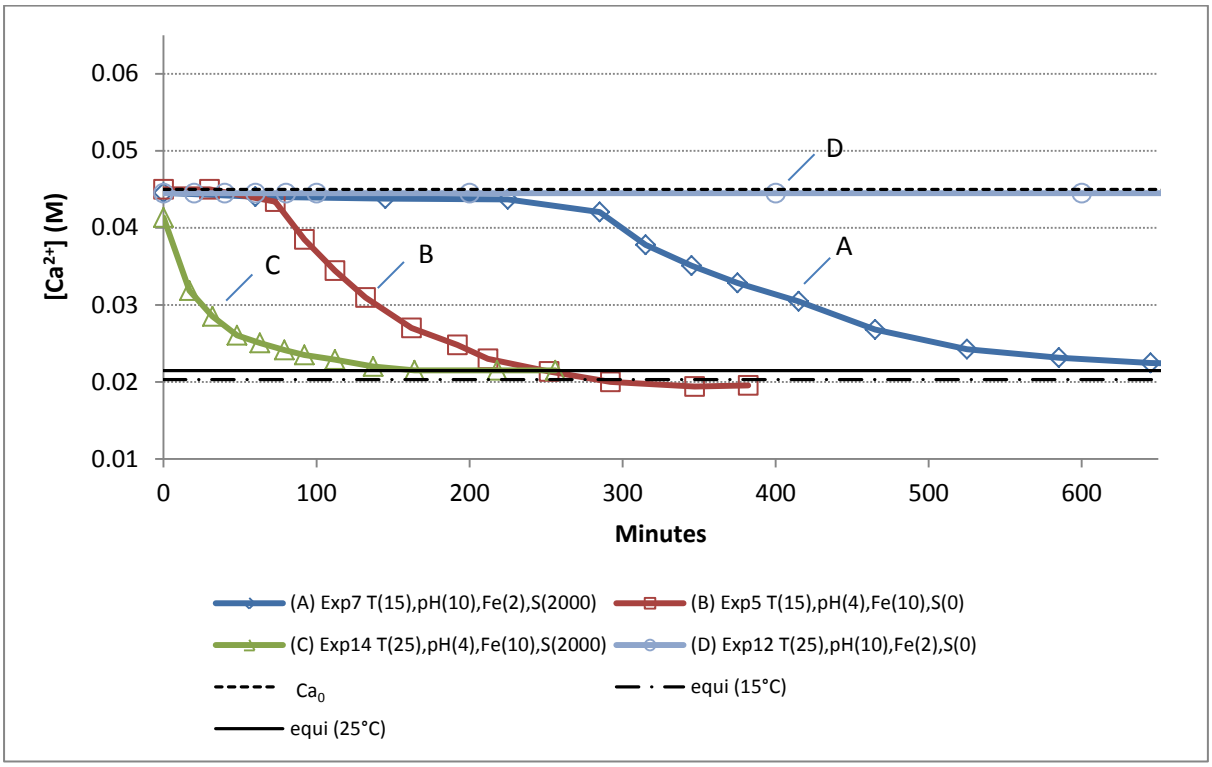

Figure 21: *Kinetic plots of gypsum precipitation, HYDREX (12 mg/l), [Ca^{2+}] = 0.045 M (1804 mg/l)*

Table 19: *Summary of kinetic data: antiscalant concentration (12 mg/l), [Ca^{2+}] = 0.055 M*

Exp ID	Conditions	Induction time (minutes)		t_{C80} (minutes)		k' ($M^{-1}min^{-1}$)	
		HYDREX	BULAB	HYDREX	BULAB	HYDREX	BULAB
6	T(25),pH(4),Fe(2),S(0)	90	30	25	30	2.87	1.88
8	T(25),pH(10),Fe(10),S(2000)	0	0	60	101	1.83	0.79
13	T(15),pH(10),Fe(10),S(0)	150	550	87	99	1.27	0.62
15	T(15),pH(4),Fe(2),S(2000)	0	0	200	206	0.29	0.26

Table 20: *Summary of kinetic data: antiscalant concentration (12 mg/l), [Ca^{2+}] = 0.045 M*

Exp ID	Conditions	Induction time (minutes)		t_{C80} (minutes)		k' ($M^{-1}min^{-1}$)	
		HYDREX	BULAB	HYDREX	BULAB	HYDREX	BULAB
5	T(15),pH(4),Fe(10),S(0)	70	30	124	80	0.34	0.4
7	T(15),pH(10),Fe(2),S(2000)	250	210	211	n/a	0.22	0.08
12	T(25),pH(10),Fe(2),S(0)	>1440	>1440	-	-	-	-
14	T(25),pH(4),Fe(10),S(2000)		0	57	45	2.10	2.7

6.4 Statistical analysis of data from experimental design

Multiple linear regression was performed on the raw data output. Variables used for regression include 1) induction times and 2) growth rates produced during precipitation tests. Raw data is presented for BULAB (**Table 47**) and HYDREX (**Table 35**) individually. Data analyses are presented in **Table 118** and **Table 119** in the appendix, c.f. section 11.11. The factors evaluated include: temperature, pH, antiscalant concentration, ferric concentration, calcium concentration and seed concentration.

The statistical significance of a factor is indicated by the P-value, which when lower than 0.05 indicates a high level of significance (Montgomery *et al.*, 1998). "P" refers to a statistical probability (1- X), where X is the probability that a factor will be significant. Therefore when the P-value of a factor is 0.05, it means that the probability that this factor will have a significant effect on the response is 95 % (or 0.95 expressed as a fraction). When a factor does not comply with these constraints, it does not necessarily mean that it has no effect on the response variable. It could be that factors having a larger effect on the response variable will mask the influence of other factors. It could also be that, within the studied range, that a given factor does not have a significant influence on the response.

Refer to **Table 21** and **Figure 22**. Both pH and seed concentration (having P-values smaller than 0.05) are considered to have a significant influence on the induction time. However, all other factors have P-values exceeding 0.05 and are therefore statistically speaking not important with regard to a change in the induction time.

Regarding the growth rate, **Table 22** and **Figure 23** indicates that temperature has a most overwhelming influence on the growth rate in the presence of both BULAB and HYDREX, having a P-value << 0.05. Statistically speaking, the calcium concentration would also have an important effect (in the presence of HYDREX) on the growth rate within the governing range of conditions. All other factors are statistically insignificant regarding the growth rate.

Table 21: *Statistical data: response variable-Induction time*

Factor	P-value	
	HYDREX	**BULAB**
Temperature	0.18	0.15
Seed concentration	0.04	0.04
Calcium concentration	0.27	0.58
pH	0.02	0.03
Antiscalant concentration	0.08	0.49
Ferric concentration	0.12	0.62

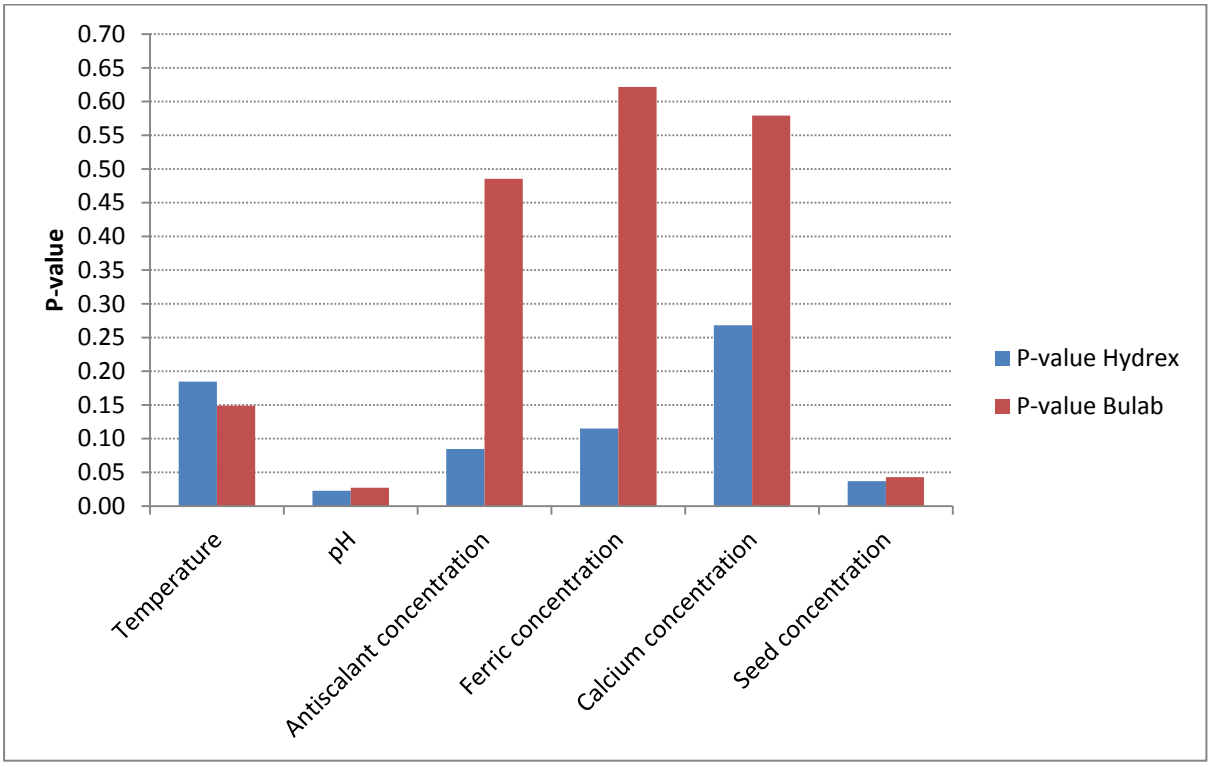

Figure 22: *Graphical display of P-values, response variable: Induction time*

Table 22: *Statistical data: response variable-* t_{C80}

Factor	P-value	
	HYDREX	**BULAB**
Temperature	0.00	0.01
Seed concentration	0.12	0.12
Calcium concentration	0.03	0.96
pH	0.37	0.27
Antiscalant concentration	0.19	0.30
Ferric concentration	0.19	0.22

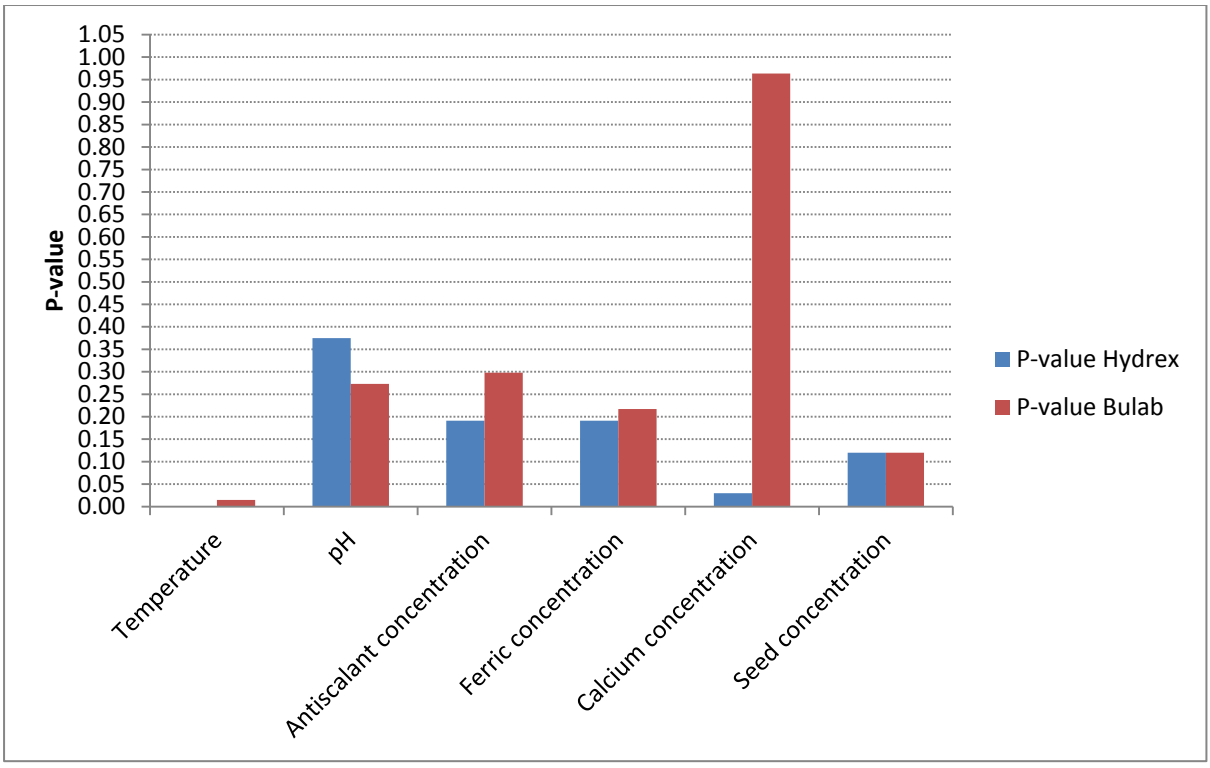

Figure 23: *Graphical display of P-values, response variable:* t_{C80}

6.5 Discussion

The following discussion will help to relate the changes in the induction period and the crystal growth rate to the changes in temperature, pH, antiscalant concentration, ferric concentration, calcium concentration, seed type and seed concentration.

6.5.1 Induction time

6.5.1.1 Temperature

In literature it is observed (classical nucleation theory) that the induction time of precipitation is a strong function of temperature (Söhnel and Mullin, 1988). Literature further points out that the induction period will typically decrease by a factor of two for every 10°C increase in temperature (Liu and Nancollas, 1975; Amjad and Hooley, 1986; Amjad, 1988). The same observation was made during baseline tests. At a calcium concentration of 0.045 M, ($[Ca^{2+}]=[SO_4^{2-}]$), the induction time of a solution supersaturated with gypsum decreased from 50 minutes to 25 minutes when the temperature was increased from 15°C to 25°C. When the calcium concentration in solution was increased to 0.055 M, the induction time changed from 25 minutes to 12 minutes for a 10°C change in temperature (15°C to 25°C). In both cases the induction time decreased by a factor 2 for a 10°C increase in temperature.

Under the governing experimental conditions, the relationship between the temperature and the induction time is not clear. According to the statistical analysis on the current range of data (considering only the P-value), it is apparent that the temperature has a less pronounced effect on the induction time than the pH or the seed concentration.

On the contrary, when the data in **Figure 24** is considered, the temperature - induction time relationship appears to be prominent. For a given antiscalant (either BULAB or HYDREX), the induction times are on average noticeably higher at 15°C compared to 25°C. There is however no clear mathematical relationship that can be formulated.

In some cases BULAB appear to be more effective at low temperatures than HYDREX: consider the induction times of experiment 3, experiment 13 and experiment 19. However, when experiment 5 and experiment 7 are considered, HYDREX seems to be the more efficient antiscalant. At high temperatures, experiment 4 and experiment 6 do not exhibit consistency with regard to the effectiveness of BULAB or HYDREX. It is therefore uncertain which of BULAB or HYDREX is more efficient at a given temperature.

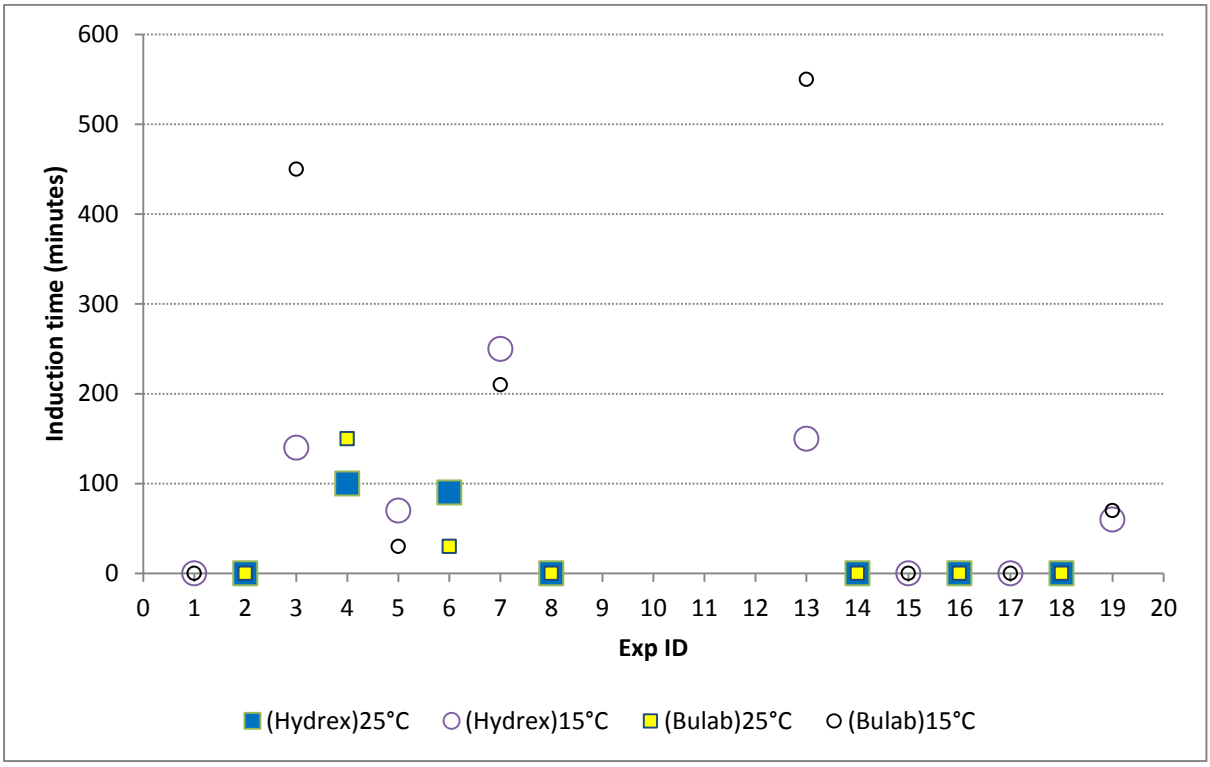

Figure 24: *Induction times at 15°C and 25°C*

6.5.1.2 Seed

6.5.1.2.1 Homogeneous seeded precipitation

According to Amjad and Hooley (1986), Amjad (1985), and Liu and Nancollas (1970), when a sufficient amount of seed is added to a super saturated solution (and their growth sites are not occupied by impurities), crystal growth will take place in the absence of a nucleation phase or **induction time**. This means that seed provides the nuclei for further growth to continue. When no seed is present, or when the amount of seed is insufficient, nuclei are first formed (induction period) after which crystal growth takes place.

At low antiscalant concentrations (4 mg/l), seed addition (2000 mg/l) appears to be effective in order to completely remove the induction period (Refer to **Figure 14** through to **Figure 17**). There is a clear distinction between the nucleation period of the un-seeded and seeded solutions. Un-seeded solutions (experiment 3, experiment 4 and experiment 19) exhibit clearly defined induction times. In addition induction times for BULAB are longer compared to HYDREX.

At higher antiscalant concentrations (12 mg/l), again the impact of seed addition on the induction period is evident (refer to **Figure 18** though to **Figure 21**). In most cases, seed addition eliminated the induction period. Of the seeded solutions, the exception is experiment 7, which displayed an

induction time for both BULAB and HYDREX solutions. A number of reasons could be provided, which will become clear during later discussion. Take note of the following in this experimental run: low temperature, high pH and low ferric concentration. Low temperature causes nucleation kinetics and crystal growth to slow down and increases the induction time. A change in pH affects the inhibitory quality of the antiscalant: at a high pH both BULAB and HYDREX are more effective (c.f. section 6.5.1.4). Ferric chloride will complex with antiscalant molecules (c.f. section 6.5.1.6). When the concentration of ferric chloride is low, the interaction between ferric and antiscalants are therefore limited and the antiscalant are more effective in lengthening the induction period.

For the un-seeded solutions, the induction times vary between zero minutes at the minimum and induction times larger than 24 hours, depending on the interaction of the other factors.

Experiment 18 is an example of an un-seeded solution exhibiting zero induction time. In this experiment both the temperature (25°C) and the calcium concentration (0.055 M) promote a larger nucleation rate whereas the higher ferric concentration (10 mg/l) and low pH (4) promote reduced antiscalant efficiency. At a low antiscalant concentration of 4 mg/l, all the conditions are suitable for rapid nucleation.

Conversely the 'un-seeded' experiment which attracts some attention is experiment 12, displaying an induction period in excess of 24 hours. Although this run was performed at a high temperature (25°C), a high antiscalant concentration (12 mg/l) combined with a high pH and low ferric concentration promote high antiscalant efficiency and therefore inhibited nucleation kinetics.

To illustrate the induction time-seed effect, refer to **Figure 25**. (Notice that the 'filled' markers represent all the runs where seed was added and the 'un-filled' markers represent the un-seeded solutions.)

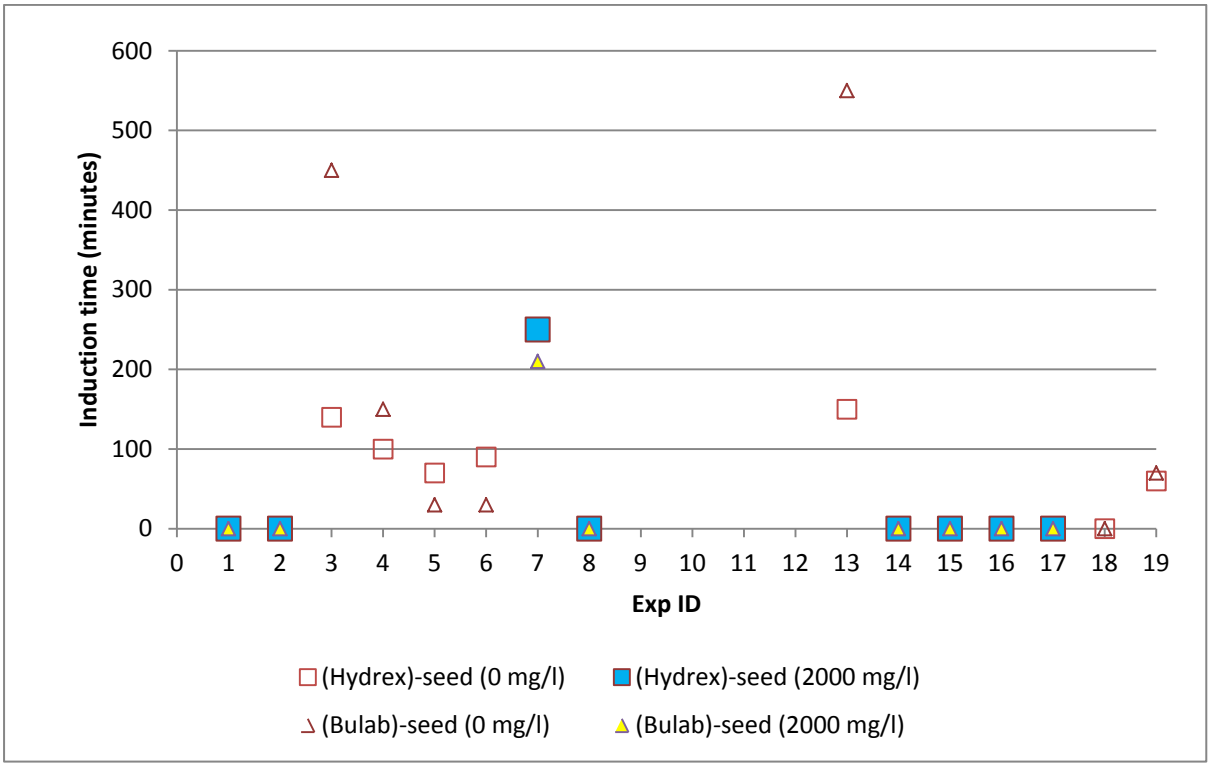

Figure 25: *Induction times at different seed concentrations*

6.5.1.2.2 Heterogeneous seeded precipitation

All cases referred to thus far have only related to the use of pure gypsum seed. **Figure 26** compares the use of lime seed, gypsum seed and mixed seed (lime and gypsum). The conditions of experiment 8 were selected for comparative study of different seed since at these conditions the most effective precipitation was obtained: zero induction time and a moderate growth rate (compared to the average growth rate when all runs are taken into account).

When only gypsum was used (refer to **Figure 26** and **Table 23**), zero induction time was observed. When only lime was used, induction times both in the presence of HYDREX (150 minutes) and BULAB (50 minutes) was observed. In addition to the observed induction time for the 'lime-experiment', the use of lime instead of gypsum caused the growth rate to increase by roughly a factor two (for an explanation on the effect of seed on the growth rate, c.f. section 6.5.2.2). Moreover the use of a combination of lime and gypsum caused the induction time to be eliminated with the added benefit of a growth rate comparable to when only lime was used.

During heterogeneous seeded precipitation (such as the use of lime, although lime-seeding is not strictly seeding since it also causes some chemical change in solution), an induction time prior to precipitation will occur, when there is a lack of identifiable growth sites for the

precipitating phase (Gill & Nancollas,1979; Yang *et al.,* 2008). With the addition of lime to the solution (super saturated with gypsum), immediately a lack of 'identifiable' growth sites exist in which case additional nucleation in the bulk solution and on the crystal (lime) surface need to take place before crystal growth (gypsum) can commence, hence forming an induction period.

Lime partially dissolves to increase the calcium concentration and free hydroxyl ions in solution. The free hydroxyl ions result in an increase in the pH of the working solution to approximately 12.3. It is probable that the increase in the pH causes the inhibitory power of the antiscalant (both BULAB and HYDREX) to increase, resulting in the extension of the induction time (c.f. section 6.5.1.4). In addition, the free calcium (added by the dissolution of lime) increases the total dissolved calcium 0.055 M to 0.075 M, which increases the saturation level. Nonetheless, the combination of a lack of growth sites as well as the enhanced antiscalant efficiency (by pH increase) causes the nucleation to be retarded to such an extent that the increased benefit of a higher precipitation potential (due to calcium addition) appears to be insignificant.

When gypsum and lime seed are used in combination, gypsum provide nucleation sites (sufficient to effect precipitation), whilst the addition of lime increases the calcium concentration to enhance the precipitation potential of the solution. In this case it appears that the increase in pH has little or no effect on the nucleation phase. Antiscalants may adhere to gypsum crystals or free calcium, whilst there is still sufficient nucleation sites left to attract excess free calcium (provided by lime dissolution) to precipitate. Rahardianto *et al.* (2010) used lime addition to scavenge (neutralise) antiscalant behaviour through $CaCO_3$ precipitation, which necessitates the presence of HCO_3^{-1} or CO_3^{-2} in solution. The extent of the scavenging process was found to be a factor of the lime concentration (1.35-2.7 mM lime was used). In this study, the concentration of lime added is much higher (34 mM). However, because no carbonate ions are present, $CaCO_3$ precipitation and therefore scavenging of antiscalants by the same method that Rahardianto *et al.* (2010) used is impossible.

It is interesting to note that HYDREX produced longer induction times (3 times larger than BULAB) in the presence of lime. It is possible that the shorter induction time in the presence of BULAB could be a result of stronger adsorption of BULAB molecules onto the lime crystals.

When seeding is applied to RO concentrate as a de-super saturation mechanism (before water is recycled back to the RO-feed), great care should be taken to make sure even the slightest trace of seed is removed from the solution. Even traces of seed can easily trigger precipitation, causing unwanted scaling in the system.

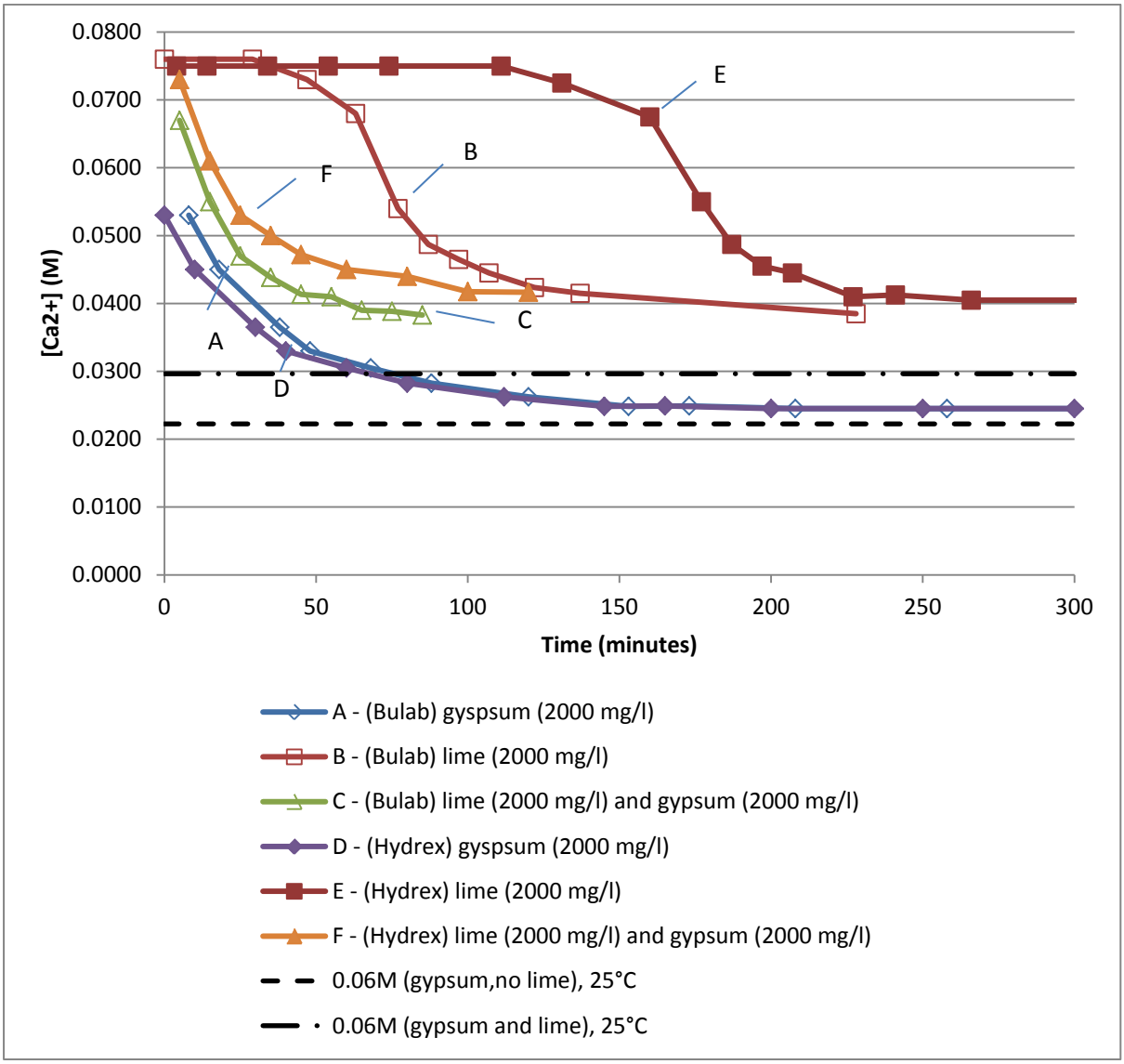

Figure 26: *Kinetic plots of experiment 8, T (25), pH (10), Fe (25), S (2000); AS (12 mg/l); [Ca^{2+}] =0.055 M using different seed types, raw data in* **Table 58** *and* **Table 59**. *(Dotted lines signify equilibrium concentrations)*

Table 23: *Summary of kinetic data: antiscalant concentration (12 mg/l), [Ca^{2+}] = 0.055 M*

Exp ID	Conditions	Induction time (minutes)		t_{c80} (minutes)	
		HYDREX	BULAB	HYDREX	BULAB
8	T(25),pH(10),Fe(10),S(2000) gypsum	0	0	60	100
8	T(25),pH(10),Fe(10),S(2000) lime	150	50	36	45
8	T(25),pH(10),Fe(10),S(2000) gypsum and lime	0	0	39	48

6.5.1.3 Calcium concentration

Literature points out that the process of nucleation is strongly affected by the level of super saturation (calcium concentration) of a precipitating solution. In contrast statistical analyses (**Table 21**) indicate that a change in 0.01 M in the calcium concentration from 0.045 M to 0.055 M under the governing experimental conditions does not have a significant effect on the change in the induction period, both in the presence of HYDREX and BULAB. It could be reasoned that factors such as the addition of seed (discussed in the previous subsection) or a change in pH, which more strongly affects the induction period, causes the effect which a change in calcium concentration has on the induction period to be subordinate. Consider the 'no-seed' cases both in the presence of HYDREX and BULAB in **Figure 27** and **Figure 28** and **Table 24**. One would naturally suspect that when the level of super saturation is increased it would lead to an increase in the nucleation kinetics. However within the studied range of conditions it seems as if the effect of the pH (In the 'no-seed' cases) overshadows the effect of a changing solution concentration. Both in the presence of HYDREX and BULAB, a high pH causes the induction period to be higher irrespective of the solution concentration.

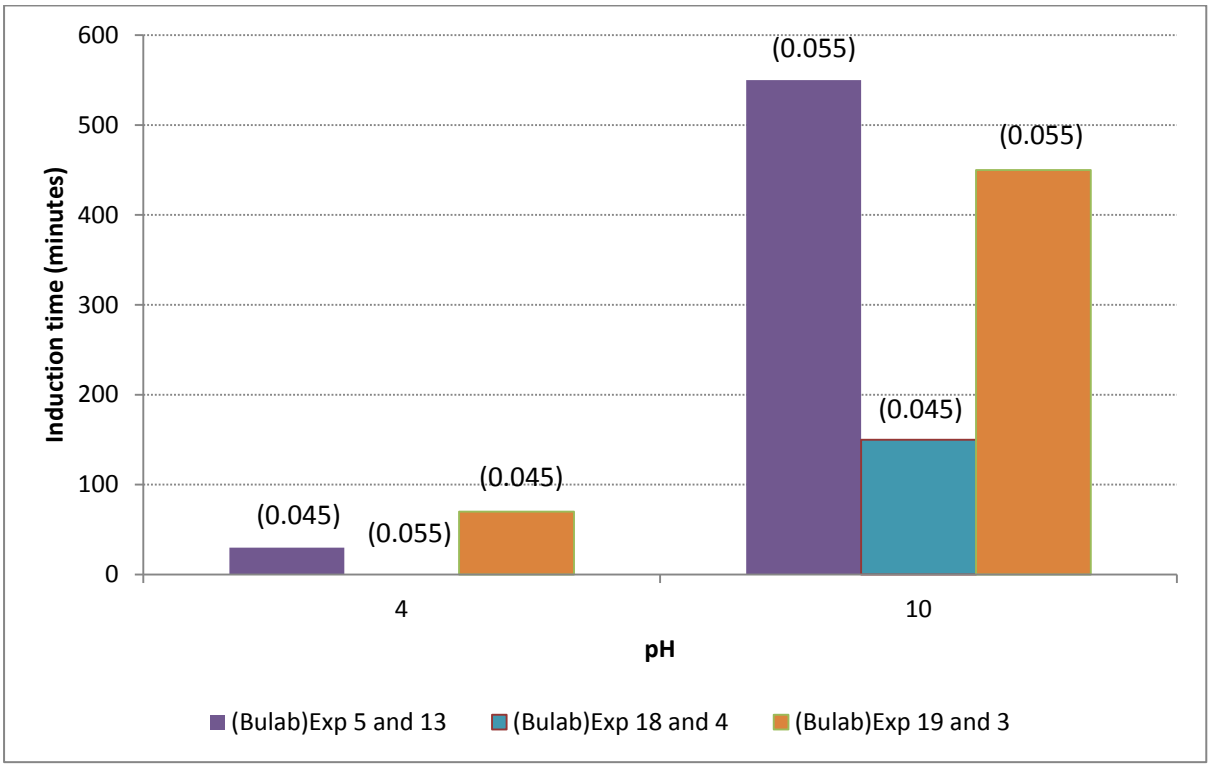

Figure 27: *Interaction between calcium concentration and pH on the induction time (BULAB)-bracketed values indicates the calcium concentration at the corresponding pH value.*

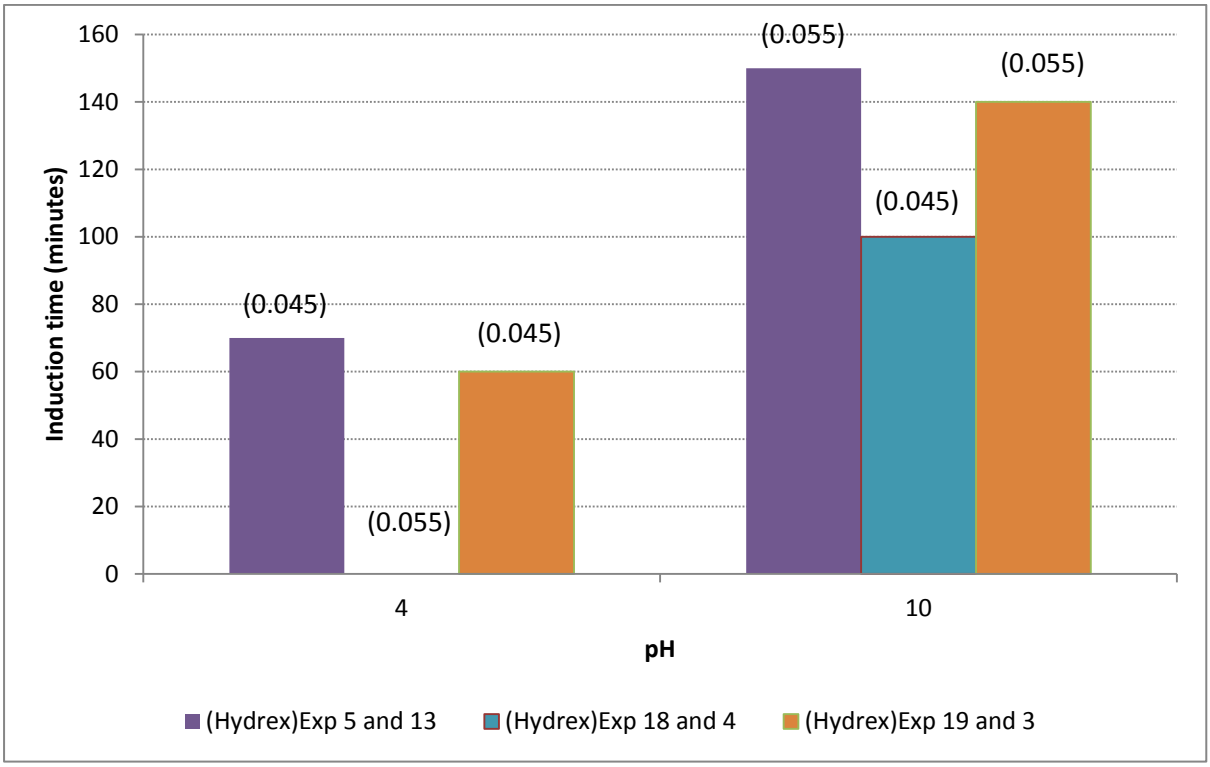

Figure 28: *Interaction between calcium concentration and pH on the induction time (HYDREX) - bracketed values indicates the calcium concentration (M) at the corresponding pH value.*

Table 24: *Interaction between calcium concentration and pH on the induction time (shown in* **Figure 27** *and* **Figure 28**.*)*

Exp ID	Conditions	Induction time (minutes)	
		HYDREX	BULAB
5	T(15),pH(4),AS(12),Fe(10),Ca(0.045),S(0)	70	30
13	T(15),pH(10),AS(12),Fe(10),Ca(0.055),S(0)	150	550
18	T(25),pH(4),AS(4),Fe(10),Ca(0.055),S(0)	0	0
4	T(25),pH(10),AS(4),Fe(10),Ca(0.045),S(0)	100	150
19	T(15),pH(4),AS(4),Fe(2),Ca(0.045),S(0)	60	70
3	T(15),pH(10),AS(4),Fe(2),Ca(0.055),S(0)	140	450

6.5.1.4 pH

Gypsum precipitation is not pH dependent. However, in the previous sections the very strong influence of a change in pH on the induction period cannot be ignored.

The pH-induction time relationship probably depends on the relationship or interaction between the pH, antiscalant adsorption efficiency and ferric speciation. The effect of the ferric speciation will be ruled out in this study as the ferric species are relatively constant within the studied pH range (4-10) where $Fe(OH)_3$ is the predominant molecular species.

Research has shown that the dissociation of both phosphate based antiscalants (HYDREX) as well as polyacrylate antiscalants (BULAB) strongly depends on a change in pH. At a low pH, antiscalants are in an un-dissociated state, causing the anionic charge density of the antiscalant (very important for interaction of the polymer with the crystal surface- which is positively charged), to be reduced. Consequently it reduces the electrostatic interaction between the antiscalant and the crystal surface. At a low pH, there is a weak interaction between the antiscalant and the gypsum crystal. At a high pH, the antiscalant molecules are in their fully dissociated state (high anionic charge density) and the antiscalant is strongly attracted to the crystal surface.

The observations concerning the pH-induction time relationship in the current study is congruent to what literature suggests. At low pH values (4), lower induction times are observed (0-70 minutes for HYDREX and BULAB) and at higher pH values (10), larger induction times are observed (100-150 minutes for HYDREX; 150-550 minutes for BULAB). The effect of pH is probably most clearly observed in **Figure 27** and **Figure 28** in the 'no-seed' cases. The effect of pH on the efficiency of the antiscalants under consideration appears to be stronger with regard to BULAB. At a low pH (4), the induction times for experiments conducted in the presence of BULAB were roughly equal (experiment 19) or lower (experiment 5) compared to experiments conducted in the presence of HYDREX. On the other hand, at a high pH (10), the induction times for experiments in the presence of BULAB were considerably larger compared to experiments carried out in the presence of HYDREX (refer to **Table 24**). The difference between the two antiscalants possibly lie in the fact that the more efficient antiscalant at a higher pH (which according to data from the designed experiments is BULAB), produces more dissociated groups that would increase its bonding capacity.

In an extreme case, the strong adsorption capacity of both HYDREX and BULAB (experiment 12 - **Figure 20** and **Figure 21**) is displayed at a pH of 10. In these cases the induction time exceeds 24 hours for both HYDREX and BULAB, even though these tests were performed at a relatively high temperature of 25°C which normally produces relatively fast kinetics.

To further evaluate the pH-antiscalant-induction time relationship, some tests were performed by only changing the pH (refer to **Figure 29**). Again at the lower end of the pH values evaluated (3.1), the BULAB was less efficient, exhibiting a lower induction time compared to HYDREX. An increase in the pH to 9 caused the efficiency of both antiscalants to increase to a considerable extent (refer to **Table 25**). It is interesting to note however that HYDREX exhibits a larger induction period (greater efficiency) even at the higher end of pH values evaluated. From the material specifications (**Table 13**) it can be observed that the acidity of BULAB (polyacrylic acid) is slightly higher than that of BULAB (phosphonic acid). Weijnen and van Rosmalen (1985) stated that an antiscalant with a higher acidity would produce a lower amount of dissociated groups as the pH increases, which would render it less effective than a antiscalant producing more dissociated groups, which confirms the observation made with respect to HYDREX and BULAB. The observations, with respect to the influence of pH on the induction time of precipitation in the presence of either HYDREX or BULAB (with the addition of foreign additives such as ferric chloride and seed material), show a different result to when no additives are in the water. It could be that the interaction between the ferric ions in the solution and the antiscalants distort the pure pH – antiscalant interaction.

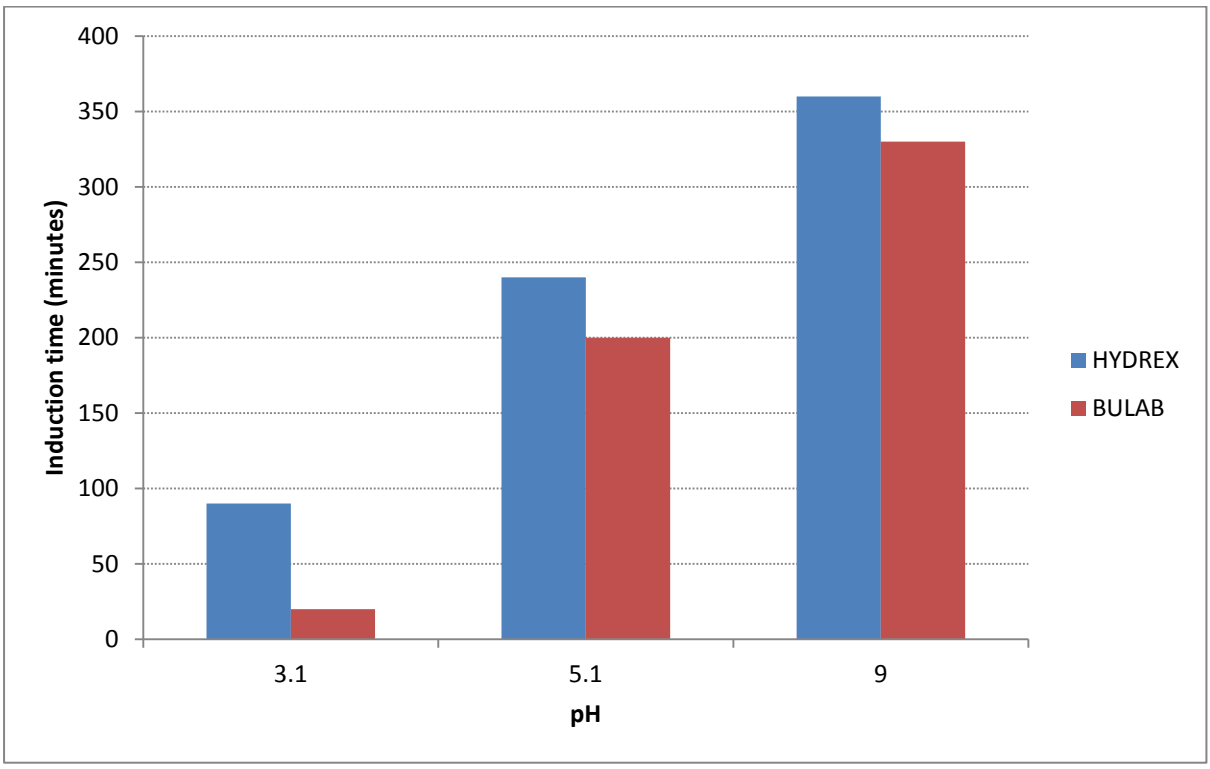

Figure 29: *pH-induction time relationship tests for HYDREX and BULAB, T (25°C), AS (4 mg/l), Ca (0.055 M)*

Table 25: *Summary of pH-induction time tests for HYDREX and BULAB (shown in* **Figure 29***)*

Conditions	Induction time (minutes)	
	HYDREX	BULAB
T(25),**pH(3.1)**,AS(4),Fe(0),Ca(0.055),S(0)	90	20
T(25),**pH(5.1)**,AS(4),Fe(0),Ca(0.055),S(0)	240	200
T(25),**pH(9)**,AS(4),Fe(0),Ca(0.055),S(0)	360	330

The current work corresponds well with work by Amjad (1988), Weijnen and van Rosmalen (1985) and Oner *et al.* (1998), who all showed that at low pH values (2.5-3.5) the retarding power of polyacrylic acid (such as BULAB) is insignificant. However, the increase of the antiscalant efficiency at larger pH values are contrary to findings by McCartney & Alexander (1958), Amjad (1988), Weijnen & van Rosmalen (1985) and Oner *et al.* (1998) who observed that the efficiency of polyacrylic acid antiscalants reached a plateau at a pH of 5-6. In fact these researchers did not increase the pH beyond this point to observe whether the efficiency of the antiscalant would actually further increase. In the current study the efficiency of BULAB continues to increase with an increase in pH (observed up to a pH of 9) without reaching the same observed plateau.

With respect to phosphonate based antiscalants (such as HYDREX), Weijnen *et al.* (1983), showed that at a pH of 3.5 the inhibitory capacity of a phosphonate based antiscalant was almost zero. In contrast to this finding, HYDREX is still very efficient at a pH of 3.1, resulting in an induction period of 90 minutes. He *et al.* (1994) further showed that the efficiency of a phosphonate antiscalant increased up to a pH of 7, after which no change was observed upon further increase. Again the current research refutes these findings, as the induction period and therefore the inhibiting power of HYDREX, was found to increase upon increasing the pH.

When we consider overriding the effect of an antiscalant, lowering the pH would reduce its inhibitory power in the case of both phosphonate based antiscalants and polyacrylate antiscalants.

6.5.1.5 Antiscalant concentration

Research (c.f. section 2.9.1) has shown that an increase in the antiscalant concentration should cause an increase in the induction period. This was confirmed by preliminary tests where it was shown that an increase from 1 mg/l to 2 mg/l antiscalant [T (25°C), Ca (0.045 M)] caused an increase in the induction time from +120 minutes to +200 minutes, which is almost a two-fold increase.

Some additional tests (refer to **Figure 30**) were performed at antiscalant concentrations of 0 mg/l, 2 mg/l and 4 mg/l for both HYDREX and BULAB. For both antiscalants a considerable increase in induction time was observed with an increase in antiscalant concentration. At 2 mg/l the induction times for BULAB (110 minutes) and HYDREX (100 minutes) were comparable. When the antiscalant concentration was increased to 4 mg/l, a clear difference between the two antiscalants (BULAB: 200 minutes; HYDREX: 260 minutes) was observed.

The considerable increase in the induction period with only an increase of 2 to 4 mg/l of antiscalant suggests that the mechanism of inhibition could not be that of chelation as explained by Liu & Nancollas (1973), but that adsorption is the prevalent mechanism. Antiscalants adsorb onto the most active growth sites on the surface of the already formed crystals or interact with the forming nuclei, while growth sites of lower energy continue to grow (Amjad, 1985). This growth process is suggested to continue until the inhibitor molecule is completely overgrown and absorbed into the crystal lattice, after which growth will commence again at a measurable rate. When the antiscalant concentration increases, more growth sites on the crystal surface are occupied and fewer growth sites of lower energy are able to grow. This extends the time necessary to overgrow and absorb the inhibitor molecule into the crystal structure.

Contrary to what literature and preliminary test results have shown, the statistical data (**Table 21**) give the idea that the change in antiscalant concentration (4 mg/l to 12 mg/l) of both HYDREX and BULAB plays an insignificant role with respect to the change in the induction time at the governing conditions of the designed experiments. Again it could be argued that other factors such as seeding and pH (which we have shown to have a significant effect on the induction time) mask the effect of the changing antiscalant concentration on the induction time.

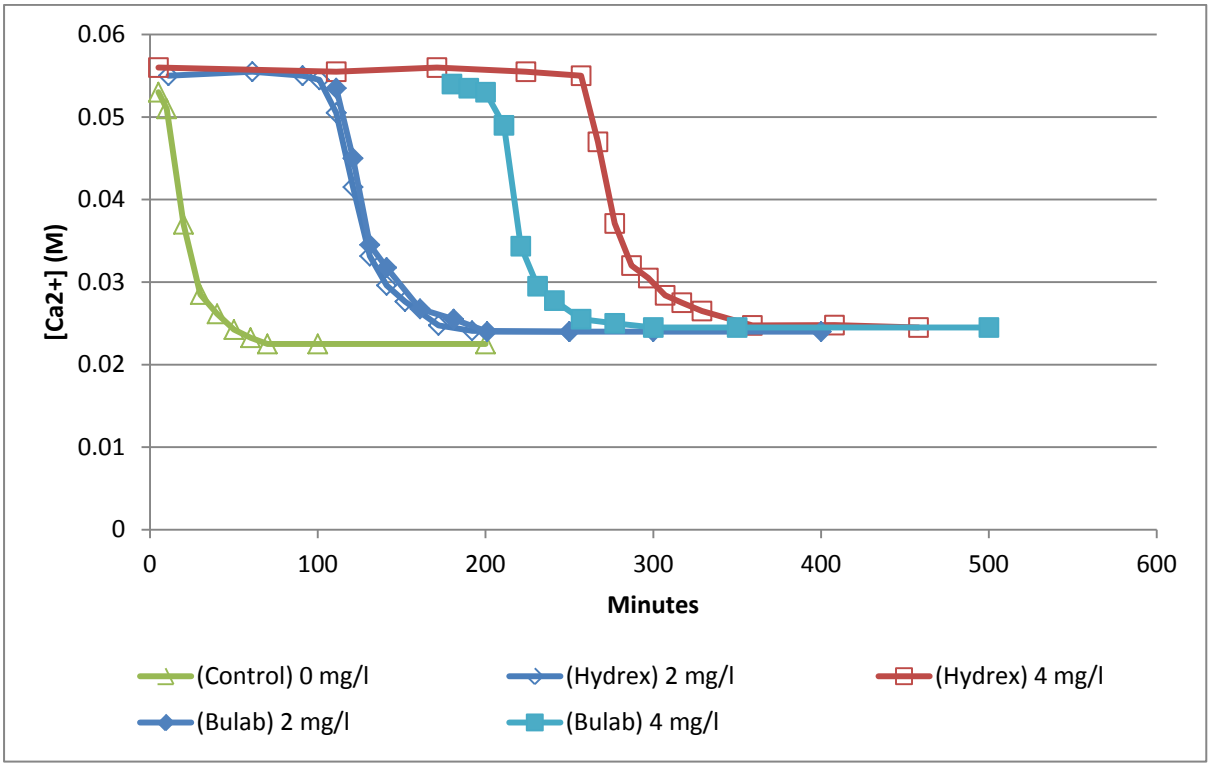

Figure 30: *Antiscalant-induction time relationship for HYDREX and BULAB, T (25°C), Ca (0.055 M), theoretical*

However, if we consider the kinetic data, there are certain data pairs where only the antiscalant concentration and ferric concentration vary (refer to **Figure 31** and **Figure 32**). In the majority of these cases, irrespective of the ferric concentration, the induction period is higher at the higher antiscalant concentration (which again confirms literature observations). Note that no clear mathematical relationship can be drawn between the change in antiscalant concentration and the change in induction time. Keep in mind that the relative differences between the induction times are as a result of a complex interaction of changing factors.

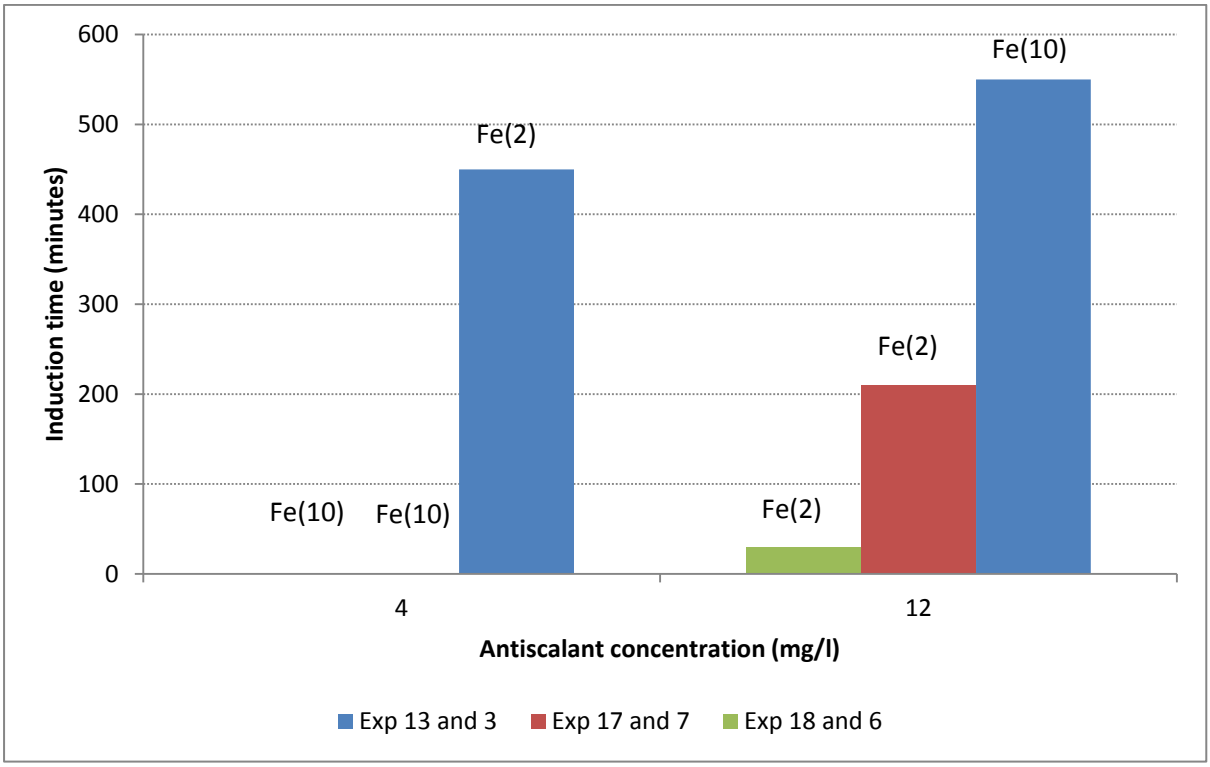

Figure 31: *Antiscalant concentration (BULAB) – induction time relationship- bracketed values indicate the ferric chloride concentration (mg/l) at the corresponding antiscalant concentration.*

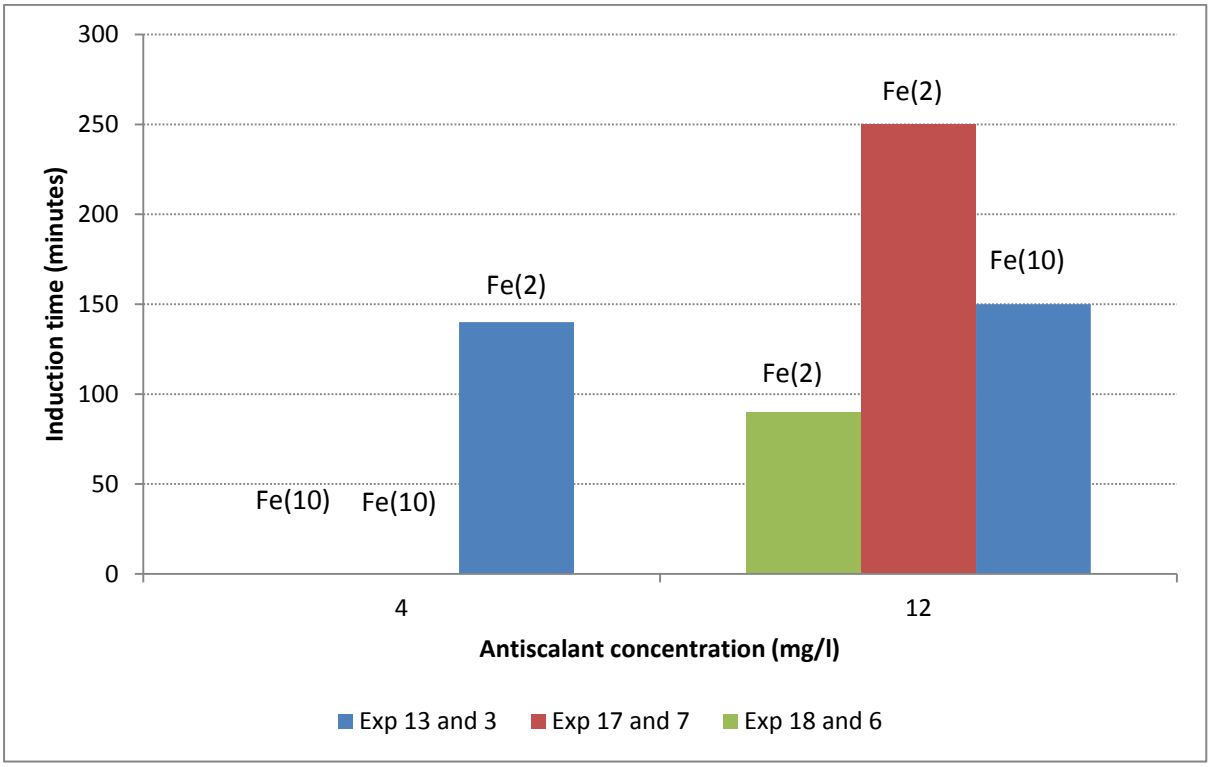

Figure 32: *Antiscalant concentration (HYDREX) – induction time relationship- bracketed values indicate the ferric chloride concentration (mg/l) at the corresponding antiscalant concentration.*

Table 26: *Interaction between antiscalant concentration and the ferric concentration on the induction time, (shown in* **Figure 31** *and* **Figure 32***)*

Exp ID	Conditions	Induction time (minutes)	
		HYDREX	BULAB
13	T(15),pH(10),AS(12),Fe(10),Ca(0.055),S(0)	150	550
3	T(15),pH(10),AS(4),Fe(2),Ca(0.055),S(0)	140	450
17	T(15),pH(10),AS(4),Fe(10),Ca(0.045),S(2000)	0	0
7	T(15),pH(10),AS(12),Fe(2),Ca(0.045),S(2000)	250	210
18	T(25),pH(4),AS(4),Fe(10),Ca(0.055),S(0)	0	0
6	T(25),pH(4),AS(12),Fe(2),Ca(0.055),S(0)	90	30

6.5.1.6 Ferric chloride concentration

Preliminary experiments have shown that the addition of ferric chloride to a super saturated solution containing antiscalants could considerably reduce the induction period with respect to the control conditions by interaction with the antiscalant molecules. The addition of 10 mg/l of ferric chloride to a solution [T (25°C), Ca (0.045)] reduced the induction period from 200 minutes to 20 minutes (which is equivalent to a complete restoration of the pure precipitating system with no antiscalant) in the presence of BULAB (2 mg/l). This means that the ferric successfully neutralized the effect of the antiscalant.

However, the statistical analyses of the data give the impression that a change in ferric chloride concentration (2 mg/l to 10 mg/l) has a negligible effect on the induction time under the governing experimental conditions. Consider the data from **Figure 31** and **Figure 32**, as well as **Figure 33** and **Figure 34** and re-evaluate the statement made according to the statistics. One gets the impression that ferric at a high concentration (10 mg/l) causes the induction period to be considerably reduced when the antiscalant concentration is at the low end (4 mg/l), both in the case of HYDREX and BULAB. When a low concentration of ferric (2 mg/l) is added to a solution spiked with 12 mg/l antiscalant, the ferric does not seem to be sufficient to override the effect of the antiscalant.

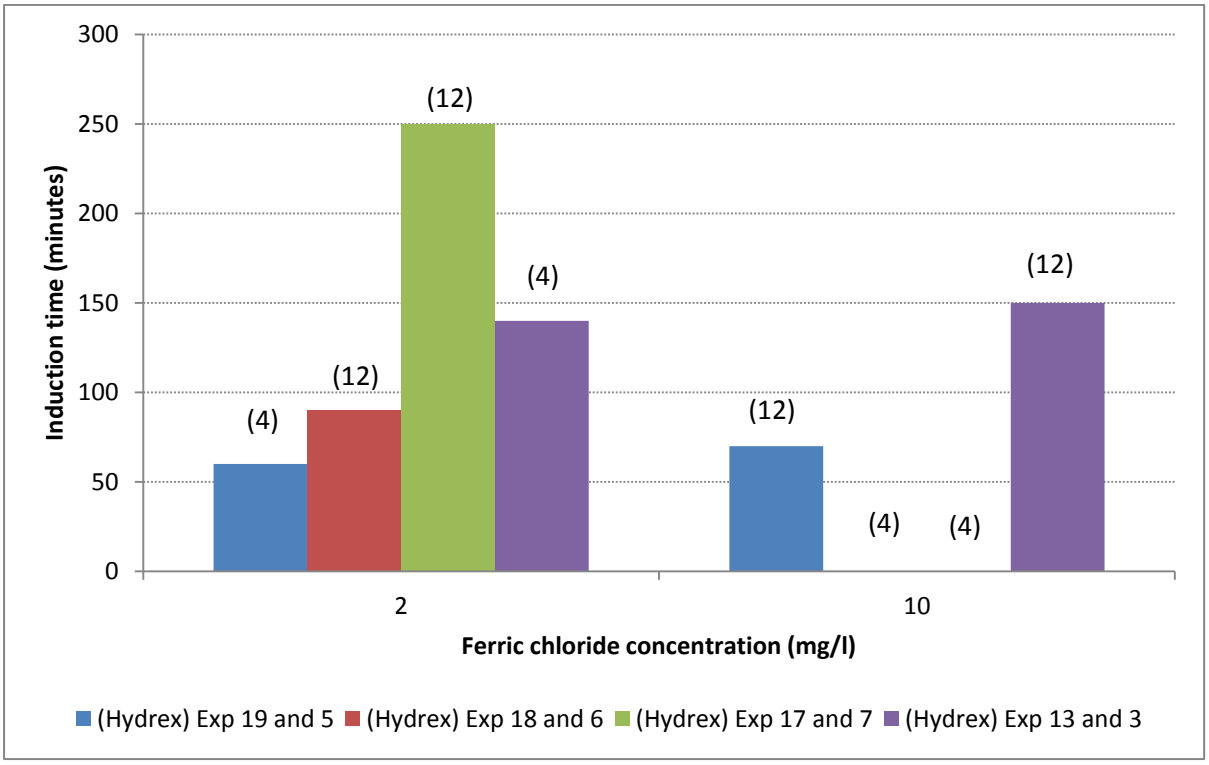

Figure 33: *Ferric chloride concentration – induction time relationship- bracketed values indicate the antiscalant concentration (HYDREX, mg/l) at the corresponding ferric chloride concentration.*

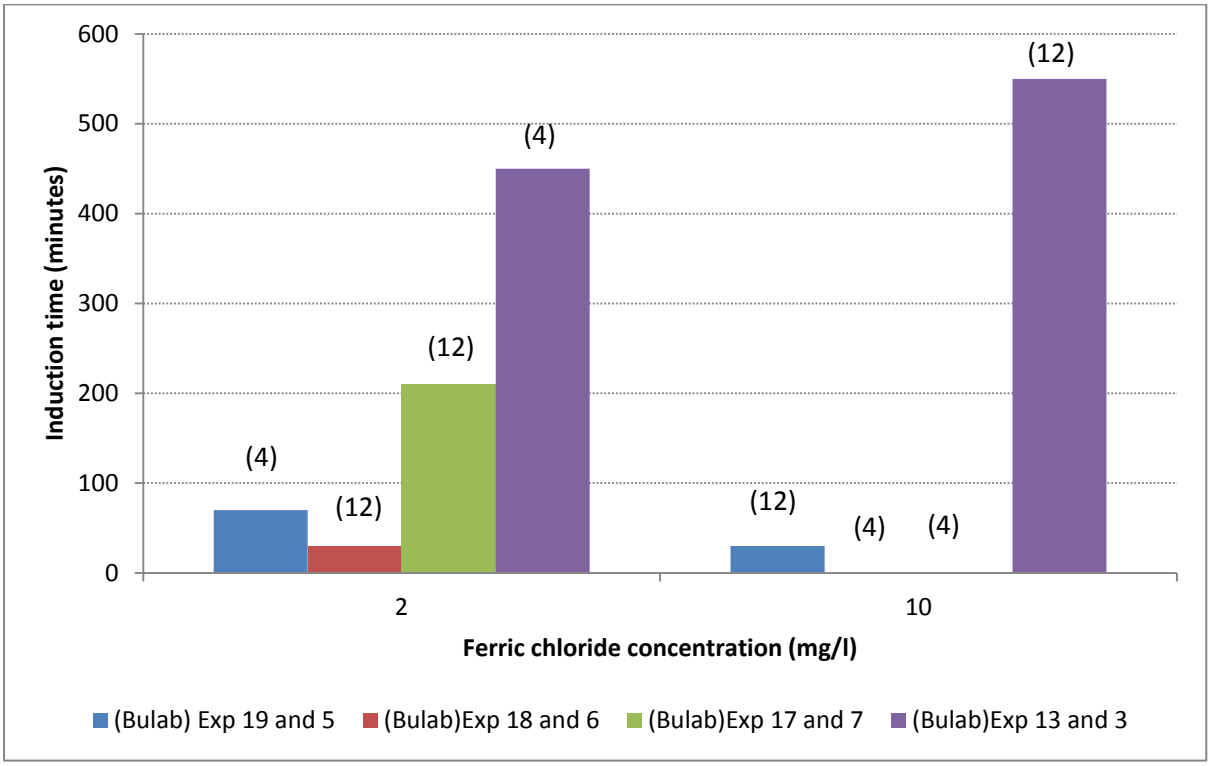

Figure 34: *Ferric chloride concentration – induction time relationship- bracketed values indicate the antiscalant concentration (BULAB, mg/l) at the corresponding ferric chloride concentration.*

Now consider the pairs experiment 13 and experiment 3 as well as experiment 19 and experiment 5. In these cases 10 mg/l ferric is as effective in reducing the effect of 12 mg/l antiscalant as 2 mg/l ferric is in reducing the effect of 4 mg/l antiscalant. The influence of ferric chloride on reducing the effectiveness of the antiscalant (both HYDREX and BULAB) cannot be ignored under these conditions.

In the case of experiment 7 and experiment 6, HYDREX is more effective than BULAB. What is particularly striking is that the antiscalant concentration is high under these conditions and that the ferric concentrations are low. The ferric-antiscalant interaction is negligible and HYDREX is more effective than BULAB irrespective of the pH.

Now refer to the pairs of experiment 13 and experiment 3. In both cases BULAB is far more efficient that HYDREX. In experiment 13 it could be argued that, due to the very high ferric concentration, HYDREX is more strongly influenced, causing a large reduction in the induction time relative to BULAB, which then rules out the idea that BULAB is naturally more efficient at a higher pH. In the case of experiment 3 the antiscalant concentration is low (4 mg/l), but due to the high pH, the antiscalant molecules are more prone to adsorption. Although the ferric concentration is low it can sufficiently reduce the effect of HYDREX relative to BULAB and hence causes a higher induction time in the presence of BULAB.

The influence of ferric on the induction periods in the presence of antiscalants can be as a result of one of two effects:

1) Ferric ions complex (anion-cation interaction) with the antiscalant molecules to partially or completely inactivate its effect.
2) Ferric species develop as large macromolecules $Fe(III)OH_3$ under the governing pH range (4-10) and present a surface for preferential adsorption of antiscalants to take place. Antiscalants would adsorb onto ferric molecules rather than on crystals, causing crystal growth to take place unhindered.

6.5.2 Growth rate

In the following discussion, the inferential variable t_{C80} is mostly used as a means to describe the growth rate. A high value for t_{C80} indicates a slow growth rate and *vice versa*. In addition, k' values (as presented in literature) are provided with the t_{C80} values (in table from). This is merely to provide additional information. As mentioned in section 4.2.3, k-values are not used in this study as the primary indicator of the growth rate because of a large variability (sensitivity) in its calculation.

6.5.2.1 Temperature

According to literature an exponential relationship exists between the temperature and the rate of precipitation (crystal growth rate). As the temperature increases so does the rate of precipitation. During baseline testing this relationship is first practically observed (within this study). An increase in 10°C caused the growth rate to increase by a factor of 2 (which as mentioned earlier is in good agreement with data from literature). Again consider the kinetic baseline data in **Table 16**, also shown in **Figure 35**.

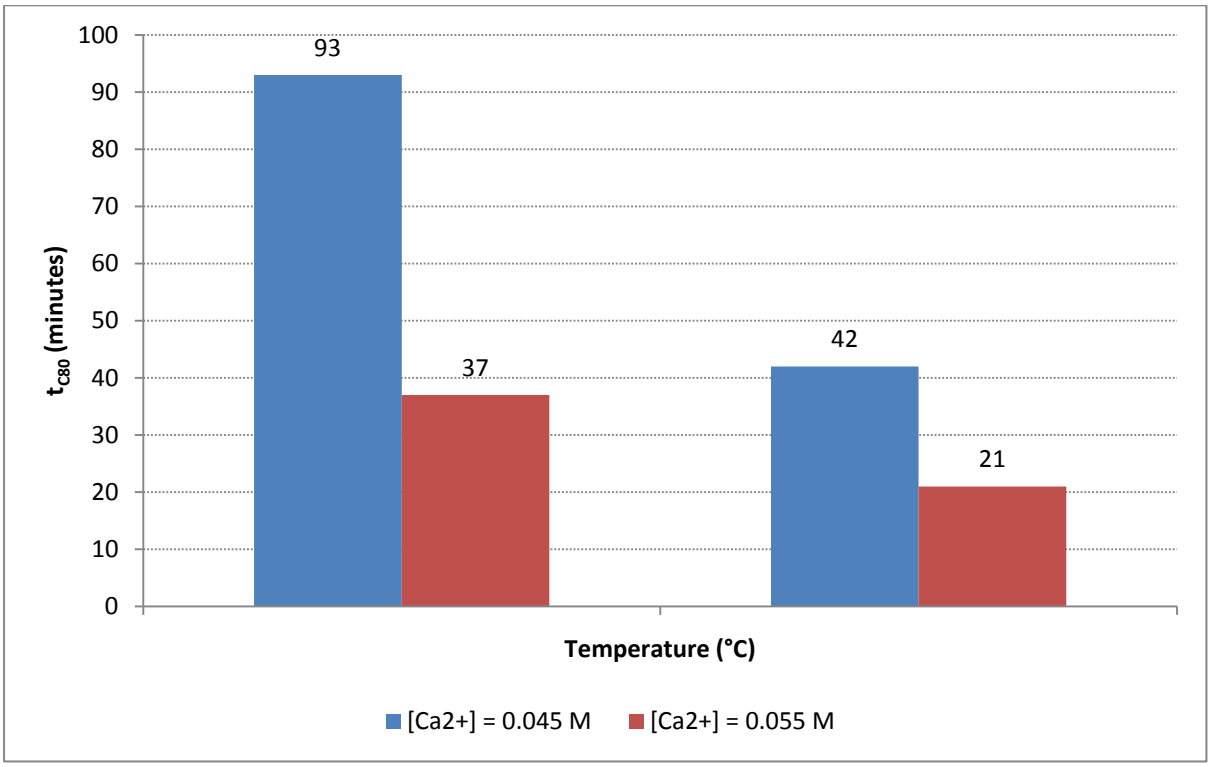

Figure 35: *The influence of temperature on the growth rate (kinetic baseline data)*

Table 16: *Kinetic baseline data (c.f. section 5.2)*

Baseline ID	Temp (°C)	$[Ca^{2+}] = [SO^{2-}_4]$ (M)	Induction time (minutes)	t_{C80} (minutes)	k' ($M^{-1}min^{-1}$)
B(1)	15	0.045	50	93	0.83
B(3)	25	0.045	25	42	2.023
B(2)	15	0.055	25	37	2.3
B(4)	25	0.055	10	21	3.32

The significance of temperature on the rate of precipitation in the presence of both HYDREX and BULAB (under the governing experimental conditions) is confirmed by statistical analyses in **Table 22** (c.f. section 6.4), where the effect of temperature on the inferential variable t_{C80} exhibits a very low P-value (almost zero).

To visually compare the data sets performed at 15°C and at 25°C, the values for t_{C80} are displayed according to their experimental ID (**Figure 36**). A '60 minute'-division line is used to separate all data with t_{C80}-values greater than 60 minutes from those with lower values. Interesting enough, all experiments (both in the presence of HYDREX and BULAB) performed at a temperature of 15°C has a t_{C80}-value> 60 minutes. In simple terms this means that under the governing experimental conditions, no test performed at 15°C will reach 80 % completion (from the moment precipitation starts) within one hour. On the other hand the majority of experiments performed at 25°C have shown to exhibit t_{C80}-values smaller than 60 minutes.

In the case of both HYDREX and BULAB the value of t_{C80} at 25°C is ≈ 0.5 times as large as at 15°C, which comes to a difference of factor 2 -congruent with the observation made during preliminary testing. This observation can be made easily by observing the t_{C80} values in **Table 27**. Because of large variability in the calculation of k', this is not as easily observed.

In addition, pairs of experimental data in which case only the temperature and seed concentration were varied are displayed in **Figure 37** (HYDREX) and **Figure 38** (BULAB). In all cases the experiment with the higher temperature displayed a higher growth rate (lower value for t_{C80}) largely independent of the seed concentration. This is also noticed when comparing k'-values in **Table 27**. In all instances the k'-values are in good agreement with literature - 0-8 $M^{-1}.min^{-1}$ (Liu & Nancollas, 1970; Amjad & Hooley, 1986; Amjad, 1988).

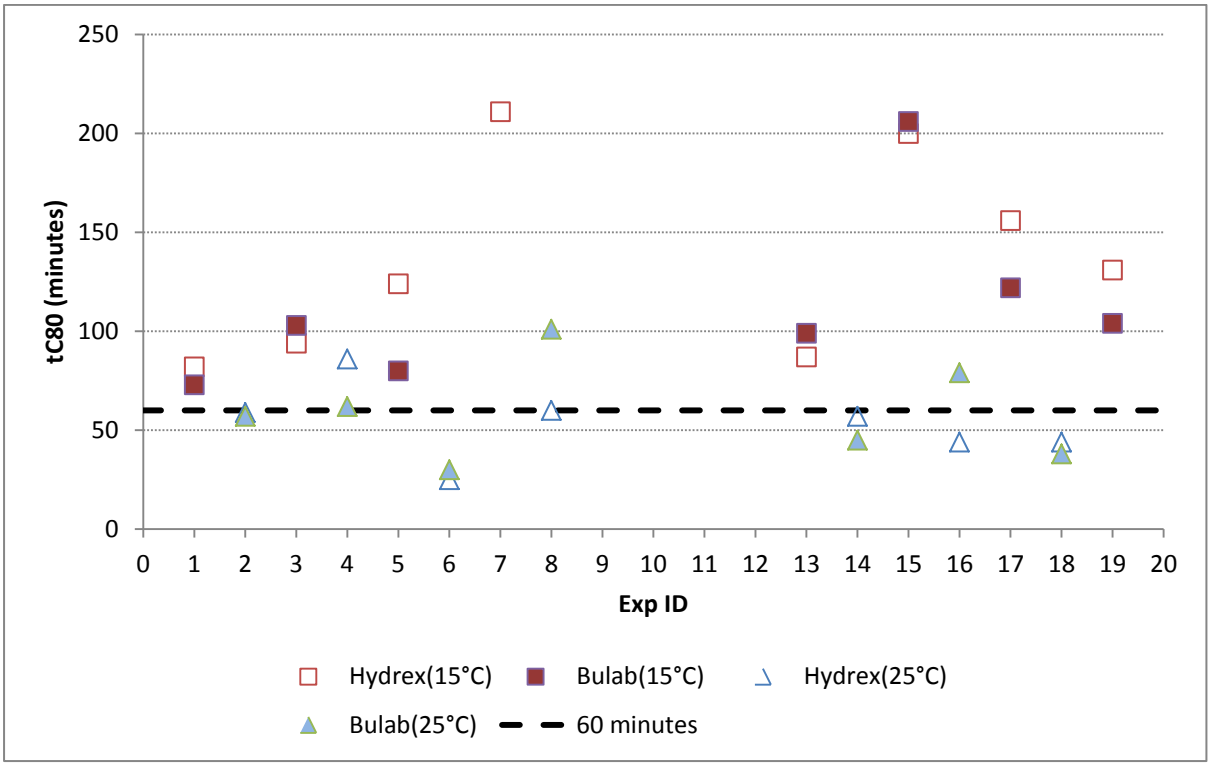

Figure 36: *Influence of temperature on the growth rate (t_{C80})*

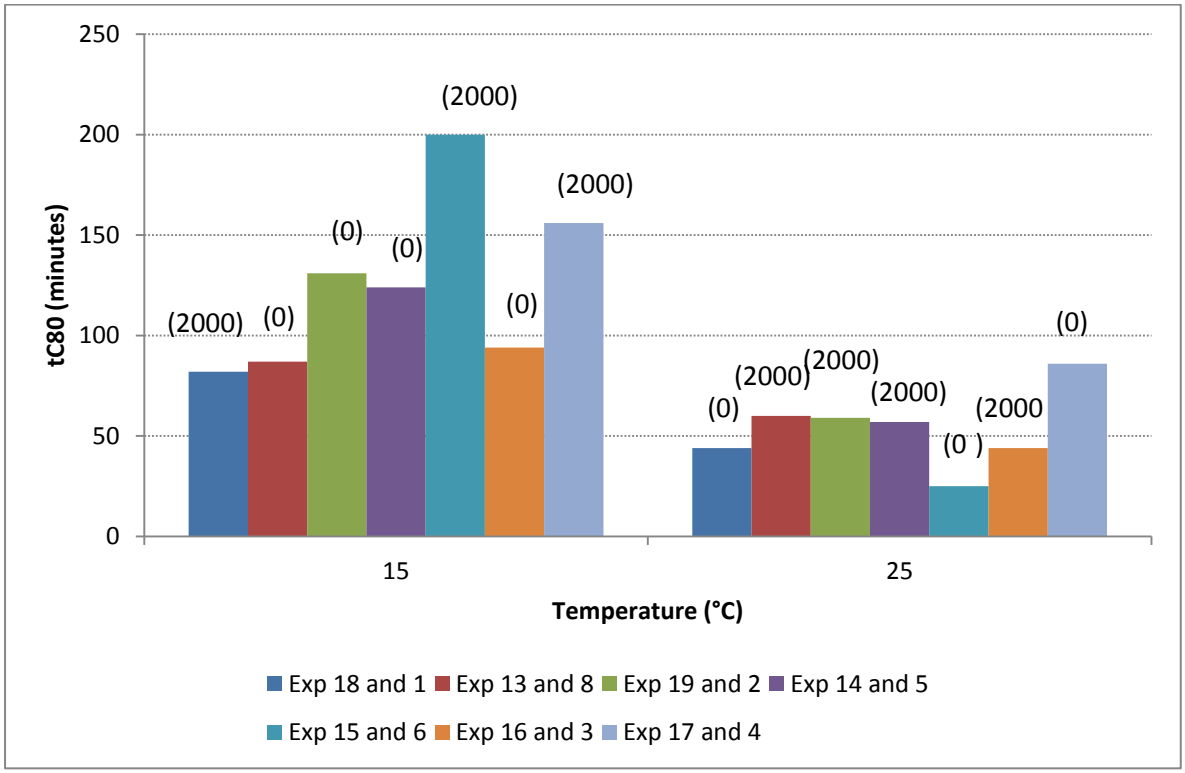

Figure 37: *Influence of temperature on the growth rate (t_{C80}) in the presence of HYDREX- bracketed values indicate the seed concentration (mg/l) corresponding to a given temperature.*

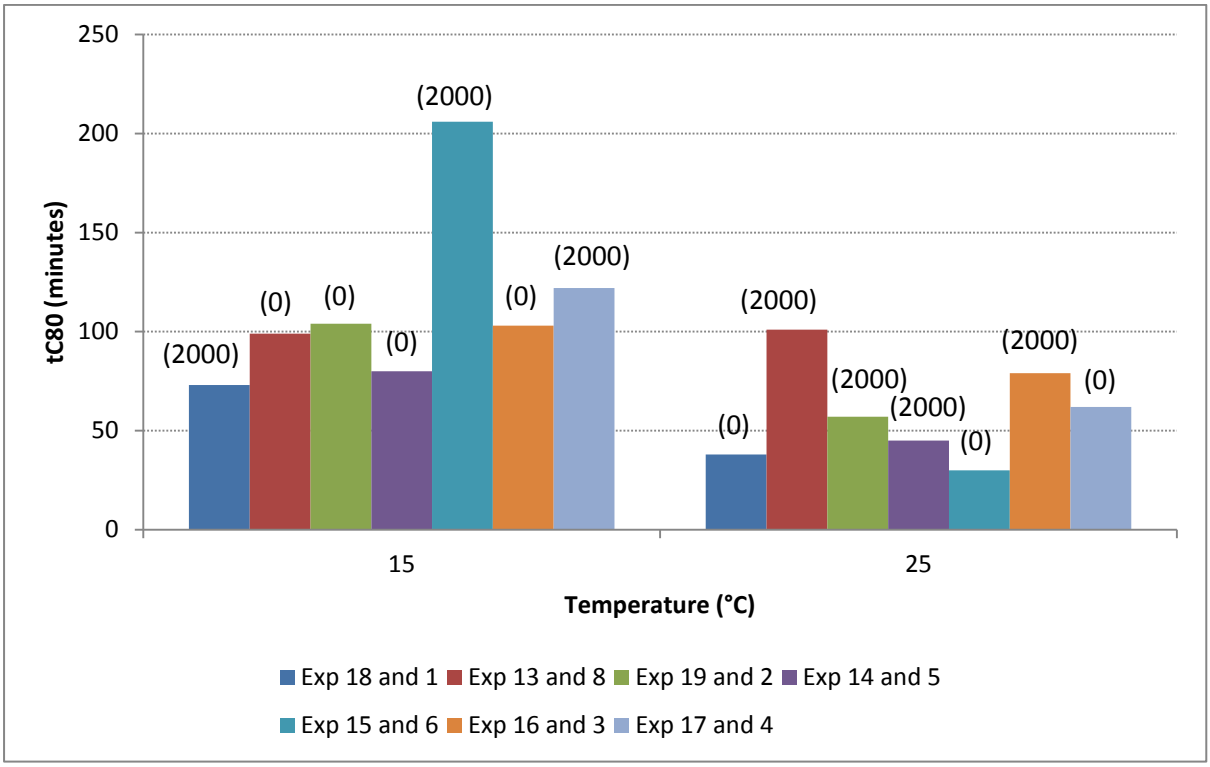

Figure 38: *Influence of temperature on the growth rate (t_{C80}) in the presence of BULAB - bracketed values indicates the seed concentration (mg/l) corresponding to a given temperature.*

Table 27: *The Influence of temperature on the growth rate (t_{C80})*

Exp ID	Conditions	Induction time (minutes)		t_{C80} (minutes) k' ($M^{-1}min^{-1}$)	
		HYDREX	BULAB	HYDREX	BULAB
18	T(25),pH(4),AS(4),Fe(10),Ca(0.055),S(0)	0	0	44 **(1.42)**	38 **(0.97)**
1	T(15),pH(4),AS(4),Fe(10),Ca(0.055),S(2000)	0	0	82 **(1.07)**	73 **(1.1)**
13	T(15),pH(10),AS(12),Fe(10),Ca(0.055),S(0)	150	550	87 **(1.27)**	99 **(0.62)**
8	T(25),pH(10),AS(12),Fe(10),Ca(0.055),S(2000)	0	0	60 **(1.83)**	101 **(0.79)**
19	T(15),pH(4),AS(4),Fe(2),Ca(0.045),S(0)	60	70	131 **(0.67)**	104 **(0.72)**
2	T(25),pH(4),AS(4),Fe(2),Ca(0.045),S(2000)	0	0	59 **(2.08)**	57 **(1.76)**
14	T(25),pH(4),AS(12),Fe(10),Ca(0.045),S(2000)	0	0	57 **(2.10)**	45 **(2.70)**
5	T(15),pH(4),AS(12),Fe(10),Ca(0.045),S(0)	70	30	124 **(0.34)**	80 **(0.40)**

Table 27 *Continues*

15	T(15),pH(4),AS(12),Fe(2),Ca(0.055),S(2000)	0	0	200 **(0.29)**	206 **(0.26)**
6	T(25),pH(4),AS(12),Fe(2),Ca(0.055),S(0)	90	30	25 **(2.87)**	30 **(1.88)**
16	T(25),pH(10),AS(4),Fe(2),Ca(0.055),S(2000)	0	0	44 **(1.87)**	79 **(0.47)**
3	T(15),pH(10),AS(4),Fe(2),Ca(0.055),S(0)	140	450	94 **(0.54)**	103 **(0.61)**
17	T(15),pH(10),AS(4),Fe(10),Ca(0.045),S(2000)	0	0	156 **(0.56)**	122 **(0.48)**
4	T(25),pH(10),AS(4),Fe(10),Ca(0.045),S(0)	100	150	86 **(0.92)**	62 **(1.48)**

6.5.2.2 Seed

It was observed in the previous section that the effect of temperature largely overshadows the effect of seeding on the growth rate under the governing experimental conditions (refer again to **Figure 37** and **Figure 38**). To support this notion, the statistical analysis has also found that the influence of seeding on the growth rate is insignificant (Consider the P-values of 0.12 in **Table 22**).

To expand the investigation, the effect of seed type on the precipitation kinetics was evaluated. A number of experiments were conducted using lime or a combination of lime and gypsum instead of only gypsum seed (conditions in **Table 23**). We reiterate that lime is somewhat different to mere seed addition in that it also causes a chemical reaction to take place in a solution: the hydroxyl ions that get released upon dissociation of the lime causing the pH to increase and the subsequent release of free calcium ions, which again increases the saturation level of calcium salts in solution such as gypsum. Nonetheless, lime qualifies as a seed material as it adds foreign nuclei to the solution. In section 2.7.3.1 it was discussed how a difference in seed type affects the nucleation kinetics with respect to a change in the induction time. Now consider the data on the effect of seed-type on the growth rate (refer to the last column of **Table 23**). The growth rate obtained by using lime in the presence of both HYDREX and BULAB increased almost twofold (refer to t_{C80} values) compared to using gypsum seed (only t_{C80}- values are used for this purpose). Note also that the growth rate in the presence of lime is preceded by a very lengthy induction period.

Table 23: *Summary of kinetic data: antiscalant concentration (12 mg/l), [Ca^{2+}] = 0.055 M (c.f. section 6.5.1)*

Exp ID	Conditions	Induction time (minutes)		t_{C80} (minutes) k' ($M^{-1}.min^{-1}$)	
		HYDREX	BULAB	HYDREX	BULAB
8	T(25),pH(10),Fe(10),S(2000) gypsum	0	0	60 **(1.83)**	100 **(0.79)**
8	T(25),pH(10),Fe(10),S(2000) lime	150	50	36 **(1.77)**	45 **(1.61)**
8	T(25),pH(10),Fe(10),S(2000) gypsum and lime	0	0	39 **(0.75)**	48 **(0.12)**

Amjad & Hooley (1986), Amjad (1985) and Liu & Nancollas (1970) showed that the growth rate is proportional to the amount of available growth sites in solution. When seeded growth takes place in the absence of an induction period it is accepted that no additional nucleation (addition of growth sites) takes place prior to precipitation and growth takes place only on the available growth site in a solution initially present. When seeded growth is preceded by an induction time it is assumed that more growth sites are formed through additional nucleation both on the crystal surface and/or in the solution until enough sites are available to produce spontaneous precipitation. This increase in growth sites can lead to an increase in the growth rate. When lime is added, the calcium concentration initially spikes to a concentration above 0.075 M. There are no identifiable growth sites to de-super saturate the solution and an induction period precedes the growth phase (which is initiated upon commencement of precipitation) during which additional growth sites develop before precipitation commences.

A similar observation was made by Gill and Nancollas (1979) using calcite and barite seed to de-super saturate a solution containing gypsum as main precipitant. Growth was preceded by an induction period and again the growth rate following the induction period was considerably higher than in the presence of pure gypsum, which is assumed to be as a result of the increase in growth sites.

On the other hand, when gypsum and lime were added in combination, no induction time was observed. It however produced the benefit of an increased growth rate almost identical (a bit slower) to the one in the presence of only lime. The lime increased the precipitation potential by increasing the level of super saturation, whereas the gypsum seed presented readily available receivers (sites) for precipitating ions.

When only gypsum seed was used, one observed that precipitation in the presence of BULAB is quite slow compared to precipitation in the presence of HYDREX. In section 6.5.1.4 it is shown that HYDREX is more effective than BULAB at higher pH values when NO additives are present in the solution. In this case a high concentration of ferric is added. If it can be assumed that the ferric-HYDREX interaction is stronger, it means that a given amount of ferric can cause a stronger de-activation of the same amount of HYDREX, compared to BULAB. When lime (or a combination of lime and gypsum) is added instead of gypsum, there seems to be almost no difference between the effectiveness of HYDREX and BULAB even though the pH is increased far beyond 10 (actual pH=12.3) in which case one would expect both HYDREX and BULAB to perform better. However it can be assumed that the release of calcium ions, which is positively charged, during lime dissociation interacts with the negatively charged antiscalant molecules and causes their deactivation and subsequently causes precipitation.

6.5.2.3 pH

It is well known that calcium sulphate dehydrate precipitation is not pH dependent.

It has been established however that there is a strong interaction between the pH and the antiscalant adsorption capacity in the case of both HYDREX and BULAB (c.f. section 6.5.1.4).

When the (gypsum) growth rate-pH relationship in the presence of HYDREX (**Figure 39**) is evaluated there appears to be no consistent correlation between the change in pH and the change in growth rate following the induction period. If the growth kinetics should follow the same philosophy as the nucleation kinetics (resembled by the induction period) with regard to the antiscalant- pH interaction, it would mean that high pH values would cause growth kinetics to slow down as a result of the increased inhibitory efficiency of HYDREX antiscalants at higher pH values (c.f. section 6.5.1.4). In some experimental runs (with reference to HYDREX) slow growth rates have been witnessed in runs with high pH (10) values (refer to pairs of experiment 1 and 17, experiment 18 and 4 and experiment 14 and 8). It is interesting to note that the slow growth rates in all of these experimental pairs took place at the lower calcium concentrations. In the case of experiments 19 and 3, experiments 5 and 13 and experiments 2 and 16, faster growth rates have been witnessed at conditions where the pH was high (10). Again note that the slower growth rates correspond to lower calcium concentrations. Clearly the slower growth rates correspond to the lower calcium concentration regardless of the pH in the presence of HYDREX. The experimental pair 14 and 6 (t_{C80} values of 57 and 60 minutes) is the only exception and shows a slightly higher growth rate at the lower calcium concentration.

During studies by Liu & Nancollas (1975) it has been theorized that phosphonate molecules, because of their small size, are absorbed by the advancing (growing) crystal faces during precipitation until the molecules are completely enveloped by a growing crystal mass. At this point (when all antiscalants are overgrown) crystal growth is assumed to commence at a growth rate comparable to that of a pure precipitating solution. The same logic could be followed in this instance: since the growth rate, in the case of HYDREX, appears not to be influenced by the pH, it could be argued that at any pH (which determine the attraction between the antiscalant and the crystal surface) the phosphonate molecules (because if their size) are enveloped by growing crystal in which case the growth rate depends on other factors, not the extent of adsorption.

In contrast to the pH-growth rate relationship for HYDREX, it appears as if there is a stronger relationship between the pH and growth rate (gypsum) in the presence of BULAB (refer to **Figure 40**). In all of the observed experimental pairs for BULAB, a slower growth rate corresponds to a high pH (10) and the faster growth rate corresponds to a lower pH (4), regardless of the calcium concentration. At a pH of 10, the adsorption capacity of BULAB is very high (as explained in setion 6.5.1.4). Polyacrylate molecules have a larger chain structure, which increases their bonding possibilities and prevents them from being easily absorbed within the crystal (Ohara and Reid, 1973). Being larger than the phosphonate molecules, BULAB would naturally bond at a larger portion of the very active fast growth sites on the crystal surface, allowing mostly the sites of low energy to continue growing. If only these sites of lower energy continue to grow it would cause the overall growth rate to be reduced as proved to be the case with BULAB.

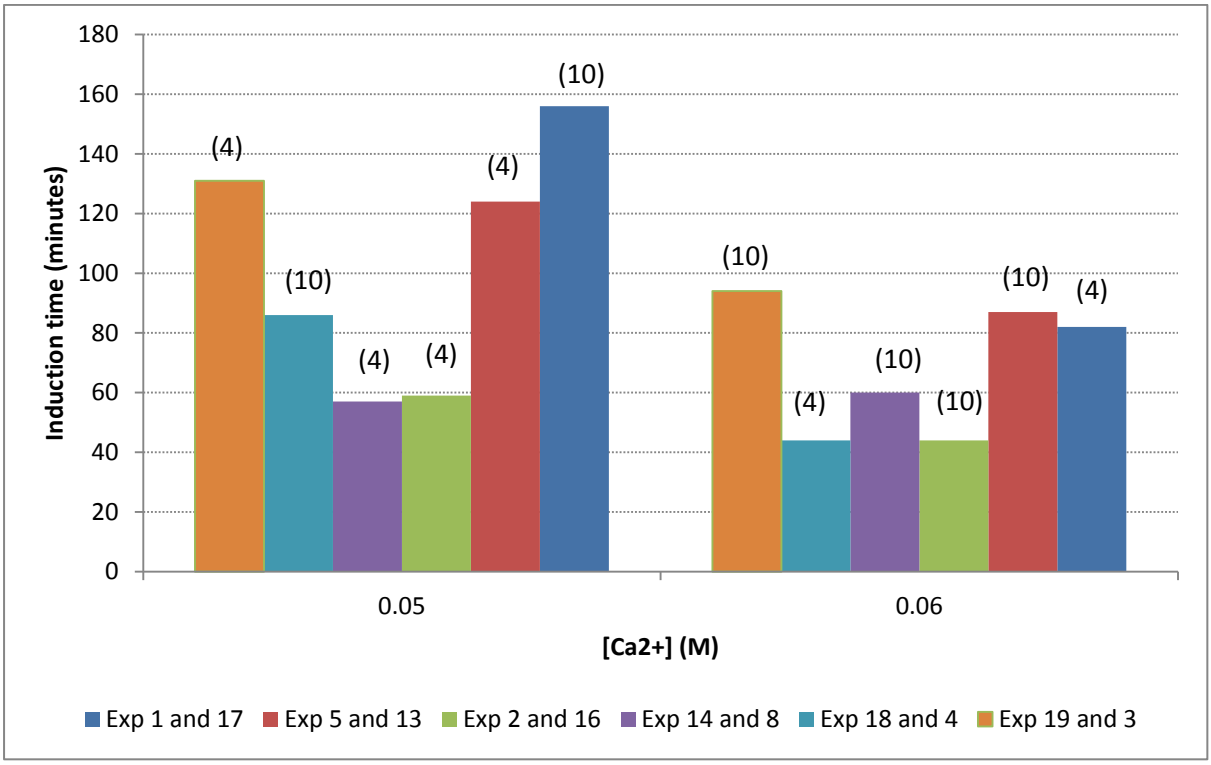

Figure 39: *Calcium concentration – growth rate interaction (HYDREX) - bracketed values indicate the pH corresponding to a given calcium concentration.*

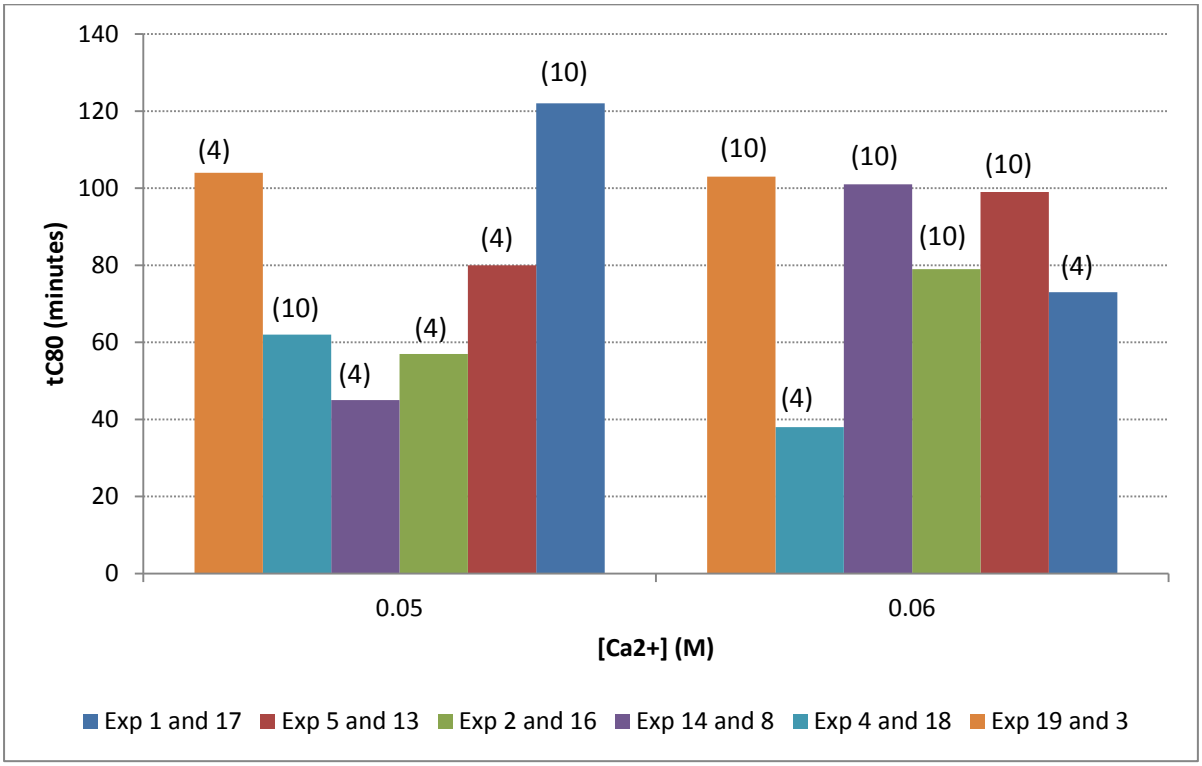

Figure 40: *Calcium concentration – growth rate interaction (BULAB) - bracketed values indicate the pH corresponding to a given calcium concentration.*

6.5.2.4 Calcium concentration

Literature has shown that the growth rate (during gypsum precipitation) can exhibit variable order reaction rates with respect to the level of super saturation. Nevertheless, the growth rate is a strong function of the saturation level. As the saturation level is proportional to the calcium (and sulphate) concentration, so the growth rate would therefore be proportional to the calcium concentration.

Baseline data (**Figure 41**) confirmed that the growth rate has a strong dependency on the change in calcium concentration. An increase in 0.01 M of calcium caused the growth rate to increase by slightly more than a factor of two at 15°C (t_{C80} changed from 93 minutes to 37 minutes) as well as at 25°C (t_{C80} changed from 42 minutes to 21 minutes).

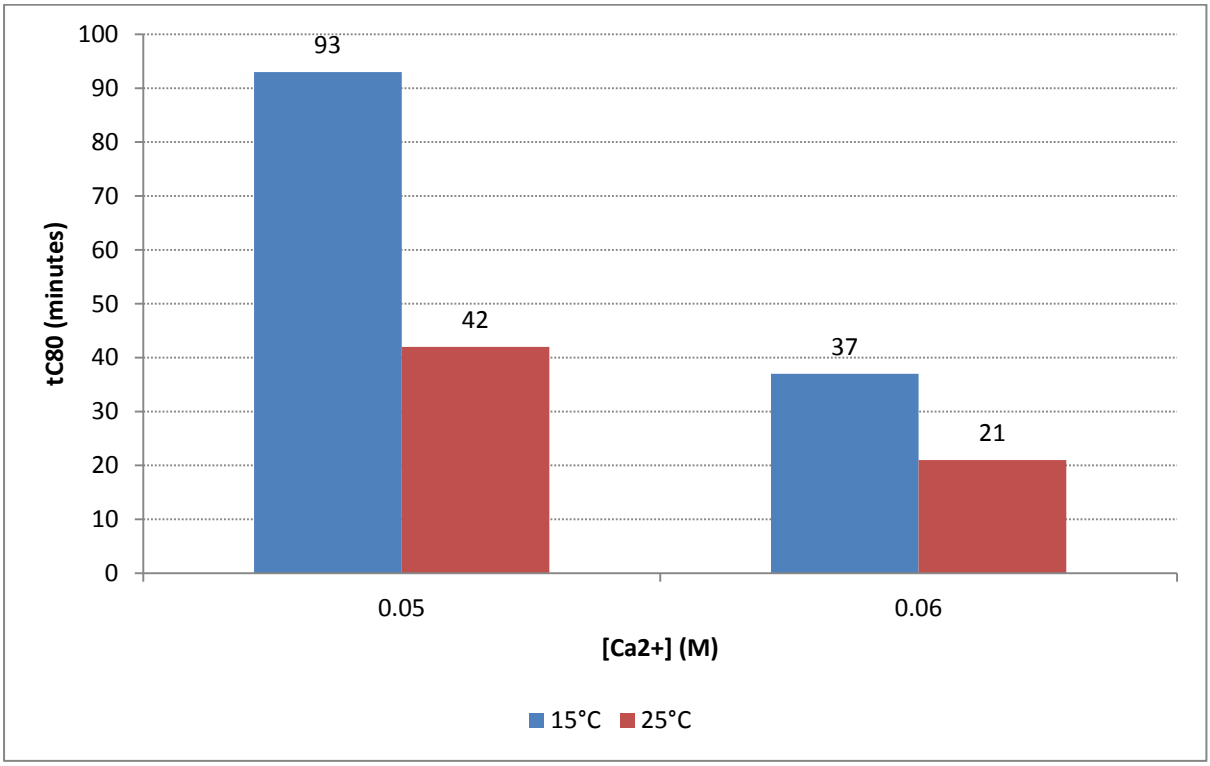

Figure 41: *The influence of calcium concentration on the growth rate (kinetic baseline data)*

For experiments conducted in the presence of HYDREX, the statistical analyses have shown that the change in calcium concentration has a significant effect on the growth rate. This is indicated by a sufficiently small P-value = 0.03<0.05 and is also confirmed by the discussion in section 6.5.2.3. The contrary is however true for BULAB. According to statistics, there appears to be very little correlation between a change in the calcium concentration and the growth rate under the governing experimental conditions. In section 6.5.2.3 it is explained that a change in pH (since it affects the

efficiency of BULAB adsorption to the precipitating crystal surface) governs the change in growth rate, rather than the change in calcium concentration.

6.5.2.5 Antiscalant concentration and ferric concentration interaction

Neither the antiscalant concentration nor the ferric concentration seems to affect the growth rate to a considerable extent when considering only the results of the statistical analysis. This could be truthful or it could be that there is such a strong interaction between these factors that when each factor is considered individually it appears to have no effect.

During seeded growth, an increase in the antiscalant concentration causes the growth rate to slow down. At closer inspection, it is noted that the ferric-antiscalant interaction is important. In all cases where the antiscalant concentration is at a maximum (12 mg/l) a ferric concentration of 10 mg/l appears to be sufficient to dampen the inhibitory effect of the antiscalant by lowering the value of t_{C80} compared to when only 4 mg/l antiscalant is applied. A combination of 12 mg/l antiscalant and 10 mg/l ferric chloride and a combination of 4 mg/l antiscalant and 2 mg/l ferric chloride, give similar growth rate results (examine the results for the combinations: experiment 5 and 19, experiment 3 and 13, experiment 14 and 2 as well as experiment 8 and 16). This could mean that the extent to which 2 mg/l ferric overrides the effect of 4 mg/l antiscalant is similar to the extent to which 10 mg/l ferric overrides the effect of 12 mg/l antiscalant. The observation made on the pairs: experiment 7 and 17 as well as on experiment 15 and 1 (which shows that the increase in antiscalant causes the growth rate to slow down) is probably caused as a result of this ferric-antiscalant interaction. The high ferric concentration (10 mg/l) easily overrides the low antiscalant concentration (4 mg/l). However the low ferric concentration (2 mg/l) fails to successfully override the very high antiscalant concentration (12 mg/l) causing the growth rate to be very slow.

It is very difficult to state whether the antiscalant concentration effect is more pronounced in the presence of HYDREX or BULAB, since the antiscalant-ferric interaction causes the results to be quite similar in both cases (refer to **Figure 42**, **Figure 43** and **Table 28**).

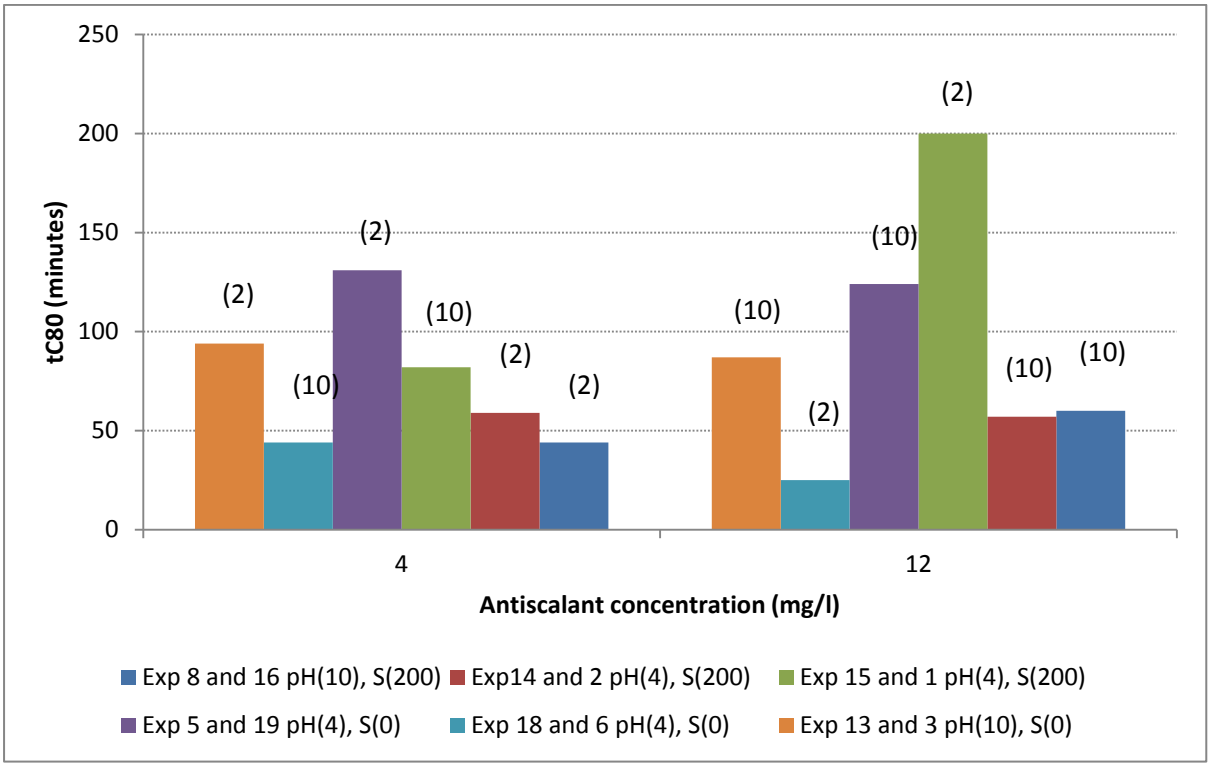

Figure 42: *Antiscalant-growth rate interaction (HYDREX) – bracketed values indicate ferric concentrations (mg/l) corresponding to a given antiscalant concentration.*

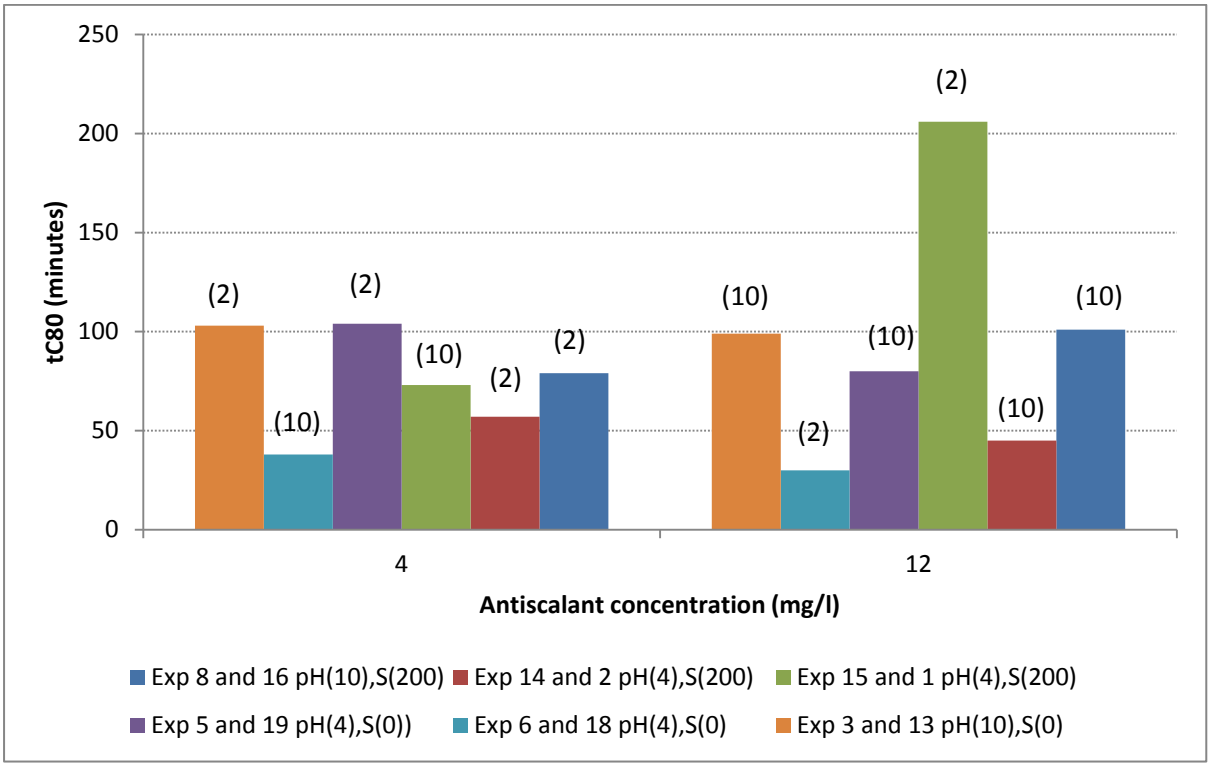

Figure 43: *Antiscalant-growth rate interaction (BULAB) - bracketed values indicate ferric concentrations (mg/l) corresponding to a given antiscalant concentration.*

Table 28: *Antiscalant-growth rate interaction (summary)*

Exp ID	Conditions	Induction time (minutes)		t_{C80} (minutes) k' ($M^{-1}min^{-1}$)	
		HYDREX	BULAB	HYDREX	BULAB
8	T(25),pH(10),AS(12),Fe(10),Ca(0.055),S(2000)	0	0	60 **(1.83)**	101 **(0.79)**
16	T(25),pH(10),AS(4),Fe(2),Ca(0.055),S(2000)	0	0	44 **(1.87)**	79 **(0.47)**
7	T(15),pH(10),AS(12),Fe(2),Ca(0.045),S(2000)	250	210	211 **(0.22)**	n/a **(0.08)**
17	T(15),pH(10),AS(4),Fe(10),Ca(0.045),S(2000)	0	0	156 **(0.56)**	122 **(0.48)**
14	T(25),pH(4),AS(12),Fe(10),Ca(0.045),S(2000)	0	0	57 **(2.10)**	45 **(2.70)**
2	T(25),pH(4),AS(4),Fe(2),Ca(0.045),S(2000)	0	0	59 **(2.08)**	57 **(1.76)**
15	T(15),pH(4),AS(12),Fe(2),Ca(0.055),S(2000)	0	0	200 **(0.29)**	206 **(0.26)**
1	T(15),pH(4),AS(4),Fe(10),Ca(0.055),S(2000)	0	0	82 **(1.07)**	73 **(1.1)**
5	T(15),pH(4),AS(12),Fe(10),Ca(0.045),S(0)	70	30	124 **(0.34)**	80 **(0.4)**
19	T(15),pH(4),AS(4),Fe(2),Ca(0.045),S(0)	60	70	131 **(0.96)**	104 **(0.72)**
6	T(25),pH(4),AS(12),Fe(2),Ca(0.055),S(0)	90	30	25 **(2.87)**	30 **(1.88)**
18	T(25),pH(4),AS(4),Fe(10),Ca(0.055),S(0)	0	0	44 **(1.42)**	38 **(0.97)**
3	T(15),pH(10),AS(4),Fe(2),Ca(0.055),S(0)	140	450	94 **(0.54)**	103 **(0.61)**
13	T(15),pH(10),AS(12),Fe(10),Ca(0.055),S(0)	150	550	87 **(2.17)**	99 **(0.62)**

6.5.3 Optimum ('best') conditions

In this section, the factors that had the most significant effect on both the induction time and the growth rate within the scope of this study will be highlighted. These conditions will then serve as guidelines to selecting the input conditions for tests on AMD water.

6.5.3.1 Induction time

During experimentation, the aim was always to reduce the induction time as far as possible and, if possible, remove it completely.

Both at high and low antiscalant concentrations, the factors that had the most significant effect on the induction time were the pH and the seed concentration.

At low pH values (4), lower induction times are observed (0-70 minutes for HYDREX and BULAB) and at higher pH values (10) larger induction times are observed (100-150 minutes for HYDREX; 150-550 minutes for BULAB). To reduce the induction period, the pH should be at the low level of 4.

Comparing the 'un-seed' cases with the seed cases indicated that the induction time was reduced to zero in almost all the cases where seed at 2000 mg/l was added. Adding seed would therefore be the best option to minimise induction time.

With respect to the other factors, a high temperature (25°C) and high calcium concentration favoured a low induction time.

6.5.3.2 Growth rate

In practice the goal would always be to increase the growth rate as far as possible to reduce retention time of a process.

Both at high and low antiscalant concentrations the major factor that influenced the growth rate proved to be the temperature which overshadowed the influence of seed and the other factors on the growth rate. An increase in temperature from 15°C to 25°C caused the growth rate to double in almost all cases.

The addition of lime seed caused the growth rate of gypsum (precipitating from solution) to increase considerably compared to when only gypsum was added as seed. An issue that occurred with the addition of lime was the occurrence of a large induction time prior to precipitation. This was overcome by adding gypsum in addition to the lime seed. Both lime and gypsum were added at concentrations of 2000 mg/l. This combined seeded precipitation added the benefit of a higher growth rate without the presence of a lengthy induction period.

A high pH again caused the growth rate to be slowed down in the cases where no lime was added. To optimise the growth rate, the pH would therefore need to be reduced.

Although the effect of the ferric on the growth rate was never significant, a higher ferric concentration proved to have an increasing effect on the growth rate of gypsum in the presence of HYDREX and BULAB nonetheless

6.5.3.3 Summary

Incorporating all of the benefits discussed in the previous subsections into a single experiment, which would support both the reduction of the induction period and the increase of the growth rate, resulted in the selection of the conditions of experiment 14 and experiment 8. These test conditions would therefore serve as input conditions for AMD precipitation tests (c.f. chapter 7). In addition, the use of lime in combination with gypsum would also be considered (during AMD water tests) at the same conditions indicated for experiment 14 and experiment 8. The conditions are presented in the following table:

Table 29: *Optimum conditions*

Exp ID	Conditions	Induction time (minutes)		t_{C80} (minutes)	
		HYDREX	BULAB	HYDREX	BULAB
14	T(25), pH(4), AS(12), Fe(10), Ca(0.045), S(2000)	0	0	57	45
8	T(25),pH(10), AS(12), Fe(10), Ca(0.055), S(2000)	0	0	39	48

Chapter 7 - Results and discussion: gypsum batch crystallization from AMD

7.1 Introduction and approach

In the previous chapter (c.f. 6.5.3), it was established that the conditions present in experiment 14 and 8 (refer to **Table 29**) were most effective in 1) reducing the induction time and 2) improving the rate of precipitation during the precipitation of gypsum from a super saturated solution. This was observed both in the presence of HYDREX and BULAB at an antiscalant concentration of 12 mg/l.

In addition, tests performed in the presence of both lime and gypsum (also at experiment 8 conditions) showed that the combination of lime and gypsum assisted to a faster growth rate (compared to the use of only gypsum seed). Another benefit observed in using this combination of seed was the elimination of the induction time, which was an apparent problem when only lime was used, although the addition of lime produced a very fast rate of precipitation.

The decision was made to perform precipitation tests using AMD RO concentrate, instead of a synthetic aqueous solution, in the presence of BULAB as well as HYDREX at the conditions of experiment 8 (with a combination of gypsum and lime) and at the conditions of experiment 14.

The aim of this part of the study was to evaluate whether the conditions found to be most effective in synthetic solutions 1) to override the inhibitory effect of antiscalants (HYDREX and BULAB) and 2) to produce precipitation of gypsum from a super saturated solution, could also be applied to real AMD RO concentrate with the same success.

A comparison of the synthetic and AMD tests are presented in **Figure 44** and **Figure 45**. The experimental conditions and response variables are presented in **Table 30** and **Table 31**.

7.2 Results

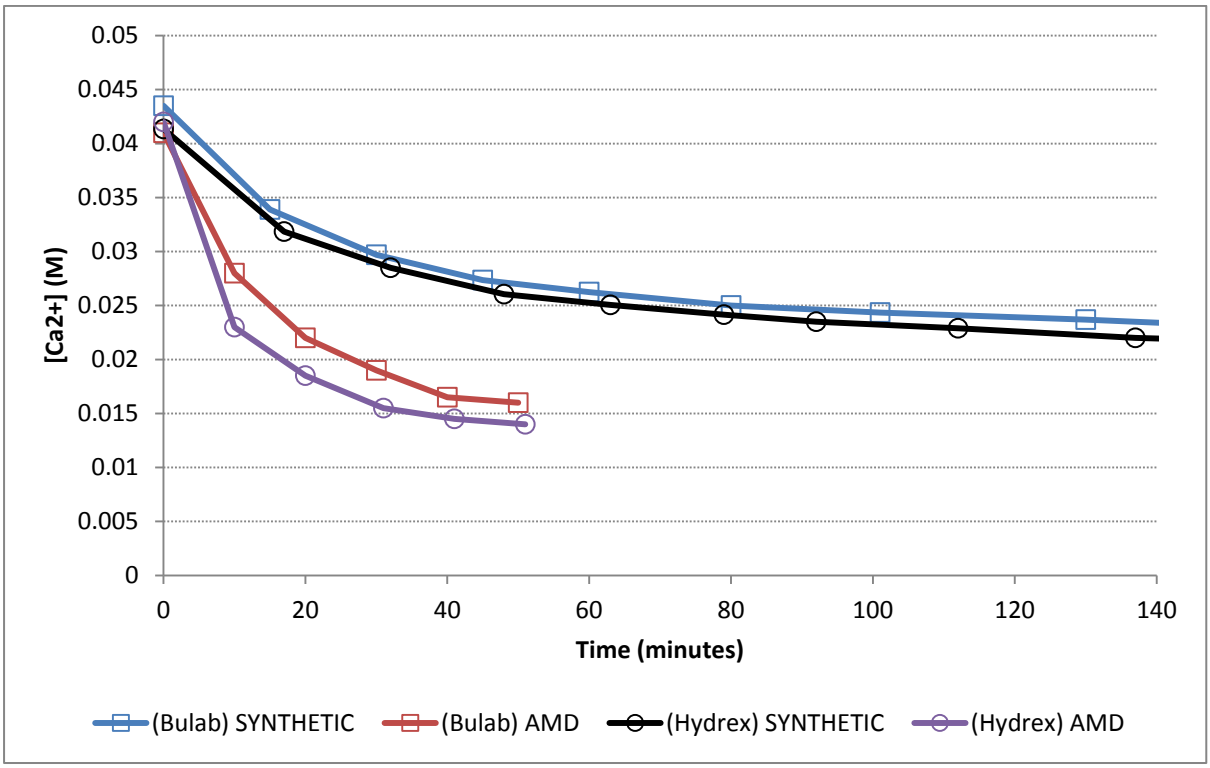

Figure 44: *Comparison of experiment 14 conditions, AMD and SYNTHETIC tests*

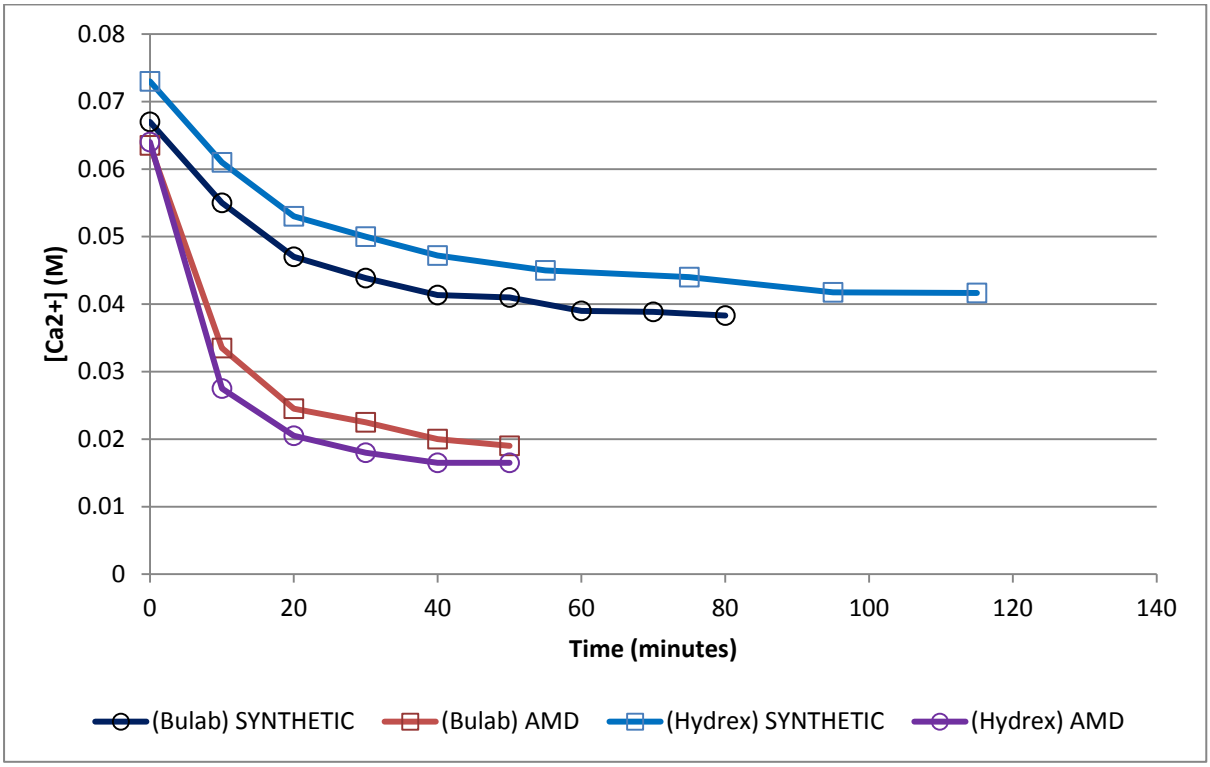

Figure 45: *Comparison of experiment 8 conditions, AMD and SYNTHETIC tests*

Table 30: *Comparison of synthetic and AMD kinetic data; experiment 14 conditions (S)-synthetic, (M)-AMD*

Exp ID	Conditions	Induction time (minutes)		t_{C80} (minutes)	
		HYDREX	BULAB	HYDREX	BULAB
14S	T(25), pH(4), AS(12), Fe(10), Ca(0.045), S(2000)	0	0	57	45
14M	T(25), pH(4), AS(12), Fe(10), Ca(0.045), S(2000)	0	0	18	23

Table 31: *Comparison of synthetic and AMD kinetic data; experiment 8 conditions (S)-synthetic, (M)-AMD (*gypsum *and* lime seed*)*

Exp ID	Conditions	Induction time (minutes)		t_{C80} (minutes)	
		HYDREX	BULAB	HYDREX	BULAB
8S	T(25),pH(10), AS(12), Fe(10),Ca(0.055), S(2000)	0	0	39	48
8M	T(25),pH(10), AS(12), Fe(10),Ca(0.055), S(2000)	0	0	12	16

7.3 Discussion

Refer to **Table 30**. Under experiment 14 conditions, the combination of a low pH of 4, a high temperature (25°C), high ferric concentration (10 mg/l) and gypsum seed addition (2000 mg/l), was sufficient to totally reduce the induction period (to zero minutes) of the complex AMD concentrate and force precipitation of gypsum in the presence of both HYDREX and BULAB. The crystal growth rate (gypsum) also seemed to be much faster in the AMD concentrate compared to the synthetic aqueous solution. For HYDREX the rate was approximately 3 times faster (57 minutes vs. 18 minutes) and for BULAB approximately 2 times faster (45 minutes vs. 23 minutes).

Synthetic aqueous solutions are prepared from pure anhydrous salts and almost pure water (de-mineralized). There are very few particles in addition to the pure minerals (which could provide nucleation sites), that could further assist in the precipitation process of gypsum. Moreover the only precipitate that can form is calcium sulphate dehydrate. This means that the rate or process of precipitation depends totally and utterly on the kinetics of gypsum nucleation and growth.

The AMD concentrate on the other hand is far more complex in composition and includes (in this case) ions of potassium, sodium, calcium, magnesium, aluminium, manganese, nickel, sulphate, chloride and fluoride. The combination of these ions creates an opportunity for a multitude of precipitates (in addition to gypsum) to form, of which the most abundant (according to a chemical analysis of the AMD concentrate, using OLI Analyser) are $Al(OH)_3$, $CaSO_4$ (calcium sulphate anhydrite) and $MgSO_4.7H_2O$. Any small hint of these precipitates in the water adds a nucleation or growth site and can possibly result in speeding up of the crystal growth therefore the rate of precipitation.

Moreover, when one considers the molar product of $[SO_4^{2-}]x[Ca^{2+}]$ which relates directly to the scaling tendency of gypsum, this scaling tendency (c.f. section 11.10 in the appendix) is slightly higher (3.73) for AMD concentrate than for the synthetic aqueous solution (3.46). A higher scaling tendency simply means a higher growth rate which could add to why the t_{C80} values are smaller in the case of AMD concentrate compared to the synthetic aqueous solutions.

It is interesting to note that the effect of BULAB (polyacrylate) which was easier to override than HYDREX (phosphonate) during the synthetic testing at a low pH, produced a slightly slower precipitation rate than HYDREX during the AMD tests. It is agreed that the values are in very close agreement and that it is hard to determine whether there is really a difference. Nonetheless, phosphonate antiscalants have been found to form complexes with aluminium (at concentrations of aluminium of approximately 100 µg/l) in solution (Gabelich *et al.*, 2002; 2006). This leads one to argue that the phosphonate in the HYDREX antiscalant and the minute amounts of aluminium in solution interact, causing a reduction of the effective amount of antiscalant available to adhere to gypsum nuclei. This probably causes the rate of precipitation in the presence of HYDREX to be increased. This was only witnessed during conditions of experiment 8 and therefore this argument is purely theoretical.

The low pH, which was formally discussed in section 6.5.1.4 and 6.5.2.3, also contributes to the lower induction period and faster growth rate in that it causes the adsorption of antiscalants to the surface of the forming crystal (and therefore its inhibitory power) to be reduced.

Refer to **Table 31**. The conditions for experiment 8 are very close to the conditions of experiment 14 with the exception that the pH is raised to 12.3 and that lime is added with the gypsum seed increasing the calcium concentration from 0.6 to 0.75 M. Moreover, the result is almost exactly the same as for experiment 14, with zero induction periods and a very fast growth rate, if not faster than observed during experiment 14 conditions.

The addition of the combination of lime and gypsum has been found to be extremely effective in reducing the induction period of synthetic solutions of gypsum and now also in the presence of AMD. As already noted in all four cases witnessed in this section, the induction period was totally eliminated. Compared to synthetic tests, the growth rate of gypsum from AMD is 3 times faster in the presence of both HYDREX (39 minutes vs. 12 minutes) and BULAB (48 vs. 16 minutes). During the synthetic runs, the addition of lime (instead of gypsum) caused the growth rate of gypsum to increase considerably. It was reasoned that the increase in growth rate was mainly because of the increase in the level of saturation of gypsum caused by the increase in calcium ions which resulted from the addition of lime.

It is notable that neither the induction period nor the growth rate was negatively affected by the large increase in pH in the presence of antiscalants. Lime increases the pH, which increases the adsorption capacity of both HYDREX and BULAB and will ultimately lead to better inhibition: longer induction times and slower precipitation rates. On the other hand the increase in pH promotes the increase of natural carbonate in the water. An increase in carbonate in the presence of calcium, promotes $CaCO_3$ (calcite) formation, which presents more nuclei which would promote additional precipitation. Now, if an increase in pH promotes both an increase in the inhibitory capacity of the antiscalants in solution as well as the production and sustainability of calcite formation, one could argue that a large portion of the antiscalants (now very active) would adsorb onto the calcite, rather than on the gypsum crystals, causing the gypsum crystals to be free to grow and cause precipitation of gypsum. The addition of calcite to an antiscalant containing super saturated solution of gypsum has been shown by Rahardianto *et al.*, (2010) in their CESP process, to cause antiscalant molecules to be scavenged. This leads to the inactivation of antiscalants and an improvement of precipitation kinetics. This then confirms the proposed argument.

The $[SO_4^{2-}]$:$[Ca^{2+}]$ ratio is presumed not to be as prominent as during experiment 14's conditions since the ratio is reduced in both cases (synthetic and AMD) by the increase in calcium through the addition of lime. When comparing the growth rates of experiment 8 and 14 conditions, this ratio does not seem to play a major role in experiment 8 when lime is added. This leads one to think that the mechanism of both antiscalant inhibition and precipitation is slightly different for the two cases studied.

To observe the full extent of the inhibitory effect of the antiscalants and the success of the forced precipitation process (through the manipulation of process variables and experimental conditions), some of the AMD RO concentrate was not de-super saturated and left to precipitate in clean glass containers at room temperature (Approximately 20-25°C). In all the cases no precipitation took place

within the first 48 hours of leaving the concentrations of concentrate. This happened both in the presence of HYDREX and BULAB. After 5 days the two containers of concentrate containing BULAB still indicated no concentration change indicating that precipitation had not yet taken place. In the case of HYDREX equilibrium had been reached within 5 days.

7.4 Implications for practical operation of RO with AMD

Practically, the knowledge contained within this study reveals how process parameters, operating conditions, (and in this section) the process (during treatment of RO concentrate from AMD) could be manipulated in order to improve overall water recovery during RO treatment of AMD.

It was explained in the earlier chapters that antiscalants are used as one method to pre-treat RO feed water in order to slow down the precipitation kinetics of the super saturated salts in solution. This would enable the water recovery through the membrane system to be maximised, while scaling is reduced.

This study confirmed that brine, super saturated with gypsum (containing either a phosphonate antiscalant or polyacrylate antiscalant) can be treated by deactivating the antiscalant and forcing precipitation of the super saturated salts (gypsum) in solution, causing a great deal of the salt to be separated from the brine. Manipulation of the brine (according to the 'best' conditions) is performed by changing the pH (reduce), adding ferric chloride, increasing the temperature (if too low), increasing the saturation level of calcium by the addition of lime and using seed (gypsum) to both scavenge antiscalants and stimulate precipitation.

After separation of precipitated salt from brine, the cleaner water is first filtered by ultra filtration (UF) to rid the water of seed and then be fed back to the RO unit as feed water.

With a compound separation process (explained on the following page), recoveries well above 98% can be obtained.

Conceptually the process would be as follows (refer to **Figure 46**):

- Before water is fed to the RO modules, the water is pre-treated. This would include among other processes, the addition of antiscalant (which would prevent scaling and improve recovery) correcting the pH (membranes are pH sensitive and antiscalants are effective within a certain pH range) and removal of seed crystals (the presence of which would result in major mineral scaling). Seed crystals can be removed effectively by ultra-filtration.
- During RO, a large portion of the salt in the feed (as well as antiscalants) are separated from the clean water (permeate). The salt and chemicals form the so-called brine.
- During brine treatment, chemical manipulation (change in pH and ferric addition) and seeding (addition of gypsum and lime) takes place (if necessary, temperature adjustment). All these process changes, except perhaps temperature adjustment, can easily be performed in correctly designed reactors and clarifiers. Clarified water is returned to the pre-treatment step and precipitated sludge (including very concentrated brine) is removed as final concentrate.

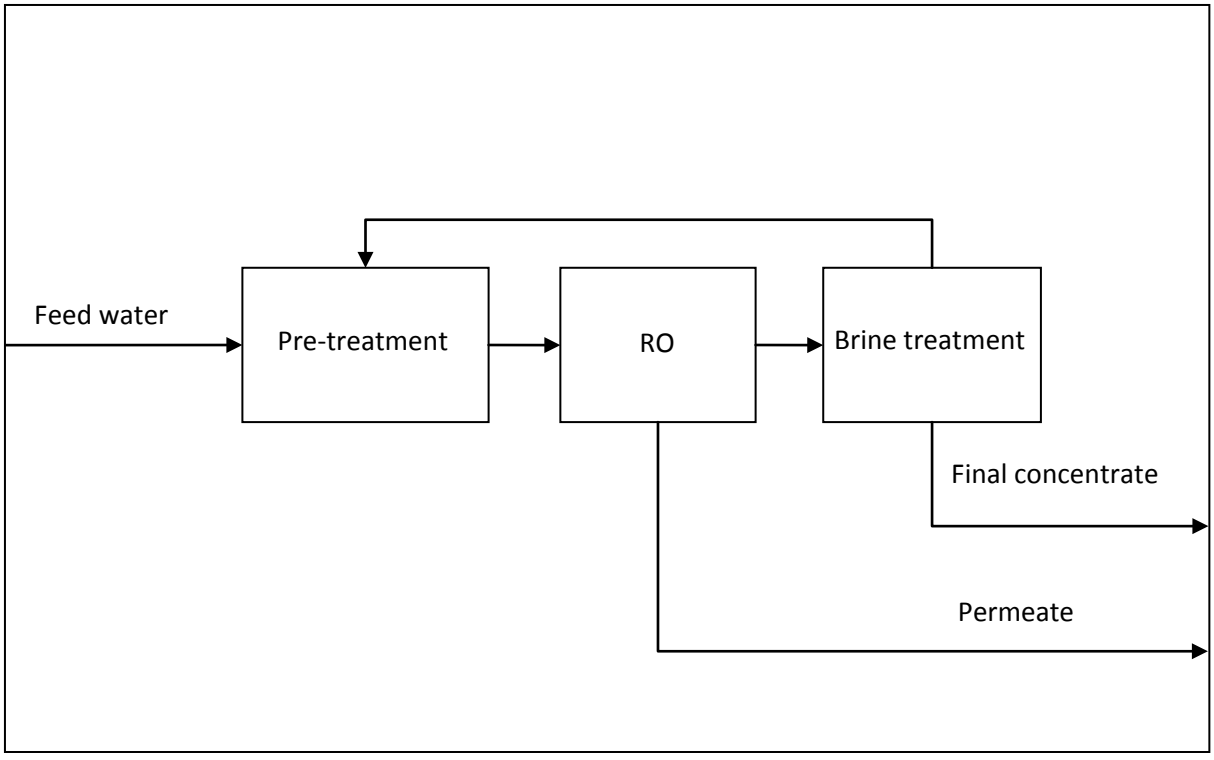

Figure 46: *Schematic to improve water recovery during RO treated AM*

Chapter 8 - Conclusions

8.1 Synthetic precipitation tests – main findings

The batch crystallization technique (using ISE to monitor precipitation), as employed to study the precipitation of gypsum from synthetically prepared solutions, produced reliable results. The measurements were verified with the use of atomic absorption spectroscopy. A standard deviation of approximately 3 was obtained for ISE measurements, giving an error margin of between 4 % and 6.5 %. The reproducibility of results was higher when the solution was seeded.

The inhibitory effect of both HYDREX and BULAB on the nucleation kinetics (expressed in terms of an induction time) was more difficult to override at a higher concentration of antiscalant. Induction times in the presence of HYDREX varied from 0-140 minutes at 4 mg/l to 0-250 minutes at 12 mg/l. For BULAB the induction times ranged from 0-450 minutes at 4 mg/l and from 0-550 minutes at 12 mg/l. Under the governing conditions BULAB therefore produced larger induction times, rendering it more effective.

Seeding and a change in pH had the greatest effect on the variation of the induction time. In almost every case where seed (pure gypsum) was added at a concentration of 2000 mg/l, it was sufficient to completely override the effect of the antiscalant (at both 4 mg/l and 12 mg/l) and produce zero induction time.

When lime was used (under experiment 8 conditions) instead of gypsum at the same concentration of 2000 mg/l, larger induction times (150 minutes for HYDREX and 50 minutes for BULAB) were produced. This problem was overcome by adding a combination of gypsum and lime seed.

In the ‘no-seed’ cases the influence of a pH-change on the induction time (hence the antiscalant effectiveness) was most prominent. At a pH of 10 the inhibitory capacity (adsorption capacity) of antiscalants was very large (in some cases induction times exceeded 24 hours) and produced longer induction times compared to a pH of 4 (in which case it rarely exceeded 100 minutes). BULAB appeared to produce longer induction times in the presence of impurities such as ferric, seed etc. and also rendered it more effective at a higher pH (within the scope of the conditions studied). When no impurities were present, BULAB was less effective than HYDREX (at high pH levels). BULAB is more acidic in character, which would cause it to produce a lower quantity of dissociated groups as the pH increases, lowering its inhibitory power. When impurities such as ferric is present however

it is likely that HYDREX would be more strongly affected than BULAB, causing the efficiency of HYDREX to drop, which results in a lowering of the induction time.

Temperature and calcium concentration showed to have a significant influence on the induction time in the literature and also during preliminary tests. However, the effect of these parameters on the induction period is not substantial under the governing experimental conditions. It is likely that the pH and seed effects overshadow the effect of these factors. With regard to the growth rate, a temperature change is almost completely responsible for any variation in the magnitude of the rate. A 10°C increase in the temperature causes the growth rate to double almost irrespective of the change in other factors.

Seeding the solution with pure gypsum under the governing conditions caused no real change in the growth rate. Using lime instead of gypsum however caused the growth rate to almost double, which is related to the fact that lime 1) increases the precipitation potential of the solution by increasing the calcium concentration and 2) stimulates the addition of new nuclei during the induction time, which increases the precipitation potential. A combination of lime and gypsum proved to overcome the occurrence of an induction time with the benefits of the same high growth rate.

An increase in the calcium concentration resulted in an increase in the growth rate of gypsum in the presence of HYDREX at a fixed temperature and was largely unaffected by a change in pH. The effect of calcium on the growth rate in the presence of BULAB was overshadowed by the effect of pH. At a high pH the growth rate is slower compared to a low pH. This could indicate that the antiscalant-crystal interaction is important even during the growth phase and that polyacrylate molecules could slow down the precipitation process if the adsorption capacity is enhanced, which is the case at a pH of 10.

The antiscalant-ferric interaction appears to be important with regard to the growth rate in the case of both HYDREX and BULAB. At a high antiscalant concentration (12 mg/l) a low ferric concentration (2 mg/l) corresponds to a low growth rate as the ferric is unable to override the effect of the antiscalant. This problem is overcome when the ferric concentration is increased. A high ferric concentration of 10 mg/l is sufficient to reduce the effect of 12 mg/l antiscalant in much the same way that 2 mg/l ferric reduces the effect of 4 mg/l antiscalant.

The optimum or ‘best’ conditions with regard to overriding the inhibitory effect of the antiscalant (HYDREX and BULAB) necessitate a low induction time (zero would be desirable) and a fast growth rate. The conditions found to be optimum under the governing experimental constraints was found in experiment 8 [T(25°C), pH(10), AS(12 mg/l), Fe(10), Ca(0.055 M) or 2204 mg/l, S(2000 mg/l)] and

experiment 14 [T(25°C), pH(4), AS(12 mg/l), Ca(0.045 M) or 1804 mg/l, S(2000 mg/l)] which both produced zero induction times and healthy growth rates. The growth rates for experiment 8 produced t_{C80} – values of 39 minutes for HYDREX and 48 minutes for BULAB. Moreover, the growth rates for experiment 14 produced t_{C80} – values of 57 minutes for HYDREX and 45 minutes for BULAB. Notice that seeding and a high temperature were present in both of these cases.

8.2 AMD concentrate precipitation tests – verification of best conditions

The conditions found to be most effective during synthetic testing in overriding the inhibitory effect of antiscalants (HYDREX and BULAB) and producing precipitation of gypsum from a super saturated solution, were applied to AMD concentrate with even greater success.

The first set of tests (in the presence of AMD concentrate) was performed at conditions of experiment 14. With regard to the nucleation kinetics, ~ 0 minutes induction time was obtained both in the presence of HYDREX and BULAB. In addition, the growth rate of gypsum in the AMD was three times faster for HYDREX and two times faster for BULAB compared to the synthetic aqueous solution at the same saturation level. The increase in the growth rate in the AMD is a possible result of a number of factors. First of all, the addition of precipitates of aluminium, calcium and magnesium in solution (according to OLI analyser), present more growth and nucleation sites, which could result in an increase in the rate of precipitation. The increase of the $[SO_4^{2-}]x[Ca^{2+}]$ product - from 3.46 (synthetic solutions) to 3.73 (AMD concentrate) - also adds to why the growth rate of gypsum is higher in the AMD concentrate relative to the synthetic tests. Moreover, aluminium forms complexes with phosphonate compounds such as HYDREX, which could be responsible for the difference in growth rate between HYDREX and BULAB.

At the conditions of experiment 8 (with the addition of both gypsum and lime seed) the induction time was again reduced to zero. The growth rate was found to be three times faster compared to synthetic tests for both HYDREX and BULAB and faster than the rates obtained in experiment 14. The additional lime increases the gypsum precipitation potential by increasing the concentration of calcium. Moreover, the higher pH causes the natural carbonate concentration to introduce $CaCO_3$ precipitation, which enhances antiscalant scavenging and introduces more growth sites for precipitation, hence a faster rate.

8.3 Hypotheses proven

To reiterate the hypotheses:

"*Considering a meta-stable solution, super saturated with gypsum in the presence of 4-12 mg/l antiscalants, the induction time for gypsum precipitation can be reduced by the addition of $FeCl_3$, decreasing the pH, addition of gypsum seed and an increase in temperature. These effects are interrelated and can be utilized to enhance precipitation of gypsum from RO concentrate generated from AMD.*"

The first part of the hypotheses touches on the reduction of the induction period. In the current study it was proven that the induction time could be reduced when a high concentration of ferric chloride (10 mg/l) is added, when the pH is reduced to 4, when seed is added at 2000 mg/l and when the temperature is increased. In addition, a combination of these conditions could lead to an improvement of the rate of precipitation. The last part of the hypotheses speaks of utilizing the conditions found to be optimum and applying it to AMD concentrate to promote gypsum precipitation in the presence of antiscalants. It was shown that even better results could be obtained for AMD concentrate compared to synthetic tests. The hypotheses have thus been confirmed.

Chapter 9 - Recommendations

By reducing the number of factors of the experimental design (at constant temperature and calcium concentration) a more thorough investigation on the interaction between pH, ferric chloride, antiscalant and seeding can be realised.

At constant seed concentration and temperature, the real influence of factors such as the ferric concentration, calcium concentration and pH can be investigated on the nucleation and growth kinetics.

A larger range of seed concentrations (0 mg/l up to 10 g/l) should be investigated as well as more variation in seed types (*e.g.* limestone, dolomite, soda ash etc.).

Synthetic aqueous solutions should be prepared to more closely resemble real AMD. This could however be a complicated and expensive business.

Real pilot plant work should be conducted to investigate the interactive effect of trace components such as Mg, Al, Ba, Sr etc.

A more continuous type of monitoring system should be employed such as online turbidity or conductivity measurement to increase the accuracy of the induction periods as well reduce the intensity of data collection.

The attained knowledge from this study should be put to the test under dedicated testing on pilot scale to determine its effect on continuous real life operation.

Chapter 10 - References

Akay, G., Keskinler, B., Cakici, A. and Danis, U. 1998. Phosphate removal from water by red mud using crossflow microfiltration. *Water research*, 32(3):717-726.

Amjad, Z. 1985. Applications of antiscalant to control calicum sulfate sclaing in reverse osmosis systems. *Desalination*, 54:263-276.

Amjad, Z. 1988a. Calcium sulphate dihydrate (gypsum) scale formation on heat exchanger surfaces: the influence of scale inhibitors. *Journal of colloid and interface science*, 123(2):523-536.

Amjad, Z. 1988b. Kinetics of a crystal growth of calcium sulfate dihydrate:the influence of polymer composition, molecular weight, and solution pH. *Canadian journal of chemistry*, 66:1529-1536.

Amjad, Z. and Hooley, J. 1986. Influence of polyelectrolytes on the crystal growth of calcium culfate cihydrate.*Journal of colloid and interface science*, 111(2):496-503.

Apfel, R.E. 1972. Water super saturated to 279.5°C at atmospheric pressure.*Nature physical science*, 238:63-64.

Basson, M.S., van Niekerk, P.H., van Rooyen, J.A. 1997. Overview of water resources availability and utilization in South Africa. Department of water affairs and forestry. Pretoria, South Africa.

Ben Ahmed, S., Tlili, M.M. and Ben Amor, M. 2008. Influence of a polyacrylate antiscalant on gypsum nucleation and growth. *Crystal research and technology*, 43(9):935-942.

Block, J. and Waters, O. 1968. The CaSO4-Na2SO4-NaCl-H2O system at 25°C to 100°C. *Journal of chemical engineering data*, 13:336-344.

Blount, C.W. and Dickson, F.W. 1973. Gypsum anhydrite equilibria in systems CaSO4-H2O and CaCO3-NaCl-H2O. *The American minerologist,* 58:323-332.

Bonne, P.A.C., Hofman, J.A.M.H. and van der Hoek, J.P. 2000. Scaling control of RO membranes and direct treatment of surface water. *Desalination*, 132:109-119.

Bremere, I., Kennedy, M., Johnson, A., van Emmerik, R., Witkamp, G.-J. and Schippers, J. 1998. Increasing conversion in membrane filtration systems using a desuper saturationsuper saturation unit to prevent scaling. *Desalination*, 119:199-204.

Bremere, I., Kennedy, M., Michel, P., van Emmerik, R., Witkamp, G.-J. and Schippers, J. 1999. Controlling scaling in membrane filtration systems using a desuper saturationsuper saturation unit. *Desalination* 124:51-62.

Brown, M., Barley, B. and Wood, H. 2002. *Minewater treatment: technology, application and policy*. London: IWA Publishing.

Burger, A.J. 2010.Personal interview. November 2010, Stellenbosch

Chamber of mines of South Africa. 2010. Mining: an in depth discussion of mining issues in South Africa. *Mining*, March-May.

Dalvi, A.G.I., Mohammad, N.M.K., Al-Sulami, S. and Sahul, K. 2000.Rrole of chemical constituents in recycle brine on the performance of scale control additives in MSF plants. *Desalination*,129:173-186.

De Santis, R., Grande, B. 1979. An equation for predicting third virial coefficients of nonpolar gases. *AlChE Journal,25(6):* 931-938.

Droste, R.L. 1997. *Theory and practice of water and wastewater treatment*. John Wiley & Sons Inc.

El Dahan, H.A. and Hegazy, H.S. 2000. Gypsum scale control by phosphate ester. *Desalination*, 127:111-118.

Gabelich, C.J., Ishida, K.P., Gerringer, F.W., Evangelista, R., Kalyan, M. and Suffet, I.H. 2006. Control of residual aluminum from conventional treatment to improve reverse osmosis performance. *Desalination*, 190:147-160.

Gabelich, C.J., Yun, T.I., Coffey, B.M. and Suffet, I.H. 2002. Effects of aluminum sulfate and ferric chloride coagulant residuals on polyamide membrane performance. *Desalination*, 150:15-30.

Geldenhuys, A.J., Maree, J.P., de Beer, M. and Hlabela, P. 2001. An integrated limestone/lime process for partial sulphate removal. *Conference on environmentally responsible mining in South Africa*. Pretoria.

Gill, J.S. and Nancollas, G.H. 1979.The growth of gyspum crystals on barite and calcite. *Desalination*, 29:247-254.

Gordon, M. 2010. Personal interview. January 2010, Stellenbosch

Guo, J. and Severtson, J. 2004. Inhibition of calcium carbonate nucleation with aminophosphonates at high temperature, pH and ionic strength. *Industrial and engineering chemistry research*, 43:5411-5417.

Hamdona, S.K. and Al Hadad, U.A. 2007. Crystallization of calcium sulfate dihydrate in the presence of some metal ions. *Journal of crystal growth*, 299:146-151.

Hamdona, S.K. and Al Hadad, O.A. 2008. Influence of additives on the precipitation of gyspum in sodium chloride solutions. *Desalination*, 228:277-286.

Hamdona, S.K., Nessim, R.B. and Hamza, S.M. 1993. Spontaneous precipitation of calcium sulphate dihydrate in the presence of some metal ions. *Desalination*, 94:69-80.

Hanna Instruments n.d.*HI 4104 Instruction manual*.

Hardie, L.A. 1967. The gypsum-anhydrite equilibrium at one atmosphere pressure. *The American mineralogist*, 52:171-200.

He, S., Oddo, J.E. and Tomson, M.B. 1994. The inhibition of gypsum and barite nucleation in NaCl brines at temperatures from 25°C to 90°C. *Applied geochemistry*, 9:561-567.

Hernandez, A., La Rocca, A., Power, H., Graupner, U. and Ziegenbalg, G. 2006. Modelling the effect of precipitation inhibitors on the crystallization process from well mixed over-saturated solutions in gypsum based on Langmuir-Volmer flux correction. *Journal of crystal growth*, 295:217-230.

Hoang, T.A., Ang, H.M. and Rohl, A.L. 2007. Effects of temperature on the scaling of calcium sulphate in pipes. *Powder technology*, 179:31-37.

Kim, M.-m., Au, J., Rahardianto, A., Glater, J., Cohen, Y., Gerringer, F.W. and Gabelich, C.J. 2009. Impact of conventional water treatment coagulants on mineral scaling in RO desalting of brackish water. *Industrial engineering chemistry research*, 48:3126-3135.

Klepetsanis, P.G., Dalas, E. and Koutsoukos, P.G. 1999. Role of temperature in the spontaneous precipitation of calcium sulfate dihydrate. *Langmuir*, 15:1534-1540.

Klepetsanis, P.G. and Koutsoukos, P.G. 1991. Spontaneous precipitation of calcium culfate at conditions of sustained super saturationsuper saturation. *Journal of colloid and interface science*, 143(2):299-308.

Koretsky, M.D. 2004. *Engineering and chemical thermodynamics.* John Wiley and Sons.

Le Gouellec, Y.A. and Elimelech, M. 2002. Calcium sulfate (gypsum) scaling in nanofiltration of agricultural drainage water. *Journal of membrane science*, 205:279-291.

Lee, S., Choi, J.-S. and Lee, C.-H. 2009. Behaviors of dissolved organic matter in membrane desalination. *Desalination*, 238:109-116.

Leseur, C., Pfeffer, M. and Fuerhacker, M. 2005. Photodegradation of phosphonates in water. *Chemosphere*,59:685-691.

Lewis, A., Nathoo, J. 2006. Prevention of calcium sulphate crystallization in water desalination plants using slurry precipitation and recycle reverse osmosis (SPARRO). Water research commission.

Liu, S.-T. and Nancollas, G.H. 1970. The kinetics of crystal growth of calcium sulfate dihydrate. *Journal of crystal growth*, 6:281-289.

Liu, S.-T. and Nancollas, G.H. 1973. Linear crystallization and induction-period studies of the growth of calcium sulphate dihydrate crystals. *Talanta*, 20:211-216.

Liu, S.-T. and Nancollas, G.H. 1973. The crystal growth of calcium sulfate dihydrate in the presence of additives. *Journal of colloid and interface science*, 44(3):422-429.

Liu, S.T. and Nancollas, G.H. 1975. A kinetic and morphological study of the seeded growth of calcium sulfate dihydrate in the presence of additives. *Journal of colloid and interface science*, 52(3):593-601.

Lottermoser, B. 2007.*Mine wastes: Characterization, treatment and environmental impacts*. 2nd edition. New York: Springer.

McCartney, E.R. and Alexander, A.E. 1958. The effect of additives upon the process of crystallization. *Journal of colloid science*, 13:383-396.

Montgomery, D.C., Runger, G.C. & Humbele, N.F. 1998. *Engineering Statistics*. New York: John Wiley & Sons, Inc.

Mullin, J.W. 1997.*Crystallization*. Oxford,U.K.: Butterworth-Heinemann.

Nathoo, J., Jivanji, R. and Lewis, A.E. 2009. Freezing your brines off: eutectic freezecrystallization for brine treatment. *International mine water conferenc.* Pretoria.

Nielsen, A.E. 1984. Electrolyte crystal growth kinetics. *Journal of crystal growth*, 67(2):278-288.

Ohara, M. and Reid, R.C. 1973. *Modelling crystal growth rates from solution*. N.J.: Prentice-Hall.

Oner, M., Dogan, O. and Oner, G. 1998. The influence of polyelectrolytes architecture on calcium sulfate dihydrate growth retardation. *Journal of crystal growth*, 186:427-437.

Partridge, E.P. and White, A.H. 1929. The solubility of calcium sulphate from 0 to 200°C. *Journal of American chemical society*, 51(2):360-370.

Pitzer, K.S. 1991. *Activity coefficients in electrolyte solutions*. Boca Raton,FL: CRC press Inc.

Posnjak, E. 1938. The system CaSO4-H2O. *American journal of science*, 35:247-272.

Power, W.H., Fabuss, B.M. and Satterfield, C.N. 1964. Transient solubilities in the calcium sulphate-water system. *Journal of chemical engineering data*, 9(3):437-442.

Pytcowicz, R.M. 1979. *Activity coefficients in electrolyte solutions*. Boca Raton, FL: CRC press Inc.

Rahardianto, A., McCool, B.C. and Cohen, Y. 2010. Accelerated desuper saturationsuper saturation of reverse osmosis concentrate by chemically-enhaced seeded precipitation. *Desalination*, (In Press.)

Rashad, M.M., Mahmoud, M.M.H., Ibrahim, I.A. and Abdel-Aal, E.A. 2004. Crystallization of calcium sulfate dihydrate under simulated conditions of phosphoric acid production in the presence of aluminum and magnesium ions. *Journal of crystal growth*, 267:372-379.

Sarig, S., Kahana, F. and Lesheim, R. 1975. Selection of threshold agents for calcium sulfate scale control on the basis of chemical structure. *Desalination*, 17:215-229.

Scholes, R.J., van der Merwe, M., John, J., Oosthuizen, R. 1999. National state of environment report. Department of environmental affairs and tourism. Pretoria.

Seewoo, S., Van Hille, R. and Lewis, A. 2004. Aspects of gypsum precipitation in scaling waters. *Hydrometallurgy*, 75:135-146.

Shih, W.-Y., Albrecht, K., Glater, J. and Cohen, Y. 2004. A dual-probe approach for evaluation of gypsum crystallization in response to antiscalant treatment. *Desalination*, 169:213-221.

Shih, W.-Y., Gao, J., Rahardianto, A., Glater, J., Cohen, Y. and Gabelich, C.J. 2006. Ranking of antiscalant performance fro gypsum scale suppression in the presence of residual aluminum. *Desalination*, 196:280-292.

Snoeyink, V.L. and Jenkins, D. 1980. *Water Chemistry.* New York: John Wiley and Sons, Inc.

Söhnel, O. and Garside, J. 1992. *Precipitation: basic principles and industrial application.* Butterworth-Heinemann Ltd.

Söhnel, O. and Mullin, J.W. 1988. Interpretation of crystallization induction periods. *Journal of colloid and interface science*, 123(1):43-50.

Sourinajan, S. 1970. *Reverse osmosis*. London: Logos Press.

Strohwald, H. 2010. Personal Interview. January 2010, Stellenbosch.

Stumm, W. 1992. *Chemistry of solid-water Interface*. New York: Wiley.

Tait, S., Clarke, W.P., Keller, J. and Batstone, D.J. 2009. Removal of sulphate from high-strength waste water by crystallization. *Water research*, 43:762-772.

Van den Berg, O. 2009. Overview of water resources of South Africa. Mine and metallurgical association of South Africa. Department of water affairs & forestry.

Wang, C., Li, S.-p. and Li, T.-d. 2009. Calcium carbonate inhibition by a phosphonate-terminated poly(maleic-co-sulfonate) polymeric inhibitor. *Desalination*, 249:1-4.

Weijnen, M.P.C., Marchee, W.G.J. and van Rosmalen, G.M. 1983. A quantification of the effectiveness on an inhibitor of the growth process of a scalant. *Desalination*, 47:81-92.

Weijnen, M.P.C. and van Rosmalen, G.M. 1985. The influence of various polyelectrolytes on the precipitation of gypsum. *Desalination*, 54:239-261.

Weijnen, M.P.C., van Rosmalen, G.M., Benna, P. 1986. The adsorption of additives at the gypsum crystal surface: a theoretical approach. *Journal of crystal growth*, 82:528-542.

Wilf, M. and Ricklis, J. 1983. RO desalination of brackish water overstaurated with CaSO4.

Yang, Q., Lisitsin, D., Liu, Y., David, H. and Semiat, R. 2007. Desuper saturationsuper saturation of RO concentrates by addition of coagulant and surfactant. *Journal of chemical engineering of Japan*, 40(9):730-735.

Yang, Q., Liu, Y., Hasson, D. and Semiat, R. 2008a. Scaling salt removal by addition of Inorganic particles. *Journal of chemical engineering of Japan*, 41(1):6-12.

Yang, Q., Liu, Y., Hasson, D. and Semiat, R. 2008b. Removal of CaCO3 scaling salt from RO concentrates by air-blow and inorganic inducers. *Journal of chemical engineering of Japan*, 41(1):13-20

Chapter 11 - Appendix

11.1 Calculation of sample standard deviation

The (sample) standard deviation for selected data populations (using selected data points within the populations) for a number of repeated experiments was calculated, to determine the repeatability of the current experimental method. The data populations used were experiments 9, 10, 11, 20 and 21 (c.f. section 11.4 and 11.5in the appendix for the raw data). These experiments were performed in the presence of HYDREX. At time intervals of 28, 48, 68, 88 and 108 minutes, calcium concentrations were taken. If data at that time interval was not available, linear interpolation was performed to obtain the necessary data. In the table below, observe that for each data point the standard deviation is between 3 and 4 units from the average value at a given time interval. If one could express this in an error term it would amount to between 4 and 6.5 % (refer to **Table 32**).

Table 32: *Standard deviations for a number of data populations*

Exp ID	Time (minutes)	$[Ca^{2+}]$ (mg/l)	Exp ID	Time (minutes)	$[Ca^{2+}]$ (mg/l)
9	28	78	9	48	67
10	28	83	10	48	74
11	28	75	11	48	66
20	28	78	20	48	66
21	28	78	21	48	67
StDEV		**3.072054687**	**StDEV**		**3.654787**
average		**78.4**	**average**		**68**
Error (%)		**3.92**	**Error (%)**		**5.37**
Exp ID	**Time (minutes)**	**$[Ca^{2+}]$ (mg/l)**	**Exp ID**	**Time (minutes)**	**$[Ca^{2+}]$ (mg/l)**
9	68	61	9	88	58
10	68	68	10	88	64
11	68	60	11	88	55
20	68	62	20	88	56
21	68	62	21	88	57
StDEV		**3.221005**	**StDEV**		**3.575891**
average		**62.6**	**average**		**58**
Error (%)		**5.15**	**Error (%)**		**6.17**
Exp ID	**Time (minutes)**	**$[Ca^{2+}]$ (mg/l)**			
9	108	54			
10	108	62			
11	108	53			
20	108	55			
21	108	55			
StDEV		**3.512866**			
average		**55.8**			
Error (%)		**6.29**			

11.2 **Preliminary results (raw data)**

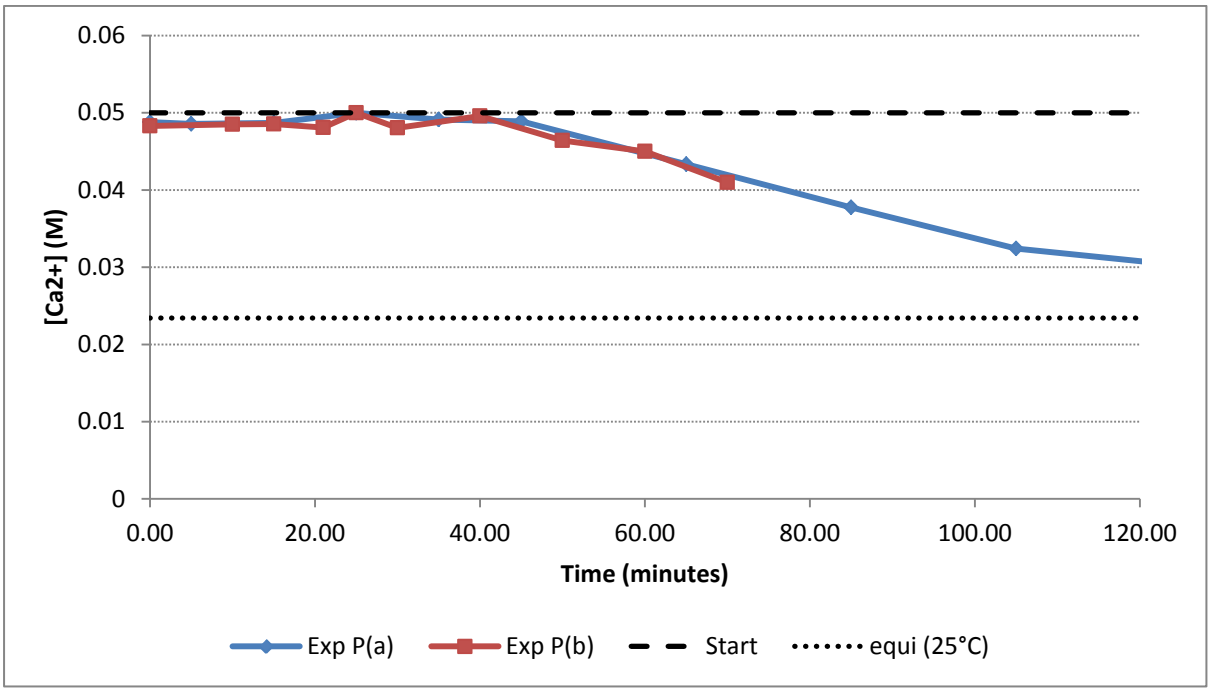

Figure 47: *Kinetics plots, [Ca^{2+}] =0.05 M, T (15°C), AS (0 mg/l)*

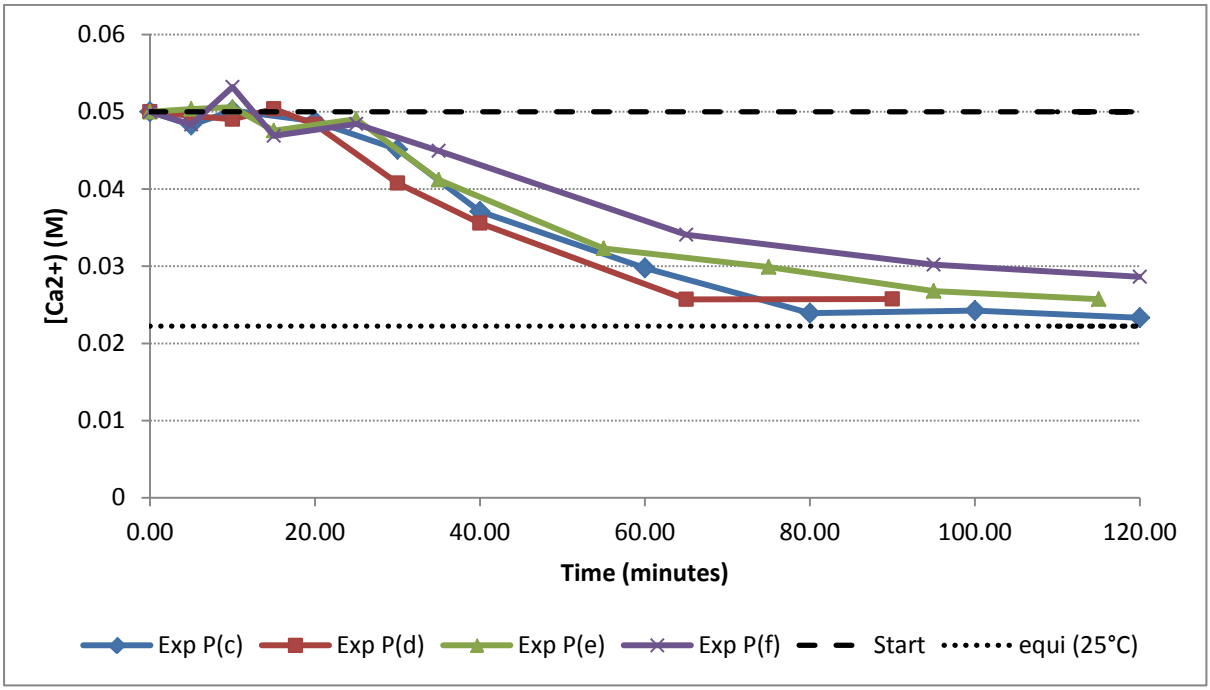

Figure 48: *Kinetics plots, [Ca^{2+}] =0.05 M, T (25°C), AS (0 mg/l)*

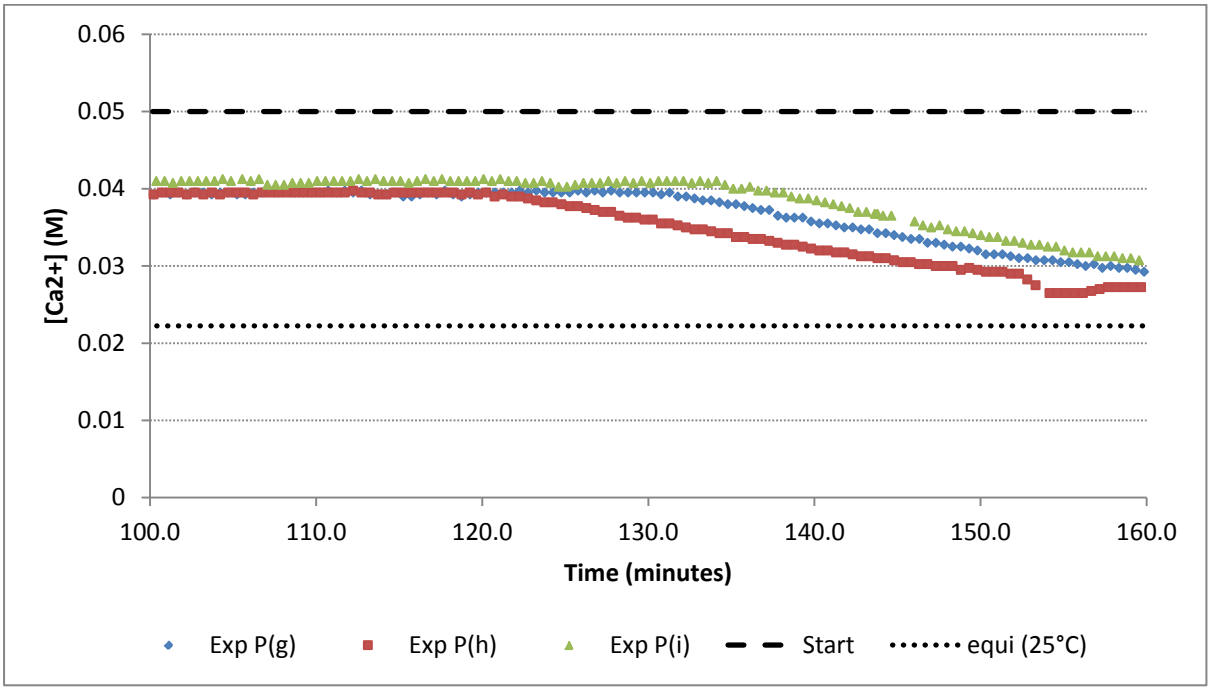

Figure 49: *Kinetics plots, [Ca^{2+}] =0.05 M, T (25°C), AS (1 mg/l), BULAB*

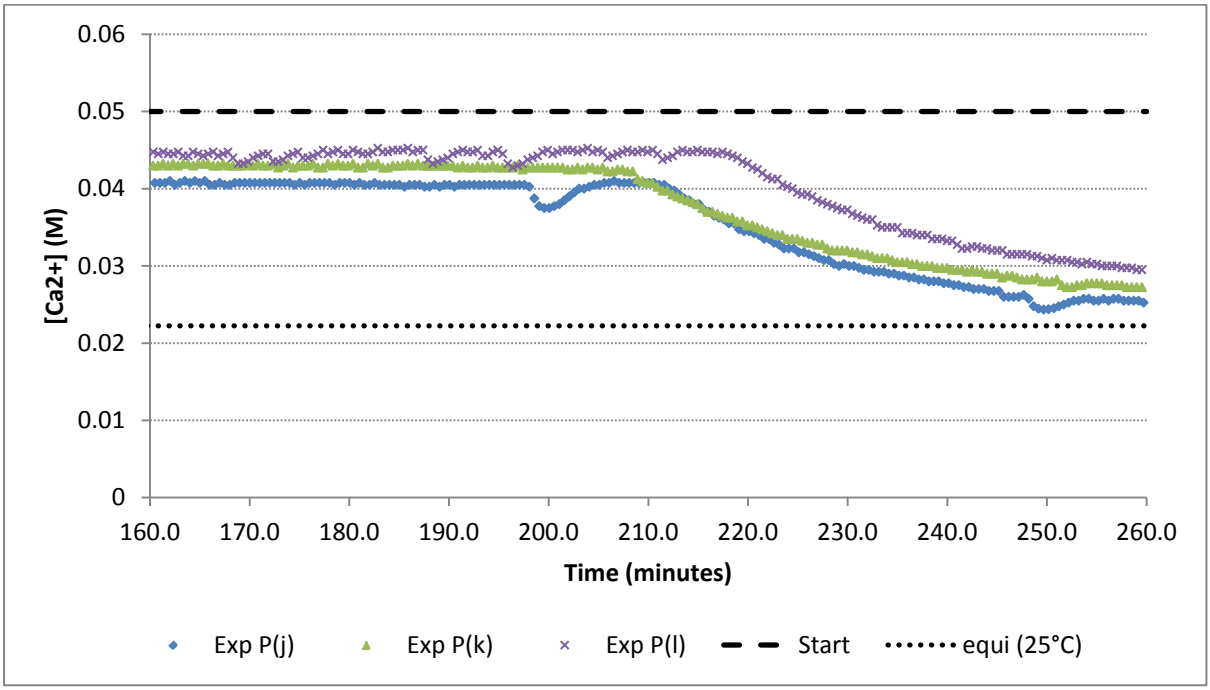

Figure 50: *Kinetics plots, [Ca^{2+}] =0.05 M, T (25°C), AS (2 mg/l), BULAB*

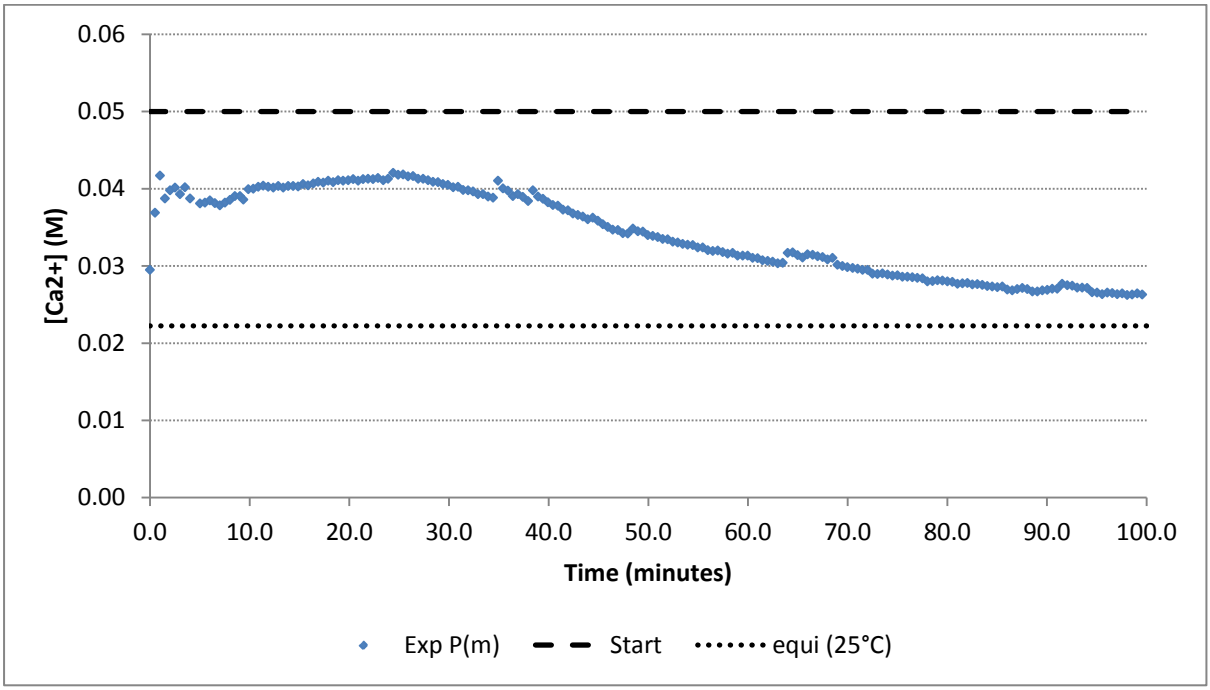

Figure 51: *Kinetics plots, [Ca^{2+}] =0.05 M, T (25°C), AS (2 mg/l), Fe (10 mg/l), BULAB*

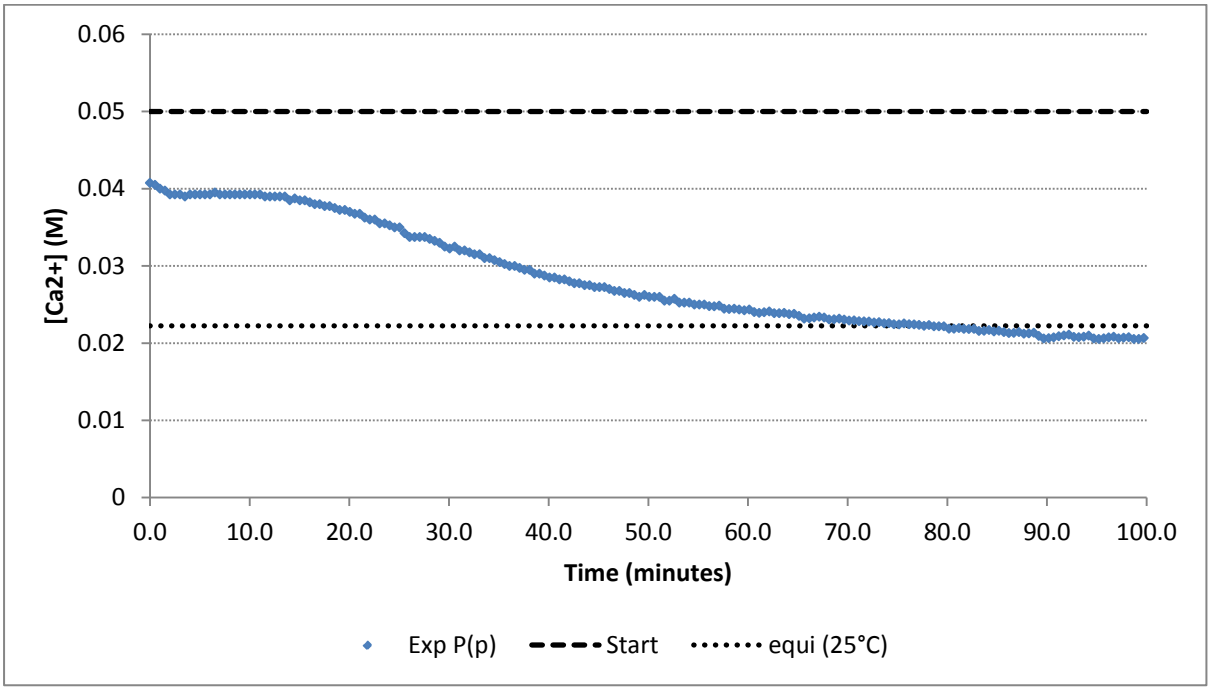

Figure 52: *Kinetics plots, [Ca^{2+}] =0.5 M, T (25°C), AS (2 mg/l), Alum (10 mg/l), BULAB*

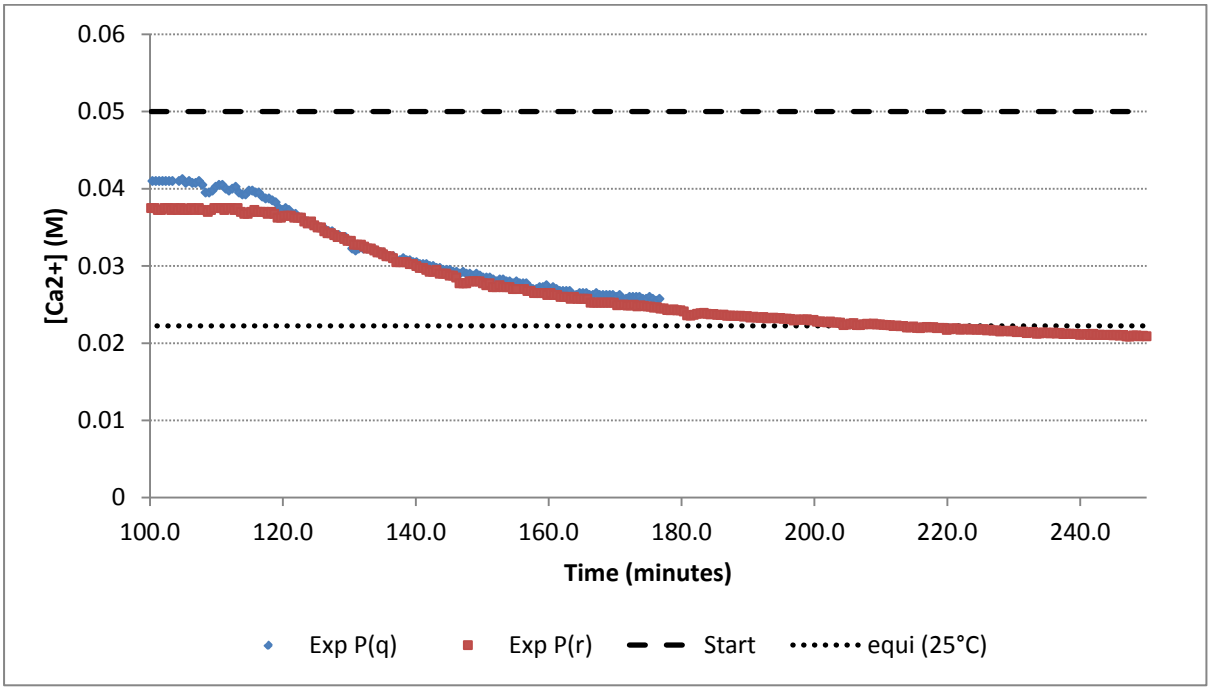

Figure 53: *Kinetics plots, [Ca^{2+}] =0.045 M, T (25°C), pH (4), AS (2 mg/l), BULAB*

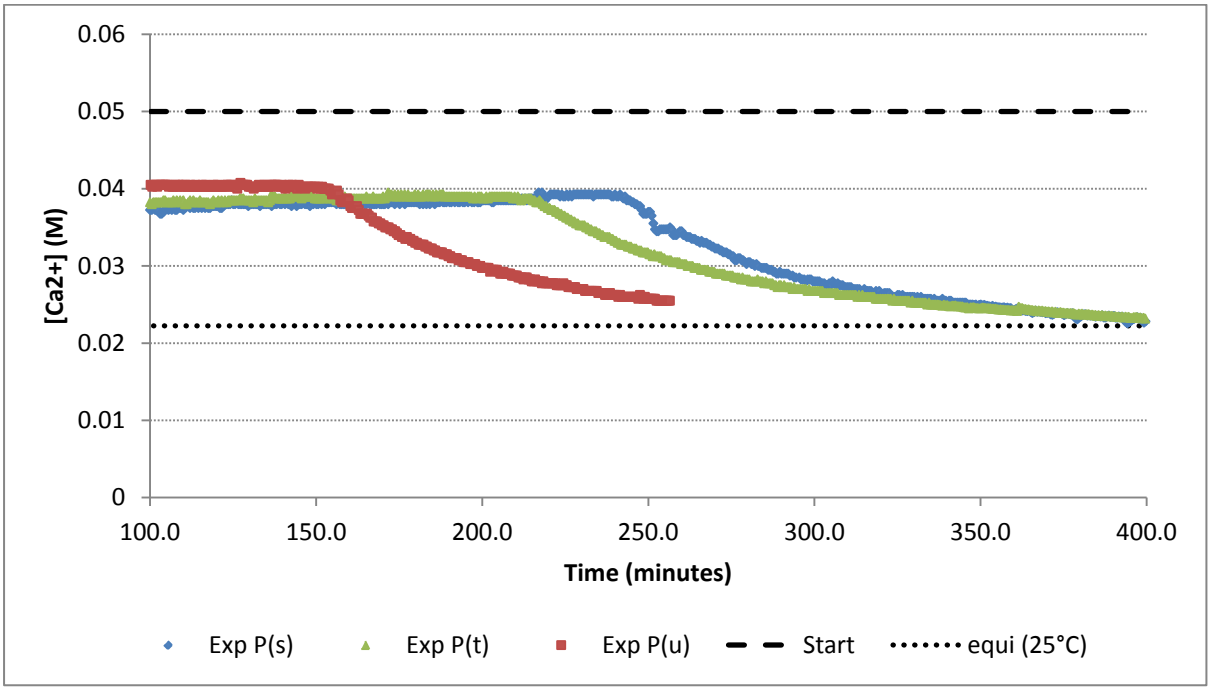

Figure 54: *Kinetics plots, [Ca^{2+}] =0.05 M, T (25°C), pH (10), AS (2 mg/l), BULAB*

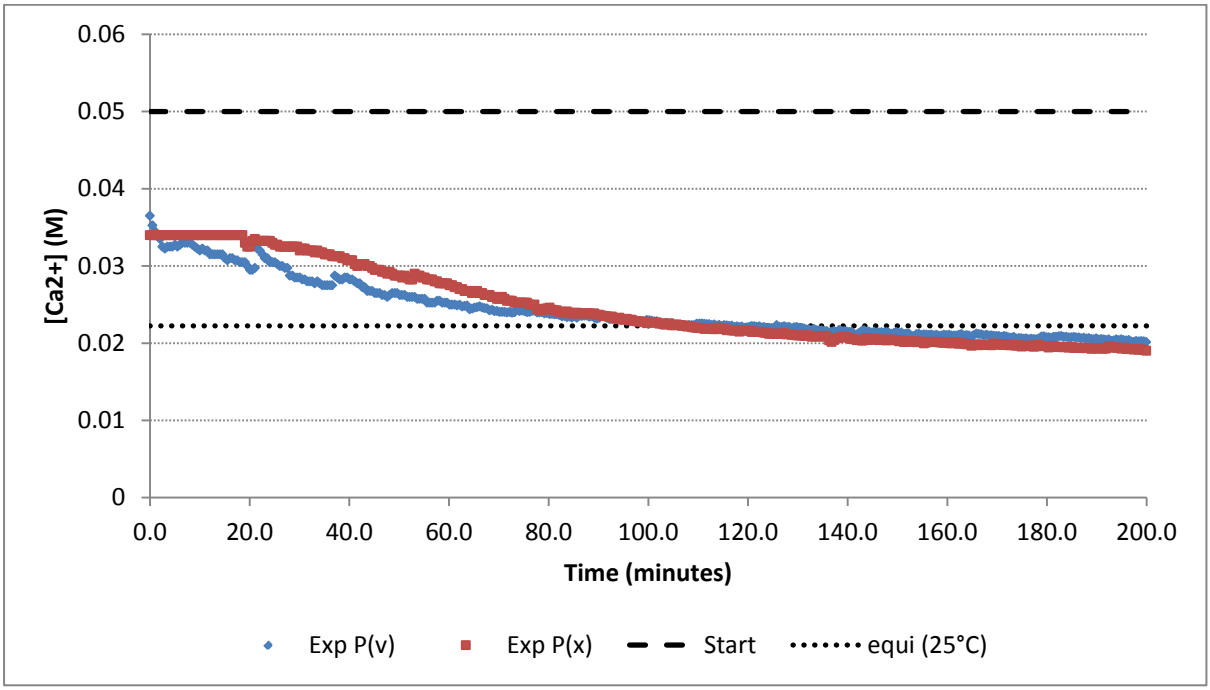

Figure 55: *Kinetics plots, [Ca^{2+}] =0.05 M, T (25°C), AS (2 mg/l), Seed, BULAB*

11.3 **Baseline data (raw data)**

Note: *all '**measured**' data is presented as displayed by the analytic instrument (remember that a 20x dilution is made before measurement). The '**actual**' values are back calculated to the original value by multiplying the '**measured**' values by 20 and dividing the answer by 40000 to obtain the molar values.*

Table 33: *Kinetic baseline data*

Exp B1 [T(15°C),Ca(0.045 M)]			**ExpB2 [T(15°C), Ca(0.055 M)]**		
Time (minutes)	**$[Ca^{2+}]$ (mg/l) measured**	**$[Ca^{2+}]$ (M) actual**	**Time (minutes)**	**$[Ca^{2+}]$ (mg/l) measured**	**$[Ca^{2+}]$ (M) actual**
10	87.4	0.0437	7	105	0.0525
30	88.9	0.04445	19	110	0.055
40	86.8	0.0434	29	98.5	0.04925
50	87.1	0.04355	39	78.5	0.03925
60	81.3	0.04065	49	68.7	0.03435
80	71.5	0.03575	59	60.6	0.0303
102	63.5	0.03175	69	57.1	0.02855
122	56.8	0.0284	79	53.3	0.02665
140	53.7	0.02685	99	50.4	0.0252
190	45	0.0225	119	49	0.0245
215	44.3	0.02215	169	48	0.024
300	44	0.022	369	48	0.024

Table 34: *Kinetic baseline data*

Exp B3 [T(25°C),Ca(0.045 M)]			**Exp B4 [T(25°C), Ca(0.055 M)]**		
Time (minutes)	**$[Ca^{2+}]$ (mg/l) measured**	**$[Ca^{2+}]$ (M) actual**	**Time (minutes)**	**$[Ca^{2+}]$ (mg/l) measured**	**$[Ca^{2+}]$ (M) actual**
10	86	0.043	5	106	0.053
20	87	0.0435	10	102	0.051
30	81	0.0405	20	74	0.037
45	67.8	0.0339	30	57	0.0285
60	55.3	0.02765	40	52.3	0.02615
75	50.5	0.02525	50	48.5	0.02425
90	45	0.0225	60	46.5	0.02325
105	44	0.022	70	45	0.0225
120	44	0.022	100	45	0.0225
300	44	0.022			

11.4 **HYDREX designed experiments (raw data)**

Table 35: *HYDREX kinetic data (summary)*

Exp ID	Temp (°C)	pH	AS dosage (mg/l)	$FeCl_3$ dosage (mg/l)	$[Ca^{2+}]$ (M)	Seed (mg/l)	Induction time (minutes)	k' ($M^{-1}min^{-1}$)	t_{C80} (minutes)
1	15	4	4	10	0.055	2000	0	1.07	82
2	25	4	4	2	0.045	2000	0	2.08	59
3	15	10	4	2	0.055	0	140	0.54	94
4	25	10	4	10	0.045	0	100	0.92	86
16	25	10	4	2	0.055	2000	0	1.87	44
17	15	10	4	10	0.045	2000	0	0.56	156
18	25	4	4	10	0.055	0	0	1.42	44
19	15	4	4	2	0.045	0	60	0.67	131
5	15	4	12	10	0.045	0	70	0.34	124
6	25	4	12	2	0.055	0	90	2.87	25
7	15	10	12	2	0.045	2000	250	0.22	211
8	25	10	12	10	0.055	2000	0	1.83	60
12	25	10	12	2	0.045	0	>1440	-	-
13	15	10	12	10	0.055	0	150	1.27	87
14	25	4	12	10	0.045	2000	0	2.10	57
15	15	4	12	2	0.055	2000	0	0.29	200

Table 35 *Continues*

9 (C)	20	7	8	6	0.055	100	0	0.63	101
10 (C)	20	7	8	6	0.055	100	0	0.85	97
11 (C)	20	7	8	6	0.055	100	0	0.85	78
20 (C)	20	7	8	6	0.055	100	0	0.89	87
21 (C)	20	7	8	6	0.055	100	0	0.89	105
22 (C)	20	7	8	6	0.055	100	0	0.88	95

Table 36: *Kinetic raw data – (Exp 1 and Exp 2) - HYDREX*

Exp 1			Exp 2		
Time (minutes)	$[Ca^{2+}]$ (mg/l) measured	$[Ca^{2+}]$ (M) actual	Time (minutes)	$[Ca^{2+}]$ (mg/l) measured	$[Ca^{2+}]$ (M) actual
8	87	0.0435	8	82.8	0.0414
19	70.3	0.0352	23	66.8	0.0334
31	63	0.0315	38	60.1	0.0300
46	54.9	0.0275	55	55.2	0.0276
61	50.7	0.0254	70	52.2	0.0261
76	47.6	0.0238	85	50	0.0250
91	44.8	0.0224	100	48.9	0.0244
111	42.1	0.0211	115	47.9	0.0239
131	39.5	0.0198	130	47.1	0.0235
171	37.5	0.0188	180	46.1	0.0230
211	36	0.0180	230	45.4	0.0227
241	35	0.0175	250	45.4	0.0227
271	34.4	0.0172			

Table 37: *Kinetic raw data – (Exp 3 and Exp 4) - HYDREX*

Exp 3			Exp 4		
Time (minutes)	$[Ca^{2+}]$ (mg/l) measured	$[Ca^{2+}]$ (M) actual	Time (minutes)	$[Ca^{2+}]$ (mg/l) measured	$[Ca^{2+}]$ (M) actual
8	106	0.0530	8	87	0.0435
24	106	0.0530	38	87	0.0435
59	106	0.0530	68	87	0.0435
99	106	0.0530	98	87	0.0435
129	106	0.0530	118	82	0.0410
149	103	0.0515	138	70.7	0.0354
164	88.4	0.0442	158	61.5	0.0308
179	75.7	0.0379	178	53.3	0.0267
194	67.5	0.0338	198	50.7	0.0254
210	61.6	0.0308	218	47.8	0.0239
239	55.5	0.0278	408	41.8	0.0209
272	51.3	0.0257			
299	48.9	0.0245			
332	46	0.0230			
362	45.1	0.0226			
422	43.3	0.0217			
442	43	0.0215			

Table 38: *Kinetic raw data – (Exp 5 and Exp 6) - HYDREX*

Exp 5			Exp 6		
Time (minutes)	**$[Ca^{2+}]$ (mg/l) measured**	**$[Ca^{2+}]$ (M) actual**	**Time (minutes)**	**$[Ca^{2+}]$ (mg/l) measured**	**$[Ca^{2+}]$ (M) actual**
8	90	0.045	10	106	0.0530
38	90	0.045	50	106	0.0530
81	86.8	0.0434	82	106	0.0530
100	77	0.0385	97	97	0.0485
120	68.9	0.03445	107	72	0.0360
140	61.9	0.03095	117	64	0.0320
170	54	0.027	127	56.3	0.0282
200	49.6	0.0248	137	54.3	0.0272
220	46	0.023	152	50.8	0.0254
260	42.7	0.02135	167	50.7	0.0254
300	40	0.02			
355	38.8	0.0194			
390	39.1	0.01955			

Table 39: *Kinetic raw data – (Exp 7 and Exp 8) - HYDREX*

Exp 7			Exp 8		
Time (minutes)	**$[Ca^{2+}]$ (mg/l) measured**	**$[Ca^{2+}]$ (M) actual**	**Time (minutes)**	**$[Ca^{2+}]$ (mg/l) measured**	**$[Ca^{2+}]$ (M) actual**
8	89.1	0.0446	8	101	0.0505
68	88.1	0.0441	24	73.5	0.0368
153	87.6	0.0438	44	61.5	0.0308
233	87.4	0.0437	64	55.6	0.0278
293	84.1	0.0421	84	52.5	0.0263
323	75.6	0.0378	114	49	0.0245
353	70.2	0.0351	144	46.7	0.0234
383	65.7	0.0329	174	45.2	0.0226
423	60.9	0.0305	204	44.5	0.0223
473	53.6	0.0268	235	43.5	0.0218
533	48.5	0.0243			
593	46.3	0.0232			
653	44.9	0.0225			
923	42.6	0.0213			

Table 40: *Kinetic raw data – (Exp 9 and Exp 10) - HYDREX*

Exp 9			Exp 10		
Time (minutes)	**$[Ca^{2+}]$ (mg/l) measured**	**$[Ca^{2+}]$ (M) actual**	**Time (minutes)**	**$[Ca^{2+}]$ (mg/l) measured**	**$[Ca^{2+}]$ (M) actual**
8	96.1	0.0481	8	98.2	0.0491
23	81.6	0.0408	23	85.8	0.0429
38	72	0.0360	38	78	0.0390
53	64.5	0.0323	55	71.8	0.0359
69	61	0.0305	75	66.5	0.0333
107	54	0.0270	95	63	0.0315
138	49.6	0.0248	125	59.8	0.0299
168	47	0.0235	180	56.5	0.0283
198	45	0.0225	210	55	0.0275
228	44	0.0220	240	53.8	0.0269
258	43.2	0.0216	265	52.9	0.0265

Table 41: *Kinetic raw data – (Exp 11 and Exp 12) - HYDREX*

Exp 11			Exp 12		
Time (minutes)	**$[Ca^{2+}]$ (mg/l) measured**	**$[Ca^{2+}]$ (M) actual**	**Time (minutes)**	**$[Ca^{2+}]$ (mg/l) measured**	**$[Ca^{2+}]$ (M) actual**
8	93		0	89	0.0445
29	74.6		20	90	0.045
48	65.6		40	88	0.044
88	55		60	89	0.0445
108	52.6		80	89	0.0445
138	50.4		100	90	0.045
168	49.2		200	91	0.0455
208	47.5		400	88	0.044
241	46		800	89	0.0445
8	93		100	90	0.045
29	74.6		1200	89	0.0445
48	65.6		1400	89	0.0445
88	55				
108	52.6				

Table 42: *Kinetic raw data – (Exp 13 and Exp 14) – HYDREX (Brackets indicate AA reading)*

Exp 13			Exp 14		
Time (minutes)	**$[Ca^{2+}]$ (mg/l) measured**	**$[Ca^{2+}]$ (M) actual**	**Time (minutes)**	**$[Ca^{2+}]$ (mg/l) measured**	**$[Ca^{2+}]$ (M) actual**
8	104	0.052	8	82.7	0.04135
28	106	0.053	25	63.7	0.03185
48	106	0.053**(0.0535)**	40	57	0.0285
68	106	0.053	56	52.1	0.02605
98	106	0.053	71	50.1	0.02505
128	106	0.053	87	48.3	0.02415
148	104	0.052	100	47	0.0235
168	84	0.042**(0.042)**	120	45.8	0.0229
188	69	0.0345	145	44	0.022
208	60.7	0.03035	172	43	0.0215
228	56.8	0.0284	226	43	0.0215
248	53	0.0265			
268	50.3	0.02515			
288	49.5	0.02475			
355	46	0.023**(0.023)**			
422	44	0.022			
448	44	0.022			

Table 43: *Kinetic raw data – (Exp 15 and Exp 16) – HYDREX (Brackets indicate AA reading)*

Exp 15			Exp 16		
Time (minutes)	**$[Ca^{2+}]$ (mg/l) measured**	**$[Ca^{2+}]$ (M) actual**	**Time (minutes)**	**$[Ca^{2+}]$ (mg/l) measured**	**$[Ca^{2+}]$ (M) actual**
8	106	0.053	8	98	0.49
28	94.5	0.04725**(0.047)**	24	71.3	0.3565
48	88.5	0.04425	41	59	0.295
68	81.4	0.0407	54	54	0.27
88	76.4	0.0382	74	52.1	0.2605
109	74.4	0.0372	95	49.5	0.2475
149	68.5	0.03425	124	47.3	0.2365
178	64.1	0.03205	154	45	0.225
208	62.6	0.0313**(0.032)**	204	44	0.22
248	60	0.03			
308	55.6	0.0278			
368	53	0.0265**(0.0265)**			
424	51.7	0.02585			

Table 44: *Kinetic raw data – (Exp 17 and Exp 18) – HYDREX (Brackets indicate AA reading)*

Exp 17			Exp 18		
Time (minutes)	**$[Ca^{2+}]$ (mg/l) measured**	**$[Ca^{2+}]$ (M) actual**	**Time (minutes)**	**$[Ca^{2+}]$ (mg/l) measured**	**$[Ca^{2+}]$ (M) actual**
8	87	0.435	8	112	0.56
23	79	0.395(**0.03992**)	23	81	0.405
38	73	0.365	43	61	0.305
58	67	0.335	63	53.5	0.2675
79	63	0.315(**0.03019**)	83	50	0.25
100	60	0.3	103	46.4	0.232
128	57.2	0.286	123	45.2	0.226
176	52.5	0.2625	156	44.5	0.2225
238	49.2	0.246	188	44	0.22
298	47.2	0.236	248	44	0.22
360	46.4	0.232(**0.0223**)			
446	45.4	0.227			
8	87	0.435			

Table 45: *Kinetic raw data – (Exp 19 and Exp 20) – HYDREX (Brackets indicate AA reading)*

Exp 19			Exp 20		
Time (minutes)	**$[Ca^{2+}]$ (mg/l) measured**	**$[Ca^{2+}]$ (M) actual**	**Time (minutes)**	**$[Ca^{2+}]$ (mg/l) measured**	**$[Ca^{2+}]$ (M) actual**
8	86	0.04285	8	96	0.0480
31	87	0.04335(**0.0435**)	28	78.1	0.0391
46	87	0.04335	48	65.6	0.0328
61	88	0.044	68	61.7	0.0309
81	80	0.0401	88	56.3	0.0282
96	73	0.0365(**0.0375**)	138	52	0.0260
116	66	0.033	168	50	0.0250
136	62	0.0308	198	48.8	0.0244
162	57	0.0285(**0.0286**)	228	47.5	0.0238
192	53	0.0266	248	45.6	0.0228
222	50	0.02495			
251	48	0.02385			
281	46	0.02275			
368	44	0.02185			

Table 46: *Kinetic raw data – (Exp 21 and Exp 22) - HYDREX*

Exp 21			Exp 22		
Time (minutes)	**$[Ca^{2+}]$ (mg/l) measured**	**$[Ca^{2+}]$ (M) actual**	**Time (minutes)**	**$[Ca^{2+}]$ (mg/l) measured**	**$[Ca^{2+}]$ (M) actual**
8	97.2	0.0486	8	91	0.0455
19	82.4	0.0412	28	75	0.0375
34	75	0.0375	48	64	0.0320
49	66.7	0.0334	68	62.1	0.0311
64	63	0.0315	119	52.5	0.0263
83	58	0.0290	138	51.6	0.0258
103	55.8	0.0279	178	49.3	0.0247
146	51	0.0255	218	47.4	0.0237
191	47.6	0.0238	248	46.6	0.0233
236	45	0.0225			
276	44	0.0220			

11.5 **BULAB designed experiments (raw data)**

Table 47: *BULAB kinetic data (summary)*

Exp ID	Temp (°C)	pH	AS dosage (mg/l)	$FeCl_3$ dosage (mg/l)	$[Ca^{2+}]$ (M)	Seed (mg/l)	Induction time (minutes)	k' ($M^{-1}min^{-1}$)	t_{C80} (minutes)
1	15	4	4	10	0.055	2000	0	1.1	73
2	25	4	4	2	0.045	2000	0	1.76	57
3	15	10	4	2	0.055	0	450	0.61	103
4	25	10	4	10	0.045	0	150	1.48	62
16	25	10	4	2	0.055	2000	0	0.47	79
17	15	10	4	10	0.045	2000	0	0.48	122
18	25	4	4	10	0.055	0	0	0.97	38
19	15	4	4	2	0.045	0	70	0.72	104
5	15	4	12	10	0.045	0	30	0.40	80
6	25	4	12	2	0.055	0	30	1.88	30
7	15	10	12	2	0.045	2000	210	0.08	n/a
8	25	10	12	10	0.055	2000	0	0.79	101
12	25	10	12	2	0.045	0	>1440	-	-
13	15	10	12	10	0.055	0	550	0.62	99
14	25	4	12	10	0.045	2000	0	2.70	45
15	15	4	12	2	0.055	2000	0	0.26	206

Table 48: *Kinetic raw data – (Exp 1 and Exp 2) - BULAB*

Exp 1			Exp 2		
Time (minutes)	**$[Ca^{2+}]$ (mg/l) measured**	**$[Ca^{2+}]$ (M) actual**	**Time (minutes)**	**$[Ca^{2+}]$ (mg/l) measured**	**$[Ca^{2+}]$ (M) actual**
8	91.3	0.0457	8	87.2	0.0436
23	75	0.0375	23	68.9	0.03445
38	66	0.0330	38	61	0.0305
53	58.2	0.0291	53	55.2	0.0276
68	55.7	0.0279	68	53	0.0265
88	50.3	0.0252	88	50	0.025
108	49	0.0245	108	47	0.0235
128	45.5	0.0228	128	46.2	0.0231
158	44.6	0.0223	158	45.5	0.02275
221	42.5	0.0213	188	45	0.0225

Table 49: *Kinetic raw data – (Exp 3 and Exp 4) - BULAB*

Exp 3			Exp 4		
Time (minutes)	**$[Ca^{2+}]$ (mg/l) measured**	**$[Ca^{2+}]$ (M) actual**	**Time (minutes)**	**$[Ca^{2+}]$ (mg/l) measured**	**$[Ca^{2+}]$ (M) actual**
8	103	0.0515	8	91.4	0.0457
38	105	0.0525	23	93	0.0465
68	105	0.0525	38	93.3	0.04665
113	104.5	0.0523	53	92	0.046
150	102	0.0510	83	91.7	0.04585
190	103	0.0515	113	92	0.046
238	104	0.0520	143	92	0.046
270	105	0.0525	173	84	0.042
300	103	0.0515	197	65.2	0.0326
332	101	0.0505	213	60.6	0.0303
392	104	0.0520	232	54	0.027
456	101	0.0505	252	52.4	0.0262
486	95.7	0.0479	312	48.2	0.0241
523	70	0.0350	332	47.5	0.02375
543	60	0.0300	362	46.2	0.0231
565	56	0.0280			
595	51	0.0255			
636	47.6	0.0238			
680	44.7	0.0224			
800	42	0.0210			

Table 50: *Kinetic raw data – (Exp 5 and Exp 6) - BULAB*

Exp 5			Exp 6		
Time (minutes)	$[Ca^{2+}]$ (mg/l) measured	$[Ca^{2+}]$ (M) actual	Time (minutes)	$[Ca^{2+}]$ (mg/l) measured	$[Ca^{2+}]$ (M) actual
8	90	0.045	10	106	0.053
28	89.7	0.04485	15	106	0.053
48	86	0.043	28	107	0.0535
68	80	0.04	38	89	0.0445
90	70	0.035	48	71	0.0355
110	58	0.029	58	59	0.0295
130	51.5	0.02575	68	54	0.027
150	49.5	0.02475	78	51	0.0255
170	46	0.023	88	48	0.024
200	42.5	0.02125	100	47	0.0235
230	39.5	0.01975	120	47	0.0235
293	37	0.0185	250	47	0.0235
			350	47	0.0235

Table 51: *Kinetic raw data – (Exp 7 and Exp 8) - BULAB*

Exp 7			Exp 8		
Time (minutes)	$[Ca^{2+}]$ (mg/l) measured	$[Ca^{2+}]$ (M) actual	Time (minutes)	$[Ca^{2+}]$ (mg/l) measured	$[Ca^{2+}]$ (M) actual
8	88	0.0440	8	108	0.054
38	88	0.0440	18	95	0.0475
130	88	0.0440	28	89	0.0445
167	89	0.0445	48	81.2	0.0406
217	84.4	0.0422	68	76	0.038
247	86.5	0.0433	88	72	0.036
277	83.8	0.0419	135	66	0.033
307	83	0.0415	170	62	0.031
332	83.2	0.0416	206	59.7	0.02985
367	80.7	0.0404			
397	82.5	0.0413			
427	78.7	0.0394			
457	77.6	0.0388			
541	75.2	0.0376			
583	75	0.0375			
643	73	0.0365			
703	72.2	0.0361			

Table 52: *Kinetic raw data – (Exp 12 and Exp 13) - BULAB*

Exp 12			Exp 13		
Time (minutes)	**$[Ca^{2+}]$ (mg/l) measured**	**$[Ca^{2+}]$ (M) actual**	**Time (minutes)**	**$[Ca^{2+}]$ (mg/l) measured**	**$[Ca^{2+}]$ (M) actual**
0	89	0.0445	11	109	0.0545
20	91	0.0455	118	109	0.0545
40	90	0.045	211	109	0.0545
60	90	0.045	287	112	0.056
80	89	0.0445	348	109	0.0545
100	92	0.046	403	110	0.055
200	89	0.0445	463	110	0.055
400	90	0.045	493	112	0.056
800	90	0.045	550	110	0.055
100	91	0.0455	568	90	0.045
1200	89	0.0445	605	74	0.037
1400	90	0.045	625	67.7	0.03385
			659	61	0.0305
			689	59	0.0295
			717	55.7	0.02785
			774	52.5	0.02625
			842	51.2	0.0256

Table 53: *Kinetic raw data – (Exp 14 and Exp 15) - BULAB*

Exp 14			Exp 15		
Time (minutes)	**$[Ca^{2+}]$ (mg/l) measured**	**$[Ca^{2+}]$ (M) actual**	**Time (minutes)**	**$[Ca^{2+}]$ (mg/l) measured**	**$[Ca^{2+}]$ (M) Actual**
8	87	0.0435	8	107	0.0535
23	67.8	0.0339	28	95	0.0475
38	59.4	0.0297	48	88.4	0.0442
53	54.7	0.02735	68	81.4	0.0407
68	52.5	0.02625	95	77.2	0.0386
88	50	0.025	133	73	0.0365
109	48.7	0.02435	294	56	0.028
138	47.4	0.0237	324	54.5	0.02725
168	45.7	0.02285	428	53.8	0.0269
188	46.6	0.0233			

Table 54: *Kinetic raw data – (Exp 16 and Exp 17) - BULAB*

Exp 16			Exp 17		
Time (minutes)	**$[Ca^{2+}]$ (mg/l) measured**	**$[Ca^{2+}]$ (M) actual**	**Time (minutes)**	**$[Ca^{2+}]$ (mg/l) measured**	**$[Ca^{2+}]$ (M) actual**
8	108	0.054	8	89.5	0.04475
24	96	0.048	23	82.3	0.04115
37	86	0.043	38	75.5	0.03775
52	72	0.036	58	66.5	0.03325
67	62	0.031	78	63.5	0.03175
87	57.5	0.02875	98	59	0.0295
107	53	0.0265	145	53.7	0.02685
143	48.6	0.0243	173	51	0.0255
172	46	0.023	262	47	0.0235
197	46.2	0.0231	325	46.9	0.02345
258	45	0.0225			
308	45	0.0225			

Table 55: *Kinetic raw data – (Exp 18 and Exp 19) - BULAB*

Exp 18			Exp 19		
Time (minutes)	**$[Ca^{2+}]$ (mg/l) measured**	**$[Ca^{2+}]$ (M) actual**	**Time (minutes)**	**$[Ca^{2+}]$ (mg/l) measured**	**$[Ca^{2+}]$ (M) actual**
8	111	0.0555	8	87.5	0.04375
18	94	0.047	28	88	0.044
28	79	0.0395	48	87	0.0435
38	66.7	0.03335	68	86.6	0.0433
50	56.7	0.02835	88	78.7	0.03935
63	52.7	0.02635	108	70	0.035
83	47.8	0.0239	128	61.8	0.0309
103	47	0.0235	148	57.5	0.02875
128	47	0.0235	168	55	0.0275
158	47	0.0235	188	52	0.026
			218	50	0.025
			247	47.5	0.02375
			277	46	0.023
			308	45	0.0225
			358	45	0.0225

11.6 **Additional experiments**

Table 56: *Kinetic data at variable antiscalant concentrations (HYDREX)*

Exp A(1) [T(25°C),AS(2 mg/l), Ca(0.055 M)] HYDREX			**Exp A(2) [T(25°C),AS(4 mg/l), Ca(0.055 M)] HYDREX**		
Time (minutes)	**$[Ca^{2+}]$ (mg/l) measured**	**$[Ca^{2+}]$ (M) actual**	**Time (minutes)**	**$[Ca^{2+}]$ (mg/l) measured**	**$[Ca^{2+}]$ (M) actual**
11	105	0.0525	5	112	0.056
61	106	0.053	111	111	0.0555
91	106	0.053	171	112	0.056
101	105	0.0525	224	111	0.0555
111	101	0.0505	257	110	0.055
121	83	0.0415	267	94	0.047
131	66.3	0.03315	277	74.2	0.0371
141	59.2	0.0296	287	64	0.032
152	55.3	0.02765	297	61	0.0305
172	49.5	0.02475	307	56.8	0.0284
192	48.2	0.0241	317	55	0.0275
250	48	0.024	329	53	0.0265
			359	49.5	0.02475
			408	49.6	0.0248
			458	49	0.0245
			507	49	0.0245

Table 57: *Kinetic data at variable antiscalant concentration (BULAB)*

Exp A(3) [T(25°C),AS(2 mg/l), Ca(0.055 M)] HYDREX			**Exp A(4) [T(25°C),AS(4 mg/l), Ca(0.055 M)] HYDREX**		
Time (minutes)	**$[Ca^{2+}]$ (mg/l) measured**	**$[Ca^{2+}]$ (M) actual**	**Time (minutes)**	**$[Ca^{2+}]$ (mg/l) measured**	**$[Ca^{2+}]$ (M) actual**
111	107	0.0535	180	108	0.054
121	90	0.045	190	107	0.0535
131	69	0.0345	200	106	0.053
141	63.5	0.03175	211	98	0.049
161	53.5	0.02675	221	68.7	0.03435
181	51	0.0255	231	59	0.0295
201	48	0.024	241	55.5	0.02775
250	48	0.024	257	51	0.0255
300	48	0.024	277	50	0.025
400	48	0.024	300	49	0.0245

Table 58: *Kinetic data of mixed seed precipitation (experiment 8, HYDREX)*

(Exp 8, lime & HYDREX)			(Exp 8, lime & gypsum & BULAB)		
Time (minutes)	**$[Ca^{2+}]$ (mg/l) measured**	**$[Ca^{2+}]$ (M) actual**	**Time (minutes)**	**$[Ca^{2+}]$ (mg/l) measured**	**$[Ca^{2+}]$ (M) actual**
0	152	0.076	5	134	0.067
29	152	0.076	15	110	0.055
47	146	0.073	25	94	0.047
63	136	0.068	35	87.7	0.04385
77	108	0.054	45	82.7	0.04135
87	97.4	0.0487	55	82	0.041
97	93	0.0465	65	78	0.039
107	89	0.0445	75	77.7	0.03885
122	84.7	0.04235	85	76.6	0.0383
137	83	0.0415			
228	77	0.0385			

Table 59: *Kinetic data of mixed seed precipitation (experiment 8, BULAB)*

(Exp 8, lime & BULAB)			(Exp 8, lime & gypsum &HYDREX)		
Time (minutes)	**$[Ca^{2+}]$ (mg/l) Measured**	**$[Ca^{2+}]$ (M) actual**	**Time (minutes)**	**$[Ca^{2+}]$ (mg/l) measured**	**$[Ca^{2+}]$ (M) actual**
4	150	0.0750	5	146	0.0730
14	150	0.0750	15	122	0.0610
34	150	0.0750	25	106	0.0530
54	150	0.0750	35	100	0.0500
74	150	0.0750	45	94.4	0.0472
111	150	0.0750	60	90	0.0450
131	145	0.0725	80	88	0.0440
160	135	0.0675	100	83.5	0.0418
177	110	0.0550	120	83.3	0.0417
187	97.4	0.0487			
197	91	0.0455			
207	89	0.0445			
227	82	0.0410			
241	82.5	0.0413			
266	81	0.0405			
316	81	0.0405			

11.7 **AMD experiments (raw data)**

Table 60: *Kinetic data of AMD precipitation (BULAB)*

Exp 8(lime & gypsum)			Exp 14 (gypsum)		
Time (minutes)	**$[Ca^{2+}]$ (mg/l) measured**	**$[Ca^{2+}]$ (M) actual**	**Time (minutes)**	**$[Ca^{2+}]$ (mg/l) measured**	**$[Ca^{2+}]$ (M) actual**
4	127	0.0635	5	82	0.041
14	67	0.0335	15	56	0.028
24	49	0.0245	25	44	0.022
34	45	0.0225	35	38	0.019
44	40	0.02	45	33	0.0165
54	38	0.019	55	32	0.016

Table 61: *Kinetic data of AMD precipitation (HYDREX)*

Exp 8(lime & gypsum)			Exp 14 (gypsum)		
Time (minutes)	**$[Ca^{2+}]$ (mg/l) measured**	**$[Ca^{2+}]$ (M) actual**	**Time (minutes)**	**$[Ca^{2+}]$ (mg/l) measured**	**$[Ca^{2+}]$ (M) actual**
4	128	0.064	5	84	0.042
14	55	0.0275	15	46	0.023
24	41	0.0205	25	37	0.0185
34	36	0.018	36	31	0.0155
44	33	0.0165	46	29	0.0145
			56	28	0.014

11.8 **k'-values**

An estimate of the calcium concentration $[Ca^{2+}]_{calc}$, at any given time is obtained by using the integrated form of equation 2.27 and first guessing a value for k' and C*. The square of the error term between the experimental value and the calculated value is determined and all the square errors are summed. This term is then minimized by the solver function in MS Excel by changing parameters k' and C**. In this manner the value for k' is obtained.**

$$Ca_{calc}^{2+} = \left(\frac{1}{\left(Ca_{exp}^{2+} - C^{*}\right)} + t \cdot k'\right) + C * \qquad (11.1)$$

Note:

In all the tables, time "0-minutes", refer to the moment in time when precipitation starts for a given run or rather when a definite change in the calcium concentration is observed. The times were normalized according to this moment in time.

Table 62: *Exp B1 [T (15°C), Ca (0.045 M)], k'-value*

	k'	0.829149		
	C*	0.017939		
Time (minutes)	**[Ca2+] exp.**	**[Ca2+] calc.**	**SE**	**SSE**
0	0.04065	0.04065	0	1.25471E-05
20	0.03575	0.034437	1.72E-06	
42	0.03175	0.03062	1.28E-06	
62	0.0284	0.028417	2.82E-10	
80	0.02685	0.027	2.24E-08	
130	0.0225	0.024526	4.1E-06	
155	0.02215	0.023734	2.51E-06	
240	0.022	0.022054	2.87E-09	
290	0.022	0.021454	2.98E-07	
440	0.022	0.020385	2.61E-06	
940	0.022	0.019153	8.1E-06	

Table 63: *Exp B2 [T (15°C), Ca (0.055 M)], k'-value*

	k'	2.295552		
	C*	0.021072		
Time (minutes)	**[Ca2+] exp.**	**[Ca2+] calc.**	**SE**	**SSE**
0	0.04925	0.04925	0	7.90107E-06
10	0.03925	0.038182	1.14E-06	
20	0.03435	0.033357	9.86E-07	
30	0.0303	0.030655	1.26E-07	
40	0.02855	0.028927	1.42E-07	
50	0.02665	0.027727	1.16E-06	
70	0.0252	0.026169	9.4E-07	
90	0.0245	0.025203	4.94E-07	
140	0.024	0.023874	1.59E-08	
340	0.024	0.022297	2.9E-06	

Table 64: *Exp B3 [T (25°C), Ca (0.045 M)], k'-value*

	k'	2.023101428		
	C*	0.018191295		
Time (minutes)	**[Ca2+] exp.**	**[Ca2+] calc.**	**SE**	**SSE**
0	0.0405	0.0405	0	1.52705E-05
15	0.0339	0.031494108	5.79E-06	
30	0.02765	0.027668298	3.35E-10	
45	0.02525	0.025551536	9.09E-08	
60	0.0225	0.024207721	2.92E-06	
75	0.022	0.023278848	1.64E-06	
90	0.022	0.022598432	3.58E-07	
270	0.022	0.019883162	4.48E-06	
470	0.022	0.01919563	7.86E-06	
970	0.022	0.018689493	1.1E-05	

Table 65: *Exp B4 [T (25°C), Ca (0.055 M)], k'-value*

	k'	3.232905		
	C*	0.018979		
Time (minutes)	**[Ca2+] exp.**	**[Ca2+] calc.**	**SE**	**SSE**
0	0.051	0.051	0	1.3111E-05
10	0.037	0.034712	5.23E-06	
20	0.0285	0.029408	8.24E-07	
30	0.02615	0.026778	3.95E-07	
40	0.02425	0.025208	9.17E-07	
50	0.02325	0.024164	8.35E-07	
60	0.0225	0.023419	8.45E-07	
90	0.0225	0.022083	1.74E-07	
190	0.0225	0.020528	3.89E-06	

Table 66: *Exp 1: HYDREX, k'-value*

	k'	1.066468		
	C*	0.014075		
Time (minutes)	**[Ca2+] exp.**	**[Ca2+] calc.**	**SE**	**SSE**
0	0.0435	0.0435	0	1.10657E-06
11	0.03515	0.035949	6.39E-07	
23	0.0315	0.031165	1.12E-07	
38	0.02745	0.027496	2.08E-09	
53	0.02535	0.025123	5.13E-08	
68	0.0238	0.023464	1.13E-07	
83	0.0224	0.022238	2.63E-08	
103	0.02105	0.021027	5.18E-10	
123	0.01975	0.020129	1.44E-07	
163	0.01875	0.018887	1.86E-08	
203	0.018	0.018067	4.49E-09	
233	0.0175	0.017615	1.32E-08	
263	0.0172	0.017255	2.98E-09	

Table 67: *Exp 2: HYDREX, k'-value*

	k'	2.079928		
	C*	0.020482		
Time (minutes)	**[Ca2+] exp.**	**[Ca2+] calc.**	**SE**	**SSE**
0	0.0414	0.0414	0	6.30109E-07
15	0.0334	0.033139	6.79E-08	
30	0.03005	0.029556	2.44E-07	
47	0.0276	0.027352	6.16E-08	
62	0.0261	0.026139	1.54E-09	
77	0.025	0.02529	8.44E-08	
92	0.02445	0.024663	4.55E-08	
107	0.02395	0.024181	5.32E-08	
122	0.02355	0.023798	6.15E-08	
172	0.02305	0.022948	1.05E-08	
222	0.0227	0.022444	6.53E-08	
242	0.0227	0.022296	1.63E-07	

Table 68: *Exp 3: HYDREX, k'-value*

	k' 0.540392 **C*** 0.014807			
Time (minutes)	**[Ca2+] exp.**	**[Ca2+] calc.**	**SE**	**SSE**
0	0.0515	0.0515	0	2.06743E-06
15	0.0442	0.043088	1.24E-06	
30	0.0379	0.037814	1.28E-09	
45	0.0338	0.034198	2.01E-07	
61	0.0308	0.031414	3.77E-07	
90	0.0278	0.027985	5.5E-08	
123	0.0257	0.025477	2.99E-08	
150	0.0245	0.02404	1.68E-07	
183	0.0230	0.022735	7.04E-08	
213	0.0226	0.021832	5.16E-07	
273	0.0217	0.020529	1.26E-06	
293	0.0215	0.020196	1.7E-06	

Table 69: *Exp 4: HYDREX, k'-value*

	k' 0.920952 **C*** 0.0174			
Time (minutes)	**[Ca2+] exp.**	**[Ca2+] calc.**	**SE**	**SSE**
0	0.041	0.041	0	5.6297E-06
20	0.03535	0.03385	2.25E-06	
40	0.03075	0.030025	5.26E-07	
60	0.02665	0.027643	9.86E-07	
80	0.02535	0.026017	4.46E-07	
100	0.0239	0.024837	8.78E-07	
290	0.0209	0.020632	7.18E-08	
340	0.0209	0.020213	4.71E-07	

Table 70: *Exp 5: HYDREX, k'-value*

	k'	0.340818		
	C*	0.011055		
Time (minutes)	**[Ca2+] exp.**	**[Ca2+] calc.**	**SE**	**SSE**
0	0.0434	0.0434	0	4.11531E-06
19	0.0385	0.037798	4.92E-07	
39	0.03445	0.033675	6.01E-07	
59	0.03095	0.030653	8.82E-08	
89	0.027	0.027381	1.45E-07	
119	0.0248	0.025046	6.04E-08	
139	0.023	0.023828	6.85E-07	
179	0.02135	0.021933	3.4E-07	
219	0.02	0.020528	2.79E-07	
274	0.0194	0.0191	9.02E-08	
309	0.01955	0.018395	1.33E-06	

Table 71: *Exp 6: HYDREX, k'-value*

	k'	2.873435		
	C*	0.020606		
Time (minutes)	**[Ca2+] exp.**	**[Ca2+] calc.**	**SE**	**SSE**
0	0.0485	0.0485	0	1.3041E-06
10	0.0360	0.03609	8.0705E-09	
20	0.0320	0.031322	4.59381E-07	
30	0.0282	0.028799	4.21766E-07	
40	0.0272	0.027238	7.76853E-09	
55	0.0254	0.025764	1.32412E-07	
70	0.0254	0.024826	2.74707E-07	

Table 72: *Exp 7: HYDREX, k'-value*

	k'	0.224155		
	C*	0.014312		
Time (minutes)	**[Ca2+] exp.**	**[Ca2+] calc.**	**SE**	**SSE**
0	0.04205	0.04205	0	4.23579E-06
30	0.0378	0.03769	1.22E-08	
60	0.0351	0.034514	3.44E-07	
90	0.03285	0.032098	5.66E-07	
130	0.03045	0.029652	6.37E-07	
180	0.0268	0.027401	3.62E-07	
240	0.02425	0.025442	1.42E-06	
300	0.02315	0.023993	7.11E-07	
360	0.02245	0.022878	1.83E-07	
630	0.0213	0.019954	1.81E-06	

Table 73: *Exp 8: HYDREX, k'-value*

	k' 1.826433 **C*** 0.020246			
Time (minutes)	**[Ca2+] exp.**	**[Ca2+] calc.**	**SE**	**SSE**
0	0.0505	0.0505	0	6.34416E-07
16	0.03675	0.036303	2E-07	
36	0.03075	0.030367	1.47E-07	
56	0.0278	0.027635	2.72E-08	
76	0.02625	0.026064	3.44E-08	
106	0.0245	0.024658	2.49E-08	
136	0.02335	0.023799	2.02E-07	
166	0.0226	0.02322	3.84E-07	
196	0.02225	0.022803	3.06E-07	
227	0.02175	0.02248	5.32E-07	

Table 74: *Exp 9: HYDREX, k'-value*

	k' 0.625678 **C*** 0.016021			
Time (minutes)	**[Ca2+] exp.**	**[Ca2+] calc.**	**SE**	**SSE**
0	0.0481	0.04805	0	5.92322E-07
15	0.0408	0.040647	2.33E-08	
30	0.0360	0.036024	5.89E-10	
45	0.0323	0.032863	3.75E-07	
61	0.0305	0.030433	4.51E-09	
99	0.0270	0.026755	6.01E-08	
130	0.0248	0.024905	1.11E-08	
160	0.0235	0.023636	1.84E-08	
190	0.0225	0.022683	3.36E-08	
220	0.0220	0.021943	3.27E-09	
250	0.0216	0.02135	6.23E-08	

Table 75: *Exp 10: HYDREX, k'-value*

	k'	0.852873		
	C*	0.022696		
Time (minutes)	**[Ca2+] exp.**	**[Ca2+] calc.**	**SE**	**SSE**
0	0.0491	0.0491	4.81E-35	7.17411E-07
15	0.0492	0.042433	2.18E-07	
30	0.0390	0.038454	2.98E-07	
47	0.0359	0.035523	1.42E-07	
67	0.0333	0.03322	8.81E-10	
87	0.0315	0.031618	1.4E-08	
117	0.0299	0.02996	3.6E-09	
172	0.0283	0.028114	1.86E-08	
202	0.0275	0.027454	2.11E-09	
232	0.0269	0.026938	1.42E-09	
257	0.0265	0.026586	1.84E-08	

Table 76: *Exp 11: HYDREX, k'-value*

	k'	0.850548		
	C*	0.018453		
Time (minutes)	**[Ca2+] exp.**	**[Ca2+] calc.**	**SE**	**SSE**
0	0.0465	0.0465	0	9.5063E-07
21	0.0373	0.037139	2.59E-08	
40	0.0328	0.032805	2.61E-11	
80	0.0275	0.028096	3.56E-07	
100	0.0263	0.026737	1.91E-07	
130	0.0252	0.025292	8.42E-09	
160	0.0246	0.024276	1.05E-07	
200	0.0238	0.023313	1.91E-07	
233	0.0230	0.02273	7.31E-08	

Table 77: *Exp 13: HYDREX, k'-value*

	k'	1.270821		
	C*	0.019941		
Time (minutes)	**[Ca2+] exp.**	**[Ca2+] calc.**	**SE**	**SSE**
0	0.042	0.042	0	9.29751E-07
20	0.0345	0.034075	1.8E-07	
40	0.03035	0.03034	1.06E-10	
60	0.0284	0.028166	5.48E-08	
80	0.0265	0.026744	5.94E-08	
100	0.02515	0.025741	3.49E-07	
120	0.02475	0.024996	6.04E-08	
187	0.023	0.023475	2.25E-07	
254	0.022	0.022657	4.32E-07	
280	0.022	0.022434	1.88E-07	
340	0.022	0.022036	1.27E-09	
390	0.022	0.02179	4.43E-08	

Table 78: *Exp 14: HYDREX, k'-value*

	k'	2.10455		
	C*	0.019306		
Time (minutes)	**[Ca2+] exp.**	**[Ca2+] calc.**	**SE**	**SSE**
0	0.04135	0.04135	0	4.60899E-07
17	0.03185	0.03163	4.83E-08	
32	0.0285	0.028178	1.03E-07	
48	0.02605	0.026137	7.63E-09	
63	0.02505	0.024925	1.55E-08	
79	0.02415	0.024031	1.41E-08	
92	0.0235	0.02349	9.33E-11	
112	0.0229	0.022864	1.32E-09	
137	0.022	0.022303	9.17E-08	
164	0.0215	0.021867	1.34E-07	
218	0.0215	0.021289	4.43E-08	
256	0.0215	0.021018	2.32E-07	
300	0.0215	0.020784	5.13E-07	
500	0.0215	0.020217	1.65E-06	
600	0.0215	0.02007	2.04E-06	

Table 79: *Exp 15: HYDREX, k'-value*

	k'	0.294583		
	C*	0.020065		
Time (minutes)	**[Ca2+] exp.**	**[Ca2+] calc.**	**SE**	**SSE**
0	0.053	0.053	4.81E-35	1.0963E-06
20	0.04725	0.047648	1.58E-07	
40	0.04425	0.043792	2.1E-07	
60	0.0407	0.040882	3.3E-08	
80	0.0382	0.038608	1.66E-07	
101	0.0372	0.036699	2.51E-07	
141	0.03425	0.033973	7.67E-08	
170	0.03205	0.032496	1.99E-07	
200	0.0313	0.031265	1.19E-09	
240	0.03	0.02996	1.64E-09	
300	0.0278	0.028487	4.71E-07	
360	0.0265	0.027395	8.02E-07	
416	0.02585	0.026604	5.69E-07	

Table 80: *Exp 16: HYDREX, k'-value*

	k'	1.870069		
	C*	0.019402		
Time (minutes)	**[Ca2+] exp.**	**[Ca2+] calc.**	**SE**	**SSE**
0	0.049	0.049	0	1.24616E-06
16	0.03565	0.035099	3.04E-07	
33	0.0295	0.029873	1.39E-07	
46	0.027	0.027749	5.6E-07	
66	0.02605	0.025763	8.24E-08	
87	0.02475	0.024492	6.68E-08	
116	0.02365	0.023391	6.73E-08	
146	0.0225	0.022661	2.6E-08	
196	0.022	0.0219	1E-08	

Table 81: *Exp 17: HYDREX, k'-value*

	k'	0.55973		
	C*	0.019267		
Time (minutes)	**[Ca2+] exp.**	**[Ca2+] calc.**	**SE**	**SSE**
0	0.0435	0.0435	0	8.81748E-07
15	0.0395	0.039403	9.4E-09	
30	0.0365	0.036491	7.98E-11	
50	0.0335	0.033707	4.28E-08	
71	0.0315	0.031611	1.24E-08	
92	0.03	0.030047	2.23E-09	
120	0.0286	0.028489	1.23E-08	
168	0.02625	0.026658	1.66E-07	
230	0.0246	0.025149	3.01E-07	
290	0.0236	0.024179	3.35E-07	
352	0.0232	0.023463	6.93E-08	
438	0.0227	0.022758	3.37E-09	

Table 82: *Exp 18: HYDREX, k'-value*

	k'	1.420834		
	C*	0.017913		
Time (minutes)	**[Ca2+] exp.**	**[Ca2+] calc.**	**SE**	**SSE**
0	0.056	0.056	0	6.86789E-06
15	0.0405	0.038935	2.45E-06	
35	0.0305	0.031073	3.29E-07	
55	0.02675	0.027491	5.5E-07	
75	0.025	0.025442	1.95E-07	
95	0.0232	0.024115	8.37E-07	
115	0.0226	0.023186	3.43E-07	
148	0.02225	0.022141	1.2E-08	
180	0.022	0.021459	2.93E-07	
240	0.022	0.020636	1.86E-06	

Table 83: *Exp 19: HYDREX, k'-value*

	k'	0.670545725		
	C*	0.018591834		
Time (minutes)	**[Ca2+] exp.**	**[Ca2+] calc.**	**SE**	**SSE**
0	0.0401	0.0401	0	7.14083E-07
15	0.0365	0.036274626	5.08E-08	
35	0.033	0.032885089	1.32E-08	
55	0.0308	0.030585983	4.58E-08	
81	0.0285	0.028511665	1.36E-10	
111	0.0266	0.026861454	6.84E-08	
141	0.02495	0.025681975	5.36E-07	
170	0.02385	0.024822878	9.46E-07	
200	0.02275	0.024128837	1.9E-06	
287	0.02185	0.022776975	8.59E-07	

Table 84: *Exp 20: HYDREX, k'-value*

	k'	0.893388		
	C*	0.019299		
Time (minutes)	**[Ca2+] exp.**	**[Ca2+] calc.**	**SE**	**SSE**
0	0.0480	0.048	0	1.47839E-06
20	0.0391	0.038271	6.07E-07	
40	0.0328	0.033468	4.46E-07	
60	0.0309	0.030605	5.99E-08	
80	0.0282	0.028705	3.08E-07	
130	0.0260	0.025922	6.08E-09	
160	0.0250	0.024924	5.85E-09	
190	0.0244	0.024187	4.55E-08	
220	0.0238	0.02362	1.68E-08	
240	0.0228	0.023311	2.61E-07	

Table 85: *Exp 21: HYDREX, k'-value*

	k'	0.885611		
	C*	0.019284		
Time (minutes)	**[Ca2+] exp.**	**[Ca2+] calc.**	**SE**	**SSE**
0	0.0486	0.0486	4.81E-35	1.4998E-06
11	0.0412	0.042088	7.88E-07	
26	0.0375	0.036786	5.1E-07	
41	0.0334	0.033484	1.8E-08	
56	0.0315	0.031231	7.26E-08	
75	0.0290	0.029231	5.34E-08	
95	0.0279	0.027741	2.53E-08	
138	0.0255	0.025681	3.27E-08	
183	0.0238	0.024381	3.38E-07	
228	0.0225	0.023521	1.04E-06	
268	0.0220	0.022968	9.37E-07	

Table 86: *Exp 22: HYDREX, k'-value*

	k'	0.88028		
	C*	0.019223		
Time (minutes)	**[Ca2+] exp.**	**[Ca2+] calc.**	**SE**	**SSE**
0	0.0455	0.0455	0	1.65837E-06
20	0.0375	0.037189	9.69E-08	
40	0.0320	0.032872	7.6E-07	
60	0.0311	0.030227	6.77E-07	
111	0.0263	0.026589	1.15E-07	
130	0.0258	0.025781	3.68E-10	
170	0.0247	0.024551	9.87E-09	
210	0.0237	0.023709	8.34E-11	
240	0.0233	0.023234	4.36E-09	

Table 87: *Exp 1: BULAB, k'-value*

	k'	1.098661		
	C*	0.017939		
Time (minutes)	**[Ca2+] exp.**	**[Ca2+] calc.**	**SE**	**SSE**
0	0.04565	0.04565	1.78E-08	8.20176E-07
15	0.0375	0.036962	7.99E-08	
30	0.033	0.032422	1.94E-08	
45	0.0291	0.029631	8.27E-10	
60	0.02785	0.027742	3.18E-08	
80	0.02515	0.026005	1.17E-07	
100	0.0245	0.02479	2.22E-07	
120	0.02275	0.023894	3.31E-07	
150	0.0223	0.022917	4.85E-07	
213	0.02125	0.021641	7.52E-07	

Table 88: *Exp 2: BULAB, k'-value*

	k'	1.757943		
	C*	0.019487		
Time (minutes)	**[Ca2+] exp.**	**[Ca2+] calc.**	**SE**	**SSE**
0	0.0436	0.0436	0	7.53274E-07
15	0.03445	0.034227	4.97E-08	
30	0.0305	0.030101	1.59E-07	
45	0.0276	0.02778	3.24E-08	
60	0.0265	0.026292	4.34E-08	
80	0.025	0.024978	4.91E-10	
100	0.0235	0.024089	3.47E-07	
120	0.0231	0.023448	1.21E-07	
150	0.02275	0.022763	1.82E-10	
180	0.0225	0.022281	4.81E-08	

Table 89: *Exp 3: BULAB, k'-value*

	k' 0.606067 **C*** 0.015419			
Time (minutes)	**[Ca2+] exp.**	**[Ca2+] calc.**	**SE**	**SSE**
0	0.0479	0.04785	0	1.29539E-06
37	0.0350	0.034195	6.47E-07	
57	0.0300	0.030714	5.1E-07	
79	0.0280	0.028124	1.53E-08	
109	0.0255	0.02574	5.75E-08	
150	0.0238	0.023633	2.78E-08	
194	0.0224	0.022157	3.71E-08	
314	0.0210	0.019941	1.12E-06	
354	0.0205	0.019495	1.01E-06	

Table 90: *Exp 4: BULAB, k'-value*

	k' 1.478039 **C*** 0.020207			
Time (minutes)	**[Ca2+] exp.**	**[Ca2+] calc.**	**SE**	**SSE**
0	0.042	0.042	0	8.86E-07
24	0.0326	0.032498	1.04E-08	
40	0.0303	0.02973	3.25E-07	
59	0.027	0.027721	5.19E-07	
79	0.0262	0.026355	2.4E-08	
139	0.0241	0.024186	7.33E-09	
159	0.02375	0.023767	2.85E-10	
189	0.0231	0.023282	3.3E-08	

Table 91: *Exp 5: BULAB, k'-value*

	k'	0.400453		
	C*	0.009349		
Time (minutes)	**[Ca2+] exp.**	**[Ca2+] calc.**	**SE**	**SSE**
0	0.04	0.04	0	3.71867E-06
22	0.035	0.033483	2.3E-06	
42	0.029	0.029574	3.29E-07	
62	0.02575	0.026754	1.01E-06	
82	0.02475	0.024625	1.56E-08	
102	0.023	0.02296	1.62E-09	
132	0.02125	0.021047	4.12E-08	
162	0.01975	0.019606	2.09E-08	
225	0.0185	0.017497	1.01E-06	

Table 92: *Exp 6: BULAB, k'-value*

	k'	1.87807		
	C*	0.01914		
Time (minutes)	**[Ca2+] exp.**	**[Ca2+] calc.**	**SE**	**SSE**
0	0.0535	0.0535	0	5.01958E-05
10	0.0445	0.040024	2E-05	
20	0.0355	0.03414	1.85E-06	
30	0.0295	0.030843	1.8E-06	
40	0.027	0.028734	3.01E-06	
50	0.0255	0.027269	3.13E-06	
60	0.024	0.026193	4.81E-06	
72	0.0235	0.025225	2.98E-06	
92	0.0235	0.024093	3.52E-07	
222	0.0235	0.021382	4.49E-06	
322	0.0235	0.020718	7.74E-06	

Table 93: *Exp 7: BULAB, k'-value*

	k' 0.079507 **C*** 0.025194			
Time (minutes)	**[Ca2+] exp.**	**[Ca2+] calc.**	**SE**	**SSE**
0	0.0433	0.04325	0	2.33E-06
30	0.0419	0.042505	3.65E-07	
60	0.0415	0.041818	1.01E-07	
85	0.0416	0.041286	9.83E-08	
120	0.0404	0.040597	6.09E-08	
150	0.0413	0.040051	1.44E-06	
180	0.0394	0.039542	3.7E-08	
210	0.0388	0.039068	7.16E-08	
294	0.0376	0.037891	8.48E-08	
336	0.0375	0.037375	1.57E-08	
396	0.0365	0.036706	4.24E-08	
456	0.0361	0.036107	4.39E-11	
611	0.0350	0.034813	1.87E-08	

Table 94: *Exp 8: BULAB, k'-value*

	k' 0.793687 **C*** 0.025249			
Time (minutes)	**[Ca2+] exp.**	**[Ca2+] calc.**	**SE**	**SSE**
0	0.054	5.40E-02	0	3.04E-06
10	0.0475	4.87E-02	1.34E-06	
20	0.0445	4.50E-02	2.4E-07	
40	0.0406	4.03E-02	1.02E-07	
60	0.038	3.74E-02	3.79E-07	
80	0.036	3.54E-02	3.31E-07	
127	0.033	3.26E-02	1.41E-07	
162	0.031	3.14E-02	1.37E-07	
198	0.02985	3.05E-02	3.71E-07	

Table 95: *Exp 13: BULAB, k'-value*

	k' 0.621128			
	C* 0.020566			
Time (minutes)	**[Ca2+] exp.**	**[Ca2+] calc.**	**SE**	**SSE**
0	0.055	0.055	0	1E-06
18	0.045	0.045428	1.83E-07	
55	0.037	0.036388	3.75E-07	
75	0.03385	0.033789	3.74E-09	
109	0.0305	0.030902	1.62E-07	
139	0.0295	0.029233	7.13E-08	
167	0.02785	0.028098	6.13E-08	
224	0.02625	0.026512	6.87E-08	
292	0.0256	0.025318	7.93E-08	
324	0.0256	0.024908	4.79E-07	

Table 96: *Exp 14: BULAB, k'-value*

	k' 2.698883			
	C* 0.02147			
Time (minutes)	**[Ca2+] exp.**	**[Ca2+] calc.**	**SE**	**SSE**
0	0.0435	0.0435	0	9.75855E-07
15	0.0339	0.033114	6.17E-07	
30	0.0297	0.029384	1E-07	
45	0.02735	0.027463	1.29E-08	
60	0.02625	0.026293	1.85E-09	
80	0.025	0.025297	8.8E-08	
101	0.02435	0.024615	7E-08	
130	0.0237	0.023993	8.61E-08	
160	0.02285	0.023565	5.11E-07	
180	0.0233	0.023352	2.73E-09	

Table 97: *Exp 15: BULAB, k'-value*

	k'	0.260658		
	C*	0.018938		
Time (minutes)	**[Ca2+] exp.**	**[Ca2+] calc.**	**SE**	**SSE**
0	0.0535	0.0535	0	3.14675E-06
20	0.0475	0.048223	5.23E-07	
40	0.0442	0.044344	2.09E-08	
60	0.0407	0.041373	4.53E-07	
87	0.0386	0.038313	8.21E-08	
125	0.0365	0.035194	1.71E-06	
286	0.028	0.028601	3.61E-07	
316	0.02725	0.027922	4.52E-07	
420	0.0269	0.026162	5.44E-07	

Table 98: *Exp 16: BULAB, k'-value*

	k'	0.471606		
	C*	0.014261		
Time (minutes)	**[Ca2+] exp.**	**[Ca2+] calc.**	**SE**	**SSE**
0	0.054	0.054	0	3.77961E-05
16	0.048	0.044833	1E-05	
29	0.043	0.040007	8.96E-06	
44	0.036	0.036041	1.65E-09	
59	0.031	0.033133	4.55E-06	
79	0.02875	0.030281	2.35E-06	
99	0.0265	0.028178	2.82E-06	
135	0.0243	0.025518	1.48E-06	
164	0.023	0.024017	1.03E-06	
189	0.0231	0.02301	8.05E-09	
250	0.0225	0.021251	1.56E-06	
300	0.0225	0.020262	5.01E-06	

Table 99: *Exp 17: BULAB, k'-value*

	k'	0.479852		
	C*	0.017339		
Time (minutes)	**[Ca2+] exp.**	**[Ca2+] calc.**	**SE**	**SSE**
0	0.04475	0.04475	0	2.96187E-06
15	0.04115	0.040233	8.41E-07	
30	0.03775	0.036994	5.71E-07	
50	0.03325	0.033875	3.9E-07	
70	0.03175	0.03161	1.96E-08	
90	0.0295	0.029891	1.53E-07	
137	0.02685	0.027121	7.37E-08	
165	0.0255	0.025985	2.35E-07	
254	0.0235	0.023653	2.35E-08	
317	0.02345	0.022641	6.54E-07	

Table 100: *Exp 18: BULAB, k'-value*

	k'	0.969547		
	C*	0.015317		
Time (minutes)	**[Ca2+] exp.**	**[Ca2+] calc.**	**SE**	**SSE**
0	0.0555	0.0555	0	2.78584E-05
10	0.047	0.044234	7.65E-06	
20	0.0395	0.037902	2.55E-06	
30	0.03335	0.033845	2.45E-07	
42	0.02835	0.030559	4.88E-06	
55	0.02635	0.028103	3.07E-06	
75	0.0239	0.025562	2.76E-06	
95	0.0235	0.023864	1.33E-07	
120	0.0235	0.022397	1.22E-06	
150	0.0235	0.021188	5.35E-06	

Table 101: *Exp 19: BULAB, k'-value*

	k'	0.720312		
	C*	0.017825		
Time (minutes)	**[Ca2+] exp.**	**[Ca2+] calc.**	**SE**	**SSE**
0	0.03935	0.03935	0	9.42079E-07
20	0.035	0.034255	5.55E-07	
40	0.0309	0.031111	4.44E-08	
60	0.02875	0.028977	5.13E-08	
80	0.0275	0.027433	4.47E-09	
100	0.026	0.026265	7.02E-08	
130	0.025	0.024963	1.35E-09	
159	0.02375	0.024037	8.24E-08	
189	0.023	0.023302	9.12E-08	
220	0.0225	0.022705	4.21E-08	
270	0.0225	0.021976	2.75E-07	

Table 102: *Exp 8, lime & BULAB, k'-value*

	k'	1.614634		
	C*	0.03459		
Time (minutes)	**[Ca2+] exp.**	**[Ca2+] calc.**	**SE**	**SSE**
0	0.068	0.068	0	7.44E-07
14	0.054	0.053625	1.41E-07	
24	0.0487	0.04915	2.02E-07	
34	0.0465	0.046378	1.48E-08	
44	0.0445	0.044493	4.36E-11	
59	0.04235	0.042578	5.18E-08	
74	0.0415	0.041283	4.72E-08	
165	0.0385	0.037964	2.87E-07	

Table 103: *Exp 8, lime & HYDREX, k'-value*

	k' 1.765194 **C*** 0.036301			
Time (minutes)	**[Ca2+] exp.**	**[Ca2+] calc.**	**SE**	**SSE**
0	0.0675	0.0675	0	1.63E-05
17	0.055	0.052414	6.69E-06	
27	0.0487	0.048846	2.13E-08	
37	0.0455	0.046571	1.15E-06	
47	0.0445	0.044995	2.45E-07	
67	0.041	0.042953	3.82E-06	
81	0.04125	0.042014	5.84E-07	
106	0.0405	0.040864	1.32E-07	
156	0.0405	0.039554	8.96E-07	
206	0.0405	0.038828	2.8E-06	

Table 104: *Exp 8, lime & gypsum & BULAB, k'-value*

	k' 0.121345196 **C*** 0.044427206			
Time (minutes)	**[Ca2+] exp.**	**[Ca2+] calc.**	**SE**	**SSE**
0	0.0730	0.073	0	1.70718E-07
10	0.0610	0.060673287	1.07E-07	
20	0.0530	0.052825275	3.05E-08	
30	0.0500	0.049889193	1.23E-08	
40	0.0472	0.047163178	1.36E-09	
55	0.0450	0.044997819	4.76E-12	
75	0.0440	0.043998333	2.78E-12	
95	0.0418	0.041664744	7.27E-09	
115	0.0417	0.04153803	1.25E-08	

Table 105: *Exp 8, lime & gypsum & HYDREX, k'-value*

	k'	0.749644175		
	C*	0.031424067		
Time (minutes)	**[Ca2+] exp.**	**[Ca2+] calc.**	**SE**	**SSE**
0	0.073	0.067394517	3.14E-05	4.36856E-05
10	0.061	0.059755055	1.55E-06	
20	0.053	0.054792112	3.21E-06	
30	0.05	0.051308767	1.71E-06	
40	0.0472	0.048729188	2.34E-06	
55	0.045	0.045910307	8.29E-07	
75	0.044	0.043325441	4.55E-07	
95	0.04175	0.041523364	5.14E-08	
115	0.04165	0.040195252	2.12E-06	

Table 106: *Exp 8, lime & gypsum & HYDREX (AMD), k'-value*

	k'	1.153119313		
	C*	0.017872076		
Time (minutes)	**[Ca2+] exp.**	**[Ca2+] calc.**	**SE**	**SSE**
0	0.064	0.064	0	9.7066E-07
10	0.0275	0.026537907	9.26E-07	
20	0.0205	0.020349833	2.26E-08	
30	0.018	0.017999436	3.18E-13	
40	0.0165	0.016407299	8.59E-09	
50	0.0165	0.016382133	1.39E-08	

Table 107: *Exp 8, lime & gypsum & BULAB (AMD), k'-value*

	k'	0.598816173		
	C*	0.022186906		
Time (minutes)	**[Ca2+] exp.**	**[Ca2+] calc.**	**SE**	**SSE**
0	0.0635	0.0635	0	6.46715E-07
10	0.0335	0.032782224	5.15E-07	
20	0.0245	0.024437649	3.89E-09	
30	0.0225	0.022498249	3.07E-12	
40	0.02	0.019879113	1.46E-08	
50	0.019	0.018663834	1.13E-07	

Table 108: *Exp 8, gypsum & HYDREX (AMD), k'-value*

	k'	0.598769746		
	C*	0.015936906		
Time (minutes)	**[Ca2+] exp.**	**[Ca2+] calc.**	**SE**	**SSE**
0	0.042	0.042	4.81E-35	1.0556E-07
10	0.023	0.02271341	8.21E-08	
20	0.0185	0.018423671	5.83E-09	
31	0.0155	0.015496428	1.28E-11	
41	0.0145	0.014447459	2.76E-09	
51	0.014	0.013878234	1.48E-08	

Table 109: *Exp 8, gypsum & BULAB (AMD) , k'-value*

	k'	0.497764514		
	C*	0.014807258		
Time (minutes)	**[Ca2+] exp.**	**[Ca2+] calc.**	**SE**	**SSE**
0	0.041	0.041	0	9.57171E-07
10	0.028	0.027187035	6.61E-07	
20	0.022	0.021519373	2.31E-07	
30	0.019	0.01875296	6.1E-08	
40	0.0165	0.016444809	3.05E-09	
50	0.016	0.015965614	1.18E-09	

11.9 **AMD analysis**

CERTIFICATE OF ANALYSIS

Our ref: I:\Stellenbosch Analytical Laboratory\Reports\University of Stellenbosch SAL0768.doc .....

Report No: SAL0768

24 November 2010

University of Stellenbosch
Process Engineering
Private Bag X1
Matieland
7602

Attention: Derek Gerber
Tel: 072 3477524
Email: dgerber@sun.ac.za

CHEMICAL ANALYSIS - O/N 183939713

Date received: 18/11/2010

Analysis completed: 24/11/2010

Sample Description & Condition: Effluent and treat water in 200 & 500ml volumetric flasks at room temperature.

Results:

Lab No	EFF4929	EFF4930	EFF4931
Sample Id	Sample 1	Sample 2	Sample 3
Potassium as K mg/L	14	15	15
Sodium as Na mg/L	55	56	58
Calcium as Ca mg/L	521	564	872
Magnesium as Mg mg/L	235	222	38
Sulphate as SO4 mg/L	2463	2355	2195
Chloride as Cl mg/L	15.2	20.5	18.9
Alkalinity as CaCO3 mg/L	0.0	14.0	71.6
Acidity as CaCO3 mg/L	150	-	-
Iron as Fe mg/L	31.8	<0.1	<0.1
Aluminium as Al mg/L	124.0	1.1	<0.1
Nickel as Ni mg/L	28.6	15.4	0.1
Conductivity mS/m (25℃)	365	340	320
pH (Lab) (20℃)	3.2	7.2	10.3
Saturation pH (pHs) (20℃)	-	7.8	6.9
Total Dissolved Solids (Calc) mg/L	2336	2176	2048
Hardness as CaCO3 mg/L	2270	2320	2333
Sodium Adsorption Ratio (SAR)	0.5	0.5	0.5
% Difference (Standard Method)	1.90	0.43	1.88
CATIONS meq/L	53.74	49.48	49.51
ANIONS meq/L	51.73	49.91	47.68

Andrew Pascall
Laboratory Manager

Sebastian Brown
Technical Laboratory Manager

Charney Anderson
Senior Laboratory Analyst

Direct Tel. 021 888 2580

Direct Fax. 021 888 2630

Page 1 of 1

This report relates only to the samples actually supplied to CSIR. The CSIR does not accept responsibility for any matters arising from the further use of these results. This certificate shall not be reproduced except in full without the written approval of the director.

Figure 56: *Chemical analysis of raw untreated AMD (sample 1)*

CERTIFICATE OF ANALYSIS

Our ref: I:\Stellenbosch Analytical Laboratory\Reports\University of Stellenbosch SAL0873.doc .....

Report No: SAL0873

14 January 2011

University of Stellenbosch
Process Engineering
Private Bag X1
Matieland
7602

Attention: Derek Gerber
Tel: 072 3477524
Email: dgerber@sun.ac.za

CHEMICAL ANALYSIS - O/N 183939713

Date received: 21/12/2010

Analysis completed: 13/01/2011

Sample Description & Condition: Effluent and treat water in 500ml plastic bottle at room temperature.

Results:

REPORT NUMBER:	873
Lab No	EFF6510
Sample Id	Mine Water
Sample Date	
Potassium as K mg/L	14
Sodium as Na mg/L	60
Calcium as Ca mg/L	614
Magnesium as Mg mg/L	246
Sulphate as SO4 mg/L (calc)	2496
Chloride as Cl mg/L	21
Alkalinity as CaCO3 mg/L	19
Ortho phosphate as P mg/L	<0.1
Fluoride as F mg/L	1.3
Aluminium as Al mg/L	0.12
Iron as Fe mg/L	<0.01
Manganese as Mn mg/L	4.1
Nickel as Ni mg/L	0.07
Conductivity mS/m (25℃)	365
pH (Lab) (20℃)	7.3
Saturation pH (pHs) (20℃)	7.59
Total Dissolved Solids (Calc) mg/L	2336
Hardness as CaCO3 mg/L	2546
Sodium Adsorption Ratio (SAR)	0.52

Andrew Pascall
Laboratory Manager

Sebastian Brown
Technical Laboratory Manager

Charney Anderson
Senior Laboratory Analyst

Direct Tel. 021 888 2580

Direct Fax. 021 888 2630

Page 1 of 1

This report relates only to the samples actually supplied to CSIR. The CSIR does not accept responsibility for any matters arising from the further use of these results. This certificate shall not be reproduced except in full without the written approval of the director.

Figure 57: *Chemical analysis of pre-treated AMD*

11.10 OLI projections

The following speciation projections were determined with OLI Analyzer 3.

11.10.1 Synthetic aqueous solution

Synthetic aqueous soltion speciation was based on conditions of experiment 8.

Table 110: *Stream Inflows*

	Input	Calculated	Unit	% Diff
H2O	1.00000e6	9.94688e5	mg/L	-0.531154
CAION	2404.68	2391.91	mg/L	-0.531154
NAION	2758.80	2744.14	mg/L	-0.531154
CLION	4254.36	4231.76	mg/L	-0.531154
SO4ION	5763.82	5733.20	mg/L	-0.531154

Table 111: *Mixture Properties*

Stream Amt - Total Inflow	1.00535	L
Temperature	25.0000	°C
Pressure	1.00000	atm

Table 112: *Aqueous Properties*

pH	7.08980	pH
Ionic Strength	5.84462e-3	mol/mol
Osmotic Pressure	8.84945	atm
Elec Cond, specific	0.0160193	1/(ohm-cm)
Elec Cond, molar	53.6828	cm2/ohm-mol
Viscosity, absolute	0.929894	cP
Viscosity, relative	1.04398	cP/cP H2O

Table 113: *Scaling Tendencies*

solids within temperature range		Temperature Range	
CASO4.2H2O	3.46407	0.0 - 126.000 °C	inside range
CASO4	2.55269	0.0 - 455.000 °C	inside range
NA2SO4.10H2O	1.12253e-3	0.0 - 32.4000 °C	inside range
NACL	1.80519e-4	0.0 - 350.000 °C	inside range
NA2SO4	1.24887e-4	19.0000 - 241.000 °C	inside range
CACL2.6H2O	7.97616e-9	-0.0100000 - 30.1100 °C	inside range
CAOH2	4.87904e-11	data valid through range	inside range
NAHSO4	1.56555e-11	data valid through range	inside range
NAOH.1H2O	1.49282e-13	12.0000 - 60.0000 °C	inside range
NA3HSO42	1.90907e-15	0.0 - 82.5000 °C	inside range
CA2CL2O.2H2O	2.42699e-19	10.0000 - 50.0000 °C	inside range

11.10.2 AMD concentrate

Raw data in **Figure 57** was used to perform the speciation in OLI at a temperature of 25°C.

Table 114: *Stream Inflows*

	Input	Calculated	Unit	% Diff
H2O	1.00000e6	9.98091e5	mg/L	-0.190886
KION	42.0000	41.9198	mg/L	-0.190886
NAION	180.000	179.656	mg/L	-0.190886
CAION	1842.00	1838.48	mg/L	-0.190886
MGION	738.000	736.591	mg/L	-0.190886
ALION	0.360000	0.359313	mg/L	-0.190886
MNION	12.3000	12.2765	mg/L	-0.190886
NIION	0.210000	0.209599	mg/L	-0.190886
SO4ION	7488.00	7673.55	mg/L	2.47801
CLION	63.0000	62.8797	mg/L	-0.190886
FION	3.90000	3.89256	mg/L	-0.190886

Table 115: *Mixture Properties*

Stream Amt - Total Inflow	1.00192	L
Temperature	20.0000	°C
Pressure	1.00000	atm

Table 116: *Aqueous Properties*

pH	6.43755	pH
Ionic Strength	5.05047e-3	mol/mol
Osmotic Pressure	2.44460	atm
Elec Cond, specific	4.39053e-3	1/(ohm-cm)
Elec Cond, molar	26.8944	cm2/ohm-mol
Viscosity, absolute	1.04953	cP
Viscosity, relative	1.04742	cP/cP H2O

Table 117: *Scaling Tendencies*

solids within temperature range		**Temperature Range**	
ALOH3	105.439	0.0 - 100.000 °C	inside range
CAF2	5.41409	data valid through range	inside range
CASO4.2H2O	3.73424	0.0 - 126.000 °C	inside range
CASO4	2.50944	0.0 - 455.000 °C	inside range
MGF2	0.176859	data valid through range	inside range
MGSO4.7H2O	7.15774e-3	0.0 - 49.9900 °C	inside range
ALF3.3H2O	1.74316e-4	0.0 - 90.0000 °C	inside range
MNSO4.5H2O	7.61016e-5	8.60000 - 23.9000 °C	inside range
NA2SO4.10H2O	1.27516e-5	0.0 - 32.4000 °C	inside range
NIOH2	4.15677e-6	data valid through range	inside range
NAF	2.21095e-6	0.0 - 100.000 °C	inside range
NISO4.7H2O	9.77229e-7	0.0 - 31.2000 °C	inside range
NIO	9.13764e-7	data valid through range	inside range
NA2SO4	7.01145e-7	19.0000 - 241.000 °C	inside range
K2SO4	6.06035e-7	9.70000 - 292.000 °C	inside range
MGOH2	4.74570e-7	data valid through range	inside range
NACL	1.70382e-7	0.0 - 350.000 °C	inside range
KCL	1.38596e-7	0.0 - 200.000 °C	inside range
MGSO4OH.0.5H2O	1.12509e-7	data valid through range	inside range

Table 117: *Scaling Tendencies Continues*

MNOH2	8.17406e-8	data valid through range	inside range
MGSO4OH	4.30341e-9	data valid through range	inside range
MNF2.4H2O	1.55004e-9	0.0 - 23.5000 °C	inside range
MNSO4	1.17513e-9	data valid through range	inside range
KF.2H2O	2.07513e-10	17.7000 - 40.2000 °C	inside range
K1ALSO4.12H2O	1.34227e-10	0.0 - 75.0000 °C	inside range
KHSO4	9.98075e-11	data valid through range	inside range
NA3FSO4	4.32996e-11	20.0000 - 120.000 °C	inside range
ALO2H2CL	3.14846e-11	data valid through range	inside range
MNCL2.4H2O	2.31182e-11	0.0 - 58.0000 °C	inside range
NAHSO4	6.14777e-12	data valid through range	inside range
NIF2.4H2O	4.59780e-12	0.0 - 90.0000 °C	inside range
CACL2.6H2O	1.46219e-12	-0.0100000 - 30.1100 °C	inside range
NAHF2	1.22932e-12	data valid through range	inside range
CAOH2	6.77117e-13	data valid through range	inside range
MGCL2.6H2O	2.64285e-13	0.0 - 116.700 °C	inside range
NICL2.6H2O	4.54262e-14	0.0 - 28.8000 °C	inside range
NAALO2	2.41944e-14	data valid through range	inside range
KOH.2H2O	8.41546e-15	0.0 - 33.0000 °C	inside range
NAOH.1H2O	1.26377e-15	12.0000 - 60.0000 °C	inside range
MGCLOH	1.19066e-15	data valid through range	inside range
ALOHCL2	1.06125e-15	data valid through range	inside range
AL2SO43.16H2O	1.10644e-16	0.0 - 88.0000 °C	inside range
NA3HSO42	6.85731e-18	0.0 - 82.5000 °C	inside range
AL2O5H5CL	1.48366e-18	data valid through range	inside range
KOH	1.73094e-22	data valid through range	inside range
NAALO22.2.5H2O	2.56065e-24	20.0000 - 120.000 °C	inside range
CA2CL2O.2H2O	4.95296e-25	10.0000 - 50.0000 °C	inside range
ALCL3.6H2O	1.90844e-25	0.0 - 100.000 °C	inside range
AL2SO43.6H2O	3.55460e-27	data valid through range	inside range
KMGCL3.2H2O	6.05986e-29	data valid through range	inside range
AL2SO43	1.00000e-35	data valid through range	inside range
KMGCL3	1.00000e-35	data valid through range	inside range

11.11 Statistical data

Table 118: *Regression statistics performed on HYDREX kinetic data from* **Table 35**

Regression Statistics	
Multiple R	0.76
R Square	0.57
Adjusted R Square	0.39
Standard Error	54.05
Observations	21.00

ANOVA

	df	*SS*	*MS*	*F*	*Significance F*
Regression	6.00	55075.07	9179.18	3.14	0.04
Residual	14.00	40905.88	2921.85		
Total	20.00	95980.95			

	Coefficients	*Standard Error*	*t Stat*	*P-value*	*Lower 95%*	*Upper 95%*	*Lower 95.0%*
Intercept	46.47	11.97	3.88	0.00	20.80	72.14	20.80
Temperature	-19.85	14.22	-1.40	0.18	-50.36	10.65	-50.36
pH	36.40	14.22	2.56	0.02	5.89	66.90	5.89
Antiscalant	26.40	14.22	1.86	0.08	-4.11	56.90	-4.11
Ferric	-23.90	14.22	-1.68	0.12	-54.40	6.61	-54.40
Calcium	-16.40	14.22	-1.15	0.27	-46.90	14.11	-46.90
Seed	-32.65	14.22	-2.30	0.04	-63.15	-2.14	-63.15

Table 119: *Regression statistics performed on BULAB kinetic data from* **Table 47**

Regression Statistics	
Multiple R	0.83
R Square	0.68
Adjusted R Square	0.45
Standard Error	130.42
Observations	15.00

ANOVA

	df	*SS*	*MS*	*F*	*Significance F*
Regression	6.00	294221.11	49036.85	2.88	0.08
Residual	8.00	136072.22	17009.03		
Total	14.00	430293.33			

	Coefficients	*Standard Error*	*t Stat*	*P-value*	*Lower 95%*	*Upper 95%*	*Lower 95.0%*
Intercept	108.89	34.37	3.17	0.01	29.64	188.14	29.64
Temperature	-54.86	34.37	-1.60	0.15	-134.11	24.39	-134.11
pH	92.64	34.37	2.70	0.03	13.39	171.89	13.39
Antiscalant	25.14	34.37	0.73	0.49	-54.11	104.39	-54.11
Ferric	-17.64	34.37	-0.51	0.62	-96.89	61.61	-96.89
Calcium	19.86	34.37	0.58	0.58	-59.39	99.11	-59.39
Seed	-82.64	34.37	-2.40	0.04	-161.89	-3.39	-161.89

11.12 ISE specifications

Measurement range: 1.0 M to $3x10^{-6}$ M (40080 to 0.12 mg/l)

Operating temperature: 0-40°C

Operating pH: 4-10

Interferences: organic solvents and cationic detergents should be absent. Moreover cationic interferences are important. If the ratio of interfering ion to calcium exceeds the values in **Table 120**, interferences become significant.

Table 120: *Ratio of interfering ions*

Ion	Interference ratio
sodium (Na^{2+})	15000
magnesium (Mg^{2+})	7000
nickel (Ni^{2+})	700
ferrous (Fe^{2+})	300
aluminium (Al^{3+})	250
ammonium (NH_4^+)	200
cupric (Cu^{2+})	35
lead (Pb^{2+})	0.001